Structure and mobility in highly viscous silicate solutions

Elke Katharina Friederike Bahlmann

Structure and Mobility in Highly Viscous Silicate Solutions

by

Elke Katharina Friederike Bahlmann

A Thesis submitted in partial fulfilment of the requirements for the degree of doctor of Philosophy

Department of Chemistry

University of Durham

1994

"Experience was of no ethical value.
It was merely the name men gave to their mistakes."

Oscar Wilde
The Picture of Dorian Gray

Abstract

This thesis is concerned with the investigation of highly condensed, highly viscous silicate systems by means of NMR methods (mainly ^{29}Si-NMR investigations). The work focused on silicate solutions containing colloidal particles in sol and gel form with the interest of the work centred on the systems near the sol/gel-transition. Quantitative information about the behaviour of silicate species in these silicate systems is presented and some information about the role of protons and sodium cations in the silicate solutions is provided. The structure of the colloidal material existing in these highly condensed silicate systems is investigated along with the behaviour of colloidal particles in several situations such as decreasing alkalinity or changing SiO_2-concentration. Additionally an idea of the range of particle sizes in the colloidal material in highly-condensed silicate solutions has been obtained. The dynamics of the silicate systems were studied in terms of rotational mobility as well as diffusive motion. Exchange processes between silicate species were monitored using 2D-exchange spectroscopy. An investigation of the influence of additives, in particular surfactants, on highly condensed silicate systems was carried out by adding representative surfactants of the categories cationic, anionic and non-ionic.

Memorandum

The research presented in this thesis has been carried out at the Department of Chemistry, University of Durham, between October 1991 and March 1994. It is the original work of the author unless stated otherwise.

Some preliminary work on this topic was undertaken for the Diplomarbeit at the Technical University of Braunschweig, the experimental work being carried out at the University of Durham under the supervision of Prof. R.K. Harris. Although this provided valuable basic information and training, none of the detailed results are used in the present thesis except where specifically stated otherwise.

Acknowledgements

I would like to express my thanks to my supervisor Prof. Robin K. Harris for his encouragement, support and understanding and many helpful discussions.
Furthermore I like to thank Dr. Barry J. Say for his patience and support in the training to use the spectrometer systems and his willingness to tackle any problems that occurred.
Further thanks to Nicola Davies, Dr. David Apperley and Dr. Race R. Yeung, who helped the progress of my PhD in letting me use the VXR300 in the IRL, and to Dr. Alan Kenwright for helpful advice.
I am pleased to thank my industrial supervisors Dr. Ken Metcalfe and Dr. Ed G. Smith at Unilever Research Port Sunlight, who were very pleasant to work with, for always being there for discussions, suggestions, advice and encouragement. Thanks to their and their families friendliness and hospitality my stays at Port Sunlight were always enjoyable.
Thanks to Jeff Rockliffe for his help in operating the MSL300 at Port Sunlight and to the NMR-section and the OSFR-section for always being prepared to help (and for numerous coffees).
In this context I would like to mention that I am grateful to Unilever Research for provision of a Research Studentship.
I would like to mention Dr. John Parkinson and Dr. Ian Sadler, who are running the NMR service at the University of Edinburgh, for their help and advice in using the Varian VXR600.
A big ThankYou to my colleges Anna, Stefan, Abdul, Graham, Steve C., Steve B., Tim and Garry for a very friendly working atmosphere in which many discussions were possible, providing deeper insight into the mysteries of NMR as well as a number of more 'profane' subjects.
I would like to express my thanks to Julia and Barry as well as Joe and Myrial for their making me feel at home in the North and for many magic moments in Northumbrian music.
The knowledge that my parents and brothers are there when I need them, whereever I am, was (and is) of invaluable importance to me.
Last but not least I would like to give many thanks to David for providing a magnetic but NMR-free home environment.
Last and least a big pat for my hairy friends Tico and Maggie.

Publications

E. K. F. Bahlmann, R. K. Harris, B. J. Say,
Magn. Reson. Chem. **31** (1993) 266

E. K. F. Bahlmann, R. K. Harris, K. Metcalfe, E. G. Smith,
Magn. Reson. Chem. **31** (1993) 743

Conferences attended

The Royal Society of Chemistry
Tenth International Meeting on NMR Spectroscopy
University of St. Andrews, Scotland
July 1991

North East Graduate Symposium
University of Northumbria
Newcastle upon Tyne
April 1993

Presentations

"NMR investigations of Highly Condensed Silicate Solutions" (Poster)
ICI Poster Competition
University of Durham
December 1992

"Structuring and Mobility in Highly Viscous Silicate Systems" (Lecture)
North East Graduate Symposium
University of Northumbria
Newcastle upon Tyne
April 1993

"Silicon-29-NMR of Highly Condensed Silicate Solutions" (Poster)
11th International Meeting on NMR Spectroscopy
University College of Swansea, Wales
July 1993

Contents:

3. Experimental

1. INTRODUCTION

Aim of the work and the industrial importance of silicate solutions

This thesis is concerned with the investigation of highly condensed, highly viscous silicate systems by means of NMR methods (mainly ^{29}Si-NMR investigations). The work focused on silicate solutions containing colloidal particles which are of considerable technological importance.

Soluble silicates are among the most widely used inorganic chemicals. They have properties not shared by other alkaline salts. Silicates are often preferred to other alkalis as soda ash because of their corrosion inhibition properties and detergent attributes[1]. Additionally to this their production can be done at relatively low cost. Sodium silicate is used in far greater quantities than silicates based on other alkali metals. The range of applications falls into the main categories - detergent, adhesive and chemical. Sodium and potassium silicates are practically the only inorganic materials used as adhesives because of their reasonably rapid set and high strength which also qualifies them for the production of paper products, particularly tubes and drums. They are suitable for use in the treatment of potable and industrial waters as very efficient coagulation aids and corrosion preventers in the water distribution systems[2]. Coatings based on soluble silicates are used for various purposes such as the sealing of porous surfaces, heat insulation, the binding of loose fibres[6] and the formulation of certain paints[2,3]. Another important application of silicates is as a binder for water-resistant compositions of siliceous cement, which can be used as a filter medium[7], for sand in foundry operations providing a longer period for shaping without increasing the set-time[8] and as binders for organic,

inorganic and mineral fibres in products such as paper[9]. Most silicate applications require the material in the form of an aqueous solution.

Several investigations have been carried out on a variety of silicate solutions in the past using methods based on physical properties[10,11], chemical reactions[12,13], diffraction and scattering techniques[14,15], microscopic methods[16] and other spectroscopic methods than NMR[17]. The first published ^{29}Si-NMR spectrum of a silicate solution can be attributed to Marsmann[18]. Amongst all these analytical techniques NMR methods can provide a wealth of information without interfering with the structuring in the silicate.

The NMR investigations carried out so far, however, mainly focused on silicate solutions with a low degree of condensation and without colloidal particles[19,20]. Because of several experimental difficulties highly condensed, highly viscous silicate solutions have not been intensively investigated so far in spite of their extreme importance and usefulness. These investigations are the first ones considering the importance of the quantitative aspect in the NMR-analysis of highly condensed silicate systems and providing a method for the quantification in silicate systems. In this work substantial valuable quantitative information about the behaviour of silicate units in silicate systems with colloidal particles is presented and some information about the role of the protons and sodium cations in the silicate solutions is provided.

Silicate systems on both sides of the sol/gel-transition were considered, with the interest of the work centred on the systems (sols and gels) near the transition. The work was mainly focused on the investigation of sodium silicate systems. Nevertheless some valuable new information was obtained on the behaviour of potassium silicate systems.

The main aspects under which the silicate solutions were studied are the structure of the colloidal material existing in these highly condensed silicate systems and the behaviour of colloidal particles in several situations such as decreasing alkalinity or changing SiO_2-concentration. The dynamics of the

silicate systems were investigated in terms of rotational mobility, which provided a deeper understanding of the relaxation times as well as diffusive motion. Although self-diffusion measurements are routine for protons and fluorine in one-component systems[21], the use of field gradients in the measurement of silicon self-diffusion in highly condensed multicomponent systems is unique. Exchange between silicate units was monitored using 2D-exchange spectroscopy and for the first time qualitative as well as quantitative information about the exchange of highly condensed silicate units was obtained.

Almost any process or product that involves the interaction of a solid and a liquid phase (e.g. in colloidal systems) will be affected by surfactant adsorption. Therefore this area represents a major segment of the technological application of silicates. One of the very early uses of viscous silicate solutions is in detergent systems in combination with surfactants and/or soaps in detergent systems. This is clearly due to their soapy feel, which combined with a lower alkalinity than that of caustic soda, make them good builders for detergents[4]. Their role in today's detergents is a combination of several effects, so they are proposed to assist in the deflocculation of soil and prevention of its redeposition and they help structure the spray-dried soap-powder. Fabric washing powder, for instant, can contain up to 15wt% sodium silicate in a range of SiO_2:Na_2O-ratios[5].

An important part of this work is concerned with the influence of surfactants on silicate systems. There is some information available on the interaction of surfactants with the surface of suspended solid silica[22-24] but on the effect of the surfactant on silicate systems near the sol/gel-transition no information was available beforehand. Representative surfactants of the categories cationic, anionic and non-ionic were added to silicate systems, and

novel information was obtained on the "reaction" of highly condensed silicates on the surfactant addition.

Literature:

1 J. S. Falcone (Ed.), Soluble Silicates, ACS Symposium Series 194, Washington D.C. (1982)

2 Crosfield Soluble Silicates, issued by Crosfield Chemicals, Warrington (1989)

3 Ullmans Encyklopaedie der Technischen Chemie, 4.Auflage, Band 22, Verlag Chemie (1982)

4 W. Gossage, Brit.Pat., 762 (1854)

5 G. C. Schweiker, J.Am.Oil Chemists Soc. **55** (1978) 36

6 R. F. Nickerson, United States Patent Office 3,024,145 (1962)

7 D. A. Kuhn, N. J. Wyckoff, United States Patent Office 3,449,139 (1969)

8 F. J. Boston, V. W. Nery, United States Patent Office 3,920,460 (1975)

9 R. K. Iler, A. G. Jelinek, United States Patent Office 2,886,466 (1959)

10 R. W. Harman, J. Phys. Chem. **32** (1928) 44

11 D. Hoebbel, W. Wieker, Z. Anorg. Allg. Chem. **405** (1974) 267

12 L. S. Dent-Glasser, E. E. Lachowski, J. Chem. Soc. Dalton (1980) 393

13 J. D. H. Strickland, J. Am. Soc. **74** (1952) 862, 868, 872

14 H. Graetsch, A. Mosset, H. Gies, J. of Non-Cryst. Solids **119** (1990) 173

15 A. Ja'nosi, O. Kratky, O. Sekora, Monatsh. Chem. **100** (1969) 1973

16 G. B. Alexander, R. K. Iler, J. Phys. Chem. **57** (1953) 932

17 P. K. Dutta, D. C. Shieh, Applied Spectroscopy **39** (1985) 343

18 H. C. Marsmann, Chem. Zeitung **97** (1973) 128

19 G. Engelhardt, D. Zeigin, H. Jancke, D. Hoebbel, W. Wieker, Z. Anorg. Allg. Chem. **418** (1975) 17

20 A. V. Mc Cormick, A. T. Bell, C. J. Radke, Zeolites **7** (1987) 183

21 E. G. Smith, J. W. Rockliffe, P. I. Riley, J. of Colloid and Interface Science **131** (1989) 29

22 R. Denoyel, J. Rouquerol, J. of Colloid and Interface Science **143** (1991) 555

23 P. Somasundaran, E. D. Snell, E. Fu, Q. Xu, Abstracts of Papers of the American Chemical Society **200** (1990) 134

24 E. M. Lee, E. A. Simister, R. K. Thomas, Langmuir **6** (1990) 1031

2. THEORY

A NMR-theory

1. General theory

1.1 Resonance condition

Nuclear magnetic resonance spectroscopy can only be applied to nuclei with a non-zero nuclear spin . The nuclear spin is characterised by the angular momentum quantum number I. In most cases the magnetic moment μ_I is parallel to the vector describing the nuclear spin of a nucleus. However, in the case of ^{29}Si they are antiparallel. The magnetic moment is characterised by the magnetogyric ratio, γ, which is a constant specific for each isotope[1].

$$\mu_I = \gamma * \hbar * [I(I+1)]^{1/2} \qquad [1]$$

Under the influence of a strong magnetic field B_0 the spin-axis of a nucleus with I # 0 will orient at an angle to the field B_0 with a quantization of energy taking place, the orientation giving rise to 2I+1 energy-levels. The energy E of these energy-levels relative to the energy at zero-field is:

$$E = \gamma * \hbar * B_0 * m_I \qquad [2]$$

where m_I is the magnetic quantum number, which can adopt numbers between

$$I , I-1 , I-2 , I-3 \ldots . \text{and} \ldots . -I+3 , -I+2 , -I+1 , -I \qquad [3]$$

For nuclei with I = 1/2 (e.g. protons, silicon) this results in two m-values (m= +1/2 and m= -1/2).

The radiation-induced transitions are generally restricted to:

$$\Delta m_I = \pm 1 \qquad [4]$$

There is a constant interval between neighbouring energy-levels.

$$\Delta E = \gamma * \hbar * B_0 \qquad [5]$$

Nuclear magnetic resonance is the phenomenon observed if an external oscillating magnetic field B_1 with the correct polarisation is applied, which fulfils a special frequency condition. This condition, widely known as resonance, implies that the frequency at which B_1 is oscillating is equal to ν_0, which is the Larmor frequency of an observed nucleus in B_0, and that B_1 has the same direction of rotation as the precessing nuclear dipoles[2]. In this case the nucleus absorbs energy from the B_1-field and is promoted to an excited state. This absorption of energy is measured in NMR-spectroscopy.

$$\hbar * 2\pi\nu_0 = \Delta E = \gamma * \hbar * B_0$$

$$\nu_0 = \frac{\gamma}{2\pi} * B_0 \qquad [6]$$

[7]

This equation, commonly called the Larmor equation, describes the basic phenomenon of nuclear magnetic resonance[1,2,3].

2. Classical picture

2.1 Rotating frame of reference

If a magnetic field B_1, which rotates with the Larmor frequency of the observed nucleus, is applied perpendicular to the static magnetic field B_0 along the x-direction, the nuclear moments interact with the magnetic vector of this electromagnetic irradiation. The result is that their equilibrium is disturbed and the overall magnetisation is not parallel to the B_0-field any more.

In all cases of the macroscopic magnetisation being in equilibrium or being perturbed, the Larmor frequency is superimposed on all movements of the spins in the static field. Since in a fixed co-ordinate system movements of M_0 are very difficult to describe, a rotating co-ordinate system is used which rotates with the same frequency as B_1[2].

The angle of the perturbation caused by electromagnetic irradiation with the frequency νo (B_1) is dependant on the pulse duration τp, B_1 and γ.

$$\theta = \gamma * B_1 * \tau_p \qquad [8]$$

3. Relaxation

3.1 General theory

The quantum mechanical view of the NMR experiment is based on time-dependent perturbation theory, where the energy of a nuclear spin state is a function of two perturbations[5]. The larger of the two results from the influence of the external field B_0. When the sample is placed in a magnetic field, there are transitions from states of high energy to states of lower energy. These transitions are governed by the longitudinal relaxation time, T1. The smaller of the two perturbations is time dependent. It results from the rf field B_1, which causes transitions from lower to upper states within an energy

manifold. These are governed by the transverse relaxation time, T2. The energy states are illustrated in Figure 2-1.

Figure 2-1

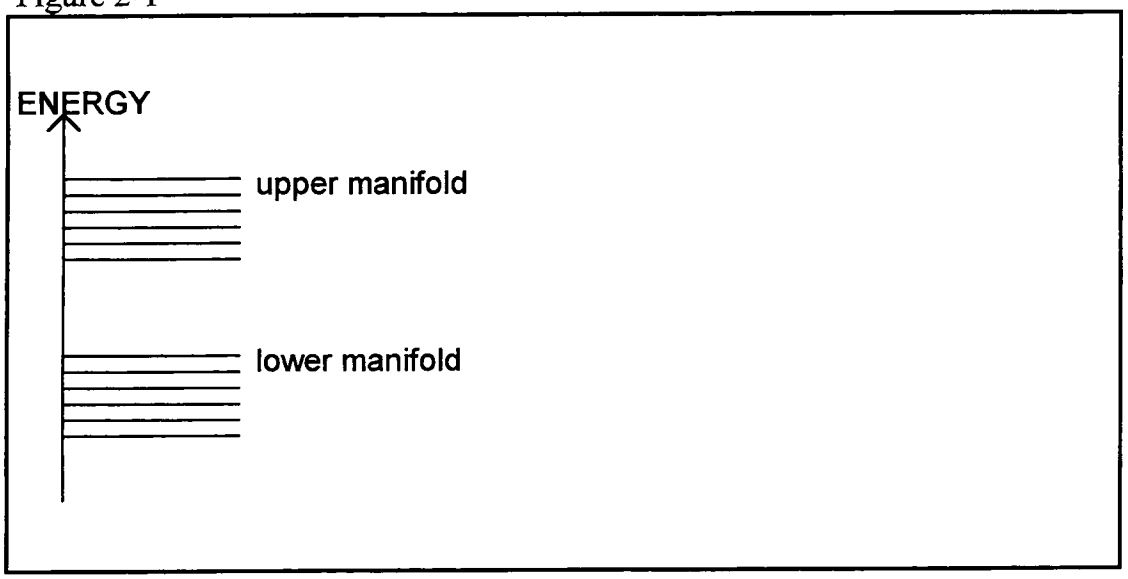

The longitudinal relaxation time T1, also referred to as the spin-lattice relaxation time, describes the change of nuclear magnetisation in a direction parallel to that of the static field, B_0. In other words T1 characterises the rate at which thermal equilibrium between spin-states is restored following the absorption of energy from a radio frequency signal or following the exposure to a static magnetic field.

The transverse relaxation time T2, also referred to as the spin-spin relaxation time, characterises the process of precessing nuclear spins gradually losing their phase coherence, which means an entropy increase for the system[6]. Chemical exchange processes in the system cause loss of phase coherence and thus affect T2[5].

In the solution state there are rapid and random motions which include rotational tumbling of individual molecules, relative translational motion and migrations of atoms or groups from one molecule to another. (Vibrations are usually too rapid to make effective relaxation pathways.) These motions

considerably reduce the coupling between nuclear spins so that the spins can be considered as individual systems coupled to the lattice. By "lattice" usually the translational or rotational degrees of freedom of the molecules in which the nuclei are located are meant. The energy transfer for the relaxation process can occur if the coupling vectors are functions of time. It is the differences between these functions over intervals of time τ that determine the correlation function[7]. The longer these intervals are the less correlation is found. The correlation time expresses the duration of a correlation between configurations of a molecule at two different times. It is a characteristic value which is shorter the faster the motions are. The correlation function is frequently considered to decay exponentially in the time domain[6,7] as illustrated in Figure 2-2.

$$G(\tau) = G(0)e^{-(t/\tau)} \qquad [9]$$

The Fourier transformation of the correlation function yields a function in the frequency domain. The resulting spectrum of frequencies is known as the spectral density $J(\omega)$[3,4,6].

$$J(\omega) = \frac{2\tau}{1+\omega^2\tau^2} \qquad [10]$$

Figure 2-2

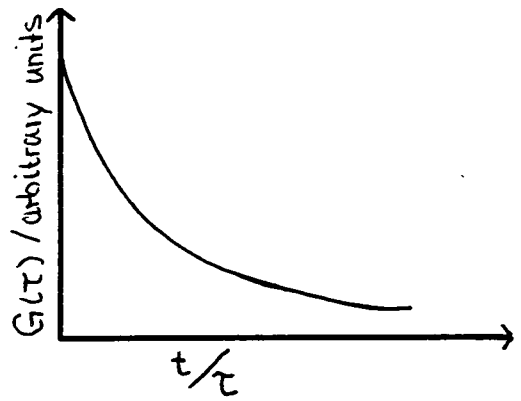

Figure 2-3

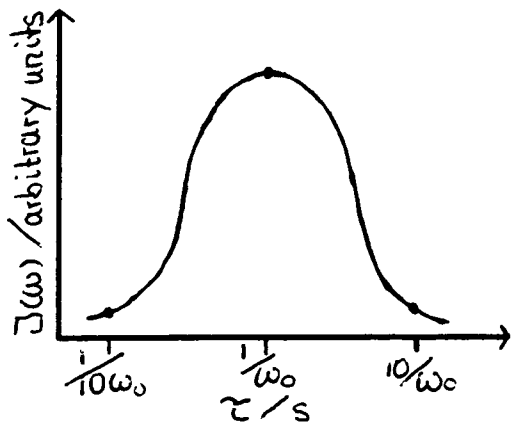

The spectral density can be represented as a function of τ at constant ω as illustrated above in Figure 2-3 or as a function of the frequency ω at constant τ as shown in Figure 2-4 below.

Figure 2-4

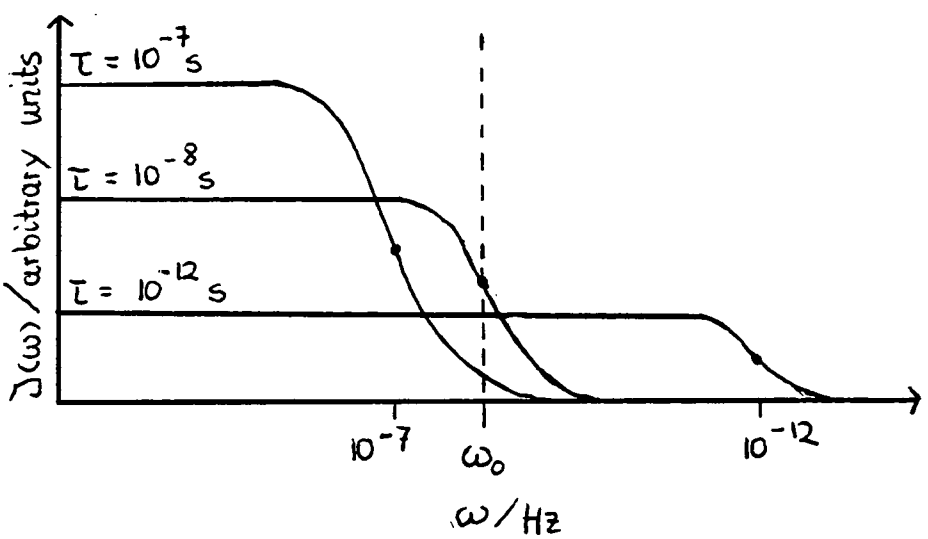

The point at half intensity characterises the inverse correlation time $1/\tau$. In both plots it can easily be seen that at a working field of Bo and a working frequency of ωo the spectral density J(ω), which can be described as the frequency distribution of the components of the motionally induced local fluctuating field, is a maximum at the point where $\tau=1/\omega_0$[3,7]. Both the spin-lattice and the spin-spin relaxation time are dependent on the spectral density. Only in the case of the spin-lattice relaxation time does a correlation time τ equal to ωo cause most effective relaxation and give rise to a maximal relaxation rate[3]. The behaviour of the spin-lattice and the spin-spin relaxation time as a function of increasing correlation time τ (decreasing mobility) and the operating field B_0 is illustrated in Figure 2-5. The functions reflect the dependency on τ and are independent of the distance separating the nuclei. It has to be noted that in the region where $\tau^2 >> 1/\omega_0^2$ not only the spin-lattice relaxation time but also the spin-spin relaxation time show a field-dependency[3,30].

Figure 2-5 shows the dependency of spin-lattice and spin-spin relaxation times on the correlation time and the spectrometer operating frequency assuming a single type of isotropic motion (and no sudden variation at phase changes).

Figure 2-5

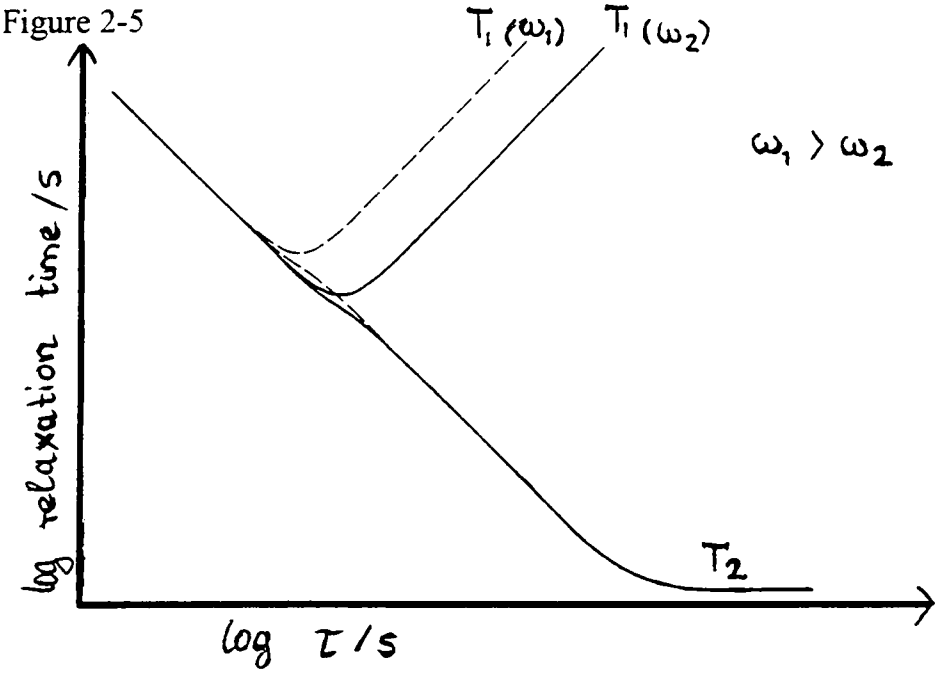

The lifetimes of spin states are generally influenced by fluctuations in the local magnetic field. In relaxation via dipole-dipole interactions, for instance, each spin experiences a fluctuating magnetic field which is produced by neighbouring spins and induces transitions among its levels. There are several other mechanisms causing relaxation of a spin, which are discussed in section 4.2.

The possible transitions between the various eigenstates of an AX spin system are given by their mixing under the influence of the local fields, and the transition rates W are obtained by solving the Schroedinger equation with the perturbation Hamiltonian $\mathcal{H}(t)$, which represents a randomly varying interaction with average value zero fluctuating in the interval t.

In quantum mechanical terms the dipole-dipole interaction between two spins I and S can be written as[5] :

$$\hbar^{-1}\mathcal{H}_1 = \sum F^{(q)} A^{(q)} \qquad [11]$$

$F(q)$ are random functions of the relative positions of two spins, and the spectral density describes all their time variations during an interval $t+\tau$

$A(q)$ are operators acting on the spin variables

If the correlation time for the random change of $\mathcal{H}_1(t)$ is very short, i.e. much shorter than the Larmor period, all spectral densities $J(\omega X-\omega A)$, $J(\omega X+\omega A)$ and $J(\omega A)$ become independent of ω and equal to $J(0)$[5]. This is the condition of extreme narrowing[3,5].

In the T1-process (z magnetisation) spin states can only exchange energy with components in x- and y-direction. The T2-process (y magnetisation) can only be influenced by spin states with gradient components in x- and z-direction. The influencing of spin states by the z-component of a

fluctuating field is an adiabatic process described by the term J(0), which only occurs in the characterisation of the T2-process[7,8].

At the T1-minimum the molecules undergo motion which is equal to the period of Larmor precession, and the correlation time τ equals $1/\omega o$. In systems with molecules undergoing motion which is slow compared with the period of Larmor precession, the transverse relaxation time T2 is considerably shorter than T1[3,5].

3.2 Spin-lattice relaxation and its mechanisms

There are several mechanisms, all of which are dependent on molecular parameters which can contribute to the local fluctuating field, i.e. the gradient causing transitions and thus relaxation. All these relaxation interactions are modulated by molecular rotation or translation. The transition probabilities between levels i and j must be summed over all possible mechanisms to give the total transition probability[1,4].

$$W_{ij} = \sum_{m} W_{ij}^{m} \qquad [12]$$

Similarly, the sum of relaxation rates due to the single contributions of mechanisms yields the overall relaxation rate measured in the NMR-experiment.

$$\frac{1}{T1} = \frac{1}{T1_Q} + \frac{1}{T1_{SC}} + \frac{1}{T1_{UE}} + \frac{1}{T1_{SA}} + \frac{1}{T1_{DD}} \qquad [13]$$

Relaxation by electric quadrupole interactions:

$$\frac{1}{T1_Q} = \frac{3\pi^2(2I+3)}{10I^2(2I-1)}\chi^2(1+\frac{1}{3}\eta^2)\frac{\tau}{1+\omega_0{}^2\tau^2} \qquad [14]$$

$I > 1/2$

χ is the nuclear quadrupole coupling constant

η is the asymmetry parameter measuring the deviation of the electronic environment (electric field gradient) of the nucleus from axial symmetry

The term $\tau/(1+\omega_O{}^2\tau^2)$ can be replaced by τ if the extreme narrowing condition $\omega_O{}^2\tau^2 << 1$ is fulfilled. Relaxation by electric quadrupole interactions can be described as an indirect energy transfer as it is not a strictly magnetic mechanism but rather involves an electric interaction between the nuclear electric quadrupole moment and electric field gradients arising from the surrounding electrons. The quadrupolar energy is modulated *via* electric field gradients. If this occurs at the transition frequency, spin-lattice relaxation is caused. Rapid isotropic molecular tumbling averages the quadrupolar interactions, which are affected by the direction of the electric field gradient. Any sites of tetrahedral, octahedral, cubic or spherical symmetry have a zero field gradient and are thus not affected by quadrupolar relaxation[3,4,6].

Relaxation by scalar coupling to spin X of quantum number S:

$$\frac{1}{T1_{SC}} = \frac{8}{3}\pi^2(J_{AX})^2S(S+1)\left[\frac{\tau_1^s}{1+(\omega_A-\omega_X)^2(\tau_1^s)^2}\right] \qquad [15]$$

J_{AX} is the coupling constant

τ_1 is the inverse of the rate at which J_{AX} is modulated

Relaxation by scalar coupling can frequently be disregarded. The ^{29}Si spins in natural abundance silicates are too dilute to give rise to ^{29}Si-^{29}Si

couplings. No ^{29}Si-^{1}H coupling can be observed (Chapter 3-2). Scalar relaxation occurs when one partner of a strongly coupled pair is in chemical exchange at a rate comparable to (ω_A-ω_X). The more the frequency at which J_{AX} is modulated (proton exchange frequency) differs from (ω_A-ω_X), the stronger the coupling between the AX spins has to be for scalar relaxation to be operative. The scalar coupling between Si and H spins has to be in the range of MHz for relaxation by scalar coupling to contribute to the overall relaxation rate. These requirements for strong coupling combined with fast exchange are very rarely observed in heteronuclear systems and only then if the gyromagnetic ratios of the two nuclei are very similar[3,31]. In fact the coupling constants for two-bond couplings between silicon and protons are typically of the order of 1 to 13Hz[1,32,33], the larger couplings (^{2}J(Si-H) = 9 to 13Hz) occurring with the silicon carrying strongly electronegative ligands[33]. These couplings are far too small to cause any contribution of scalar relaxation to the relaxation rate, which can thus be disregarded for the silicates under investigation.

Relaxation *via* unpaired electrons of spin S:

$$\frac{1}{T1_{UE}} = \frac{\mu_0^2\gamma_A^2\gamma_e^2\hbar^2 S(S+1)}{120\pi^2 r^6}\left[\frac{3\tau_P}{1+\omega_I^2\tau_p^2}+\frac{7\tau_P}{1+\omega_S^2\tau_P^2}\right]+\frac{\mu_0^2\gamma_e^2 a_N^2 S(S+1)}{24\pi^2}\left[\frac{\tau_e}{1+\omega_S^2\tau_e^2}\right] \quad [16]$$

τ_e is the electron spin relaxation time

Relaxation *via* unpaired electrons occurs *via* a dipolar relaxation mechanism or a scalar relaxation mechanism[3] both of which are very effective as the magnetogyric ratio γ of the electron is 658 times as large as the γ of the proton[4]. The relaxation *via* paramagnetics is often referred to as outer-sphere relaxation[11]. There are two major terms, the first one describing the dipole-dipole contribution, the second one depends upon a_N, the nuclear electron

hyperfine coupling constant which characterises the contact interaction[4]. Modulation of the interactions with unpaired electrons can occur by exchange of the electron between different molecules or by spin-lattice relaxation of the electron itself[3].

Relaxation by nuclear shielding anisotropy:

$$\frac{1}{T1_{SA}} = \frac{\mu_0 \gamma_A^2 B_0^2 \Delta\sigma^2}{30\pi} \frac{\tau}{1+\omega_0{}^2\tau^2} \qquad [17]$$

$\Delta\sigma$ is the shielding anisotropy of the relevant molecule which can be modulated by molecular motion thus providing a local fluctuating magnetic field. Equation 17 describes the case of an axially symmetric molecule[1,4].

3.3 Relaxation *via* dipole-dipole interactions

Relaxation *via* dipole-dipole interactions is the most important mechanism in the relaxation of silicon in viscous silicate systems. The polarisations of the spins I and S are coupled so that the fluctuating field produced by spin I acts on spin S and induces energy transitions[12]. Dipolar relaxation can be divided into intramolecular dipolar relaxation and intermolecular dipolar relaxation[4,9]. These two mechanisms can be distinguished by dilution studies (e.g. dilution with D_2O) as long as it is assured that there is no viscosity change in the system which would change the correlation time and thus T1. In the case of intramolecular dipolar relaxation the T1-value will not be affected whereas in the case of intermolecular dipolar relaxation the T1-value will be affected.

3.3.1 Intramolecular dipolar interaction :

In the interior of a molecule the intramolecular dipolar relaxation of spins arises from the rotation of the molecule, the variation in the distance between the spins due to vibrations being negligible[5].

The equations below are for a given pair of spin-1/2 spins A and X :

$$\frac{1}{T1A} = W0 + 2W1A + W2 \qquad [18]$$

$$W0 = \frac{1}{20}(2\pi R)^2 J(\omega x - \omega A) \qquad [19]$$

$$W1A = \frac{3}{40}(2\pi R)^2 J(\omega A) \qquad [20]$$

$$W2 = \frac{3}{10}(2\pi R)^2 J(\omega x + \omega A) \qquad [21]$$

$$J(\omega) = \frac{2\tau}{(1+\omega_0{}^2\tau^2)} = \frac{2\tau}{(1+4\pi^2\nu_0{}^2\tau^2)} \qquad [22]$$

The equations below are for the case of intramolecular A-X interaction[3,5,10] :

$$\frac{1}{T1} = \frac{1}{20}(2\pi R)^2[J(\omega x - \omega A) + 3J(\omega A) + 6J(\omega x + \omega A)] \qquad [23]$$

$$\frac{1}{T1} = \frac{1}{10}\tau(2\pi R)^2[\frac{1}{1+(\omega x - \omega A)^2\tau^2} + \frac{3}{1+\omega A^2\tau^2} + \frac{6}{1+(\omega x + \omega A)^2\tau^2}] \qquad [24]$$

$$\frac{1}{T2} = \frac{1}{40}(2\pi R)^2[4J(0) + J(\omega x - \omega A) + 3J(\omega A) + 6J(\omega x) + 6J(\omega x + \omega A)] \qquad [25]$$

$$\frac{1}{T2} = \frac{1}{20}\tau(2\pi R)^2[4 + \frac{1}{1+(\omega x - \omega A)^2\tau^2} + \frac{3}{1+\omega A^2\tau^2} + \frac{6}{1+\omega x^2\tau^2} + \frac{6}{1+(\omega A + \omega x)^2\tau^2}] \qquad [26]$$

R is the dipolar coupling constant and is proportional to r_{AX}^{-6}.

In cases of interest in this thesis r_{AX} is the Si-H distance.

$$R^2 = \left[\left(\frac{\mu o}{4\pi}\right) \gamma_A \gamma_X \left(\frac{\hbar}{2\pi}\right) \right]^2 \left[r_{AX}^{-3} \right]^2 \qquad [27]$$

$$R^2 = 5.703 * 10^{-52} * r_{AX}^{-6} \qquad [28]$$

3.3.2 Intermolecular dipolar interaction:

For the intermolecular interactions the relative translation of molecules must be considered as in this case the vector connecting the nuclei A and X becomes time dependent[4,5].

$$\frac{1}{T1dd(inter)} = \frac{\mu_0^2 N_X \gamma_A^2 \gamma_X^2 \hbar^2}{120\, Da\, \pi^2} \qquad [29]$$

D mutual translational self-diffusion coefficient of the molecules containing A and X

a distance of closest nuclear approach

N_S concentration of spins X per unit volume

4. Solid state NMR

4.1 General theory

There are two factors determining the appearance of the NMR-spectrum for nuclei with spin 1/2 in solids.

Dipolar interactions

The direct coupling interaction or dipolar coupling interaction depends on the angle θ_{AX} between the field-vector of B_0 and the vector connecting the nuclei i and j. It is characterised by the average over all magnetic dipoles with an orientation in the magnetic field. Therefore it is usually averaged to zero in solutions (rare exceptions are molecules which even in solution are partially oriented in the field) and only occurs in anisotropic systems[13]. In the solid state the molecules (i.e. the nuclei) are usually fixed. Thus dipolar interactions cannot be averaged to zero. A heteronuclear AX two-spin system in a crystal with only one possible orientation for r_{AX} and only one θ_{AX} has a dipolar splitting[3]:

$$(\frac{\mu_0}{4\pi})\gamma_A\gamma_X(\frac{\hbar}{2\pi})r_{AX}^{-3}(3\cos^2\theta-1) \qquad [30]$$

Isolated two-spin systems, which are in microcrystalline assemblies, show a variety of orientations for the angle θ. Therefore, instead of a doublet a characteristic splitting pattern is observed called the powder pattern[2] (Figure 2-6).

Figure 2-6

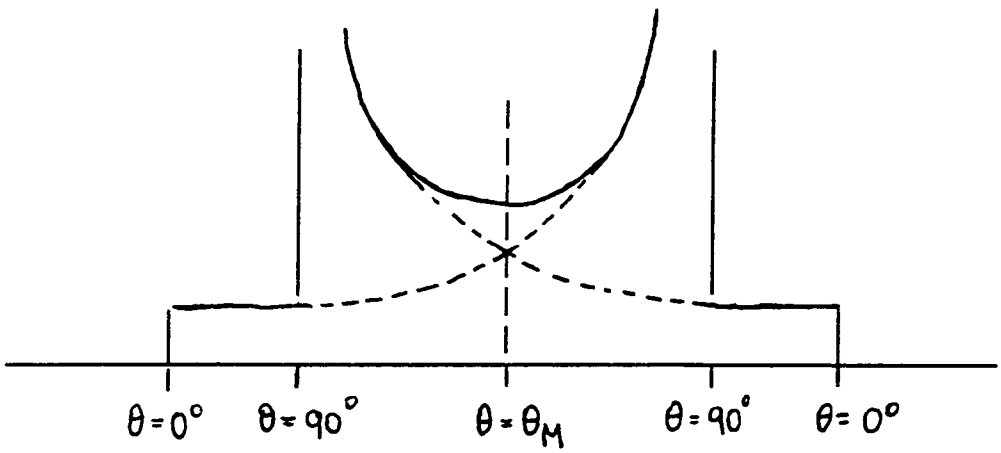

However there are only very few solids containing isolated two-spin systems. For the majority of solids there are long-distance interactions which cause a considerable broadening of the lines observed in the NMR-spectrum[2,3].

Shielding anisotropy

Shielding anisotropies are dependent on the orientation of the solid in the magnetic field. The shielding constant is a typical tensor with major contributions for the orientations characterised by the principal axes in a fixed molecule. The only case when the shielding is independent of the orientation is in the case of cubic local symmetry. The shielding constant σ_{ZZ}, observed in its dependency of θ_j, is described by[3]:

$$\sigma_{zz} = \sigma_{iso} + \frac{1}{3}\sum_{j=1}^{3}(3\cos^2\theta_j - 1)\sigma_{jj} \qquad [31]$$

σ_{jj} = principal component of the shielding
σ_{iso} = isotropic value of the shielding
θj = angle between principle axis and field

4.2 MAS (magic-angle spinning)

Dipolar coupling as well as shielding anisotropy can cause a substantial broadening of the lines in the NMR spectrum.

If the sample rotates with an angle of 54.7°, called the magic angle, in the magnetic field both dipolar interactions and shielding anisotropy can be eliminated[2,3].

$$(3\cos^2(54.7^\circ) - 1) = 0 \qquad [32]$$

The rotation frequency, however, determines the degree of elimination of the two effects. The frequency of rotation needed to eliminate the shielding anisotropy has to exceed the value of the shielding anisotropy in Hz. The rate of rotation required to eliminate the dipolar interactions must be bigger than the dipolar interaction in Hz. Frequently the frequency of rotation that can be achieved suffices to fulfil the first condition but not the second condition. The remaining effect of heteronuclear dipolar coupling can be eliminated by high-power proton decoupling[3].

4.3 CP (Cross-polarisation)

By using the method of cross-polarisation a problem can be solved which occurs with the acquisition of solid-state NMR spectra. Spin-lattice relaxation times in solids can be extremely long. Thus the accumulation of spectra requires a long time. The procedure of cross-polarisation transfers magnetisation from the ^{1}H-spins to the ^{29}Si spins using the pulse-sequence given in figure 2-7:

Figure 2-7

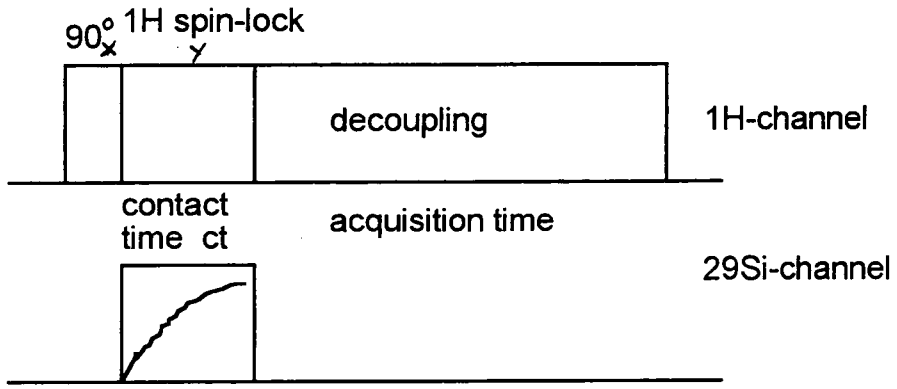

The first step is a 90°-pulse in the x-direction in the proton channel. This is followed by a spin-lock of the proton-magnetisation in the y-direction of the rotating frame and the simultaneous switching on of the radio frequency in the ^{29}Si channel. The amplitude of the radio frequency field B_{1Si} is chosen in order to match the amplitude of the B_{1H}-field according to the Hartmann-Hahn condition[14].

$$\gamma_{1H} B_{1H} = \gamma_{29Si} B_{29Si} \qquad [33]$$

This condition implies that proton- and silicon nuclei precess at equal rates so that a rapid transfer of magnetisation (i.e. spin-energy) can take place. The pulse-sequence includes high-power decoupling of the protons during the acquisition of the FID. In comparison to the magnetisation of the ^{29}Si-spins in equilibrium, the magnetisation of the ^{29}Si-spins after the energy transfer according to the Hartmann-Hahn condition is a factor of γ_H/γ_{Si} stronger. Another considerable advantage of this sequence is that the time required to get back to equilibrium after the thermal contact with the ^1H-spin-system is $5*T1_H$ instead of $5*T1_{Si}$[15].

2. THEORY

B Application of NMR to characterise silicate solutions

1. Nomenclature

1.1 Nomenclature of Silicon Sites

In this work the commonly used Q^ny-notation, according to Engelhardt, is adopted in order to describe the structure of building units in silicate solutions and silicate gels[16,17,18] (figure 2-8). A silicon atom bonded to four oxygen atoms is represented by Q. The superscript n denotes the number of other Q-units attached to the SiO_4-tetrahedron, i.e. the connectivity. The subscript y is the number of units of same connectivity in a silicate anion.

Figure 2-8

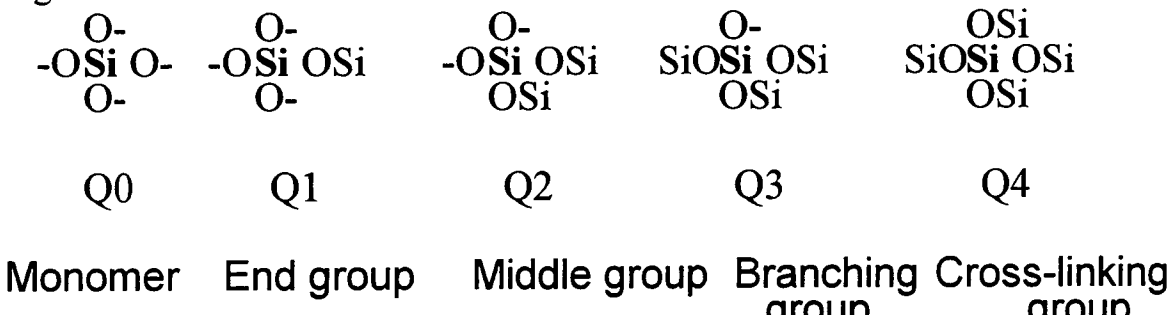

1.2 Nomenclature of silicate solutions

The nomenclature which is commonly used to characterise industrial silicate solutions is adopted here. The concentration of silica is reported in terms of weight percent fumed silica (see chapter 3-4.1.1) per total weight of the solution (wt% SiO_2). The composition of the silicate solution with respect to SiO_2 and M_2O (M=alkali metal) is reported in molar ratio of SiO_2 to M_2O (Rm-value). Values from cited literature are calculated into these units when possible.

2. NMR of silicate solutions

Silicate solutions have been analysed with a range of different methods[19-26]. The advantage of the NMR method in contrast to chemical methods is that information can be obtained without affecting the speciation in the silicate solution. The advantage of the NMR method in contrast to other spectroscopic methods is that it is extremely versatile and just by varying the sequence and duration of pulses a wealth of information can be obtained.

2.1 Chemical shifts of structural units

The first published ^{29}Si-NMR spectrum of a silicate solution was acquired in 1973 by Marsmann[27].

In the ^{29}Si-NMR silicate spectra five separable subdivisions of chemical shift regions can be observed[18]. On the high-frequency side of the NMR spectrum, at about -70 ppm from the signal of TMS, the resonance of the monomeric silicate anion is found. The more condensed the silicate unit is the lower is the frequency at which its signal is found. This occurs because the shielding of the silicon atom in the silicate unit increases with increasing degree of polymerisation. Figure 2-9 shows the regions where the main silicate resonances are found on the NMR scale[16]. The resonances of the main silicate structural units are approximately 10ppm apart[16,29].

Figure 2-9

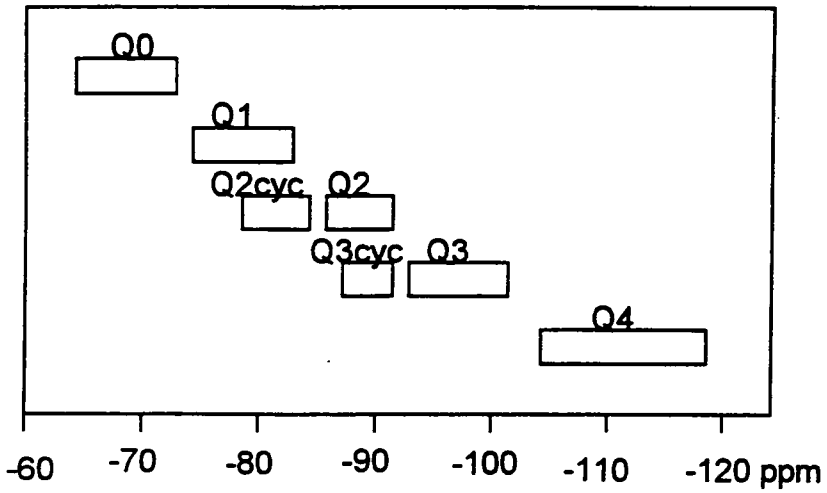

The resonances of Q^n-silicon sites in small rings (Q^ny) are shifted to higher frequency compared to the corresponding Q^n-silicon sites which do not form rings[28]. This is due to the longer Si-O bonds and smaller Si-O-Si bond angles found in ring structures causing less-efficient Si-O σ- and π-orbital overlapping and hence decreasing the shielding[29]. An apparent increase of linewidth with increasing connectivity of the silicon site makes it impossible to deduce any information on individual silicate anions for highly condensed solutions as the observed resonances involve overlapping of resonance lines of similar Si-environments in different species[16].

structural unit	number of different possible arrangements	
Q0	0	statistical combinations
Q1	4	"
Q2	10	"
Q3	20	"
Q4	35	"

Literature:

1 R. K. Harris, B. E. Mann, NMR and the Periodic Table, Academic Press, London, New York (1978)

2 E. Fukushima, S. B. W. Roeder, Experimental Pulse NMR, Addison-Wesley Publishing Company, London (1981)

3 R. K. Harris, Nuclear Magnetic Resonance Spectroscopy, Longman Scientific & Technical, New York (1986)

4 I. Ando, G. A. Webb, Theory of NMR Parameters, Academic Press, London, New York (1983)

5 A. Abragam, The Principles of Nuclear Magnetism, Oxford University Press, London, Glasgow (1961)

6 R. G. Kidd in: NMR of Newly Accessible Nuclei, P. Laszlo (Ed.), Vol.1 Academic Press, London, New York (1983)

7 J. Reisse in: The Multinuclear Approach to NMR Spectroscopy, J. B. Lambert, F. G. Riddel (Ed.), D. Reidel Publishing Company, Dordrect, Boston (1982)

8 T. C. Farrar, E. Becker, Pulse and Fourier Transform NMR, Academic Press, New York (1971)

9 J. H. Noggle, R. E. Schirmer, The Nuclear Overhauser Effect, Academic Press, London, New York (1971)

10 J. McConnell, The Theory of Nuclear Magnetic Relaxation in Liquids, Cambridge University Press, Cambridge, New York (1987)

11 G. A. Webb in: Annual Reports on NMR Spectroscopy, E. F. Mooney (Ed.), Vol.6A, Academic Press, London, New York (1975)

12 B. C. Gerstein, C. . Dybowski, Transient Techniques in NMR of Solids, Academic Press, London, New York (1985)

13 C. Brevard, P. Granger, Handbook of High Resolution Multinuclear NMR, John Wiley & Sons, New York, Toronto (1981)

14 S. R. Hartmann, E. l. Hahn, Phys. Rev. **128** (1962)2042

15 C. A. Fyfe, Solid State NMR for Chemists, C. F. C. Press, Guelph/Ontario (1983)

16 G. Engelhardt, D. Michel, High Resolution Solid State NMR of Silicates and Zeolites, John Wiley & Sons, New York, Toronto (1987)

17 G. Engelhardt, D. Zeigin, H. Jancke, D. Hoebbel, W. Wieker, Z. Anorg. Allg. Chem. **418** (1975) 17

18 G. Engelhardt, H. Jancke, D. Hoebbel, W. Wieker, Z. Chem. **14** (1974) 109

19 R. W. Harmann, J. Phys. Chem. **32** (1928) 44

20 D. Hoebbel, W. Wieker, Z. Anorg. Allg. Chem. **405** (1974) 267

21 L. S. Dent-Glasser, E. E. Lachowski, J. Chem. Soc. Dalton (1980) 393

22 L. S. Dent-Glasser, E. E. Lachowski, J. Chem. Soc. Dalton (1980) 399

23 J. D. H. Strickland, J. Am. Chem. Soc. **74** (1952) 862

24 G. B. Alexander, R. K. Iler, J. Phys. Chem. **57** (1953) 932

25 P. K. Duta, D. C. Shieh, Applied Spectroscopy **39** (1985) 343

26 A. Ja'nosi, O. Kratky, O. Sekora, Monatsh. Chem. **100** (1969)1973

27 H. C. Marsmann, Chem. Zeitung **97** (19773) 128

28 R. K. Harris, R. H. Newman, J. Chem. Soc. Faraday Trans. II **73** (1977) 1204

29 S. D. Kinrade, T. W. Swaddle, Inorg. Chem. **27** (1988) 4253

30 M. L. Martin, G. J. Martin, J-J. Delpuech, Practical NMR Spectroscopy, Heyden, London, Philadelpia (1980)

31 D. Neuhaus, M. Williamson, The Nuclear Overhauser Effect in Structural and Conformational Analysis, VCH, Weinheim, Cambridge (1989)

32 J. Mason (Ed.), Multinuclear NMR, Plenum Press, New York, London (1987)

33 J. Schraml, J. M. Bellama in: Determination of Organic Structures by Physical methods, F. C. Nachod, J. J. Zuckerman, E. W. Randall (Eds.), Vol.6, Ch.4, Academic Press, New York, London, San Francisco (1976)

3. Experimental

1. NMR-spectrometers

The experiments were carried out on six different NMR-spectrometers, three of which are solid-state machines.

T1-experiments were carried out on a BRUKER AC250 spectrometer with an operating field of 5.9 Tesla, a BRUKER AMX500 machine working at a field of 11.7 Tesla (both located in Durham) and a VARIAN VXR600 machine operating at 14.1 Tesla (located in Edinburgh). All these machines are solution-state spectrometers.

The majority of ^{29}Si silicate spectra were recorded on the BRUKER AMX500. Additionally, for a considerable number of ^{29}Si-spectra a VARIAN VXR300 operating at a field of 7.5 Tesla or a BRUKER CXP200 instrument operating at 4.7 Tesla were used. The latter two instruments are solid-state spectrometers with MAS probes. Spectra acquired on the VARIAN VXR300 were referenced to external Tetrakis-trimethylsilyl methane (δ=0.0ppm), whereas on the BRUKER CXP200 external silicon-gum (δ=22.06ppm) was used for referencing.

Proton and sodium spectra were recorded using the BRUKER CXP200, both static and with MAS.

Proton T2 as well as ^{29}Si, ^{1}H and ^{23}Na diffusion-constant measurements were carried out on a BRUKER MSL300 spectrometer working at a field of 7.5 Tesla (located at UNILEVER RESEARCH, Port Sunlight).

For all solution-state measurements 10mm tubes have been used with Teflon inserts to prevent interaction of the silicate solution with the glass of the tube.

2. Pulse sequences

2.1 Single pulse

For the acquisition of most of the solution-state spectra the technique of inverse gated decoupling has been used. The pulse sequence is given in figure 3-1.

Figure 3-1

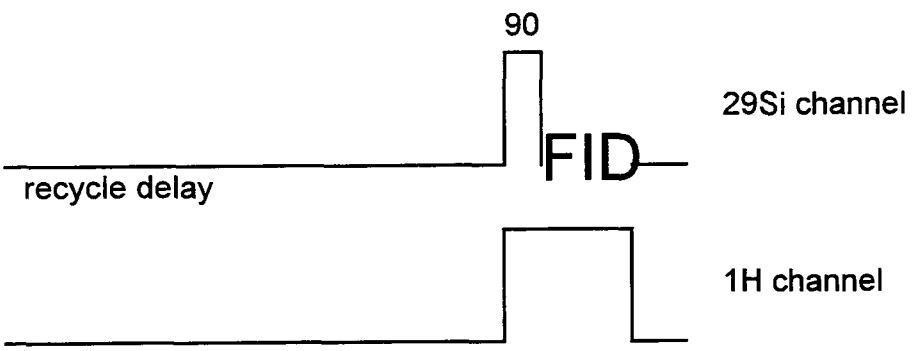

This technique assures that full $^{29}Si\{1H\}$ decoupling is applied without affecting the intensities of the resonances by the NOE-factor. This is achieved by gating the decoupler with the transmitter and receiver, and switching it off during the relaxation delay[1]. However, care has to be taken that the recycle delay is at least 10 times as large as the acquisition time[2]. In the systems investigated the acquisition times are about a factor of 100 shorter than the longest relaxation time. Therefore a recycle delay of 5*T1 is appropriate to eliminate any effects of the NOE on the signal intensities and to ensure that relative intensities within a given spectrum are accurate.

The acquisition time was chosen to be about 1.5 times as long as the length of the FID. All spectra were zero-filled[3] so that the number of

transformed points was twice or four times as large as the number of acquired data points.

The D_2O signal served as a field/frequency lock. For silicate solution-state spectra no suitable internal reference which is not interacting with the silicate structures could be found. The monomer provides a more convenient than accurate reference as its chemical shift is dependent on the composition of the silicate system and is especially varying with the pH[4,5,6]. Thus an external reference has to be taken, which was HMDSO (hexamethyldisiloxane), with δ=6.53ppm.

A baseline correction was carried out for every spectrum prior to the integration of the signals. The errors in the speciation percentages, derived from the integrated intensities, are likely to be in the region of 5-10% of the reported values. Intensity data (integrals) are averages from three to four measurements.

2.2 T1

The spin-lattice relaxation times in the silicate solutions were measured by the inversion-recovery method[7]. The pulse-sequence is shown in figure 3-2:

Figure 3-2:

$$\left[-T_D - 180\,^{o}{}_{x} - vd - 90\,^{o}{}_{x} - FID -\right]_{NS}$$

T_D is the relaxation delay (5 times as long as the longest T1), the $180^{o}{}_{x}$-pulse inverts the magnetisation, and vd is the variable delay-time applied before the $90^{o}{}_{x}$ observe pulse, after which the FID is acquired.

The majority of T1-measurements were carried out on the BRUKER AMX500. Measurements of all ^{29}Si spectra on solution-state spectrometers show a background signal from glass inserts in the probe and the glass of the

sample-tube (see section 3.1). This background signal was subtracted by hand for every single spectrum in an inversion-recovery sequence before calculating the T1-values. For this purpose a T1-experiment with a blank has to be carried out under the same conditions as the silicate T1-measurement. Errors on the values of T1 are estimated to be in the region of 8-9%.

2.3 T2

T2-values have been measured with a pulse program for a Hahn-echo as well as with a custom-written CPMG-sequence. The Hahn-echo pulse sequence[16] shown in figure 3-3 should be used only in the case of systems with no chemical exchange, since the intensities of resonances in the spectra with long variable delays may be decreased not only by T2-effects but by exchange.

Figure 3-3

$$\left[-T_D - 90^\circ_x - (vd)_n - 180^\circ_y - (vd)_n - FID\right]_{NS} \quad n=0,1,2,3,.....$$

In the case of chemical exchange, the CPMG-sequence[10] shown in figure 3-4 is of advantage as the value of the delay stays constant and only the number of 180°y-pulses is increased.

Figure 3-4

$$\left[-T_D - 90^\circ_x - (vd - 180^\circ_y - vd)_n - FID\right]_{NS} \quad n=1,2,3,.....$$

It was found that when the Hahn-echo experiment was used, deviations in the logarithmic fit occur which are typical for chemical exchange between silicate units (see chapter 6-4.1). Thus for measurements of the T2-values the CPMG-sequence was employed.

2.4 Exchange spectroscopy (EXSY)

The effect of gradual collapse and subsequent exchange narrowing of resonant lines separated by the interval 2A about a centre frequency ω_o takes place when the exchange rate ω_{ex} increases beyond $\omega_{ex}/A = 1$.

In systems where the exchange at room temperature is not fast enough to produce the phenomenon of collapsing lines and the temperature cannot be drastically increased to produce faster exchange, the exchange between different structures can be monitored by means of 2D-exchange spectra[11]. In these experiments it is necessary to not only carefully estimate the required mixing time but also the relaxation rate, since the longitudinal relaxation components which exchange relax at the same time. In extremely simple systems the constant of exchange can be calculated from the ratio of cross-peak and diagonal peak intensities. In more complicated systems where several exchange mechanisms or whole exchange networks exist it becomes necessary to run a series of 2D exchange spectra with varying mixing time. This in effect represents a change from a 2D to a 3D experiment[9].

The following pulse-sequence was used:

Figure 3-5

$$[T_d - 90^\circ{}_x - t_1 - 90^\circ{}_x - t_M - 90^\circ{}_x - FID]_{NS}$$

The first $90^\circ{}_x$-pulse creates the transverse magnetisation, with the magnetisation vectors belonging to the silicon groups rotating with different frequencies in the x',y'-plane. During the evolution period characterised by t_1 these magnetisations travel different angles. The second $90^\circ{}_x$-pulse selects the y'-components of the precessing magnetisations and rotates them into the direction of the z-axis. The non-equivalent groups of spins are partially

exchanged and take with them their respective z-magnetisation components. Magnetisation transfer by this mechanism requires a period of time referred to as the mixing time, t_M, which has to be selected so that the maximum amount of exchange takes place. The mixing time for the maximum exchange is comparable to the reciprocal rate of exchange. After the exchange a third 90^o_x-pulse rotates the z-axis components into the x',y'-plane for detection. Diagonal peaks identify individual groups, whereas cross-peaks indicate the exchange process which during the mixing time has transferred magnetisation of frequency ω_1 to a frequency ω_2[3,9]. Chemical exchange that is detected by 2D-exchange spectroscopy is not in the fast exchange region and an upper limit can be determined taking the chemical shift differences into account. The lower region of the exchange rate is limited by longitudinal relaxation. If the exchange is much slower than 1/T1 the frequency-labelled z-magnetisation will disappear before the magnetisation exchange. For exchange at rate k between equally populated sites the optimum mixing time is 0.5/k for k in the region of 1/T1 and 1.5/k for k in the region of 10/T1[9].

2.5 INADEQUATE

2D INADEQUATE spectra show the ^{29}Si-^{29}Si couplings. They identify two coupled nuclei not by their coupling constant but by the frequency of their double-quantum coherence[1,3,9]. With a natural abundance silicate this experiment would take an unreasonably long time. Thus this experiment was performed with a silicate solution enriched in ^{29}Si. The 2D INADEQUATE experiments in the present work were carried out with a conventional sequence shown in figure 3-6, where the value of d4 is chosen to maximise the connectivities for a particular J-coupling value[9,32]. This sequence works in four major steps. During the preparation time double-quantum coherence is created, which is allowed to evolve during an incremented delay, vd, during the evolution period. After this the result is converted into observable

magnetisation by a mixing pulse. The last step is the acquisition of the FID. A double fourier transformation is carried out on the resulting set of FIDs. The delay, d4, for weakly coupled spins is given as

$$d4 = \frac{2n + 1}{4 J_{AX}}$$

in order to maximum coherence transfer. Usually the value of n is chosen to be zero[33]. Typical values for the scalar coupling between silicon in siloxy systems are 2J(Si-O-Si) of 1 to 1.5 Hz[35]. Therefore the value of the fixed delay d4 is chosen to be 20ms in order to get optimum double quantum coherence. This matches the value for d4 which was chosen as found by Fyfe et al. for optimum double-quantum coherence[34].

Figure 3-6

$$\left[T_d - 90^\circ_x - d4 - 180^\circ_{\pm y} - d4 - 90^\circ_x - vd - 120^\circ - FID\right]_{NS}$$

$d4 = (4J)^{-1} = 20$ ms

2.6 Self-diffusion constant measurement

The attenuation of the spin-echo which arises from diffusive dephasing under the influence of a steady gradient can be used to determine molecular self-diffusion. The gradient is applied in the form of rectangular pulses inserted in the dephasing and rephasing parts of the echo sequence and gated off during r.f. pulse transmission and signal detection.

The pulsed-gradient spin-echo sequence (PGSE) which was first used by Stejskal and Tanner[12,13,14] is given in figure 3-7 below:

Figure 3-7

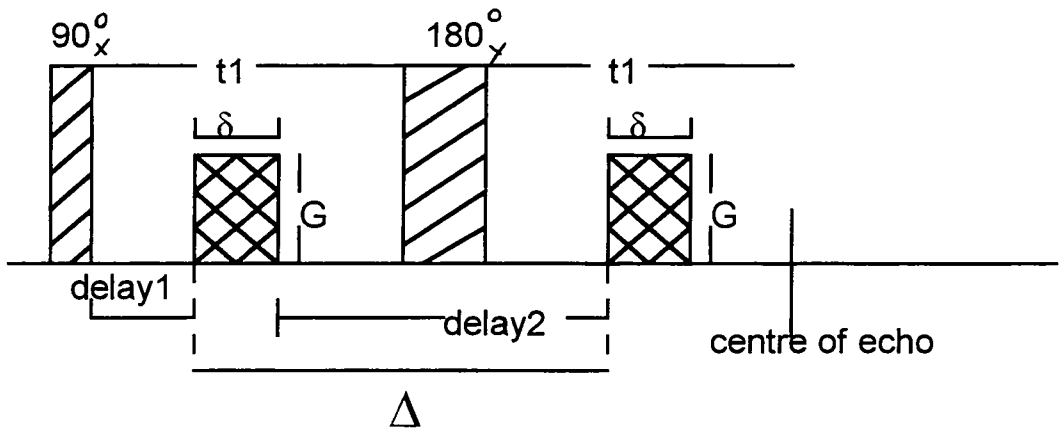

δ : is the pulse gradient duration which is the parameter varied for each experiment

delay2 : is the delay which has to be varied accordingly to δ so that Δ stays constant

$$\delta = \Delta - \text{delay2} \qquad [1]$$

Δ : remains constant (50ms or 25ms)

G : is the gradient strength which stays fixed during the experiment and is measured in arbitrary units

The measurement of the self-diffusion coefficient by PGSE NMR is limited by the loss of phase coherence due to transverse relaxation. The spacing between the 90°x and the 180°y-pulse is limited by the T2-process, which in turn limits the field-gradient pulse duration δ so that in the case of short T2-values and slow self-diffusion the classical PGSE cannot be applicable[15].

A method of avoiding this problem is to store the transverse magnetisation existing at some point of time t1 for later recall to see how far the molecules have moved. This is done by applying a single 90°x-pulse a time t1 after the first 90°x-pulse, which has the effect of rotating the y-component of

the magnetisation into longitudinal polarisation where only T1-relaxation will occur. Any x-magnetisation will be unaffected by the second pulse so that part of the transverse magnetisation is lost during this storage. The magnetisation is recalled after a time t2 using another 90^{o}x-pulse, which leads to an echo a time t1 after the pulse. This echo, which occurs at an interval after the third pulse equal to that between the first two 90^{o}x-pulses, has been named by Hahn the stimulated echo[16]. He showed that the relaxation attenuation of this echo has a T1-dependence during the interval between the second and the third pulse which is not a problem, however, in the experiments described in this thesis. The pulse sequence for such a stimulated echo is shown in figure 3-8.

Figure 3-8

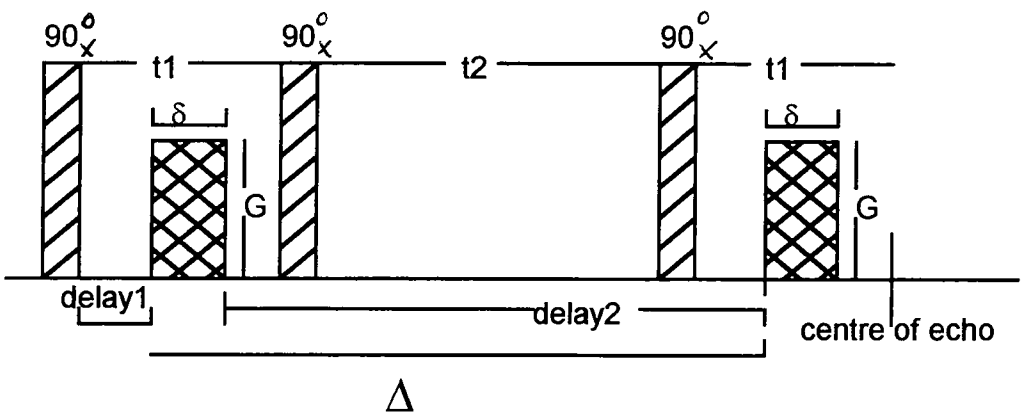

In the presence of a *steady* gradient G_0 the expressions for the stimulated echo show a dependency on the delay between the 90^{o}-pulse and the start of the first gradient and on the delay between the end of the second gradient pulse and the centre of the echo[17]. Therefore the equations for the two types of PFG sequences are different due to the term G_0. This however is only of importance in poorly-shimmed systems whereas in modern well-

constructed systems any residual gradients are eliminated and terms involving G_o can be neglected.

The general expression for the attenuation of the spin-echo amplitude with time, taking into account the T2-relaxation and the self-diffusion under the influence of a magnetic field gradient, is for the normal and the stimulated echo[8,12,15]:

$$A = A_0 \exp\left[\left(\frac{-2\tau}{T2}\right) - \gamma^2 D \delta^2 G^2 \left(\frac{\Delta - \delta}{3}\right)\right] \qquad [2]$$

τ : is the radio-frequency pulse separation (90^o - τ - 180^o)

D : is the self-diffusion coefficient

The contributions to the signal attenuation from the T2-process and the diffusion process can be isolated by recording the spin-echo sequence with and without applying a pulsed field-gradient (PFG). Taking the ratio of these two experiments for every field-gradient pulse gives:

$$A' = \frac{A_{PFG\,(on)}}{A_{PFG\,(off)}} \qquad [3]$$

$$A' = \exp\left[-\gamma^2 D \delta^2 G^2 \left(\frac{\Delta - \delta}{3}\right)\right] \qquad [4]$$

The achieved attenuation A' is measured against a reference of known D for every sample while keeping the PFG-current constant. Since a silicon reference cannot be used because of the low sensitivity of ^{29}Si, water was chosen as the reference.

A semilogarithmic plot of A' versus $\delta^2(\Delta-\delta/3)$ yields a slope, S, which can be correlated to the slope of the water diffusion experiment under equal conditions and the known diffusion constant of water[19].

$$\frac{D_{sample}}{D_{reference}} = \frac{S_{sample}}{S_{reference}} \qquad [5]$$

$D_{reference} = D_{water} = 2.3*10^{-5}cm^2s^{-1}$ at 27°C [20]

All self-diffusion experiments were carried out on a Bruker MSL300 equipped with a custom-built probehead containing anti-Helmholz coils for applying linear field gradients (no residual gradients G_0) in the B_0-direction.

3. Background

3.1 Background subtraction

All ^{29}Si silicate spectra recorded on a solution-state machine show a background signal from the glass of the NMR tube and of glass inserts in the probe, the latter contributing 79% of the background signal.

Figure 3-9 illustrates where glass in a typical solution-state probe is located.

Figure 3-9

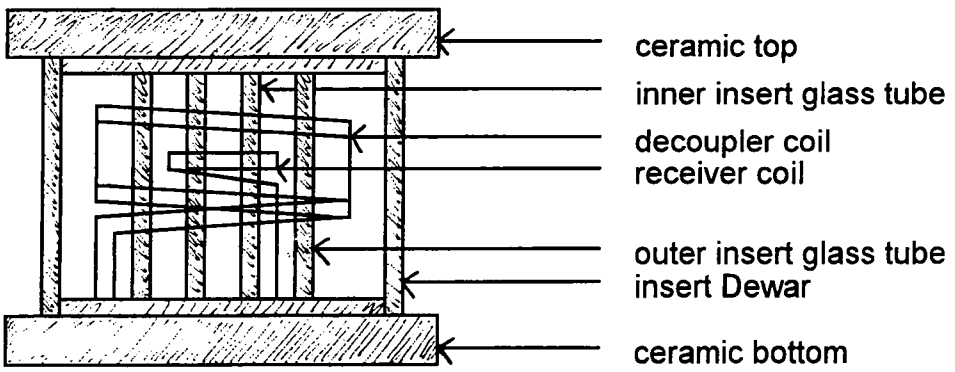

Therefore the method of background subtraction, which has already been successfully used[21,22], was employed (Fig. 3-10 illustrates its effectiveness). This method implies the acquisition of the FID of a blank with

the same pH as the relevant sample with every spectrum and its subtraction from the FID of the silicate. This means that the time involved to obtain a ^{29}Si NMR spectrum is doubled. Additionally there is a $(2)^{1/2}$ increase in the noise of the spectrum after subtraction of the background.

In these investigations it was proved that the method of background subtraction can be used with sufficient accuracy[22] by a comparison of subtracted spectra recorded on a solution-state instrument with spectra recorded using the VXR300 spectrometer with a Doty probe which does not contain glass. ^{29}Si NMR spectra acquired on both spectrometers are shown in figure 3-11. The deviation between these spectra over all structural units is 4.5%. This is negligible if it is considered that the general error in speciation percentages is likely to be in the region of 5-10%.

Figure 3-10

^{29}Si NMR-spectra of a sodium silicate solution with 30wt% SiO_2 and Rm=2.6

a) with background

b) with background subtraction

c) ^{29}Si NMR-spectrum of probe and tube background

a) to c) acquired on the Bruker AMX500 with 160 transients, acquisition time 0.06s, spectral width 200ppm, relaxation delay 80s

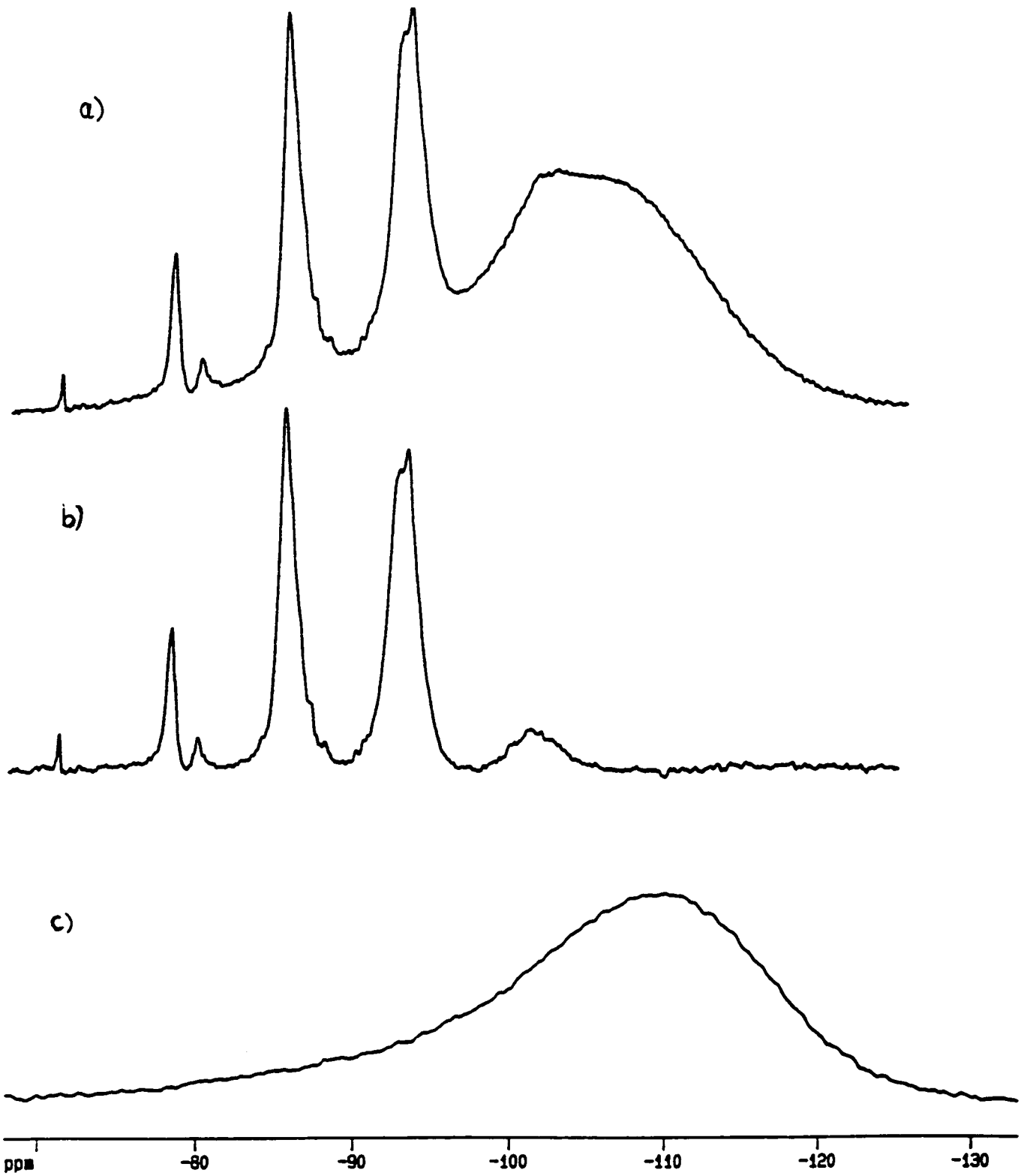

Figure 3-11

^{29}Si NMR-spectra of a sodium silicate solution with 30wt% SiO_2 and Rm=2.6

a) with background subtraction (acquired on a solution-state machine)

b) without background (acquired on a solid-state machine)

a) acquired on the Bruker AMX500 with 160 transients, acquisition time 0.06s, spectral width 200ppm, relaxation delay 80s

b) acquired on the Varian VXR300 with 1060 transients, acquisition time 0.06s, spectral width 300ppm, relaxation delay 80s

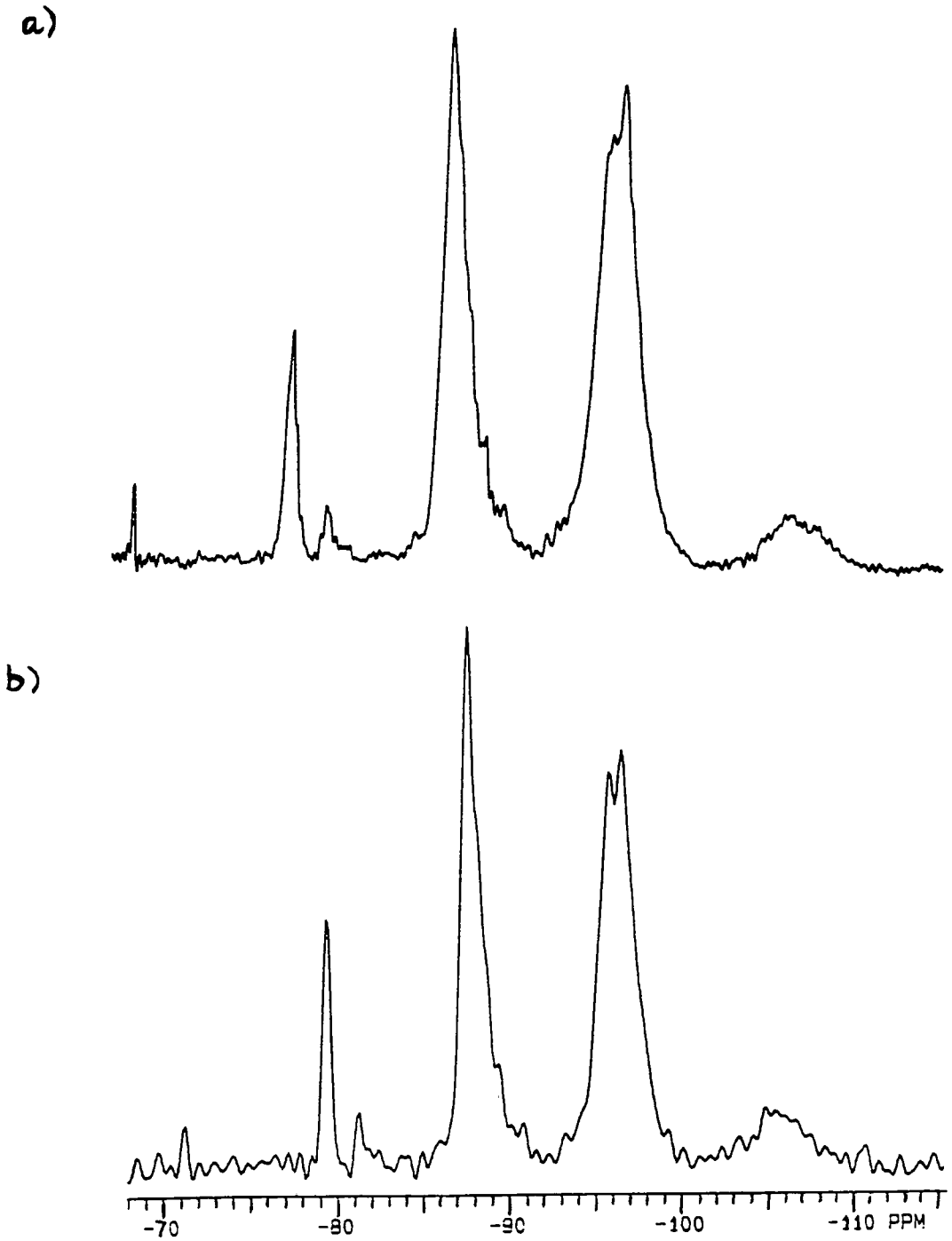

3.2 A pulse sequence to eliminate the background in T1- and T2-experiments

A pulse-sequence was found which eliminates the 29-Si background from the probe and the sample tube by making use of their short T2 and the fact that they are not in the homogeneous region of the field. In a single-pulse spectrum this was achieved by using an extra 180-degree pulse which is 90-degree phase-shifted with respect to the other pulses. Figure 3-13 illustrates the success of this method.

Figure 3-12

$[T_D - 90^o x - d2 - 180^o y - d2 - FID]_{NS}$

The results, of course, are influenced by the T2-decay of the signals so this cannot be the method of choice for acquiring single-pulse spectra.
The minimum d2-delay which can be used for effective elimination of the background is 9ms.

Figure 3-13

^{29}Si NMR-spectra of a sodium silicate solution with 30wt% SiO_2 and Rm=2.6

a) with a single pulse sequence (section 2.1)

b) with background-elimination using the sequence given in figure 3-12

a) and b) acquired on the Bruker AMX500 with 160 transients, acquisition time 0.06s, spectral width 200ppm, relaxation delay 80s

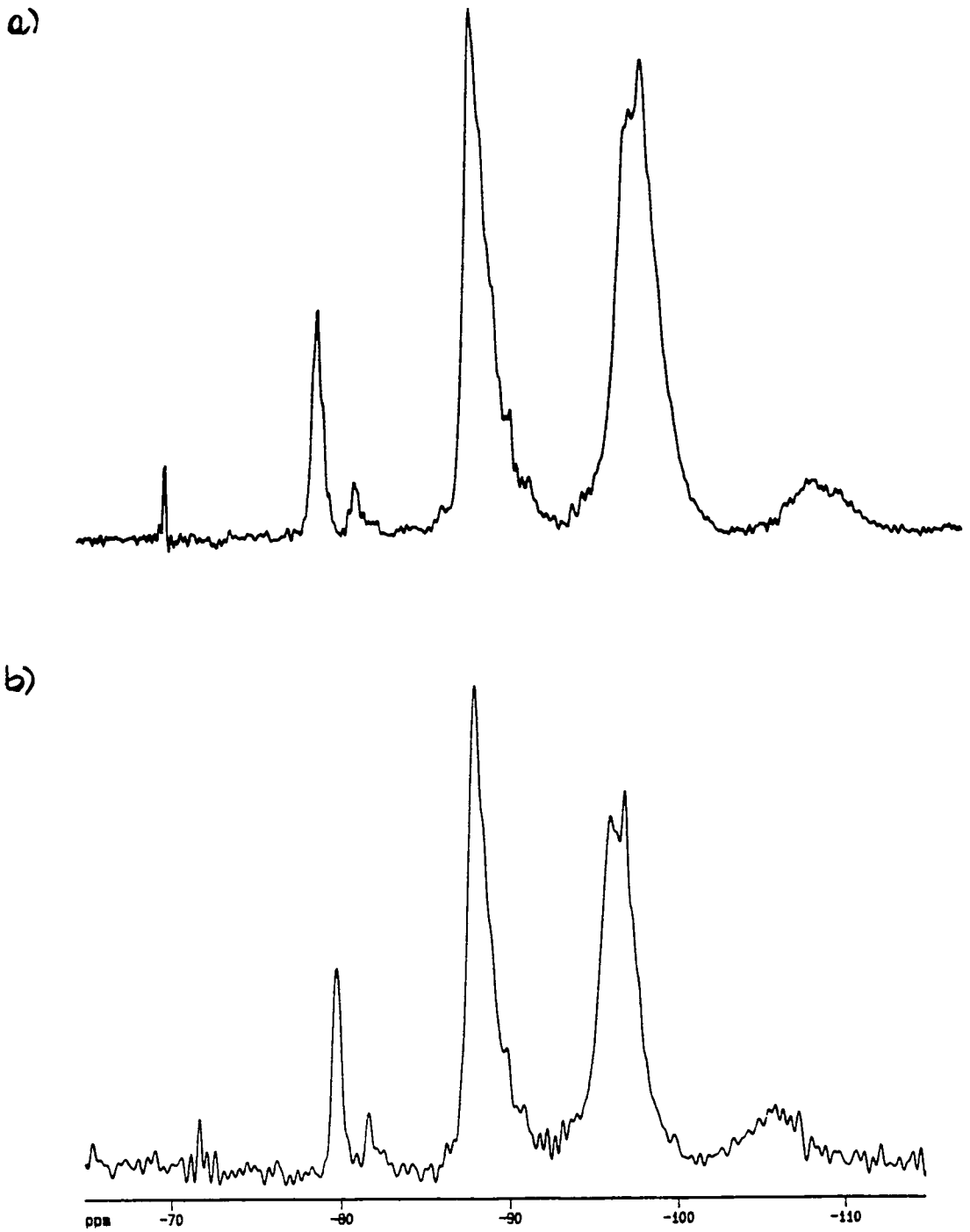

T1-measurements with inversion recovery

In T1-experiments the method of applying an extra 180°y-pulse which is 90° phase-shifted with respect to the 180° and 90° pulses can be successfully employed to eliminate the background for every vd-delay as illustrated in figure 3-14. The sequence shown in figure 3-15 can only be successfully used if the ^{29}Si T2-values are long enough to provide sufficient signal intensity for the T1-experiment. The attenuation of the signal due to the T2-decay during d2 is the same for all vd-values.

Figure 3-15

$$[\ T_D - 180^{o}x - vd - 90^{o}x - d2 - 180^{o}y - d2 - FID]_{NS}$$

Table 3-1
T1-values, given in s, for a :
sodium silicate solution 30wt%SiO2, Rm=2.6 + laurylether

	without background-subtraction	with manual background-subtraction	with "echo" background-elimination
Q0	4.0	7.0	7.2
Q1	5.2	8.2	8.5
Q2cyc	4.3	8.0	8.2
Q2	6.5	8.9	8.6
Q3	7.6	9.5	9.8
Q4	15.2	14.4	13.7

d2=10ms

Table 3-1 shows that the calculation of spin-lattice relaxation times from the spectra in an inversion-recovery sequence without background subtraction is not accurate compared to those obtained with background elimination. It demonstrates that the method of manual background subtraction described in section 2.2 can be used with sufficient accuracy. However the method of background-elimination is the method of choice as it is much less time consuming than a manual subtraction of the glass background. Values of T1 are estimated to be accurate to *ca.* 8%.

Figure 3-14
^{29}Si T1-measurement
for a sodium silicate solution with 25wt% SiO_2 and Rm=4.0
on the Varian VXR600 with background elimination :
relaxation delay 100s, acquisition time 0.05s, 16 transients, d2=11ms

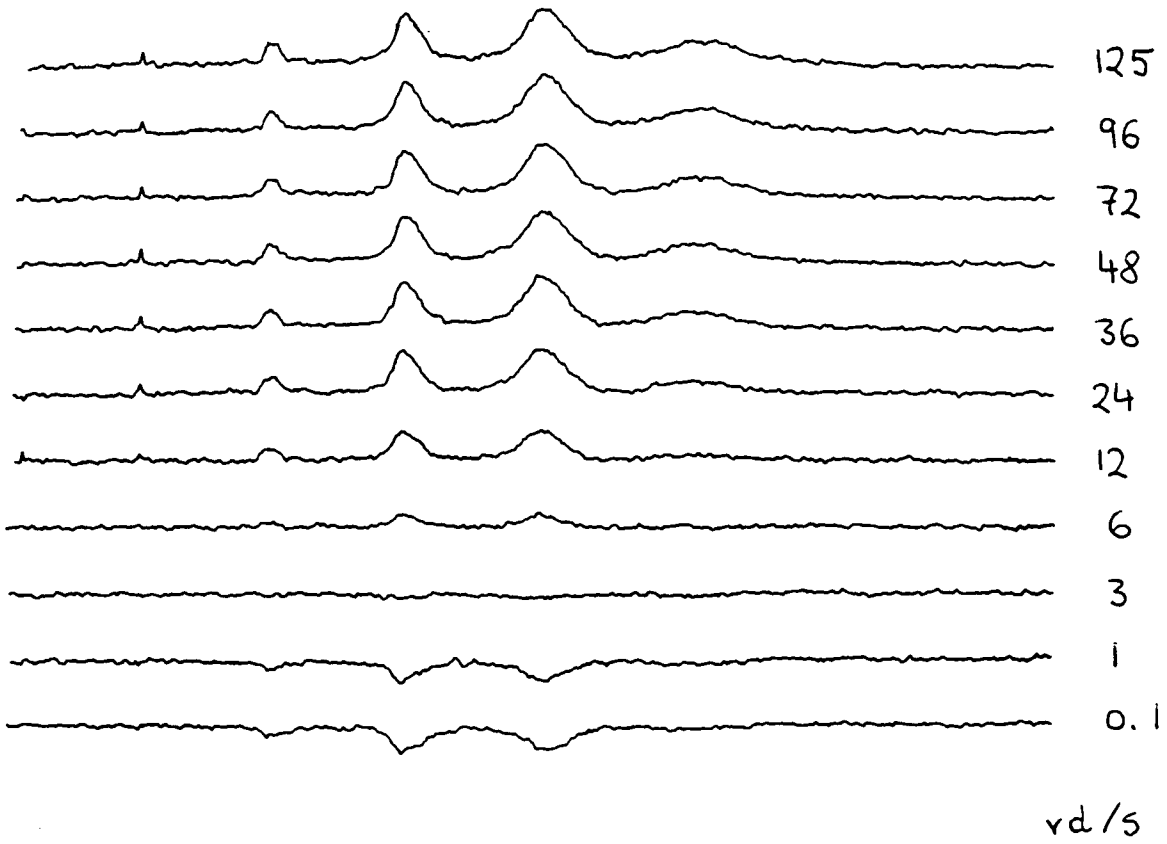

T2-measurements

In T2-experiments carried out with the Hahn-echo sequence the delay d2 of 10ms is added to each vd-value. Therefore this way of eliminating the background only works if the respective T2-values are sufficiently long. If the T2-values are very short, the signal will be fully attenuated within a time of the order of 10ms. In the calculation of the T2-value this extra d2 added to the vd-value can be ignored as it is the same for all spectra in the Hahn-echo sequence and the resulting extra attenuation in the signal is identical for every change in the vd-value.

Figure 3-16

$$[\, T_D - 90^0x - d2 - vd - 180^0y - vd - d2 - FID]_{NS}$$

Table 3-2
T2-values, given in s, for a sodium silicate solution :
32wt%SiO2, Rm=2.0

	with background-subtraction	with background-elimination d2=10ms
Q0	0.23	0.34
Q1	0.13	0.23
Q2cyc	0.12	0.18
Q2	0.09	0.18
Q3	0.07	0.13
Q4	-	-

Table 3-2 compares the spin-spin relaxation times calculated from ^{29}Si spectra in the echo sequence with background elimination with those obtained with manual background-subtraction.

3.3 The silicon-free probe

In January 1993 the specially-built silicon-free 10mm probe (built by Bruker) arrived and went into use. This probe's outstanding feature is that 29-Si spectra can be acquired without any background signal from glass inserts in the probe. This renders the application of the method of background-subtraction unnecessary and thus makes the acquisition of silicate spectra a more precise and less time-consuming process.

The maximum resolution for this probe, established for TMS in $CDCl_3$ is good : linewidth at half height of 0.4Hz on Si-29.

A special sample set-up (demonstrated in figure 3-17) had to be used to completely eliminate the silicon background as otherwise the background of the sample tube would still remain. Every sample was measured in an insert made of Teflon FEP^R which was placed in a NMR glass tube. This sample-tube was cut off at the bottom so that only the Teflon-insert with the silicate solution was in-between the coils.

Figure 3-17

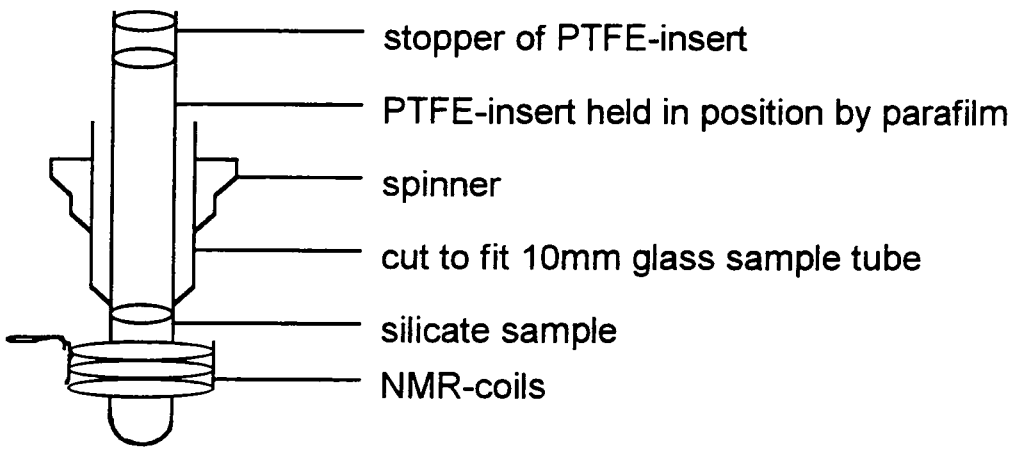

The quantitative comparison of signal intensities for the silicon-free probe (narrowband probe) and a 10mm broadband probe used for Si-29

acquisitions previously show that the signals are slightly more intense for the narrowband probe (see tables 3-3 and 3-4 below). The structural distributions of all spectra recorded on the Bruker AMX500 with the 10mm broadband probe were double-checked using the silicon-free probe.

Table 3-3
Intensity in arbitrary units of the signal for neat TMS:

intensity	**10mm broadband probe**	**silicon-free probe**
	9.1	10.0

Table 3-4
Intensities in arbitrary units of the silicate signals for a sodium silicate solution with 25.5 wt% SiO_2 and Rm=3.8 :

intensity	**10mm broadband probe**	**silicon-free probe**
Q0	0.20 (-65%)	0.31
Q1	2.11 (-92%)	2.29
Q2	10.27 (-87%)	11.81
Q3	24.85 (-91%)	27.17
Q4	9.45 (-90%)	10.46

4. Silicate systems

4.1 Natural abundance silicate solutions (sols)

4.1.1 Preparation

All silicate solutions have been prepared by dissolving fumed silica (from the hydrolysis of distilled $SiCl_4$) in caustic soda solution at 70 to 80°C. The time for the dissolution of all the silica can be up to 6 weeks. The equilibrium in the distribution of structures is established after approximately 10 weeks (see section 4.1.2).

To assure maximum purity of the silicate samples sodium hydroxide pellets of high purity (AristaR-grade NaOH from BDH), distilled water and fumed silica were taken for the preparations. Fumed silica is obtained from the hydrolysis of distilled silicon tetrachloride with distilled water so that the content in impurities is kept to a minimum.

Great care has been taken to avoid contamination with atmospheric carbon dioxide (which would cause a decrease in the pH of the solution) and oxygen (which could act as a paramagnetic) as well as impurities which could possibly leak out of glass containers if in contact with the solution. Thus samples were prepared, stored and handled under a N_2-atmosphere using high-quality alkali-resistant polyethylene and polypropylene bottles.

To keep errors in the preparation to a minimum, sodium hydroxide solutions used for the preparation of silicate solutions were titrated with 1M HCl to establish the accurate concentrations. The water content of the fumed silica was investigated by heating to 100°C under slight vacuum for 12 hrs and weighing and was determined to be 1.4%. This was considered in the sample preparation.

4.1.2 Equilibration

The complete dissolution of the silica at elevated temperature (70°C to 80°C) takes up to 1 week in the case of a moderately alkaline silicate solution (32wt% SiO_2 and Rm=2.0) whereas it takes up to 10 weeks at temperatures of 70°C to 80°C in the case of the lowest alkalinity (highest Rm) which can be produced (25wt% SiO_2 and Rm=4.0). Nevertheless the distribution of structural units in the former solution changes at room temperature with time until after a period of 8 weeks it stays stable (see chapter 5.1.2) whereas the speciation of the latter solution at room temperature does not change with time after complete dissolution of the silica. Therefore it can be concluded that the

equilibration of sodium silicate solutions takes up to 8 to 10 weeks in the case of any silicate system.

4.2 Natural abundance silicate gels

4.2.1 Preparation

For the preparation of sodium silicate gels of a certain Rm the silicate solutions with the corresponding Rm were taken initially. These were heated to 80°C to 90°C in a water bath or an oven. The heated silicate solution was taken out of the water bath (or oven) and water in the form of water vapour was displaced using a stream of nitrogen gas over the solution. When the solution had reached room temperature the above procedure was repeated if the silicate was still fluid until it had reached the gel point so that actually the gel point was approached in very small steps. The new SiO_2 concentration was determined through weighing using the water loss to obtain the increase in the SiO_2 concentration.

4.3 Silicate solution enriched in ^{29}Si

4.3.1 Preparation

The natural abundance of the isotope ^{29}Si in silicon is 4.7%. For all experiments but especially for 2D-experiments it is of great advantage if the percentage of the isotope ^{29}Si can be increased.

97.29 mg of $^{29}SiO_2$ enriched in ^{29}Si to the 95.65 %-level were available. A representative silicate solution with a high degree of condensation (Rm=4.0) was prepared using exactly the same method described in section 4.1.1 of this chapter. However the difficulty with the silicate solution enriched in ^{29}Si is that the amount of silicate solution obtained from 97.29 mg of enriched silica is very small and the transfer from any container into the sample tube would cause an insupportable loss of sample. Thus the silicate

solution in this case was prepared directly in the 10 mm Teflon FEP-insert used for the NMR investigations.

The actual SiO_2-concentration was determined by employing the method of quantification[23] described in chaper 4. It was determined to be 25wt% SiO_2.

The distribution of structural units (see table 3-5 below) shows less Q4-units than were found in a sodium silicate solution of 24.3 wt% SiO_2 Rm=4.0 made with fumed silica. It has been reported that different sources of silica can be of paramount influence on the properties of the silicate sample[8]. Clearly fumed silica has undergone a different procedure from that of the silica enriched in ^{29}Si, which is assumed to be the reason for the difference in structuring.

As shown in table 3-6 the T1-values for the enriched silicate solution are shorter than the T1-values of a corresponding non-enriched silicate solution. This reinforces the conclusion that the source of the silica enriched in ^{29}Si is in fact different from that of the fumed silica.

The intensity of a spectrum of the silicate solution made with the ^{29}Si-enriched silica is in principle 20-times higher than the intensity of a corresponding silicate solution with natural-abundance silica for the same number of transients. Alternatively, the same signal-to-noise can be achieved in a time which is a factor of 400 lower for the enriched sample.

Table 3-5
Distribution of structural units:

structural unit	^{29}Si-enriched 25 wt% SiO_2 Rm=4.0 /%	non-enriched 25 wt% SiO_2 Rm=4.0 /%
Q0	0.2	0.7
Q1	2.8	3.3
Q2cyc	0.0	0.0
Q2	25.9	21.4
Q3	55.5	52.3
Q4	15.6	22.3

Table 3-6
T1-values:

structural unit	^{29}Si-enriched 25 wt% SiO_2 Rm=4.0 /%	non-enriched 25 wt% SiO_2 Rm=4.0 /%
Q0	5.2	8.4
Q1	5.8	8.8
Q2	6.0	8.5
Q3	7.0	10.2
Q4	12.1	18.5

4.3.2 Recovery of silica enriched in ^{29}Si

It is essential to recover as much enriched silica as possible from the silicate solutions. This is done by adding HCl to the point where the pH of the instability region is reached and silica precipitates out of the silicate solution, which is then evaporated to dryness. The residue which consists of NaCl and

silica is then put onto an extremely fine filter paper and water is passed over the silica salt mixture in order to wash the salt out (solubility of silica in cold water $0.1*10^{-3}$g/l at 25°C; solubility of NaCl in cold water 35.7g/l at 25°C[24]). The powder remaining on the filter paper is dried in an oven at 110°C for 24 hours and stored in a plastic container. The procedure is repeated on the washings to increase the yield. Afterwards the filter papers are placed in an oven and dried at 250°C for 2 days to recover any silica still on the filter paper.

5. Doping with paramagnetics

The addition of paramagnetics should effectively suppress the negative NOE for dipolar Si-H interactions, and ^{29}Si T1-relaxation times should be shortened[25]. The effect of the paramagnetic is, however, subject to its solubility in the medium. and to the viscosity of the solution according to studies made by Levy et al[25]. Furthermore, it was found that not all paramagnetic metal ions are efficient relaxation agents. For instance Ni^{2+}, Co^{2+} and Fe^{2+} ions do not significally shorten relaxation times[26]. O_2 dissolved in the solution is reported to shorten relaxation times via its paramagnetic properties in some cases whereas in others it has no effect[27,28]. Not in all cases are the T2 relaxation times affected in the same way as T1 relaxation times, as Cr^{3+}-ions cause considerable shortening of T1-values without noticeably affecting the linewidth whereas Mn^{2+}-ions cause substantial line broadening[28]. The majority of paramagnetics affect the relaxation times via electron-nuclear dipole-dipole interactions[29]. For some paramagnetics like Mn^{2+}-ions, however, there is an additional contribution of scalar coupling between nuclear spins and electron spins[26].

The T1-relaxation times of ^{29}Si in highly viscous silicate solutions can be as long as almost 30 seconds, which makes the investigations fairly time-

consuming. Thus several representative silicate solutions have been doped with various paramagnetic metal ions, which have been added to the point of saturation, in order to investigate their effect on the ^{29}Si spin-lattice relaxation times. If not otherwise mentioned, the paramagnetic metal ions were left for at least 3 days to equilibrate with the silicate solutions before the T1 measurements. The concentrations of the dissolved paramagnetics were determined by atomic adsorption spectroscopy.

Further information on the paramagnetic ions used is presented in table 3-7 below.

Table 3-7
Paramagnetics used :

ion	nuclear spin I	spin state	free electrons	salt
Cu^{2+}	1/2	$3d^9$	1 (1)	CuSO4
Cr^{3+}	3/2	$3d^3$	3 (3)	CrCl3
Ni^{2+}	1	$3d^8$	2 (2)	NiSO4
Gd^{3+}	7/2	$4f^7$	7	Gd(dpm)3
Fe^{3+}	2	$3d^5$	1 (5)	FeCl3
Fe^{2+}	2	$3d^6$	0 (4)	FeSO4

If a high-spin state and a low-spin form exist the number of unpaired electrons in the high-spin state is given in brackets.

This doping with Cr^{3+}, Cu^{2+}, Ni^{2+}, Fe^{2+}, Fe^{3+} and Gd^{3+} ions does not exert any noticeable effect on the distribution of the structural building units in the silicate solutions, which stays constant within the experimental 5%-error limits. Moreover there is no perceptible effect on the linewidth of the Q0-resonance (which is the only resonance caused by a single structure) or on the chemical shifts.

Amongst the paramagnetic cations, Fe^{3+} ions exert the biggest effect on the shortening of T1, achieving an average shortening of 75%, and Cu^{2+} ions, although dissolved in higher concentrations than Fe^{3+} ions, only cause the second biggest shortening of T1-values in a silicate solution (tables 3-9, 3-11 and 3-12). The effect of Fe^{2+} and Ni^{2+} ions on the decrease in T1 relaxation times is negligibly small and Gd^{3+} ions exert no effect at all (tables 3-8 and 3-12). Cr3+ ions, although dissolved to a higher extent than any of the other paramagnetics, only cause a small decrease in the ^{29}Si T1-values (tables 3-8 and 3-12). The saturation of a silicate solution with oxygen did not cause any change in the ^{29}Si T1 values (table 3-8). The paramagnetic metal ion can adsorb on the SiOH-groups of the surface of the particles in the silicate solution[30]. The specific adsorption of metal ions on the silica surface can be related to the tendency of the metal atom to form covalent bonds which decreases in the order[31] :

$$Al^{3+} > Fe^{3+} > Cr^{3+} > Co^{2+} > Cu^{2+} > Ca^{2+} > K^{+} > Na^{+}$$

Out of the parmagnetic ions used in these studies Fe3+ ions are by far the most effective relaxation agents. They cause a considerable shortening of T1-values even in concentrations which are lower than for the other paramagnetic metal ions. Generally the amount of disolved paramagnetic increases with decreasing alkalinity of the silicate solution. The decrease in spin-lattice relaxation times caused by any paramagnetic is the smaller the more condensed the structural unit is. The paramagnetic is more effective in shortening the T1-values in diluted silicate solutions than in the concentrated ones (table 3-10). This is simply because the amount of parmagnetic dissolved in diluted silicate solutions increases with decreasing SiO_2 concentration (tables 3-8 and 3-12). Another result was that the effect of the salt in the silicate solutions is dependent on the time it is given to dissolve. It was found

that after three days the effect of the paramagnetic on the T1 values was fully established (table 3-9).

Table 3-8
T1 values in seconds for sodium silicate solutions :
32wt% SiO_2 Rm=2.0

structural unit	not doped	+ Fe^{3+} 3ppm	+ Cr^{3+} 160ppm	+ O_2 saturated
Q0	2.4	0.3	2.3	2.3
Q1	3.0	0.6	2.8	2.9
Q2cyc	3.0	0.8	2.9	3.1
Q2	3.9	0.9	3.2	4.0
Q3	4.9	1.5	4.1	5.0
Q4	-	-	-	-

Table 3-9
T1 values for sodium silicate solutions :
32wt%SiO_2 ; Rm=2.0

structural unit	without salt	with FeCl3 (3ppm)	with CuCl2 (6ppm) left 3hrs	with CuCl2 (30ppm) left 3 days
Q0	2.4	0.3(13%)	2.2(92%)	1.1(46%)
Q1	3.0	0.6(20%)	2.7(90%)	1.0(33%)
Q2cyc	3.0	0.8(27%)	2.8(93%)	1.4(47%)
Q2/Q3cyc	3.85	0.9(23%)	3.0(78%)	1.5(39%)
Q3	4.9	1.5(31%)	4.0(82%)	1.8(37%)
Q4	-	-	-	-

Table 3-10

T1 values for sodium silicate solutions :

15wt% SiO_2 ; Rm=2.0

structural unit	without salt	with FeCl3 (38ppm)
Q0	5.2	0.1(2%)
Q1	4.8	0.14(3%)
Q2cyc	4.3	0.3(7%)
Q2/Q3cyc	4.7	0.35(7%)
Q3	5.5	1.0(18%)
Q4	-	-

Table 3-11

T1 values for sodium silicate solutions :

30wt%SiO_2 ; Rm=2.95

structural unit	without salt	with FeCl3 (10ppm)
Q0	4.0	1.4(35%)
Q1	4.8	3.3(69%)
Q2cyc	5.1	4.0(78%)
Q2/Q3cyc	5.3	4.2 (79%)
Q3	7.3	6.4(88%)
Q4	14.7	13.4(91%)

Table 3-12
T1 values for sodium silicate solutions :
25wt% SiO_2 Rm=4.0

structural unit	not doped	+ Fe^{2+} 8ppm	+ Cu^{2+} 37ppm	+ Cr^{3+} 190ppm	+ Ni^{2+} 1ppm	+ Gd^{3+} 4ppm
Q0	8.4	1.0	5.5	7.0	8.4	7.3
Q1	8.8	1.6	5.7	7.3	8.9	7.6
Q2cyc	-	-	-	-	-	-
Q2	8.5	1.5	6.8	7.2	8.9	7.0
Q3	10.2	2.3	9.1	9.0	10.0	9.9
Q4	18.5	6.0	16.5	14.7	19.0	15.8

6. Non-NMR analytical techniques

All equipment mentioned in this section is located at Unilever Research, Port Sunlight.

6.1 Optical microscopy

Optical microscopy has been carried out with an Olympus BH-2 instrument equipped with a Linkam TP 91 temperature control unit. The observation of silicate systems under the microscope has to be fast, since it is not possible to work under CO_2-free conditions. Lenses with a range of magnifications were used and in some cases a polarising lens was used for the observation of liquid crystalline phases. The microscopic pictures were monitored with a Panasonic WV-CM 140 Video Monitor, and photos of the picture shown on the monitor were taken using a Sony Video Graphic Printer VP-850.

6.2 Transmission electron microscopy (TEM)

There are several experimental techniques used in TEM. In the experiments described in this thesis copper grids supported by a carbon film were used as sample carriers. The instrument used is a JEOL JEM-200 CX electron microscope equipped with a camera control display unit of the type 1570 Agar. It works at a vacuum of 10^{-7}bar. If the sample was put onto the grid and immediately placed in the vacuum to prevent changes of the silicate solution (25.5wt% SiO_2 and Rm=3.8 with surfactant) occurring in the atmosphere, the film on the grid was very thick but allowed the resolution of agglomerated particles on the edges. The dilution of the sample with a factor 1/10 and immediate shock-freezing at liquid nitrogen temperature, with observation of the sample in the instrument in the frozen state, allowed agglomerated particles on the film to be seen.

6.3 Rheology

Two different types of experiments have been carried out. Experiments with varied temperature and constant stress to measure phase transitions as a function of temperature were carried out using a 4^{o}-cone and a stress of 4774 N/m^2 in the temperature range -10°C to +80°C. The shear rate is adjusted throughout the experiment according to the increased temperature to keep a constant stress. Experiments with varied stress at a constant temperature of 25°C to measure flow behaviour used a 4^{o}-cone. The instrument adjusts the shear rate according to the changed stress at a constant temperature.

6.4 Differential Scanning Calorimetry (DSC)

For these experiments a Perkin-Elmer DSC-instrument with a 7 Series Thermal Analysis System was used. The temperature range investigated was -60°C to +100°C with a step size of 5°C per minute.

The literature value for the enthalpy needed for the melting of ice, ΔH_m (H2O) is 319.73 J/g.

The experimental value for ΔH_m (H2O) is 321.83 J/g.

For the calculations the latter value for ΔH_m (H2O) is taken.

6.5 Water activity measurements

The water activity was measured in % with a 3-channel Novasina AW-centre which detects the aw-value (0-1) of the humidity of the air layer between the sensing head and the sample with an electronic humidity sensor. The equilibration of the sample with the air layer takes approximately 2 hours. All three channels are calibrated with special samples on which the aw-values are set.

For the measurement of water activities of the silicate samples it was established that the H2O/D2O-ratio does not affect the result (see table 3-13). Solutions of NaCl saturated in H2O, 50% H2O/50% D2O and D2O were measured:

Table 3-13
Water activity values

	aw-value
100% H2O	75.1%
50% H2O/50% D2O	75.9%
100% D2O	73.9%

Literature:

1 R. K. Harris, Nuclear Magnetic Resonance Spectroscopy, Longman Scientific & Technical, New York (1986)

2 R. H. Newman, PhD Thesis, University of Durham (1978)

3 A. E. Derome, Modern NMR Techniques for Chemistry Research, Vol.6, Pergammon Press, Oxford, New York (1987)

4 H. C. Marsmann, Z Naturforsch. **29b** (1974) 495

5 S. D. Kinrade, T. W. Swaddle, Inorg. Chem. 27 (1988) 4253

6 R. K. Harris, C. T. G. Knight, J. Chem. Soc. Faraday Trans. II, **79** (1983) 1525, 1539

7 E. Fukushima, S. B. W. Roeder, Experimental Pulse NMR, Addison-Wesley Publishing Company, London, Amsterdam (1981)

8 A. J. Walker, N. Whitehead, J. Appl. Chem. **16** (1966) 230

9 J. Schraml, J. M. Bellama, Two-Dimensional NMR Spectroscopy, Vol.97, Wiley-Interscience, New York, Chichester (1988)

10 S. Meiboom, D. Gill, Rev. Scient. Instrum. **29** (1958) 688

11 J. Jeener, B. H. Meier, P. Bachman, R. R. Ernst, K. J. Wuethrich, J. Magn. Reson. **56** (1984) 207

12 E. O. Stejskal, J. E. Tanner, J. Chem. Phys. **42**, No.1, (1965) 288

13 J. E. Tanner, Rev. Scient. Instrum. **36** (1965) 1086)

14 E. O. Stejskal, J. E. Tanner, J. Chem. Phys. **49** (1968) 1768

15 J. E. Tanner, J. Chem. Phys. **52**, No.5 (1970) 2523

16 E. L. Hahn, Phys. Rev. **80** (1950) 580

17 P. Stilbs in: Progress in NMR Spectroscopy, J. W. Emsley, J. Feeney, L. H. Sutcliffe (Ed.) **19** (1987) 1

18 D. E. Woessner, J. Chem. Phys. **43** (1961) 2057

19 E. G. Smith, J. W. Rockliffe, P. I. Riley, J. Colloid Interface Sci. **131**, No.1 (1989) 29

20 M. Holz, H. Weingaertner (Dept. Phys. Unversity of Karlsruhe), A. Sacco (Dept. Chem. University of Bari) in: Bruker Almanac 1992, printed by Bruker/Germany, Nov 1991

21 R. K. Harris, R. H. Newman, Org. Magn. Res. **9**, No.7 (1977) 429

22 E. K. F. Bahlmann, R. K. Harris, K. Metcalfe, E. G. Smith, Magn. Reson. Chem. **31** (1993) 743

23 E. K. F. Bahlmann, R. K. Harris, B. J. Say, Magn. Reson. Chem. **31** (1993) 266

24 Handbook of Chemistry and Physics, K. C. Weast, M. J. Astle, W. H. Beyer (Ed.), 64th edition (1983-1984), CRC Press, Inc., Boca Raton, Florida

25 C. G. Levy, . D. Cargioli, P. C. Juliano, T. D. Mitchell, J. Am. Chem. Soc. **95** (1973) 3445

26 R. A. Bernheim, T. H. Brown, H. S. Gutowski, D. E. Woessner, J. Chem. Phys. **30** (1959) 950

27 S. D. Kinrade, T. W. Swaddle, J. Am. Chem. Soc. **108** (1986) 7159

28 R. K. Harris, R. H. Newman, J. Chem. Soc. Faraday Trans. II **72** (1977) 1204

29 I. Ando, G. A. Webb, Theory of NMR Parameters, Academic Press, London, New York (1983)

30 R. K. Iler, The Chemistry of Silica, Wiley-Interscience, New York (1979)

31 T. Wakatsuki, H. Furukama, K. Kawaguchi, Chem. Abstr. **82** (1974) 160671r

32 J. K. M. Sanders, B. K. Hunter, Modern NMR Spectroscopy, Oxford University Press, Oxford, New York, Toronto (1987)

33 A. Bax, R. Freeman, S. P. Kemsell, J. Magn. Reson. **41** (1980) 349

34 C. A. Fyfe, Y. Feng, H. Gies, H. Grondey, G. T. Kokotailo, J. Am. Chem. Soc., **112** (1990) 3264

35 J. Schraml, J. M. Bellama in: Determination of Organic Structures by Physical methods, F. C. Nachod, J. J. Zuckerman, E. W. Randall (Eds.), Vol.6, Ch.4, Academic Press, New York, London, San Francisco (1976)

4. THE QUANTITATIVE ASPECT

1. Introduction to the problem

A very important aspect in the NMR investigations of viscous, highly-condensed silicate solutions is ensuring that every silicon atom in the solution is represented in the NMR spectrum. It has been stated that silicon atoms located in colloidal particles cannot be detected by solution-state NMR[1] because there could be silicon atoms, especially in the core of colloidal particles, having long spin-lattice relaxation times which would make detection difficult. Moreover, such nuclei may give rise to extremely broad lines for reasons of short T2 or shift dispersion, so that signals may be unduly affected by the spectrometer dead time[2]. The investigated silicate solutions do contain varying amounts of Q4-units[3] (in some silicate solutions up to 25%, see chapter 5-1.2), the existence of the Q4-unit being evidence for the existence of colloidal particles[4,5]. Thus the investigation of colloidal particles plays a dominant role in the silicate solutions studied, and it is vital to check if their silicon atoms are represented in the NMR spectrum. The quantitative determination of the amount of nuclei between the coils is not straightforward and has not been tackled in the literature so far. A new procedure was worked out for the present studies in which physical approaches had to be taken into account[3].

2. Theory

The quantification procedure is complicated by two major factors. The magnitude of the detected NMR signal is influenced by the flip-angle of the pulse and the coupling of the spins on the receive side[5]. The flip-angle depends on the duration of the pulse and the strength of the rf magnetic field. The latter in turn depends on the coupling between the spectrometer and the

spins on the transmit side[2,6]. The transmit and receive coupling are complementary, so that cases which lead to spins experiencing a high magnetic field also lead to large received signals in the spectrometer. The coupling is not uniform in space, since spins at the extreme of the NMR coil are not as well-coupled as those in the centre[7]. There is also a potential variation in an annular sense, spins near the centre of the coil being coupled differently to those at the periphery. The extent of this effect is influenced by the nature of the sample.

All samples affect the characteristics of the NMR coil by virtue of their relative permittivity and dielectric loss factor[8]. These describe the extent to which the electric charge distribution can be polarised by a magnetic field and exert an influence on both the inductance of the coil and its Q factor.

We can thus deduce the equation for the observed intensity of a NMR signal I, at a given pulse angle.

$$I \propto \varepsilon * S_f * N \qquad [1]$$

$$I = K * \varepsilon * S_f * N \qquad [2]$$

The proportionality constant, K, involves factors such as γ, B_0, T and gain settings on the spectrometer which stay constant for any sample[9]. N denotes the number of nuclei detected by the coil and is expressed in terms of wt% SiO_2. S_f is a shape factor which characterises the first effect described above. If this were the only effect, replacement of the sample by one of known concentration with the same shape would suffice. ε can be described as a tuning factor representing the second effect. If this were the only effect to be considered we could use a two-compartment sample holder with known volume ratio.

Both effects complicating the quantification can be cancelled out if an experimental set-up is used which connects the results of two individual experiments. The first experiment gives the integrated intensities for a silicate standard solution containing no colloidal particles and a non-silicate reference which is in a coaxial sealed capillary inside the NMR tube. The second experiment yields the integrals for the silicate solution of interest and the same reference in the same insert as used for experiment 1. In these investigations HMDSO is used as a reference.

The equations for the resulting two sets of two integrals are as follows:

Experiment 1:

$$I^{(1)}_{HMDSO} = K * \varepsilon_1 * S_f(\text{insert}) * wt\%Si_{HMDSO} \qquad [3]$$

$$I^{(1)}_{HMDSO} = K * \varepsilon_1 * S_f(\text{tube}) * wt\%Si_{standard} \qquad [4]$$

Experiment 2:

$$I^{(2)}_{HMDSO} = K * \varepsilon_2 * S_f(\text{insert}) * wt\%Si_{HMDSO} \qquad [5]$$

$$I^{(2)}_{HMDSO} = K * \varepsilon_2 * S_f(\text{silicate}) * wt\%Si_{silicate} \qquad [6]$$

Connecting these equations in the form of taking the ratios

$$\frac{[3]}{[4]} \div \frac{[5]}{[6]} \qquad [7]$$

yields an equation for the amount of Si in a silicate solution detected by the coils which is not dependent on K, ε and S_f any more.

It can easily be solved with the accessible data[3].

$$wt\%Si_{silicate} = \frac{I^{(1)}_{HMDSO} * I^{(2)}_{silicate} * wt\%Si_{standard}}{I^{(1)}_{standard} * I^{(2)}_{HMDSO}} \qquad [8]$$

3. Practice

To check the reliability and applicability of equation [8], two different standards were investigated, both sodium silicate solutions containing no colloidal particles[10,11]. These standards were :

1) 0.1wt% SiO_2 , Rm=1.6

2) 20.0wt% SiO_2 , Rm=0.7

When these standards are measured against each other, the correct values for the silicon contents were obtained. Thus there is proof that by using this quantification method the usually qualitative NMR measurement can be turned into a quantitative experiment.

The next step was the investigation of two relevant sodium silicate solutions with a high degree of condensation, both showing considerable amounts of Q4-units. Since the existence of Q4-units can be taken as an indication that colloidal particles are formed in the silicate system[4,5], it can be concluded that both silicate solutions contain colloidal particles. In silicate solutions with ratios in the range of those used here particles of sizes in the low-size range of colloidal particles were found by Iler[5,12,13].

Experimental values for the total silica concentration have been obtained using the set of experiments described before and solving equation [8] with the measured data. They represent the amount of Si nuclei detected by the coils.

30wt% SiO_2 , Rm=3.4

Theoretical : 14.03wt% Si

Experimental : 14.0 +/- 0.46 wt% Si

(average of two experiments)

25wt% SiO_2 , Rm=4.0

Theoretical : 11.69wt% Si

Experimental : 11.6 +/- 0.64 wt% Si

(average of three experiments)

These results show that, within experimental error, every silicon atom in the silicate solutions can be detected by the coils and is thus represented in the NMR spectrum no matter whether it is located in colloidal particles or in much smaller units[3].

Literature:

1 A. V. McCormick, A. T. Bell, C. J. Radke, Zeolites 7 (1987) 183

2 E. Fukushima, S. B. W. Roeder, Experimental Pulse NMR, Addison-Wesley Publishing Company, Inc. (1981)

3 E. K. F. Bahlmann, R. K. Harris, B. J. Say, Magn. Reson. Chem. **31** (1993) 266

4 R. K. Iler, The Chemistry of Silica, Wiley-Interscience, New York (1979)

5 E. K. F. Bahlmann, R. K. Harris, K. Metcalfe, E. G. Smith, Magn. Reson. Chem. **31** (1993) 743

6 A. E. Derome, Modern NMR Techniques for Chemistry Research, Pergamon Press, Oxford, New York (1987)

7 M. L. Martin, G. J. Martin, J-J. Delpuech, Practical NMR Spectroscopy, Heyden, London, Philadelphia (1980)

8 J. B. Hasted, Aqueus Dielectrics, Chapman and Hall, London (1973)

9 R. K. Harris, Nuclear Magnetic Resonance Spectroscopy, Pitman (1983)

10 H. C. Marsmann, Z. Naturforsch. **29b** (1974) 495

11 I. L. Svensson, S. Sjoberg, L-O. Oehman, J. Chem. Soc. Faraday Trans. I **82** (1986) 3635

12 R. K. Iler, Soluble Silicates, J. S. Falcone (Ed.), ACS Symposium Series **194** (1982) 95

13 Hackh's Chemical Dictionary, J.Grant (Ed.), 4th edition, Mc Graw Hill, New York (1969)

5. COLLOIDAL PARTICLES AND STRUCTURING OF SILICATE SYSTEMS

1. Structures

1.1. Structure assignment for a silicate solution with Rm=2.0

Individual structures have been assigned by Harris and Knight for potassium silicate solutions which were enriched in ^{29}Si. The techniques of ^{29}Si-{^{29}Si} homonuclear decoupling[1,2] and two-dimensional ^{29}Si homonuclear correlation spectroscopy (COSY)[3,4,21] have been employed. The chemical shifts of the Si atoms forming the structures that were identified are listed in table 5-1. The chemical shift values reported here are referenced to the Q0 resonance.

A remarkably well-resolved ^{29}Si spectrum of a sodium silicate solution with 32wt% SiO_2 and Rm=2.0 was obtained which allowed the assignment of individual resonances to individual structures[35]. The spectrum is shown in figure 5-1. A similar resolution could not be obtained in any of the higher molar ratios as the overlapping of signals makes it impossible to resolve individual lines. In the comparison of reported chemical shifts care has to be taken as chemical shift values are dependent on the Rm-value and the SiO_2 concentration[1,5]. Thus for the assignment of resonances by using reported chemical shifts for comparison all chemical shifts were referred to the Q0-resonance (the chemical shifts in the table are absolute values). The structures found in this silicate solution are listed in table 5-2[35].

Table 5-1

Chemical shifts in a sodium silicate solution with 0.6/1.5 M SiO_2 and Rm=2.0 referenced to the Q0 resonance and the structures they are assigned to[1-4,21]

• denotes the silicon atoms assigned to the resonance
Oxygen atoms are generally omitted

Δδ /ppm		
0.0	Q^0	
-7.90	Q^1	
-8.06	Q^1	
-8.15	Q^1	
-8.59	Q^1_2	
-9.8	Q^2	
-9.86	Q^2	
-10.17	Q^2_3	
-10.36	Q^2	
-10.6	Q^2	
-14.22	Q^2	
-14.52	Q^2	
-15.5	Q^2	
-15.6	Q^2	
-15.7	Q^2	
-15.76	Q^2	
-16.0	Q^2	
-16.08	Q^2	
-16.09	Q^2_4	
-16.2	Q^2	
-16.3	Q^2	
-16.4	Q^2	
-16.6	Q^3	
-16.6	Q^3	
-16.6	Q^2	
-16.7	Q^2	
-16.92	Q^2	
-17.16	Q^3	
-17.22	Q^3_6	
-17.46	Q^3	
-17.8	Q^3	
-17.8	Q^3	
-17.89	Q^3	
-18.1	Q^3	
-18.22	Q^3	
-18.88	Q^3	
-20.42	Q^3	
-21.43	Q^3	
-21.94	Q^3	
-24.1	Q^3	
-24.2	Q^3	
-24.5	Q^3	
-24.72	Q^3	
-24.9	Q^3	
-25.2	Q^3	
-25.4	Q^3_4	
-26.72	Q^3	
-27.15	Q^3_{10}	
-27.31	Q^3_8	

Figure 5-1
^{29}Si NMR spectrum of a sodium silicate solution
with 32wt% SiO_2 and Rm=2.0
chemical shifts referenced to HMDSO (external), acquired on the AMX500
relaxation delay 30s, 500 transients, acquisition time 0.2 s

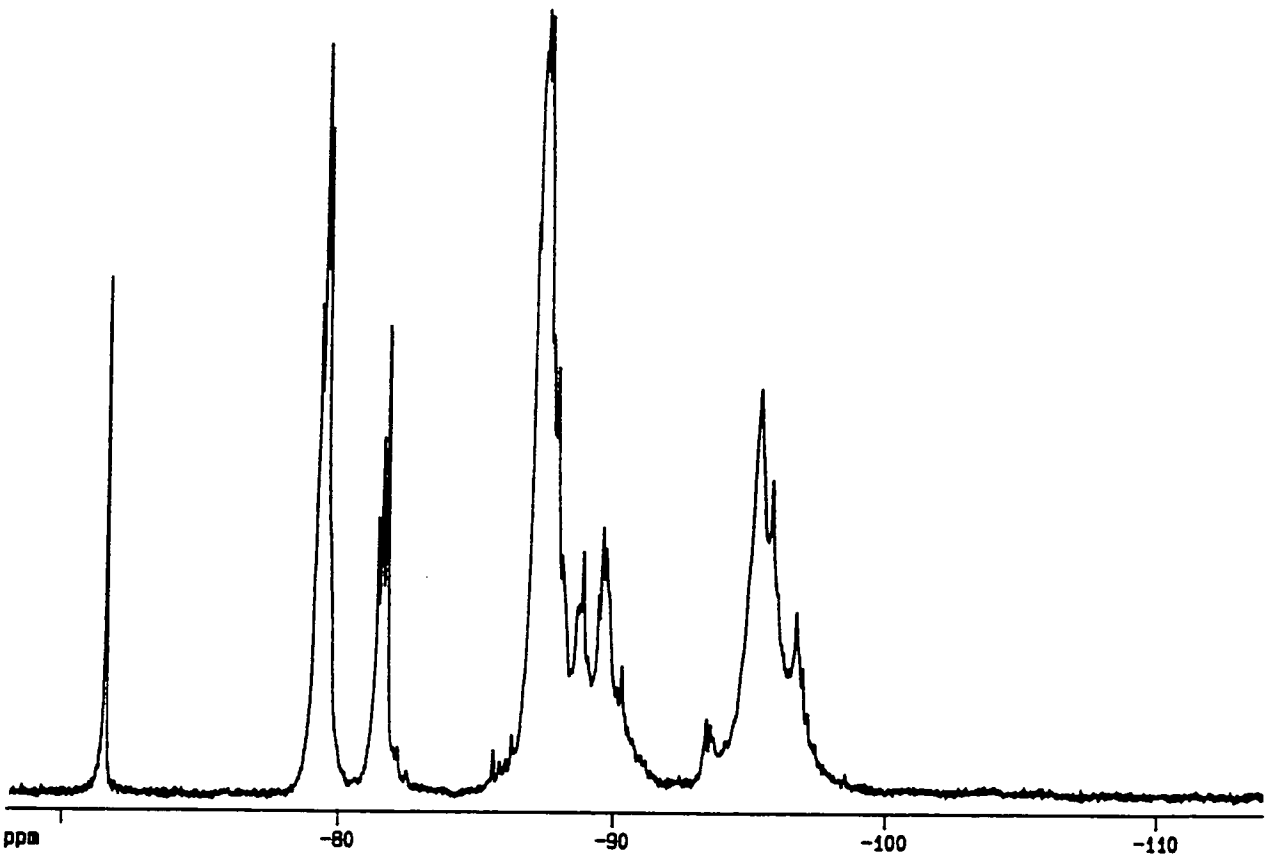

Table 5-2

Chemical shifts in a sodium silicate solution with 32wt% SiO_2 and Rm=2.0 referenced to HMDSO (external) and the structures they are assigned to according to assignments in figure 5-1

• denotes the silicon atoms assigned to the resonance

Oxygen atoms are generally omitted

δ / ppm	Δδ / ppm		
- 71.56	(0.0)	Q^0	
- 79.21	(-7.65)	Q^1	
- 79.37	(-7.81)	Q^1	
- 79.47	(-7.91)	Q^1	
- 81.35	(-9.79)	Q^2	
- 81.51	(-9.95)	Q^2	
- 81.68	(-10.12)	Q^2	
(- 85.61	(-14.05)	Q^2	)
-86.26	(-14.7)	Q^2	
-87.02	(-15.46)	Q^2	 or 
-82.2	(-15.64)	Q^2	" "
-87.31	(-15.75)	Q^2	
-87.41	(-15.85)	Q^2	
-87.84	(-16.28)	Q^2	
-88.04	(-16.48)		
-88.84	(-17.28)	Q^3	
-89.42	(-17.86)	Q^3	
-89.55	(-17.99)	Q^3	
-89.67	(-18.11)	Q^3	
(-93.41	(-21.85)	Q^3	)
-93.57	(-22.01)	Q^3	
-95.29	(-23.73)	Q^3	
-95.75	(-24.19)	Q^3	
-96.69	(-25.13)	Q^3	

According to this assignment the structures occurring in this solution are fairly small and limited in size. There are no large, extended units, for instance chains containing Q2-units. Thus the process which takes place when the pH decreases (Rm increases) is not a simple polymerisation. It is rather a random condensation of small units to bigger entities than a growth of chains.

1.2 Effect of decreasing NaOH-content (increasing Rm-value)

The distribution of structural units in silicate solutions is strongly influenced by the ratio of SiO_2 to Na_2O, the Rm-value. An increase in the Rm-value means a decrease in the alkalinity of the silicate system.

In these investigations silicate solutions were prepared by dissolving fumed silica in sodium hydroxide solution. The procedure used is described in detail in chapter 3-4.1.1. The different Rm-values were produced by varying the NaOH content in the systems. It should be noted that the silicate systems with 30wt% SiO_2 and Rm $\geq$ 3.8 are past the sol/gel-transition (see section 2). Typical ^{29}Si-spectra of sodium silicate solutions are shown in figure 5-2.

All spectra consist of six major regions which are assigned to structural units according to previous assignments[31,32]. In the chemical shift range δ = -70.5 to -72.0 ppm the monomer resonance is found. At δ = -78.8 to -80.8 ppm peaks assgned to the Q1 end-group are found. The resonance at δ = -80.9 to -82.0 ppm is characteristic for the cyclic trimer ($Q2_3$). In the chemical shift range δ = -87.0 to -89.6 ppm peaks arising from Q2 middle-groups and cyclic Q3-units are found, the cyclic Q3-units resonating at the high-field side of this region. The peaks belonging to silicon atoms in Q3-units, which can form branching groups and surface units in colloidal particles resonate in the region

δ = -95.0 to -98.5 ppm. Silicon atoms in Q4 cross-linking groups, found in the core of colloidal particles resonate at δ = -105.0 to -109.0 ppm.

The general tendency in the structural distribution at high SiO_2-concentrations ([SiO_2] = 30wt%) with increasing Rm-value is presented in figure 5-3 and table 5-3.

Table 5-3
Distribution of sructural units with incresing Rm-value ($cSiO_2$= 30wt%)

	2.0	**2.4**	**2.6**	**3.0**	**3.4**	**3.8**	**4.0**
Q0	1.2	0.8	0.7	0.9	0.8	0.0	0.0
Q1	12.7	8.6	6.7	5.7	5.5	3.0	2.4
Q2cyc	3.7	2.3	1.5	1.0	0.0	0.0	0.0
Q2	47.7	38.8	36.5	29.8	26.1	24.3	21.8
Q3	34.7	44.8	47.2	48.5	50.0	51.5	52.0
Q4	0.0	4.7	7.4	14.1	17.6	21.2	23.8

Figure 5-3
Distribution of structural units with increasing Rm-value

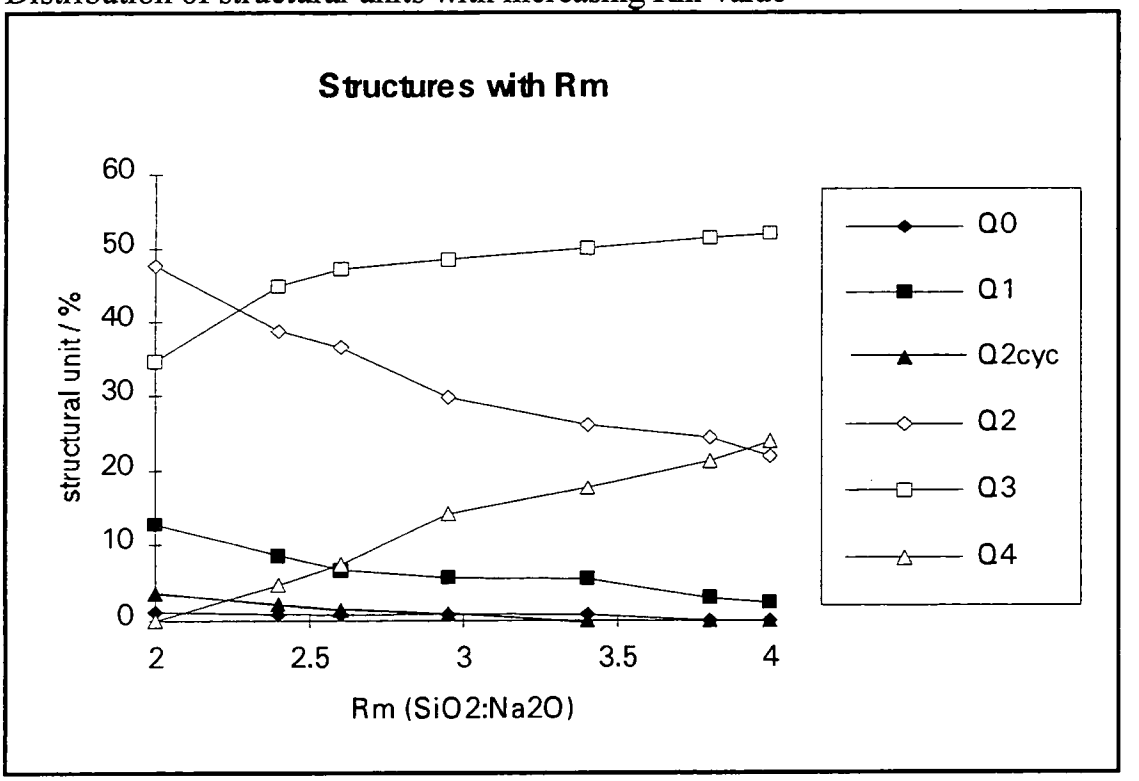

In agreement with previous results on silicate solutions with much lower SiO_2-concentrations[10,11], a general trend in the speciation can be observed with decreasing alkalinity (increasing Rm). The fraction of Si atoms in Q0-, Q1-, Q2cyc- and Q2-units decreases whereas the fraction of Si-atoms in Q3- and Q4-units increases. Thus the relative number of Si atoms in more branched environments increases with increasing Rm, indicating the formation of larger more complex silicate structures. The beginning of the formation of Q4-units, which occurs at Rm-values bigger than 2.0 at high SiO_2-concentrations, is regarded as the start of the formation of colloidal particles[6].

From the distribution of structural units with increasing Rm-value shown in figure 5-3 an equation was derived describing the Rm-value in terms of the ratio of Q4-units to the other structural units. This enables us to calculate the respective Rm-value of a silicate system of known SiO_2-content ($cSiO_2$ = 30 wt%) but unknown alkalinity from the ^{29}Si NMR-spectrum.

$$Rm = 6 * \frac{\sum Q4}{\sum Q0 + Q1 + Q2cyc + Q2 + Q3} + 2.0 \qquad [1]$$

The limit of precipitation of silica in silicate solutions has been investigated by trying to produce silicate solutions with Rm-values bigger than 4.0 and using the method of quantification described in chapter 4 to investigate the amount of silica dissolved (see chapter 7). It is found to be Rm=4.0. This agrees with previous results reported in the literature[7,8] where the Rm=4.0 was assumed to be the precipitation boundary for SiO_2 and thus the highest ratio at which silicate solutions are stable.

Two processes are involved in systems containing colloidal particles. The formation of new colloidal particles and the growth of existing colloidal

particles. Colloidal particles have Q4-units in the core and Q3-units on their surface. From the graphs in figure 5-3 conclusions can be drawn about the growth-mechanisms in silicate solutions with decreasing alkaline content. The relatively large increase in the amount of Q3-units compared with the growth of Q4-units from Rm=2.0 to Rm=2.5 suggests that in this regime the formation of new colloidal particles dominates. From Rm=2.5 onwards to Rm=4.0 the relatively small increase in the amount of Q3-units compared with that of the Q4-units suggests that the growth of existing colloidal particles is the dominating process.

The Q3/Q4-ratio versus the Rm-value was plotted for a constant SiO_2-concentration of 30wt% SiO_2 (figure 5-4). In the plot a change in the slope can be seen at a molar ratio of SiO_2 to Na_2O around 3.0. This is even obvious in the semi-logarithmic plot of the Rm-value versus the Q3/Q4-ratio (figure 5-5). This is illustrating the fact that from a molar ratio of around 3.0 and a Q3/Q4-ratio of around 3 the growth of colloidal particles dominates over the new-formation of colloidal particles. The very slowly decreasing tail of the graph also indicates that there is a limiting particle size (a limiting Q3/Q4-ratio).

Experimental findings furthermore show a limiting Q4-content which is around 25% for a silicate on either side of the sol/gel-transition where no precipitation has occurred.

The rate of particle growth depends on the distribution of particle sizes[13] which is assumed to be Gaussian. The growth occurs with smaller particles dissolving and adding silica to larger ones till the difference in the solubility of the smaller particles is negligible compared to the solubility of the larger particles.

Table 5-4
Q3/Q4 ratio and logQ3/Q4 in dependency of the Rm-value :

Rm	**2.4**	**2.6**	**2.95**	**3.4**	**3.8**	**4.0**
Q3/Q4	9.5	6.4	3.4	2.8	2.4	2.2
log Q3/Q4	0.98	0.81	0.53	0.45	0.38	0.34

Figure 5-4
Q3/Q4 versus Rm:

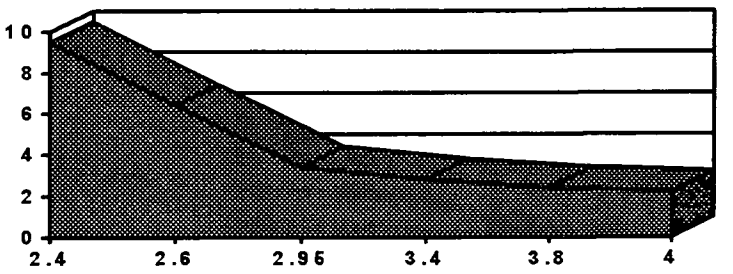

Figure 5-5
log Q3/Q4 versus Rm:

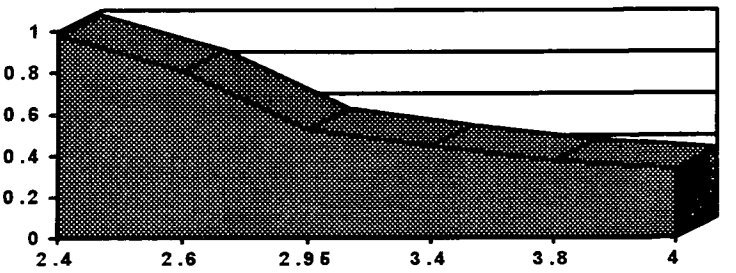

Figure 5-2

^{29}Si NMR-spectra of sodium silicate solutions

a) 32wt% SiO_2 and Rm=2.0,
acquisition time 0.2s, relaxation delay 30s, transients 500

b) 30wt% SiO_2 and Rm=3.0
acqusition time 0.04s, relaxation delay 80s, transients 80

c) 25wt% SiO_2 and Rm=4.0
acqusition time 0.02s, relaxation delay 100s, transients 100

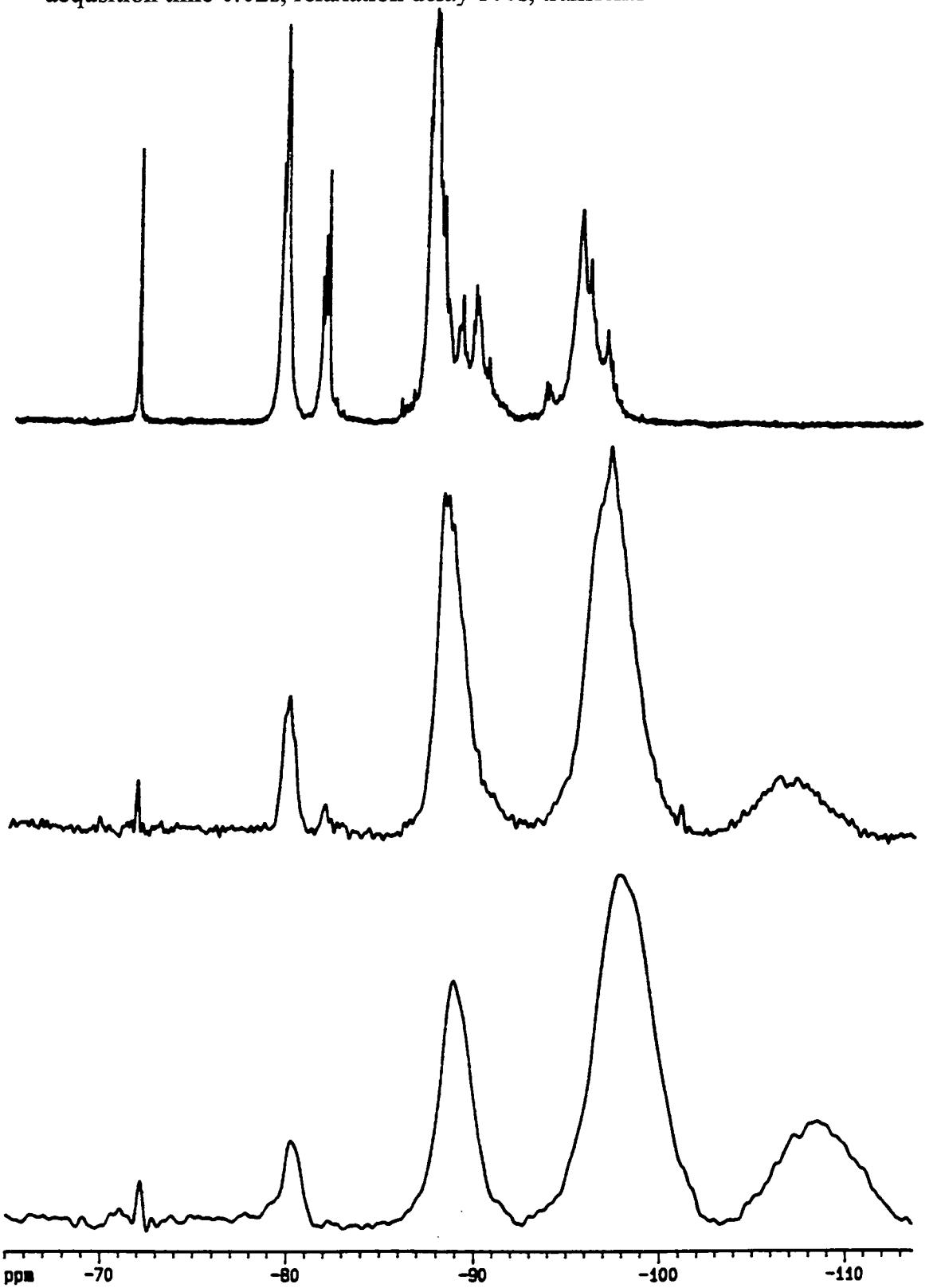

1.3 Dilution of the silicate solutions

Most studies so far involved relatively dilute silicate solutions[9,10] and highly concentrated silicate systems have received less attention. Compared to the effect of the Rm-value the distribution of Si-units is less influenced by the SiO_2-concentration[11].

1.3.1 Study on time-dependent dilution

The dilution of a sodium silicate solution containing colloidal particles has been studied as a function of time in order to find how long it takes for the structural units to establish the new equilibrium. Furthermore it might be possible to see if any Q3-units equilibrate faster than others by plotting the amount of Q3-units against the time and checking if there is more than one contribution to this time-dependency. Assuming that the colloidal particles equilibrate more slowly than small particles this would be a method of distinguishing between Q3-units in colloidal particles and Q3-units in small molecules.

A sodium silicate solution with 25.5wt% SiO_2 and Rm=3.8 was diluted 1:1 to give 12.3wt% SiO_2. ^{29}Si-spectra have been recorded in step sizes of 66 minutes after the addition of the appropriate amount of water to the silicate solution.

The results are presented in table 5-5 and figure 5-6. It can be seen that during the experiment there were no Q3- or Q4-units which equilibrated faster. This as well as the observation that the slope of the Q3-graph is about the same as the (negative) slope of the Q4-graph indicates that most of the Q3-units are on the outer or inner surface of colloidal particles.

Table 5-5

Dilution of a sodium silicate solution with 25.5wt% SiO_2 and Rm=3.8 to 12.3wt% SiO_2

^{29}Si spectra were recorded on the AMX500 with background subtraction recycle delay 150s, acquisition time 0.04s, 40 transients in step sizes of 66 minutes after the addition of the appropriate amount of water to the silicate solution

Values are for the distribution of the structural units in % of the respective unit

time/min	Q0	Q1	Q2	Q3	Q4
66	1.0	5.0	21.4	50.8	21.8
132	0.9	4.0	23.2	52.3	19.6
198	0.5	5.0	25.3	52.9	16.4
264	0.9	4.0	23.9	52.9	18.2
330	1.0	5.8	23.6	51.6	17.9
396	0.9	3.5	25.0	55.5	15.1
462	0.6	5.4	27.4	52.0	14.6
528	0.9	4.6	24.7	54.4	15.4
594	0.9	4.8	25.3	54.4	14.6
660	0.8	4.0	25.5	55.3	14.4
726	0.8	3.8	25.7	55.6	14.1
8 weeks	0.5	2.5	26.0	58.7	12.3

Figure 5-6
Dilution of a sodium silicate solution with 25.5wt% SiO_2 and Rm=3.8 to 12.3wt% SiO_2
Plot of amount of structural unit versus time after dilution
^{29}Si spectra were recorded on the AMX500 with background subtraction recycle delay 150s, acquisition time 0.04s, 40 transients in step sizes of 66 minutes after the addition of the appropriate amount of water to the silicate solution

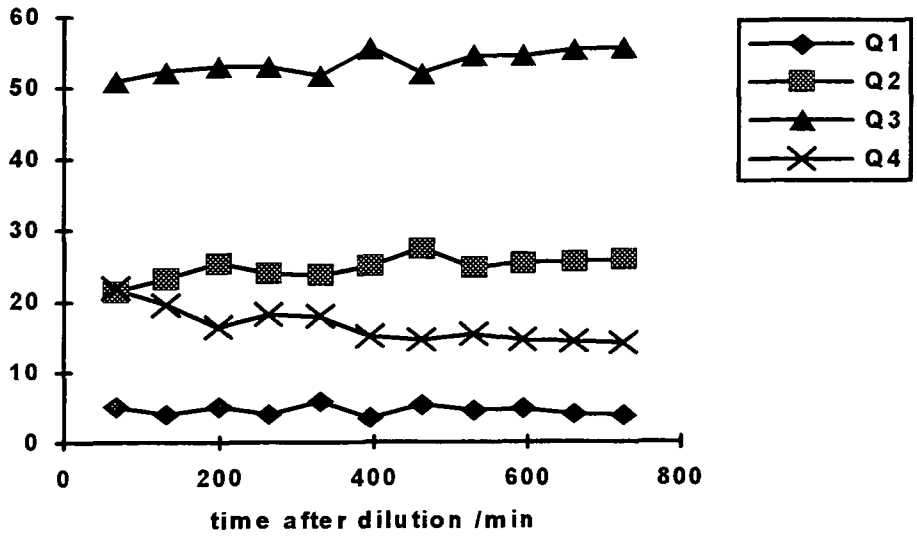

1.3.2 Dilution of a high-ratio sodium silicate solution

Iler reported that the dilution of a concentrated silicate solution by a factor of 10 almost instantly released more monomer into the solution[13]. A representative silicate solution with a high degree of condensation containing colloidal material was diluted to a factor of 1/5 of its initial concentration to investigate the effect of dilution on the structuring in a silicate containing colloidal matter. The effect of dilution is shown in table 5-6.

From the increasing amount of Q3 units, in parallel with the decreasing amount of Q4-units, when the solution is diluted by half it can be concluded that the size of the colloidal particles in the silicate solution is decreasing. Upon further dilution to a fifth of the SiO_2 content of the stock solution a decrease in the total amount of colloidal material takes place which goes along

with a general depolymerisation of all structures, shown in the drastically increased amount of Q1-units at the expense of Q2, Q3 and Q4 units. Surprisingly the amount of monomer in the silicate does not drastically increase.

Table 5-6
Distribution of structural units in a sodium silicate solution with Rm=3.8 under the influence of dilution:

structural unit	25.5wt% SiO_2 Rm=3.8	12.0wt% SiO_2 Rm=3.8	5.0wt% SiO_2 Rm=3.8
Q0	0.9	0.5	1.8
Q1	4.7	2.5	37.3
Q2cyc	0.0	0.0	0.0
Q2	23.2	26.0	17.0
Q3	51.5	58.7	35.3
Q4	19.7	12.3	8.6

1.3.3 Redilution of a silicate past the sol/gel-transition

The reversibility of the passing of the transition from a sol to a gel gives important information about the ability of silicate systems to readapt to changing conditions in both directions. A sodium silicate system past the sol/gel-transition (see section 5-2) of Rm=4.0 and 30wt% SiO_2 (which has been prepared by concentrating up a silicate solution of 25wt% SiO_2) has been rediluted to 23wt% SiO_2. It gives the expected structural distribution if given enough time to get to equilibrium (at least 6 weeks). This shows that even if physical properties like the viscosity change drastically in a gel, the system is

able to readapt if the composition is changed. This ability to readapt to the sol state proves the great flexibility of silicate systems.

Table 5-7
Distribution of structural units in a sodium silicate solution with 23wt% SiO_2 and Rm=4.0 rediluted from the gel containing 30wt% SiO_2 with Rm=4 (30R4)

structural unit	30wt% SiO_2 Rm=4.0	23wt% SiO_2 Rm=4.0 rediluted from 30R4
Q0	0.6	0.4
Q1	1.9	1.8
Q2cyc	0.0	0.0
Q2	27.0	22.3
Q3	39.6	56.3
Q4	30.9	19.2

1.4 Ageing of silicate solutions

The CO_2 in the atmosphere has a profound effect on the constitution of sodium silicate solutions especially in cases with a high sodium content (high pH). The CO_2 works in the way that sodium hydroxide is taken out of the silicate solution in the form of sodium bicarbonate.

$$NaOH + CO_2 \rightarrow NaHCO_3$$

This artificially decreases the alkalinity of the silicate and therefore has the same effect as an increase in the Rm-value. If it is assured that no water-loss occurs during the exposure to CO_2 the change in the silicate system can thus be described in terms of the Rm-value calculated with equation [1].

Two sodium silicate solutions were exposed to CO_2 atmosphere for a period of 14 and 28 weeks. Under the influence of the ageing-process both silicate solutions passed the sol/gel-transition. In CO_2-atmosphere the ageing

is increasing the Rm-value of a silicate solution with Rm=2.0 to Rm=2.3 and the Rm-value of a sodium silicate solution with 25wt% SiO_2 and Rm=4.0 which was aged in the atmosphere for 7 months to Rm=4.3 (table 5-8 and 5-9). The distribution of structural units in the latter silicate system indicates the formation of larger particles than are usually formed in solutions with Rm=4.0 without the influence of CO_2 (see section 1.2). The decreasing Q3/Q4-ratio is a good indication for this.

Table 5-8
Structural distribution for a sodium silicate solution with 32wt%SiO_2 ; Rm=2.0

structural unit	non-aged	aged in CO_2-atm for 14 weeks
Q0	1.2	0.0
Q1	12.7	4.2
Q2cyc	3.7	1.0
Q2/Q3cyc	47.7	51.0
Q3	34.7	40.1
Q4	0.0	3.7

Table 5-9
Structural distribution for a sodium silicate solution with 25wt%SiO_2 ; Rm=4.0

structural unit	25wt% SiO_2 Rm=4.0 not aged	25wt% SiO_2 Rm=4.0 aged 7 months in CO_2 atm.
Q0	0.7	0.2
Q1	3.3	3.5
Q2cyc	0.0	0.0
Q2	21.4	20.6
Q3	52.3	48.7
Q4	22.3	27.0

1.5 Temperature-influence on silicate structures

In the literature the influence of increased temperature on the linewidth of the silicate resonances has been discussed[24,25] whereas no attention was drawn to the effect of increased temperatre on the structuring in silicate solutions, which is studied in this section.

The time that a representative silicate solution takes to adjust to high temperature as well as the time the system takes to readjust to room temperature is studied. The temperature was not raised above 85°C. All investigations at increased temperature have been carried out in closed vessels where no loss of water can occur.

It was found that an increase in temperature generally causes a general depolymerisation of the silicate system which is manifested in the decrease in the amount of Q3- and Q4-units parallel to an increase in the amount of the less condensed units (table 5-10, 5-11 and 5-14). Thus not only the viscosity is decreased and the mobility of the silicate particles is increased but the structuring of the system is changed. This is caused by a shifting of the exchange equilibrium between the structural units, which is discussed in detail in chapter 6-4, towards the structures with a lower degree of condensation.

room temperature

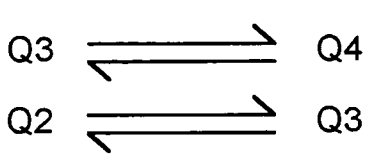

increased temperature

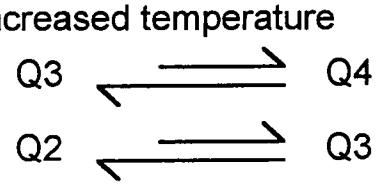

The new equilibrium between the structures at increased temperature only takes a period of 12 to 16 minutes to establish. However, the re-establishment of the

room-temperature equilibrium for the distribution of structural units after the heating of a silicate solution takes a much longer time (approximately 6 weeks). The results are presented in table 5-12 to 5-14.

The constant for the rate of exchange increases by a factor of more than 10 when the temperature is increased from 25°C to just 45°C. Thus it can be explained that during the heating process the structures adapt the new equilibrium of species much more quickly then during the cooling process. Nevertheless, the heating is reversible with respect to the structuring which shows that there are no irreversible physical changes taking place in the silicate system such as would be due to the loss of water.

Table 5-10
Distribution of structural units in a
sodium silicate solution with 30wt% SiO_2 and Rm=2.6

structural unit	T=300K	T=329K
Q0	0.75	1.0
Q1	6.7	7.0
Q2cyc	1.5	1.3
Q2/Q3cyc	36.45	37.6
Q3	47.2	46.8
Q4	7.4	6.3

Table 5-11
Distribution of structural units in a
sodium silicate gel with 33wt% SiO_2 and Rm=3.4

structural unit	T=300K	T=329K
Q0	0.0	1.0
Q1	5.6	6.1
Q2cyc	0.0	0.0
Q2/Q3cyc	25.6	29.1
Q3	50.2	49.4
Q4	18.3	14.4

Table 5-12
Distribution of structural units in a
sodium silicate solution with 25wt% SiO_2 and Rm=4.0 (enriched in ^{29}Si)
under the influence of heat as a function of time

time at 85°C/min	Q0	Q1	Q2	Q3	Q4
0	0.2	2.8	25.9	55.5	15.6
4	0.0	3.7	31.6	50.3	14.4
8	0.0	3.9	32.3	50.5	13.3
12	0.0	4.7	32.4	50.0	12.9
16	0.0	4.8	32.3	50.3	12.6

Table 5-13
Distribution of structural units in a
sodium silicate solution with 25wt% SiO_2 and Rm=4.0 (enriched in ^{29}Si),
the cooling process as a function of time after switching the heater off
(at the time of 0 min the silicate is still at 85°C)

time/min	Q0	Q1	Q2	Q3	Q4
0	0.0	4.8	32.3	50.3	12.6
8	1.0	4.0	28.5	53.2	13.3
16	0.4	3.9	25.6	56.5	13.6
24	0.2	2.6	26.8	56.6	13.8
56	0.3	3.3	26.3	57.0	13.1
88	0.5	4.2	24.6	57.3	13.4
280	0.5	3.7	26.9	55.0	14.0
536 (9hrs)	0.5	3.7	27.3	54.4	13.5

Table 5-14
Distribution of structural units in a
sodium silicate solution with 25wt% SiO_2 and Rm=4.0 (enriched in ^{29}Si)
under the influence of heat

	Q0	Q1	Q2	Q3	Q4
at 25°C	0.2	2.8	25.9	55.5	15.6
at 60°C	0.3	4.3	30.6	52.1	12.7
at 85°C	0.0	4.8	32.3	50.3	12.6
2 weeks after heating to 85°C	0.1	3.7	27.8	54.6	13.8
6 weeks after heating to 85°C	0.2	3.1	25.6	55.3	15.8

2. The sol/gel-transition in silicate systems

It is important to distinguish between the process of gelation, where colloidal particles join into chains and thereafter three-dimensional continuous networks, and the process of precipitation, where forces are present causing the colloidal particles to coagulate and form aggregates[13,23]. In the case of gelation taking place, the SiO_2 concentration of the structure formed does not exceed the SiO_2 concentration of the sol, whereas in the case of precipitation the aggregates formed contain a higher SiO_2-concentration than the original sol. Coagulants (causing precipitation) can be substantial amounts of salts, small amounts of water-miscible organic liquids, polymers or surfactants. In this chapter only the gelation process is investigated. This gelation goes *via* the formation of colloidal particles. The preparation of the silicate gels from silicate solutions is described in detail in chapter 3-4.2.

The sol/gel-transition is defined in this work as the point where the silicate solution is not easily fluid any more at room temperature though it is still fluid at 60°C. The silicate goes into a highly viscous state where it shows the property of very slow flow, i.e. it flows with a velocity of approximately 10cm/hr to 2cm/hr.

The viscosity of the silicate system shows a dramatic jump after the sol/gel-transition is passed as demonstrated in figure 5-7 (table 5-15 and 5-16).

Figure 5-7
Viscosity of sodium silicate sols and gels
The sols have the composition : 32wt% SiO_2 and Rm=2.0
25wt% SiO_2 and Rm=4.0
The gels have the composition : 39wt% SiO_2 and Rm=2.0
29wt% SiO_2 and Rm=4.0

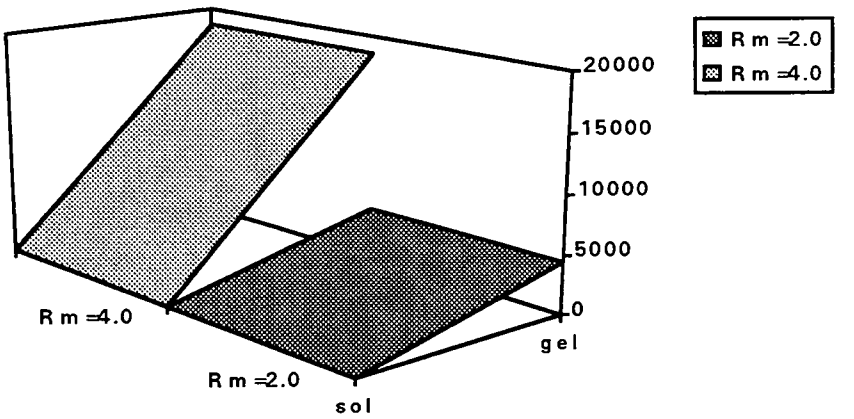

A clear change in the decline of the water activity of the silicate systems with increasing SiO_2 concentration was observed when the transition from a sol to a gel was passed (figure 5-8 and table 5-17 and 5-18).

Figure 5-8
Water activity of sodium silicates with Rm=2.0 and Rm=4.0

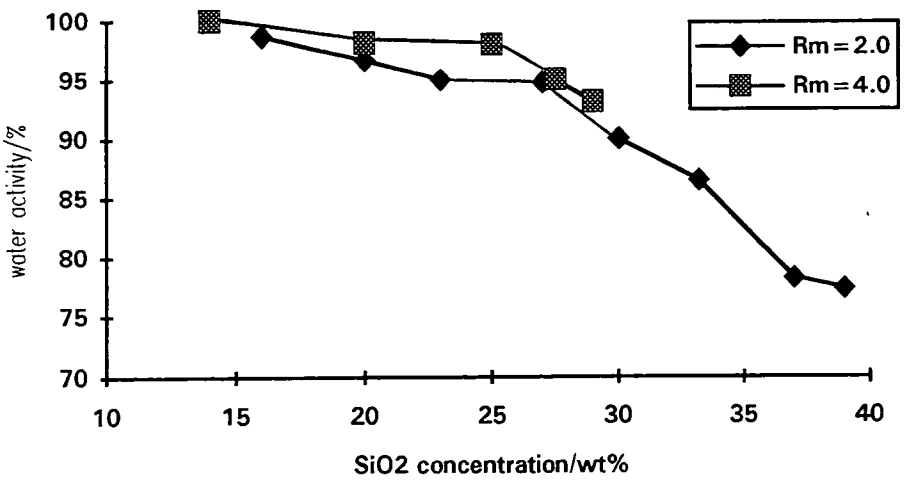

Along with the results from water activity measurements go results from DSC measurements (differential scanning calorimetry). These show an increase in the amount of water in the pore area (table 5-19) which means that the amount of colloidal material increases.

A clear transition from sol to gel can be seen in the T1 values as illustrated in figure 5-9 (table 5-20 to 5-23). When the SiO_2 concentration is increased the spin-lattice relaxation times pass a minimum exactly when the silicate solution is not fluid at room temperature any more.

The investigation of various molar ratios at increasing SiO_2 concentration shows that the sol/gel-transition, which is a constant physical parameter for each silicate system at a fixed molar ratio, is shifted to lower SiO_2 concentrations the higher the Rm-value.

The measurements show that the silicate solutions investigated are on the border of the sol/gel-transition and very near to the minimum in T1-values.

Figure 5-9

T1 relaxation times in dependency of the SiO_2 concentration and the Rm-value

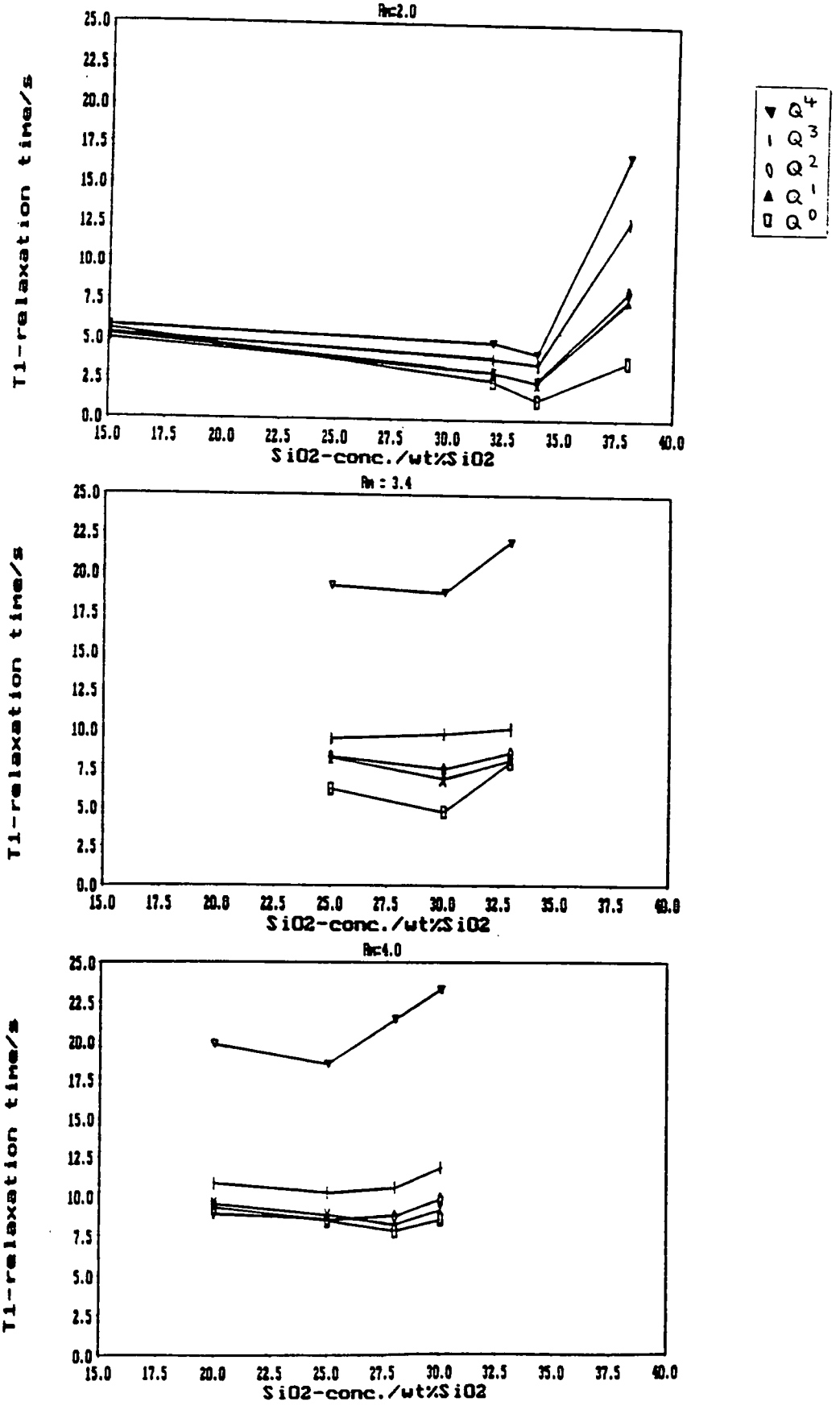

Table 5-15
Viscosity of a sodium silicate system with Rm=2.0

	25wt% SiO_2	32wt% SiO_2	39wt% SiO_2
viscosity/poise	0.3	7.1	4406.0

Table 5-16
Viscosity of a sodium silicate system with Rm=4.0

	25wt% SiO_2	29wt% SiO_2
viscosity/poise	0.9	18463.0

Table 5-17
Water activity of a sodium silicate system with Rm=2.0

SiO_2 concentration / wt%	water activity / %
16	98.7
20	96.7
23	95.0
27	94.7
30	90.0
33	86.5
37	78.2
39	77.3

Table 5-18
Water activity of a sodium silicate system with Rm=4.0

SiO_2 concentration/wt%	water activity/%
14	100.0
20	98.2
25	98.0
27.5	95.0
29	93.1

Table 5-19
DSC measurements on various sodium silicate systems

silicate	water in pore area in % of total water
Rm=2.0	
25wt% SiO_2	0.0
32wt% SiO_2	0.0
37wt% SiO_2	12.3
Rm=3.4	
30wt% SiO_2	10.0
33wt% SiO_2	15.6
Rm=4.0	
25wt% SiO_2	16.8
28wt% SiO_2	21.9

Table 5-20
T1-values
sodium silicate solution with Rm=2.0

structural unit	32wt% SiO_2	34wt% SiO_2	37wt% SiO_2	39wt% SiO_2
Q0	5.6	2.4	1.2	3.7
Q1	5.2	2.96	2.3	7.7
Q2cyc	5.0	3.0	2.4	8.2
Q2/Q3cyc	5.3	3.85	3.5	12.7
Q3	5.8	4.9	4.15	16.8
Q4	-	-	-	-

Table 5-21

T1-values in s in a sodium silicate solution with Rm=3.4

structural unit	25wt% SiO_2	30wt% SiO_2	33wt% SiO_2
Q0	6.2	4.7	7.9
Q1	8.2	6.9	8.1
Q2cyc	-	-	-
Q2/Q3cyc	8.3	7.5	8.6
Q3	9.4	50.0	10.1
Q4	19.2	18.8	22.0

Table 5-22

T1-values in s in a sodium silicate solution with Rm=3.8

structural unit	25.5wt% SiO_2	30wt% SiO_2
Q0	6.8	-
Q1	8.5	8.1
Q2cyc	-	-
Q2/Q3cyc	8.6	8.3
Q3	9.8	10.5
Q4	18.1	19.9

Table 5-23

T1-values in s in a sodium silicate solution with Rm=4.0

structural unit	20wt% SiO_2	25wt% SiO_2	28wt% SiO_2	30wt% SiO_2
Q0	9.3	8.4	7.8	8.5
Q1	9.5	8.8	8.2	9.1
Q2cyc	-	-	-	-
Q2/Q3cyc	8.9	8.5	8.7	9.8
Q3	10.8	10.2	10.5	11.8
Q4	19.8	18.5	21.4	23.3

The distribution of structural units does not show any obvious jumps when the sol/gel-transition is passed. It is characterised by a slight increase in the amount of Q4 units at the expense of the other structural units as illustrated in figure 5-10 and 5-11 (table 5-24 to 5-27).

Figure 5-10
Distribution of structural units with increasing SiO_2 concentration
The point where the sol/gel-transition is passed is marked with an asterisk

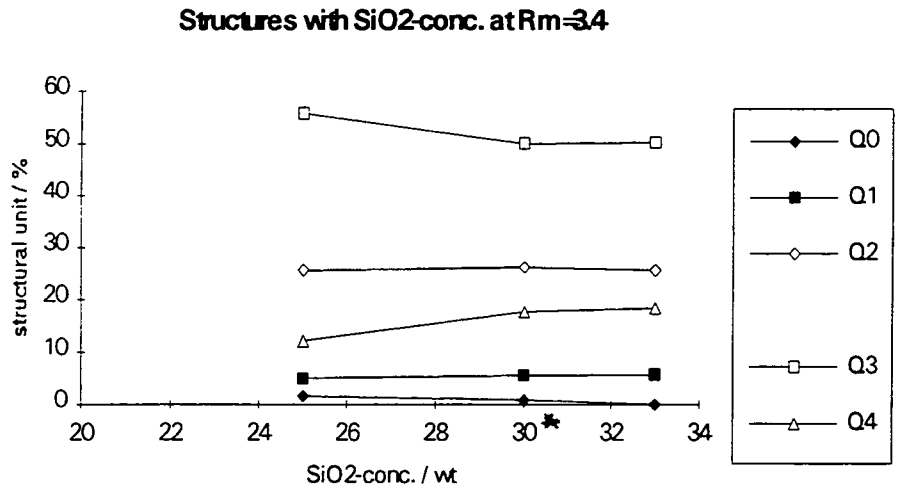

Figure 5-11
Distribution of structural units with increasing SiO_2 concentration
The point where the sol/gel-transition is passed is marked with an asterisk

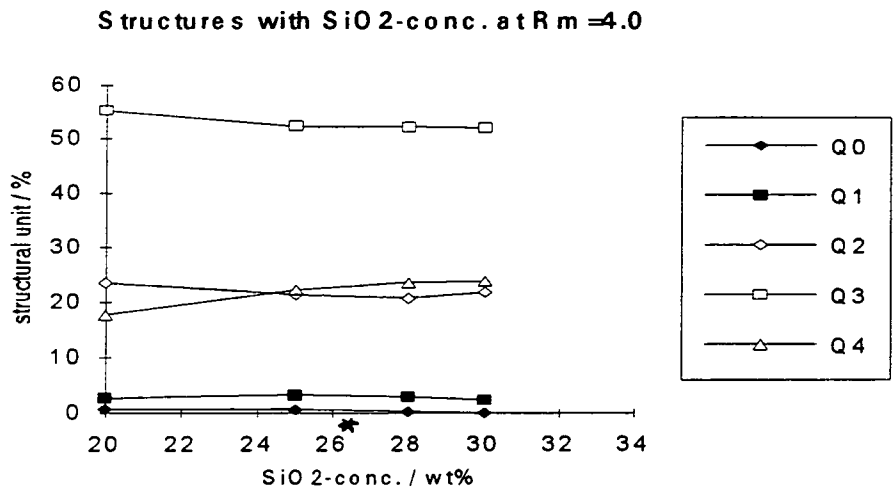

The self-diffusion coefficient for protons, which was measured using the PFG technique described in detail in chapter 3-2.6 and chapter 6-3, does not change very much when the transition from a sol to a gel is passed (table 5-28). This shows that the majority of the water molecules experiences a small restriction of their diffusive mobility in the gel.

The mobility of the sodium cations in a representative silicate is measured in terms of the spin-spin-relaxation time (measured with the CPMG sequence). Table 5-28 shows that the T2-value for sodium is decreased by a factor of about 2 in the gel. Therefore the mobility of the sodium cations in the gel is smaller than in the sol.

Considering all the experimental findings conclusions can be drawn about the formation of the gel and its nature. Considering that the colloidal particles do not have a hard-core structure (see chapter 6) only some of the Q3-units have to condense to Q4-units to cause a "lock-up" of the whole structure. This would make movements of the particles which have been condensed to a sort of inflexible "net" impossible. The "lock-up" of the whole structure is made clearly visible by viscosity measurements. These show that the viscosity of a silicate in the gel state is about 1600 times as big as the viscosity of a silicate in the sol state. The fact that the diffusional mobility of the protons is only little restricted in the gel compared to the sol suggests that the structure of the gel is not compact. The gel structure contains holes and pores just like the colloidal material in the sols and could therefore be described as an extended sol structure where silicate networks are interlinked to build largely extended networks.

Table 5-24

Distribution of structural units in a sodium silicate solution with Rm=2.0

structural unit	32 wt% SiO_2	37 wt% SiO_2	39 wt% SiO_2
Q0	1.1	0.7	0.8
Q1	12.3	12.3	11.1
Q2cyc	2.1	3.5	3.5
Q2/Q3cyc	50.1	46.4	45.1
Q3	34.4	35.6	36.7
Q4	0.0	0.6	2.8

Table 5-25

Distribution of structural units in a sodium silicate solution with Rm=3.4

structural unit	25wt% SiO_2	30wt% SiO_2	33wt% SiO_2
Q0	1.5	0.8	0.0
Q1	5.0	5.5	5.6
Q2cyc	0.0	0.0	0.0
Q2/Q3cyc	25.5	26.1	25.6
Q3	55.8	50.0	50.2
Q4	12.2	17.6	18.3

Table 5-26

Distribution of structural units in a sodium silicate solution with Rm=3.8

structural unit	25.5wt% SiO_2	30wt% SiO_2
Q0	0.9	0.0
Q1	4.7	3.0
Q2cyc	0.0	0.0
Q2/Q3cyc	23.2	24.3
Q3	51.5	51.5
Q4	19.7	21.2

Table 5-27
Distribution of structural units in a sodium silicate solution with Rm=4.0

structural unit	20wt% SiO_2	25wt% SiO_2	28wt% SiO_2	30wt% SiO_2
Q0	0.8	0.7	0.6	0.2
Q1	2.8	3.3	3.0	2.4
Q2cyc	0.0	0.0	0.0	0.0
Q2/Q3cyc	23.5	21.4	20.8	21.8
Q3	55.2	52.3	52.0	51.7
Q4	17.7	22.3	23.6	23.9

Table 5-28
Self-diffusion coefficient measured with the normal echo PFG pulse sequence (developed by Stejskal and Tanner[12]) of protons,
T2-value measured with the CPMG sequence of sodium,
in a sodium silicate system with Rm=4.0

	^{1}H D_{self}/cm^2s^{-1}	^{23}Na T2/ms
25wt% SiO_2 (sol)	7.5 E-6	2.2
28wt% SiO_2 (gel)	5.1 E-6	1.2

3. Potassium silicate solutions

It has been found that the dissolution rate of silica in caustic solution increases in the order :

LiOH ~ CsOH < RbOH ~ NaOH < KOH[14]

This is due to two contrary effects governing the dissolution rate, the strength of the hydration shell and the strength of the cation adsorption on the silica surface. Contradicting results have been found regarding the dependency of the

structuring in the silicates on the cation, some claiming that in spite of the profound effect of the cation on the silica dissolution rate there is no effect on the distribution of species[14,16,19] and others claiming that there is an effect of the cation on the silicate anion distribution[17,22] or the degree of polymerisation of the system[18].

In these studies potassium silicate solutions do not show significant differences in the distribution of structural units compared to sodium silicate solutions of the same composition as shown in table 5-29 to 5-31. Therefore it can be concluded that such a change of cation does not exert an effect on the development of structures in the silicate systems. There are no direct Si-O-cation bonds in the investigated silicate solutions. The cation exists in the silicate system in the hydrated form which is in the case of sodium and potassium, with six water molecules bound octahedrally in the hydration shell. The amount of water in the hydration shell of the cation increases with decreasing cation radius as well as the adsorption on the silica surface[15]. Nevertheless the size of the potassium ion would allow more water molecules in a second hydration shell.

In these investigations an important observation was made concerning the influence of a change of cation from sodium to potassium on the sol/gel-transition. Two potassium silicate solutions of the composition 30wt% SiO_2 and Rm=3.4 and 23wt% SiO_2 with Rm=4.0 have passed the sol/gel-transition and are behaving like gels whereas the corresponding sodium silicate solutions are still on the sol-side of the sol/gel-transition. In figure 5-12 (table 5-32 to 5-34) the difference in the mobility of the silicate units between the two silicate systems with different cations can clearly be seen.

Figure 5-12
Mobility of silicate units in terms of the rotational correlation time in s
(for calculation see chapter 6-2.2)
SOSI sodium silicate with 30wt% SiO_2 and Rm=3.4
POSI potassium silicate with 30wt% SiO_2 and Rm=3.4

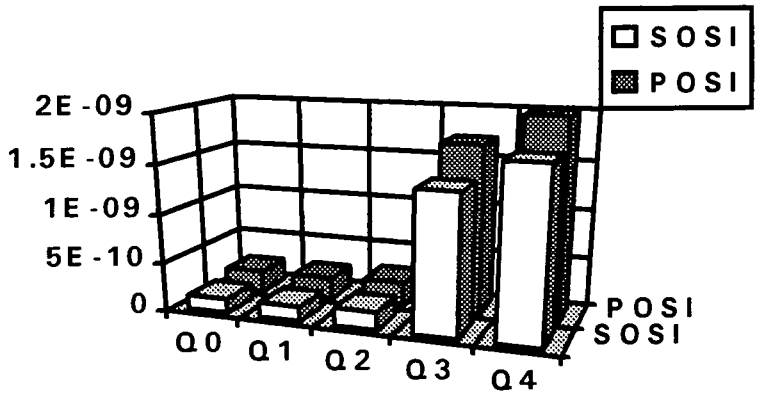

The transition from sol to gel at fixed Rm is at lower SiO_2 concentrations for potassium silicate solutions compared to sodium silicate solutions. This could be caused by the larger size of potassium ions compared to sodium ions which would allow an enlarged second hydration shell and thus take more water molecules out of the silicate system than sodium does. Another explanation is that the larger potassium ion shows a higher selectivity to ion-pairing with larger silicate anions than the sodium ions. Thus the mobility of the larger units is more restricted by silicate-cation-silicate pairing (see section 6) in potassium silicate solutions than in sodium silicate solutions.

The fact that the structural distribution of these potassium silicates past the sol/gel-transition does not differ very much in Q3 and Q4 content from the sodium silicates which still are sols supports the theory that there is a 'lock-up' of the overall structure for which only a few more Q2 and Q3 units have to condense (see section 2).

Table 5-29
Distribution of structural units in silicate solutions with 30 wt% SiO_2 and Rm=2.6

structural unit	sodium silicate	potassium silicate
Q0	0.75	0.4
Q1	6.7	6.0
Q2cyc	1.5	0.8
Q2/Q3cyc	36.45	35.1
Q3	47.2	50.4
Q4	7.4	7.3

Table 5-30
Distribution of structural units in silicate solutions with 30 wt% SiO_2 and Rm=3.4

structural unit	sodium silicate	potassium silicate
Q0	0.8	0.0
Q1	5.5	4.2
Q2cyc	0.0	0.0
Q2/Q3cyc	26.1	24.7
Q3	50.0	52.0
Q4	17.6	18.1

Table 5-31

Distribution of structural units in silicate solutions with

25wt% SiO_2;Rm=4.0(Na silicate) 23wt% SiO_2;Rm=4.0(K silicate)

structural unit	sodium silicate	potassium silicate
Q0	0.7	0.1
Q1	3.3	4.0
Q2cyc	0.0	0.0
Q2/Q3cyc	21.4	22.0
Q3	52.3	51.1
Q4	22.3	22.8

Table 5-32

T1-values in s in a sodium silicate solution with 30wt% SiO_2 and Rm=3.4

structural unit	500MHz	600MHz	$T1_{600}/T1_{500}$
Q0	4.7	5.0	1.06
Q1	6.9	7.3	1.06
Q2cyc	-	-	-
Q2	7.5	8.1	1.08
Q3	9.8	11.9	1.21
Q4	18.8	23.4	1.24

Table 5-33

T1-values in s in a potassium silicate gel with 30wt% SiO_2 and Rm=3.4

structural unit	500MHz	600MHz	$T1_{600}/T1_{500}$
Q0	6.1	6.6	1.09
Q1	7.4	8.1	1.09
Q2cyc	-	-	-
Q2	10.6	11.7	1.11
Q3	11.9	14.8	1.24
Q4	18.6	23.8	1.28

Table 5-34

Correlation times in silicate systems with 30wt% SiO_2 and Rm=3.4

structural unit	**sodium silicate sol'n**	**potassium silicate sol'n**
Q0	1.5E-10s	2.2E-10s
Q1	1.5E-10s	2.2E-10s
Q2cyc	-	-
Q2	1.8E-10s	2.5E-10s
Q3	1.4E-9s	1.7E-9s
Q4	1.7E-9s	2.0E-9s

4. Si-Si couplings

Si-Si couplings have been obtained for natural abundance zeolite structures using the method of 2D-INADEQUATE[26] and $^{29}Si/^{29}Si$ COSY[27]. The 3-D lattice connectivities for these highly crystalline and highly symmetrical materials were obtained with great accuracy.

In contrast to the zeolites investigated by Fyfe et.al.[26,27], highly viscous silicate systems such as the ones investigated in this thesis contain

material of no higher order formed by random condensation of silicate units (see section 6). This complicates the determination of the connectivities in such a silicate solution. In order to obtain 2D-INADEQUATE data in a reasonable time a silicate solution containing 25wt% SiO_2 with Rm=4.0, which is enriched in ^{29}Si, is used as a representative silicate solution.

The connectivities observed in the 2D-INADEQUATE spectrum are listed in table 5-35. The 2D-INADEQUATE spectrum is shown in figure 5-13. Since typical values for the scalar coupling between silicon in siloxy systems are $^{2}J(Si\text{-}O\text{-}Si)$ of 10 to 15 Hz[33], the value of the fixed delay d4 is chosen to be 20ms in order to get optimum double quantum coherence.

Table 5-35
Si-Si connectivities in a sodium silicate solution with 25wt% SiO_2 and Rm=4.0 *via* 2D-INADEQUATE (figure 5-13)

	Q0	Q1	Q2	Q3	Q4
Q0					
Q1			?		
Q2		?		×	
Q3			×		×
Q4				×	

In the 2D-INADEQUATE spectrum couplings between the Q4- and the Q3-units along with couplings between the Q3- and Q2-units are found. The intensity of the double quantum coherence for the Q2-units is very low. Thus it can not be excluded that the Q2- and Q1-units are connected and give rise to $^{29}Si\text{-}^{29}Si$ couplings although they are not resolved in the 2D-INADEQUATE spectrum due to the very low intensity of their double quantum coherence.

Figure 5-13
2D-INADEQUATE of a sodium silicate solution with
25wt% SiO_2 and Rm=4.0 enriched in ^{29}Si
relaxation delay 60s, fixed delay 20ms, transients 32, dummy transients 4,
acquisition time 0.03s, spectral width 89ppm, 128 experiments

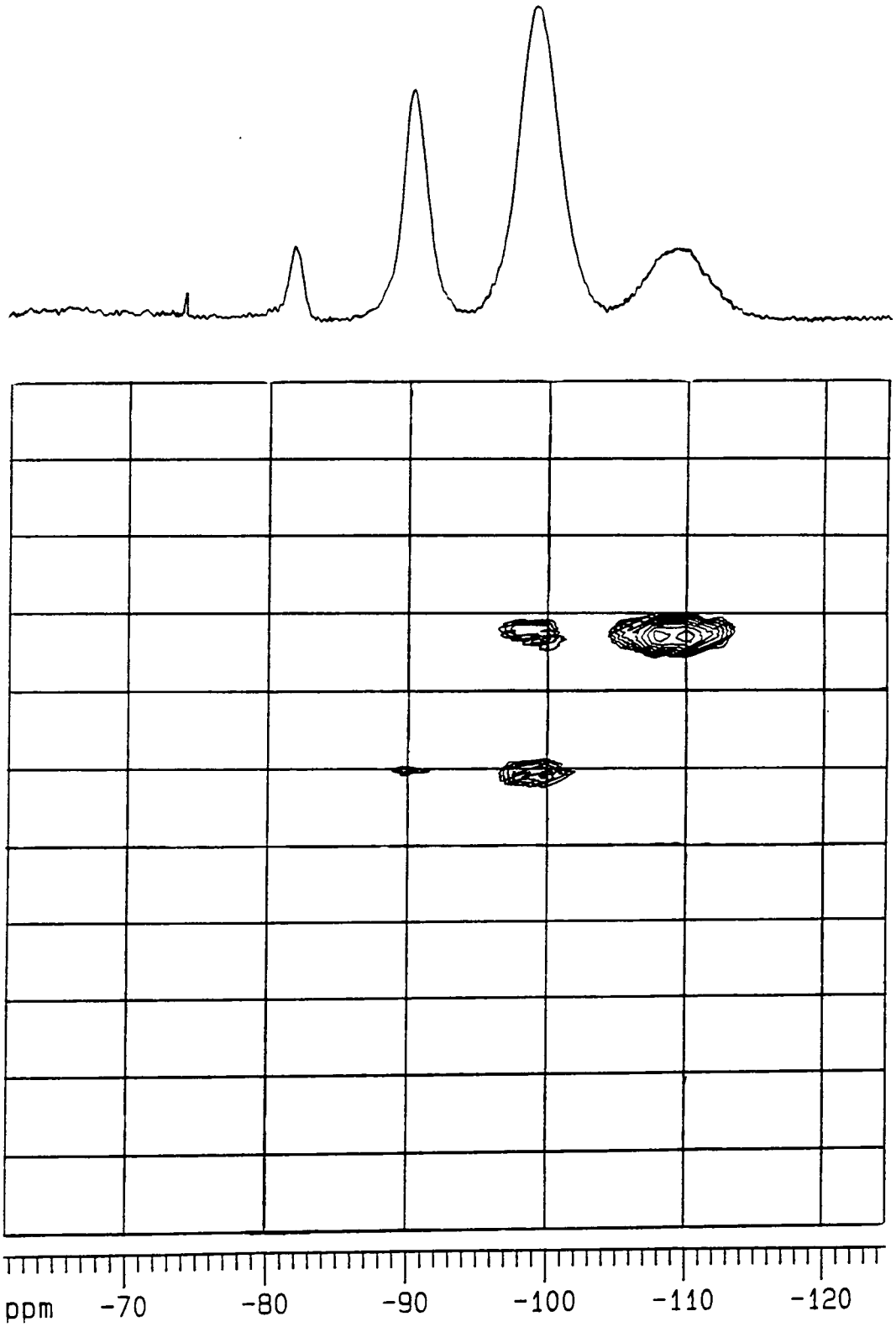

5. The nature of the particle surface

The ^{29}Si spin-lattice relaxation times for silicate systems containing the aqueous solvent in different H_2O/D_2O ratios can give information about the nature of the uncondensed silicate bonds. If the T1-values for silicates with different H_2O/D_2O ratios are identical, it can be concluded that protonated hydroxyl groups prevail in the silicate units. If, however, the T1-values differ there is a certain amount of deprotonation of the siloxane groups.

The spin-lattice relaxation times of representative silicate solutions containing 100% H_2O, 50% H_2O/50% D_2O and 2% H_2O/98% D_2O were measured by inversion recovery. The results presented in table 5-36 to 5-38 show that the silicate solution with the largest difference in T1 values is the one with the highest alkalinity (Rm=2.0). The silicate solutions with a higher degree of condensation (lower alkalinity) only show slight differences in the T1-values of the less condensed structural units, Q0 and Q1 unit, whereas the T1-values for the Q2, Q3, and Q4 units remain unchanged within the limit of errors.

It can be concluded that the higher the alkalinity of the silicate solution, the more deprotonated surface groups are found. The structural units with low connectivity, Q0 and Q1, are far more sensitive to deprotonation than the structural units with higher connectivity. Generally the difference in T1-values with increasing D_2O content is fairly small, even in the silicate with the highest alkalinity (Rm=2.0), considered that the error in the experimental T1-values can be up to 10%. Therefore the degree of deprotonation of surface groups is generally small and is negligible in silicate solutions with Rm-values bigger than 2.6.

It can be concluded that the surface acts as a potential proton donor. The proton exchange mechanism is enhanced by the presence of a structured network of adsorbed species (a monolayer), in which the molecules are interconnected, for instance by hydrogen bonds. The rate limiting process is

the back-donation to the surface sites and there is no direct correlation between the pKa of the surface and the rate of proton transfer[34]. Proton jump frequencies in completely homogeneous liquids are generally in the region of 10^{12} s^{-1}. They are smaller when a solid donor and an adsorbed acceptor are involved[34].

hydrated cation - H_2O rate of proton transfer = 10^{10} s^{-1}

Aerogel - NH3 rate of proton transfer = $5*10^{8}$ s^{-1}

Xerogel - CH3OH rate of proton transfer = $3*10^{7}$ s^{-1}

Table 5-36

T1-values in s in sodium silicate solutions with 32wt% SiO_2 and Rm=2.0

	with 100% H_2O	with 98% D_2O
Q0	2.5	3.7
Q1	3.0	4.0
Q2cyc	3.1	4.2
Q2	3.9	5.0
Q3	5.0	5.9
Q4	-	-

Table 5-37

T1-values in s in sodium silicate solutions with 30wt% SiO_2 and Rm=2.6

	with 100% H_2O	with 50% H_2O	with 98% D_2O
Q0	3.2	3.8	4.6
Q1	3.4	3.9	4.8
Q2cyc	3.4	3.7	4.0
Q2	4.5	4.9	4.7
Q3	6.9	6.5	7.0
Q4	12.4	12.1	12.0

Table 5-38
T1-values in s in sodium silicate solutions with 25.5wt% SiO_2 and Rm=3.8

	with 100% H_2O	with 50% H_2O	with 98% D_2O
Q0	5.6	6.3	7.8
Q1	7.4	8.1	8.4
Q2cyc	-	-	-
Q2	8.4	8.3	8.9
Q3	10.0	10.5	9.9
Q4	20.4	19.9	20.2

6. Model for colloidal particles

A model for the structure of colloidal particles has been obtained on the basis of the measurements described in this chapter, particularly DSC measurements, investigations of the sol/gel-transition and ^{29}Si T1 values.

Colloidal silicate particles are the result of random condensation of silicate building units. Thus a network such as the one illustrated in figure 5-14 containing holes ('pores') in which water molecules can be trapped is formed as opposed to a 'hard-core' structure which would be the result of an ordered condensation.

Figure 5-14
The structure of a colloidal particle

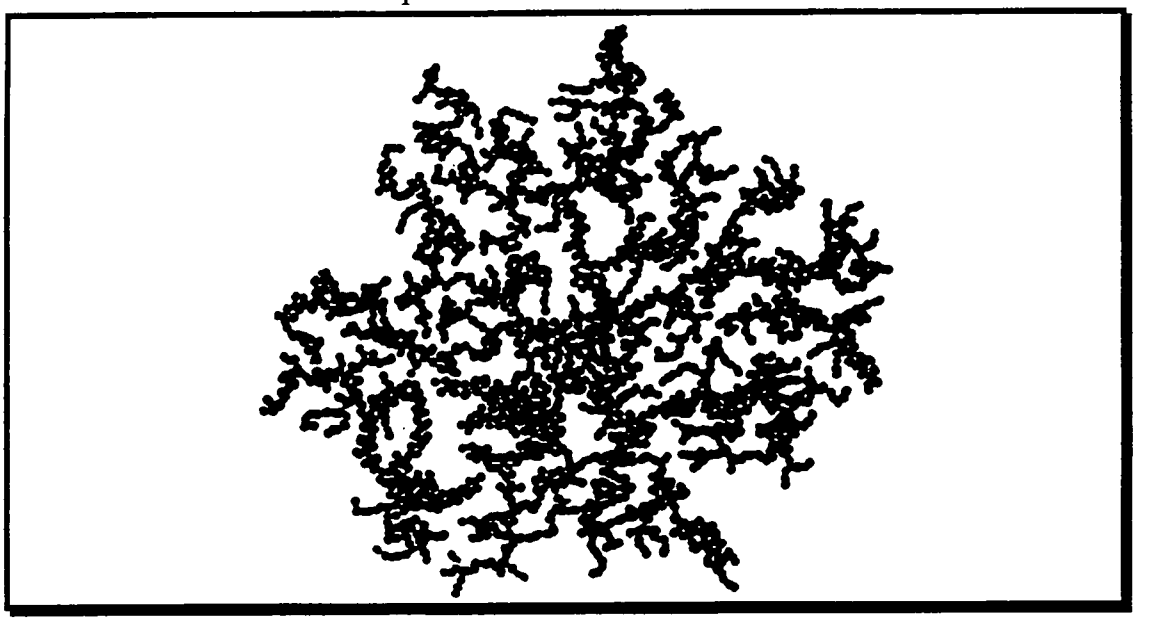

DSC measurements (table 5-19) show the existence of pore water in silicate systems in which Q4 units are found and which thus contain colloidal material[6]. Pore water can only be found in structures which can accommodate water molecules such as three-dimensional networks with channels or pores of a minimum size. In the DSC measurements the pore water is distinguished from free water by its low freezing point (-25°C as opposed to 0°C). Studies of the sol/gel-transition (see section 2) show that in silicate solutions extended networks exist which only have to extend a little further to cause a lock-up of the structure to a gel. The ^{29}Si spin-lattice relaxation times of the Q4-units are generally about a factor of 2 larger than the ^{29}Si spin-lattice relaxation times of the Q3-units. This suggests that there must be protons in the reach of the Si atoms which would be impossible if colloidal particles had a hard-core structure. Protons can only contribute to the relaxation of the Si atoms in Q4 units if there are water molecules located in pores of the network. The fact that the diffusion constant of protons undergoes no major change when the transition from a sol to a gel is passed (table 5-28) indicates that the pores or channels in the silicate networks must be large enough to allow diffusive motion of the water molecules.

In the low molar ratios of SiO_2 to Na_2O there is a larger amount of deprotonated hydroxyl groups (SiO^- bonds) on the particle surfaces than in high molar ratios (see section 5), the charge on the surface preventing further condensation to larger units.

$$SiOH + OH^- \longrightarrow SiO^- + H_2O$$

If the surface sites of the colloidal particles are negatively charged, hydrated sodium ions are adsorbed near the ionised sites to form a neutral complex. *Via* these hydrated sodium ions co-ordination links between charged particles as shown in figure 5-15 can be formed.

Figure 5-15

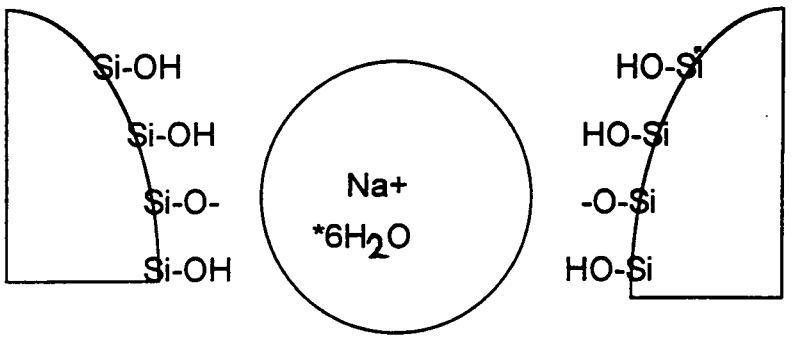

The higher the molar ratio is, the higher is the degree of condensation of the system and the more hydroxyl groups on the particle surfaces and in the pores of the network are in the protonated state (SiOH bonds). In fact spin-lattice relaxation measurements for silicate solutions with Rm-values from 2.6 up to 3.8 with varying H_2O-contents of 100 % H_2O, 50 % H_2O/ 50% D_2O and 95 % D_2O show (section 5) that the T1-values of the higher condensed structural units (Q2, Q3 and Q4 units) are independent of the proton-content of the solvent. Thus the hydroxyl groups on the surface of the colloidal particles are fully protonated. There is evidence gained from viscosity measurements that on fully protonated surfaces a monolayer of water molecules, which is fairly immobilised, is adsorbed on the uncharged surface[28]. On these surfaces the hydrated sodium ions are not directly adsorbed. The water layer on the surface can be more strongly adsorbed on OH-groups in geminal positions on Si ($Si(OH)_2$) than on isolated OH-groups (SiOH)[29]. Even on silica surfaces, which are considered to be fully dehydrated, a substantial number of residual OH sites is found on the surface part of which are in geminal position[30].

Silicate sols contain colloidal material with the above-mentioned pore-structure, which is dissolved and stabilised in the systems. Silicate gels contain a network of colloidal material interlinked by condensation. The size of the colloidal material in these gels is undefined since it is rather a porous network than discrete particles with pore structure. There is a profound difference

between colloidal and undissolved silica. Colloidal silica is dissolved and the silicate system is homogeneous, whereas undissolved silica sinks to the bottom of the system as a precipitate and the system is inhomogeneous. This distinction is of particular importance (chapter 7).

Literature :

1 R. K. Harris, C. T. G. Knight, J. Chem. Soc. Faraday Trans. II, **79** (1983) 1525

2 R. K. Harris, C. T. G. Knight, J. Chem. Soc. Faraday Trans. II, **79** (1983) 1539

3 C. T. G. Knight, J. Chem. Soc. Dalton Trans. (1988) 1457

4 R. K. Harris, C. T. G. Knight, W. E. Hull, ACS Sym. **194** (1982) 79

5 H. C. Marsmann, Z. Naturforsch. **29b** (1974) 495

6 E. K. F. Bahlmann, R. K. Harris, K. Metcalfe, E. G. Smith, Magn. Reson. Chem. **31** (1993) 743

7 I. L. Svensson, S. Sjoeberg, L-O. Oehman, J. Chem. Soc. Faraday Trans. I, 82 (1986) 3635

8 R. K. Iler, Soluble Siicates, J. S. Falcone (Ed.), ACS Symposium Series **194** (1982) 95

9 S. D. Kinrade, T. W. Swaddle, Inorg. Chem. **27** (1988) 4253

10 G. Engelhardt, D. Zeigin, H. Jancke, D. Hoebbel, W. Wieker, Z. Anorg. Allg. Chem. **418** (`1975) 17

11 A. V. McCormick, A. T. Bell, C. J. Radke, Zeolites 7 (1987) 183

12 E. O. Stejskal, J. E. Tanner, J. Chem. Phys. **42**, No.1, (1965) 288

13 R. K. Iler, The Chemistry of Silica, Wiley-Interscience, New York (1979)

14 P. W. J. G. Wijnen, T. P. M. Beelen, J. W. de Haan, Colloids and surfaces, **45** (1990) 255

15 J. Depasse, A. Watillon, J. Colloid Interface Sci., **33** (1970) 431

16 S. D. Kinrde, T. W. Swaddle, J. Am. Chem. Soc., **108** (1986) 7159

17 P. W. J. G. Wijnen, PhD Thesis, Technical University of Eindhoven (1990)

18 R. K. Harris, R. H. Newman, J. Chem. Soc. Faraday Trans. II **73** (1977) 1204

19 C. T. G. Knight, PhD Thesis, University of East Anglia (1982)

20 D. W. Sindorf, G. E. Maciel, J. Phys. Chem., **87** (1983) 5516

21 R. K. Harris, M. J. O'Connor, E. H. Curzon, O. W. Howarth, J. Magn. Reson., **57** (1984) 115

22 A. V. McCormick, A. T. Bell, C. J. Radke, Mat. Res. Soc. Symp. Proc., Vol. **111** (1988) 107

23 C. J. Brinker, K. D. Keefer, D. W. Schefer, R. A. Assink, B. D. Kay, C. S. Ashley, J. Non-Cryst. Solids, **63** (1984) 45

24 L. Griffiths, C. S. Cundy, R. J. Plaisted, J. Chem. Soc. Dalton Trans. (1986) 2265

25 R. K. Harris, J. Jones, C. T. G. Knight, R. H. Newman, J. Mol. Liquids **29** (1984) 63

26 C. A. Fyfe, Y. Feng, H. Gies, H. Grondey, G. T. Kokotailo, J. Am. Chem. Soc., **112** (1990) 3264

27 C. A. Fyfe, H. Gies, Y. Feng, J. Am. Chem. Soc., **111** (1989) 7702

28 R. L. Dalton, R. K. Iler, J. Phys. Chem., **60** (1956) 955

29 K. Klier, A. C. Zettlemoyer, J. Colloid Interface Sci., **58** (1977) 216

30 A. P. Legrand, H. Taibi, H. Hommel, P. Tougne, S. Leonardelli, J. Non-Cryst. Solids, **155** (1993) 122

31 G. Engelhardt, D. Michel, High Resolution Solid State NMR of Silicates and Zeolites, John Wiley and Sons, New York (1987)

32 G. Engelhardt, H. Jancke, D. Hoebbel, W. Wieker, Z. Chem., **14** (1974) 109

33 J. Schraml, J. M. Bellama in: Determination of Organic Structures by Physical methods, F. C. Nachod, J. J. Zuckerman, E. W. Randall (Eds.), Vol.6, Ch.4, Academic Press, New York, London, San Francisco (1976)

34 H. A. Resing, C. G. Wade, Magnetic Resonance in Colloid and Interface Science, ACS Symposium Series 34, Washington (1976)

35 E. K. F. Bahlmann, Diplomarbeit, Technical University of Braunschweig, 1992

6. Mobility

1. Rheology measurements

Viscosity measurements at constant shear rate and constant stress give an idea about the fluid behaviour of the sample, whereas viscosity measurements at varied stress are used to investigate the flow behaviour. If the viscosity is independent of the stress, the system shows Newtonian behaviour, which is typical for liquids. If the viscosity decreases with increasing stress non-Newtonian behaviour is present, which is typical for complex, highly-interlinked systems.

All experiments have to be carried out in the atmosphere due to the set-up of the instrument. Therefore the duration of the individual experiments is limited, since the samples change owing to evaporation of water and the influence of CO_2. Rheology experiments at varied stress are carried out in such a way that the instrument adjusts the shear rate according to changed stress. All experiments are carried out at constant temperature (25°C).

The results of viscosity measurements at constant stress are presented in table 6-1 below.

Table 6-1
Viscosity of sodium silicate systems measured at constant stress using a 4° cone, stress 4774 N m^{-2}, shear rate 1 s^{-1}

sample	viscosity / Pa s
25wt% SiO_2 and **Rm=2.0** (sol)	0.03
32wt% SiO_2 and **Rm=2.0** (sol)	0.71
39wt% SiO_2 and **Rm=2.0** (gel)	440.6
25wt% SiO_2 and **Rm=4.0** (sol)	0.09
29wt% SiO_2 and **Rm=4.0** (gel)	1846.3

The viscosity of sodium silicates with identical SiO_2 concentrations increases with increasing Rm-value. This shows that the rigidity of a silicate

system is directly related to the degree of condensation, which is higher for higher Rm-values. At constant Rm-value the viscosity increases with increasing SiO_2 concentration, with a very drastic change in viscosity when the transition from a sol to a gel is passed.

As illustrated in figure 6-1 the silicate sols (silicate solutions) all show Newtonian behaviour, whereas for the silicate gels non-Newtonian behaviour is found at high stress, but the decrease in viscosity with increasing stress levels off at a shear rate of ~ 1 s^{-1}. The change in flow behaviour from a sol to a gel shows that the structuring in the latter is more rigid, along with a far greater degree of interlinking than in the former.

Figure 6-1
Viscosity in Pa s as a function of the shear rate, illustrating the flow behaviour of sodium silicate solutions
[25R4 = 25wt% SiO_2 and Rm=4.0 (sol)
32R2 = 32wt% SiO_2 and Rm=2.0 (sol)
39R2 = 39wt% SiO_2 and Rm=2.0 (gel)
29R4 = 29wt% SiO_2 and Rm=4.0 (gel)]

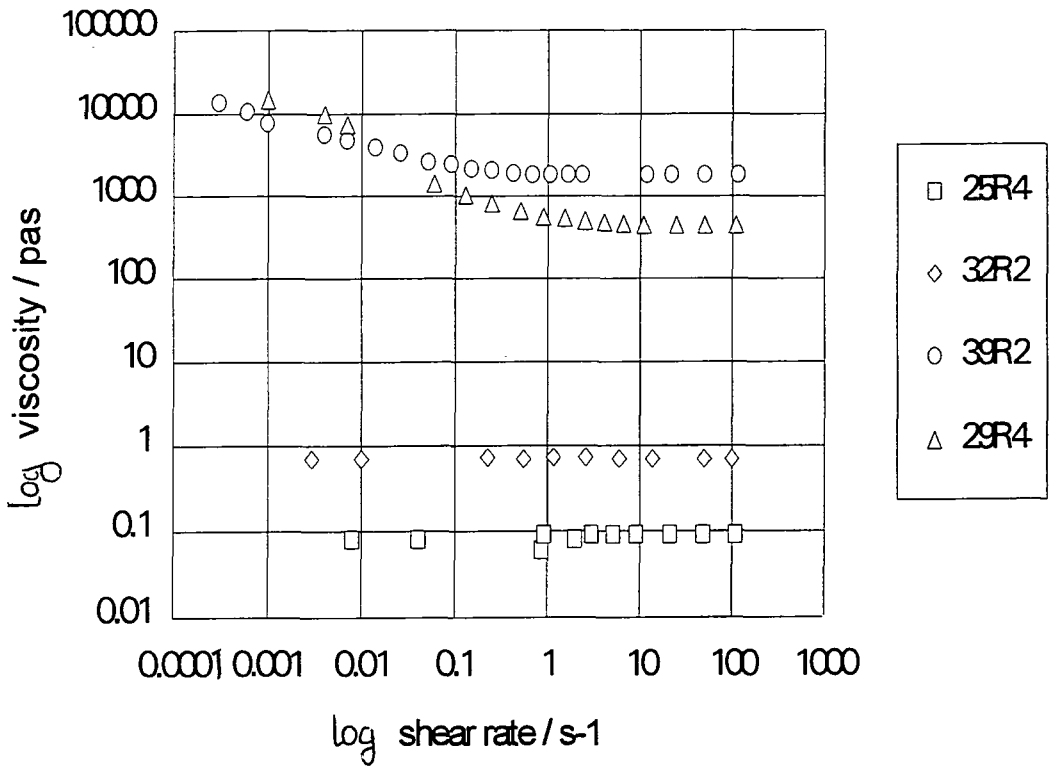

2. ^{29}Si mobility

2.1 Mobility model

2.1.1 High or low motion side of T1-minimum

There are several experimental results supporting the statement that the correlation times of the species in the silicate solutions investigated in this thesis, which are on the border of the sol/gel-transition, are not within the extreme narrowing region. The condition for extreme narrowing is that the spectral density terms J(ωX-ωA), J(ωX+ωA) and J(ωA) (discussed in detail in chapter 2-3.1) are equal (A ≡ ^{29}Si, X ≡ ^{1}H). This is the case for correlation times not longer than $1*10^{-10}$ seconds for 500 MHz (taking the average error in T1-values of ~8% into consideration) (see table 6-2). The minimum of T1 is at $\tau c = 1/\omega o = 1.6*10^{-9}$ s.

Table 6-2
Calculation of J(ωX-ωA), J(ωX+ωA) and J(ωA) as a function of τc
(the signs of wA and wX are positive since $\nu = |\gamma/2\pi| B$ [7])

τc/s	J(ωx-ωA)	J(ωx+ωA)	J(ωA)
5E-12	9.998E-12	9.997E-12	9.999E-12
1E-11	1.999E-11	1.997E-11	1.999E-11
5E-11	9.845E-11	9.66E-11	9.991E-11
8E-11	1.538E-10	1.468E-10	1.59E-10
1E-10	**1.882E-10**	**1.754E-10**	**1.992E-10**
4E-10	3.98E-10	2.47E-10	7.53E-10
8E-10	3.18E-10	1.61E-10	1.28E-9
1E-9	2.74E-10	1.33E-10	1.44E-9
8E-9	3.96E-11	1.78E-11	6.16E-10
1E-8	3.17E-11	1.43E-11	5.0E-10

The experimental observations leading to the conclusion that the correlation times of highly condensed silicate systems are not within the region where the extreme narrowing condition is fulfilled are discussed in the following paragraphs.

Temperature influence :

The T1-values decrease with increasing temperature which is only the case for solutions on the low-motion side of the T1-minimum (tables 6-3 to 6-5). To make sure that no water evaporates the temperature cannot be raised above approximately 85°C . The effect of increased temperature on the structural distribution is a decrease in the amount of highly condensed units (Q3 and Q4) parallel to an increase in the amount of units with a low degree of condensation (see chapter 5-1.5). This depolymerization of structures makes them even more mobile than the increased movement caused by the raised temperature alone does. If the correlation times of the silicate species were located on the low-motion side of the T1-minimum the T1 should decrease, whereas if they were found on the fast-motion side the T1-values would increase with increasing temperature (increasing mobility). The silicate solution with 25wt% SiO_2 and Rm=4.0 is supposed to be nearer the T1-minimum than the other solutions as the same temperature increase as for all other silicate solutions causes a comparatively smaller decrease in the T1-values.

Table 6-3

T1-values in s for a sodium silicate solution with 30wt% SiO_2 and Rm=2.6

structural unit	T=300K	T=329K
Q0	4.6	3.6
Q1	5.8	4.3
Q2cyc	5.0	3.8
Q2/Q3cyc	5.6	4.8
Q3	7.0	5.6
Q4	12.65	10.6

Table 6-4

T1-values in s for a sodium silicate solution with 25wt% SiO_2 and Rm=4.0

structural unit	T=300K	T=329K
Q0	7.3	6.8
Q1	7.6	7.0
Q2cyc	-	-
Q2/Q3cyc	8.1	7.4
Q3	9.1	8.0
Q4	17.8	16.4

Table 6-5

T1-values in s for a sodium silicate gel with 33wt% SiO_2 and Rm=3.4

structural unit	T=300K	T=329K
Q0	7.9	5.9
Q1	8.1	6.1
Q2cyc	-	-
Q2/Q3cyc	8.6	6.9
Q3	10.1	7.9
Q4	22.0	16.4

Spin-spin relaxation times :

The T2-values are much shorter than the T1-values (figure 6-2) which generally is a characteristic for systems where $\tau^2\omega o^2 >> 1$. In this case, however, it has to be considered that chemical exchange takes place between the Si-units (see section 4 of this chapter). This causes the magnetisation to fan out more quickly once it is in the xy-plane so that T2 is shortened by the exchange[16].

Figure 6-2
Comparison of T1- and T2-values in s for sodium silicate solutions :

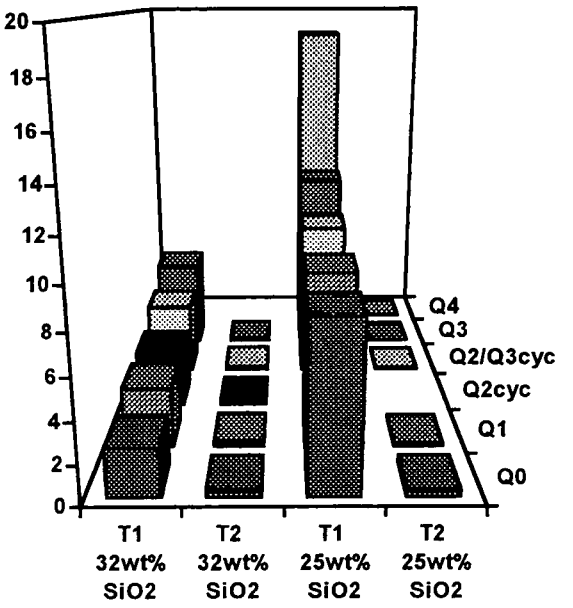

Bo-dependence of spin-lattice relaxation times :

The T1-values are field-dependent and though the difference in T1-values at different fields is not very big it is clear and consistent in all the measurements (tables 6-6 to 6-9). It can thus be concluded that the correlation time of the Si-units in the silicate solutions is not very far from the minimum in T1-values where $\tau c = 1/\omega o$.

Tables 6-6 to 6-9
T1-values at different field-strengths (proton resonance frequencies)

Table 6-6
T1-values in s for a sodium silicate solution with 30wt% SiO_2 and Rm=2.6

structural unit	250MHz	500MHz
Q0	4.1	3.8
Q1	4.5	3.9
Q2cyc	-	3.7
Q2/Q3cyc	4.0	4.9
Q3	5.4	6.5
Q4	8.3	12.1

Table 6-7
T1-values in s for a sodium silicate solution with 25wt% SiO_2 and Rm=4.0

structural unit	250MHz	500MHz	600MHz
Q0	-	8.4	8.6
Q1	6.8	8.8	8.9
Q2cyc	-	-	-
Q2/Q3cyc	7.6	8.5	9.9
Q3	8.7	10.2	12.2
Q4	12.8	18.5	23.2

Table 6-8
T1-values in s for a sodium silicate gel with 33wt% SiO_2 and Rm=3.4

structural unit	250MHz	500MHz
Q0	-	7.9
Q1	5.5	8.1
Q2cyc	-	-
Q2/Q3cyc	6.1	8.6
Q3	7.9	10.1
Q4	10.9	22.0

Table 6-9
T1-values in s for a sodium silicate gel with 30wt% SiO_2 and Rm=4.0

structural unit	500MHz	600MHz
Q0	8.5	-
Q1	9.1	10.5
Q2cyc	-	-
Q2/Q3cyc	9.8	10.4
Q3	11.8	15.2
Q4	23.3	31.6

2.1.2 Relaxation mechanism for ^{29}Si nuclei

The general requirement for spin-lattice relaxation is a magnetic interaction fluctuating at the resonance frequency. The relevant mechanisms, which can provide the appropriate conditions, are discussed in chapter 2-3.2. The mechanisms for spin-lattice relaxation in silicate solutions have only been dealt with in a fairly speculative way so far[1,2,27] using silicates with lower degrees of condensation than found in these studies. Different conclusions were drawn in the past, one assuming relaxation of ^{29}Si to be dominated by silicon-sodium interactions[1], others contradicting this theory by assuming paramagnetics to be responsible for ^{29}Si relaxation[27] and others suggesting that proton exchange between ionised and non-ionised surface units could be the major relaxation mechanism[2,28]. The mechanism for spin-lattice relaxation dominating in highly condensed silicate systems is of great interest, since it not only provides information about the major magnetic interaction but also opens the possibility to determine rotational correlation times, making use of the field-dependency of T1-values characteristic for systems that are not in the extreme narrowing region. Correlation times in turn will give us an idea about the mobility in highly condensed silicates.

To investigate the relaxation mechanism, spin-lattice relaxation times were obtained for sodium and potassium silicates of the same composition. As shown in table 6-10 to 6-12, the ^{29}Si T1-values of sodium silicate solutions do not differ greatly from the ^{29}Si T1-values of potassium silicate solutions of the same composition.

This experimental observation reveals that relaxation *via* silicon-sodium interactions, assumed to be operative in silicate solutions with relatively low SiO_2 concentrations (3 to 13wt% SiO_2) by Kinrade and Swaddle[1], can be excluded as the dominant mechanism. The sodium and potassium ions are most likely located in a hydration shell which prevents a close contact between them and the silicon atoms in SiO^- - and/or SiOH-bonds. The charge density for the sodium ion is bigger than for the potassium ion so that the hydration shell of sodium ions is even stronger than the hydration shell of potassium and direct contact between Si-O bonds and Na^+-ions is impossible. Relaxation via scalar coupling initiated by strong scalar silicon-proton coupling combined with fast proton-proton exchange[33,34,35] or extremely fast proton relaxation can be disregarded[4,5,6]. For further details the reader is referred to chapter 2-4.2 and 5-5).

Thus it can be concluded that dipolar relaxation with protons governs the relaxation of the silicon atoms. Long-range dipolar interactions over more than one bond, usually negligible for ^{13}C nuclei, can contribute significantly to the relaxation of ^{29}Si nuclei[3]. This dipolar Si-H relaxation can be intramolecular or intermolecular. Which mechanism prevails, can be found by dilution studies, discussed in detail in chapter 5-5. The silicate systems can not be simply be diluted with D_2O, since this would affect the viscosity. Therefore a silicate solution of equal composition was prepared using 95% D_2O. Generally T1-relaxation times in silicates containing colloidal material are not affected by the change in D_2O-content, and it can be concluded that the surface groups are predominantly Si-OH groups. Thus intermolecular relaxation with protons governs the relaxation rate of silicon.

Tables 6-10 to 6-12
Comparison of T1-values in s for sodium and potassium silicates

Table 6-10
T1-values in s for silicate solutions with 30 wt% SiO_2 and Rm=2.6

structural unit	sodium silicate	potassium silicate
Q0	3.8	-
Q1	3.9	3.8
Q2cyc	3.7	-
Q2/Q3cyc	4.9	6.2
Q3	6.5	6.8
Q4	12.1	11.6

Table 6-11
T1-values in s for silicate solutions with 30 wt% SiO_2 and Rm=3.4

structural unit	sodium silicate	potassium silicate
Q0	4.7	-
Q1	6.9	7.3
Q2cyc	-	-
Q2/Q3cyc	7.5	9.9
Q3	9.8	10.0
Q4	17.4	17.1

Table 6-12
T1-values in s for silicate solutions with 25wt% SiO_2 and Rm=4.0

structural unit	sodium silicate	potassium silicate
Q0	8.4	-
Q1	8.8	9.2
Q2cyc	-	-
Q2/Q3cyc	8.5	9.5
Q3	10.2	10.8
Q4	18.5	19.1

2.2 Correlation times

From the findings reported in the previous section two conclusions can be drawn which are the basis of the mobility model and the calculation of the correlation times of Si-units in highly viscous silicate solutions. First the investigated silicate solutions are not within the extreme narrowing region of T1-values, and second the relaxation of the Si-atoms is dominated by intermolecular dipolar interactions with protons. The correlation time describes the amount of rotational physical movement in the silicate systems. It expresses the duration of a correlation between two configurations of a nuclear environment at two different times and therefore is an important parameter describing the motions in a silicate system[8,26].

The correlation time τc can be calculated from T1-values at different fields (see tables 6-6 to 6-9) by taking ratios. The expression for spin-lattice relaxation times, which are not in the extreme narrowing region, is a function of τ at a constant rAX-distance as all other variables are known constants. If the exact values for the rAX-distances are not known the most accurate method of calculating τ from the experiment is to take the ratio of T1-values at different

fields. The following equations[7,8], which are discussed in more detail in chapter 2-3.3, are needed for the calculation of the correlation times:

$$\frac{1}{T1A} = W0 + 2W1A + W2 \qquad [1]$$

$$W0 = \frac{1}{20}(2\pi R)^2 J(\omega x - \omega A) \qquad [2]$$

$$W1A = \frac{3}{40}(2\pi R)^2 J(\omega A) \qquad [3]$$

$$W2 = \frac{3}{10}(2\pi R)^2 J(\omega x + \omega A) \qquad [4]$$

$$J(\omega) = \frac{2\tau c}{(1 + \omega^2 \tau c^2)} = \frac{2\tau c}{(1 + 4\pi^2 \nu^2 \tau c^2)} \qquad [5]$$

$$\frac{1}{T1} = \frac{1}{10}\tau(2\pi R)^2\left[\frac{1}{1+(\omega x-\omega A)^2\tau^2} + \frac{3}{1+\omega A^2\tau^2} + \frac{6}{1+(\omega x+\omega A)^2\tau^2}\right] \qquad [6]$$

R is the dipolar coupling constant and is proportional to rAX^{-6}

rAX is the Si-H-distance

$$R^2 = \left[\left(\frac{\mu o}{4\pi}\right)\gamma A \gamma x \left(\frac{\hbar}{2\pi}\right)\right]^2 \left[rAX^{-3}\right]^2 \qquad [7]$$

$$R^2 = 5.703 * 10^{-52} * rAX^{-6} \qquad [8]$$

The ratios of T1-values at different fields are taken to give equations [9] to [11].

$$\frac{T1(500)}{T1(250)} = \frac{\left\{\frac{1}{1+\tau c^2\,1.579E18}\right\}+\left\{\frac{3}{1+\tau c^2\,9.87E16}\right\}+\left\{\frac{6}{1+\tau c^2\,3.55E18}\right\}}{\left\{\frac{1}{1+\tau c^2\,6.3165E18}\right\}+\left\{\frac{3}{1+\tau c^2\,3.9478E17}\right\}+\left\{\frac{6}{1+\tau c^2\,1.4212E19}\right\}} \quad [9]$$

$$\frac{T1(600)}{T1(250)} = \frac{\left\{\frac{1}{1+\tau c^2\,1.579E18}\right\}+\left\{\frac{3}{1+\tau c^2\,9.87E16}\right\}+\left\{\frac{6}{1+\tau c^2\,3.55E18}\right\}}{\left\{\frac{1}{1+\tau c^2\,9.126E18}\right\}+\left\{\frac{3}{1+\tau c^2\,5.609E17}\right\}+\left\{\frac{6}{1+\tau c^2\,2.042E19}\right\}} \quad [10]$$

$$\frac{T1(600)}{T1(500)} = \frac{\left\{\frac{1}{1+\tau c^2\,6.3165E18}\right\}+\left\{\frac{3}{1+\tau c^2\,3.9478E17}\right\}+\left\{\frac{6}{1+\tau c^2\,1.4212E19}\right\}}{\left\{\frac{1}{1+\tau c^2\,9.126E18}\right\}+\left\{\frac{3}{1+\tau c^2\,5.609E17}\right\}+\left\{\frac{6}{1+\tau c^2\,2.042E19}\right\}} \quad [11]$$

A BASIC program was used to calculate the rotational correlation time τc as a function of varying T1(field1)/T1(field2)-ratios. The results are presented in figure 6-3 below. The point where it can be stated that the correlation time begins to be field dependent is very much dependent on the accuracy of the experimentally determined spin-lattice relaxation times. With an average error in T1-values of about 8% (see chapter 3-2.2)[22], the correlation time, where a difference in T1-values begins to be relevant and can not be caused by errors in the measurements, is assumed to be $\tau c = 1*10^{-10}$s.

Figure 6-3

Rotational correlation time τc as a function of the T1(field1)/T1(field2)-ratio :

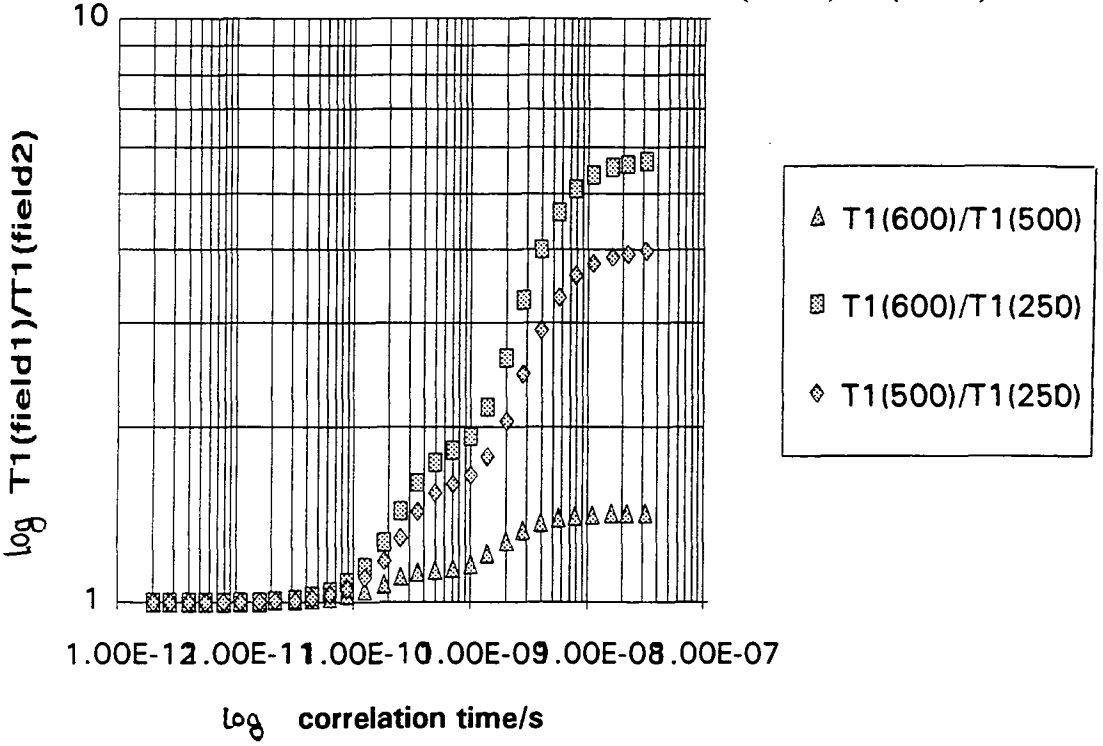

Rotational correlation times were calculated from T1-ratios for two sodium silicate solutions containing 30wt% SiO_2 with Rm=2.6 and 25wt% SiO_2 with Rm=4.0 and for two sodium silicate gels, one of them corresponding to the latter solution containing 30wt% SiO_2 and Rm=4.0. The results are presented in tables 6-13 to 6-15.

In the interpretation of these results it has to be born in mind that the deviation of the calculated correlation times from the average value will be the higher the shorter the correlation times are (the smaller the ratio of T1-values at different fields is). Thus the errors will be the smaller the nearer the calculated τc to the correlation time at or past the minimum of T1-values is. This means that rotational correlation times are the more reliable the more condensed the structural units are and the higher the degree of condensation of the silicate system is. The correlation times of the species in the two investigated silicate solutions are neither in the region of extreme motional narrowing nor are they past the minimum of T1-values, the point where $\tau c = \omega o^{-1}$, characterising the region of slow motion. It can be concluded that they are in the region of the

T1-minimum, i.e. in a transitional region towards the slow motion region where $\tau c > \omega o^{-1}$. The lower the alkalinity of the silicate solution is (the higher the Rm-value), the slower are the correlation times. The tendency of the correlation times in these solutions is shown in figure 6-3. The τc-values for the sodium silicate solution containing 25wt% SiO_2 and Rm=4.0 in this figure have been obtained by taking the average value in the range of correlation times quoted in table 6-15.

Figure 6-3
Correlation times of two silicate solutions :

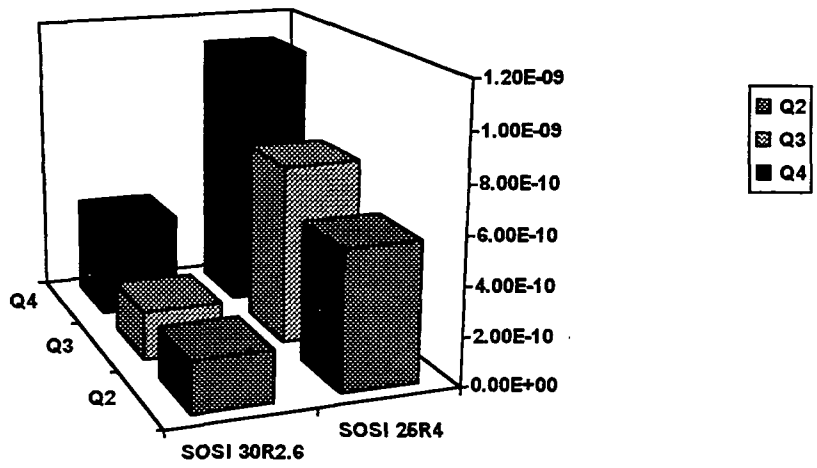

A general increase is found in the values of the correlation times when going from lower to higher condensed structural units. This might seem odd, since in colloidal particles we find Q3-units on the surface and Q4-units in the bulk so that the mobility of both should be the same. It has to be taken into account, however, that the calculated correlation times are an average over all existing colloidal particles in the silicate solution. Thus the conclusion can be drawn that there is a distribution of different particle sizes in the solution. Thus the average mobility of Q3-units is expected to be higher than for Q4-units, as Q3-units are represented to a higher degree in smaller particles with higher mobility whereas Q4-units are found to a high percentage in large, less-mobile particles.

In figure 6-5 the correlation times for a silicate gel with Rm = 4.0 (containing 30wt% SiO_2) are compared with the corresponding silicate solution with Rm=4.0 (containing 25wt% SiO_2).

Figure 6-5
Correlation times in s for a silicate sol and silicate gel :

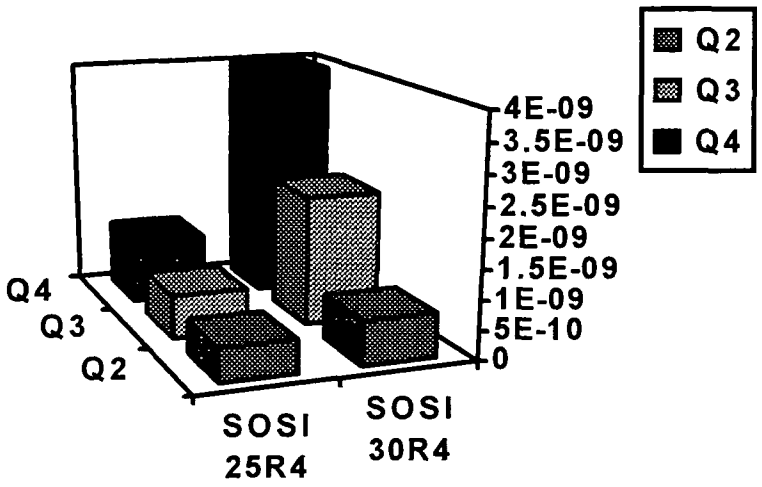

It is clearly evident that from the point where the sol/gel-transition is passed a steep increase in the Si-correlation times is observed. This is due to a severe loss of mobility of the silicate units when during further condensation a network is formed. The ratio of correlation times for Q3- and Q4-units stays constant at a factor of ~2 for silicate systems on both sides of the sol/gel-transition. Like in sodium silicate solutions, the silicate species in sodium silicate gels are the less mobile the lower the alkalinity (the higher the Rm-value) is (tables 6-16 and 6-17).

Table 6-13
Correlation times in s for T1-values at two different fields for a sodium silicate solution containing 30wt% SiO_2 with Rm=2.6 :

	T1(500) / T1(250)	τc
Q0	1.1	1.3E-10
Q1	-	-
Q2	1.23	2.1E-10
Q3	1.2	2.0E-10
Q4	1.46	4.0E-10

Table 6-14
Correlation times in s for T1-values at three different fields for a sodium silicate solution with 25wt% SiO_2 and Rm=4.0

	T1(600) / T1(500)	τc	T1(500) / T1(250)	τc	T1(600) / T1(250)	τc
Q0	1.02	1.0E-10	-	-	-	-
Q1	1.01	1.0E-10	1.29	2.5E-10	1.3	2.0E-10
Q2/Q3cyc	1.16	1.0E-9	1.12	1.4E-10	1.3	2.0E-10
Q3	1.2	1.3E-9	1.17	1.8E-10	1.4	2.4E-10
Q4	1.25	1.8E-9	1.45	3.7E-10	1.81	6.8E-10

Table 6-15
Average correlation time in the range of correlation times for the structural units in a sodium silicate solution with 25wt% SiO_2 and Rm=4.0:

structural unit	τc / s
Q0	1E-10
Q1	2E-10
Q2/Q3cyc	6E-10
Q3	7E-10
Q4	11E-10

Table 6-16
Correlation times for T1-values at two different fields for a sodium silicate gel with 33wt% SiO_2 and Rm=3.4

	T1(500)/T1(250)	τc / s
Q0	-	-
Q1	1.47	4.0 E-10
Q2/Q3cyc	1.41	3.5 E-10
Q3	1.28	2.4 E-10
Q4	2.02	20.0 E-10

Table 6-17
Correlation times for T1-values at two different fields for a sodium silicate gel containing 30wt% SiO_2 with Rm=4.0

	T1(600)/T1(500)	τc / s
Q0	-	-
Q1	1.15	8.5 E-10
Q2/Q3cyc	1.06	1.4 E-10
Q3	1.29	22.0 E-10
Q4	1.36	40.0 E-10

2.3 Tendencies of spin-lattice relaxation times

It is a general experimental fact that the spin-lattice relaxation times in silicate solutions increase with decreasing alkalinity (increasing Rm-value)[1,9]. In the past these studies were carried out with silicates which, compared to the ones investigated here, were relatively low in silica content.

In these investigations the Rm-values are systematically increased from 2.0 to 4.0 at a constant SiO_2 concentration of 30wt%. In figure 6-5 the spin-lattice relaxation times are plotted versus the Rm-value.

Analogous to the trend reported before[38], the spin-lattice relaxation times of all structural units show a steady increase with decreasing alkalinity of the silicate solution (figure 6-6).

Figure 6-6
Spin-lattice relaxation times versus the Rm-value at constant SiO_2 concentration of 30wt% :

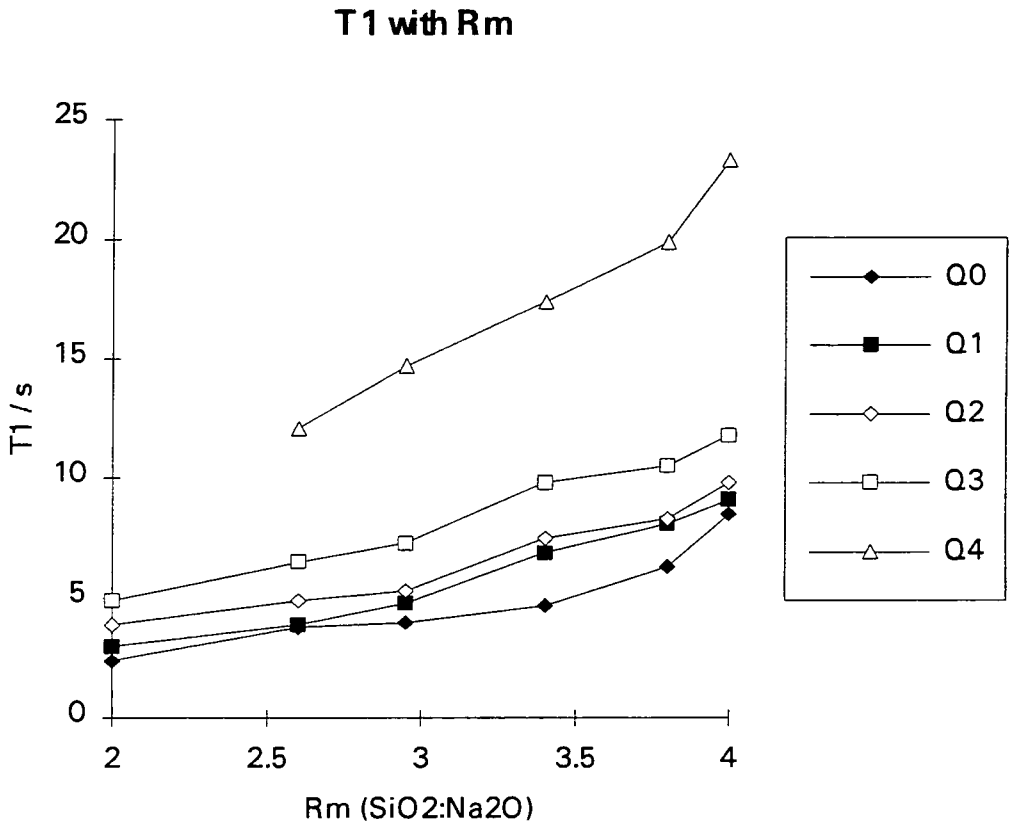

The increase in T1-values with increasing Rm-value reflects an increase in the degree of condensation (chapter 5-1.2). This can be related to a decrease in mobility showing in the correlation times, which generally increase with increasing Rm-value (section 2.2 of this chapter). The increase in T1-values with increasing connectivity of the silicate species is caused by two factors working in the same direction; decreasing mobility in combination with decreasing amount of neighbouring protons.

3. Silicon Self-diffusion and particle radii

The dephasing of the magnetisation under the influence of pulsed field gradients is a measure for the self-diffusion of the silicate units. The faster the self-diffusion, the bigger the loss of magnetisation through dephasing.

The self-diffusion constants for the Si units in the silicate solution are calculated with the following equations[10,11]. For further details the reader is referred to chapter 3-2.6.

$$\text{slope} = \frac{\ln \frac{A}{A_0}}{\delta^2 (\Delta - \frac{\delta}{3})} = -\gamma^2 * G * D \qquad [12]$$

$$\frac{\text{slope (Si)}}{\text{slope (H)}} * \frac{\gamma^2 (Si)}{\gamma^2 (H)} = \frac{D (Si)}{D (H)} \qquad [13]$$

$$D(Si) = \frac{1}{25.3} * \frac{\text{slope (Si)}}{\text{slope (H)}} * D(H) \qquad [14]$$

Particle radius :

The results can be put into the Stokes-Einstein equation which describes the diffusion of spherical particles of radius r in a medium of viscosity η. This equation is independent of the charge of the diffusing particles[12]. It is an approximation which is based on the assumption of the validity of the Stokes equation for the viscous drag and is still valid for slow self-diffusion constants (as the one for dextrose in water : D=6.7 E-10 $m^2 s^{-1}$)[12]. The Stokes equation can be used for the determination of the particle radius as the viscosity has been experimentally determined. Therefore equations like the Mooney equation, which are concerned with theoretically determining the viscosity of a complex system with the help of the intrinsic viscosity, are not relevant in this case[12].

$$r = \frac{kT}{6 \pi \eta D} \qquad [15]$$

k=1.3806 E-23 m^2 kg s^{-2} K^{-1}

T=298 K η=0.0913 Pa s

There are three cases which are possible for the investigated systems (figure 6-7 first row). The Gaussian curve for the amount of particles with a certain size versus the particle size (figure 6-7 second row) and the graph of $\delta^2*\delta-\Delta/3$ versus attenuation (figure 6-7 third row) are given for each of the three hypothetical cases. If the distribution of particle sizes matches case 2, the hypothetical contribution of Q3 and Q4 units to the distribution of structural units for the two extremes is illustrated in figure 6-7. From results discussed in section 2-2, however, we know that case 3 is the most likely of the three. Thus all contributions of Q3 and Q4 units between the two extremes illustrated in figure 6-8 are possible, with an emphasis on the medium sizes.

Figure 6-7

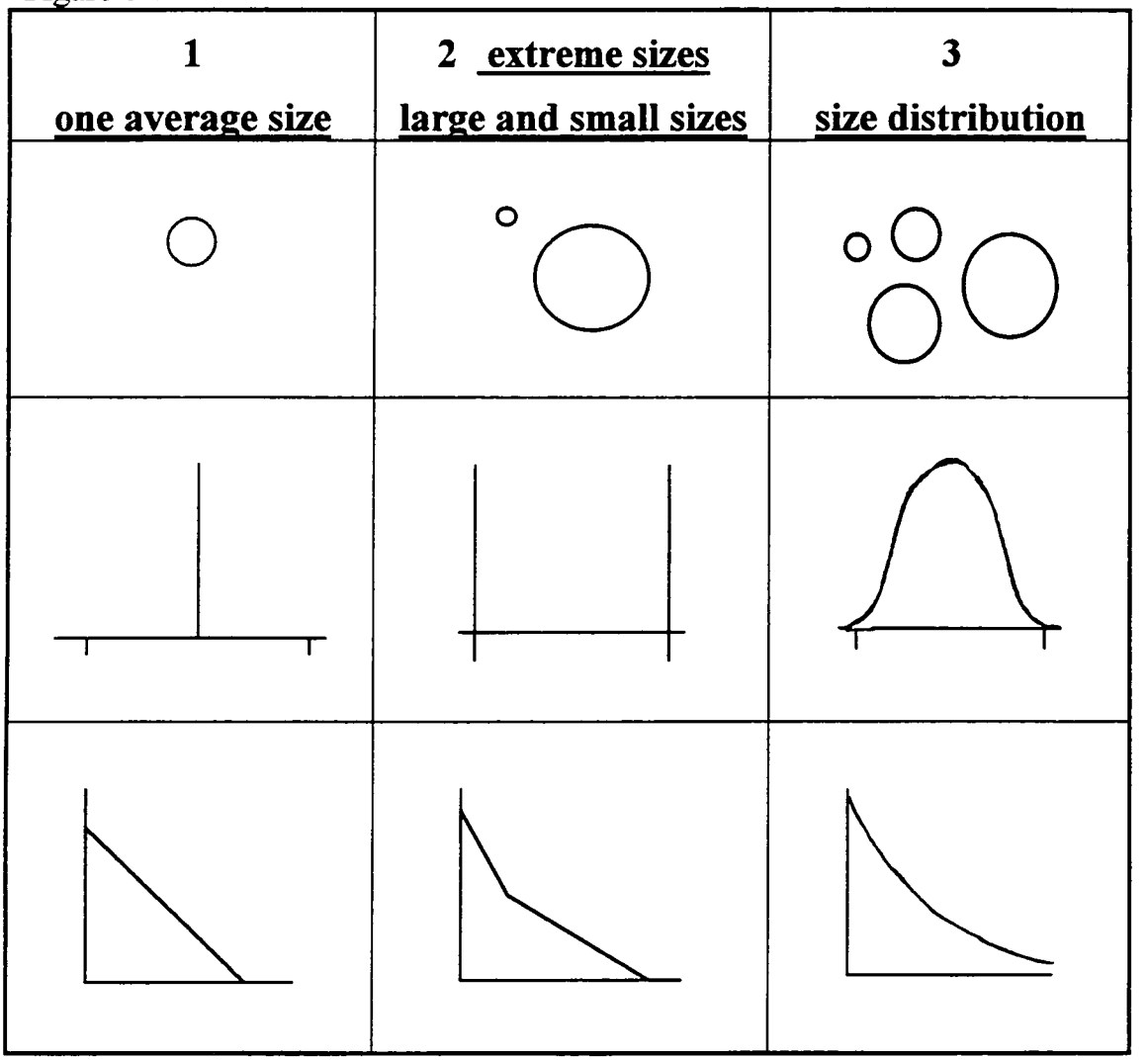

Figure 6-8
Contributions of Q3 and Q4 units to the overall distribution resulting from small and large particles

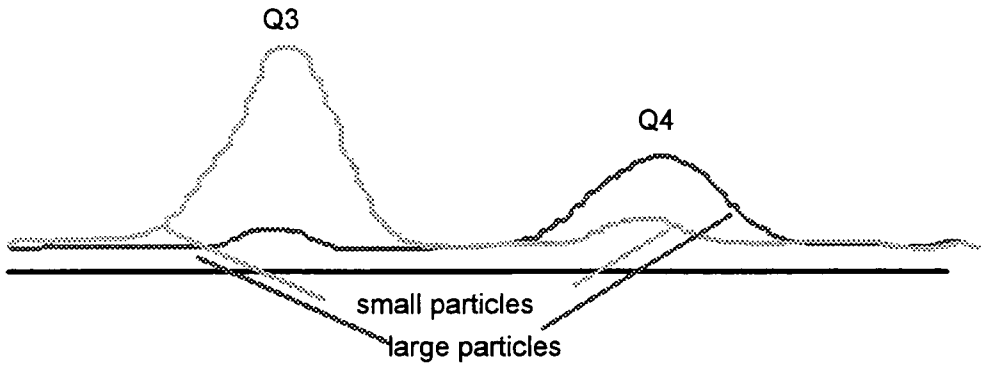

The sample investigated in this section is a sodium silicate solution with 25wt% SiO_2 and Rm=4.0. This silicate was enriched to the 95.65%-level with ^{29}Si to increase the sensitivity of the experiment. The S/N in a single-shot spectrum is between 6 and 7 for the Q3-resonance.

In the measurement of the self-diffusion coefficient using pulsed field gradients a fine adjustment of the gradient duration has to be carried out for each set of measurements. This requires the adjustment of the gradient duration for one representative gradient till the maximum FID is achieved. This should ideally be done in one-scan mode to allow optimal adjustment. This, however, can not be made on the silicate sample, since the intensity of the single-shot FID is not sufficient to allow any optimising adjustment. Thus another nucleus with a resonance frequency near ^{29}Si had to be used as intensity standard. According to table 6-22 iodine is the nucleus with a resonance frequency nearest to ^{29}Si, followed by deuterium.

Table 6-22
Resonance frequencies nearest the resonance frequency of ^{29}Si at a proton frequency of 300MHz and nuclear spin:

	SF/MHz	Spin I
Si	59.62	1/2
I	60.02	5/2
D	46.05	1

The sensitivity for iodine in a KI-solution with 4.4wt% KI should match the sensitivity of silicon in the investigated silicate solution and could therefore be used as an intensity-standard.

The following relation is used[13].

signal ~ $N * \rho * c$

N = sensitivity (absolute)

ρ = nuclear density, this is obtained by taking the ratio of the molecular weight and the number of nuclei in one molecule (unit cell)

ρ_{Si} in $Na_2O(SiO_2)_4 = 302/4 = 0.013$

ρ_I in KI = 166/1 = 0.006

c = concentration of nuclei

Thus:

$$N_{Si} * \rho_{Si} * c_{Si} = N_I * \rho_I * c_I \qquad [16]$$

Although the intensity of the first point of the FID should be the same no matter how many resonances are involved it has to be taken into account that the FID for KI-solution is a one-resonance FID (one iodine resonance), whereas the FID of the silicate solution is a five-resonance FID (five silicon resonances from Q0 to Q4). The huge advantage of the nucleus I is that the frequency is very near that of Si. The huge disadvantage is that I is quadrupolar (I= 5/2) and thus the T2-relaxation is too short (T2 << 500μs) to apply any field gradients.

Another nucleus had to be found with a resonance frequency near that of Si with a reasonably long T2 and a reasonably high absolute sensitivity where field gradients can be applied and a good FID is achieved on which to do the duration-optimisation. The only nucleus which is near to fulfilling these conditions is D in D_2O. However, the problem which arises when using D for the duration-optimisation is that the gradient-insert for the probe which is appropriate for Si is designed for frequencies from 58 to 85 MHz and the amplifiers in the spectrometer appropriate for Si have a frequency-range from 58 to 74 MHz. Using this set-up, designed for the acquisition of Si, does not yield any signal for D at all. Therefore all the tuning parameters have to be changed from D to Si, and thus the fine-adjustment of the gradient duration for deuterium is not necessarily applicable to silicon. It is concluded that the fine-adjustment of the gradient width has to be made on ^{29}Si in the silicate solution under investigation but can not be carried out in single-shot mode on the FID. However, with some experience it is possible to be carried out on the FID acquired using 8 transients and a relaxation delay of 20s.

Another problem arises if a 90^o - 180^o pulse sequence is used. This is because of the very small attenuation that is achieved for Si in the silicate units. The measurement of the diffusion constant gives optimal results when an attenuation of about 10 is achieved. The attenuation that is achieved with the above mentioned pulse sequence for the silicate units lies between 1.05 (Q4) and 1.8 (Q1). In the field-gradient experiments on silicate solutions we have two limiting factors working against each other. One is the very short T2-relaxation time, the other is a long diffusion constant (thus long δ-values are needed which require long Δ-values, which in turn require long T2-decays).
To get round the T2-problem stimulated echoes can be used in the field-gradient measurements, where we get a T1-dependence of the echo instead of a T2-dependence[11,14] (see chapter 3-2.6).
Another possibility is to do the measurements at increased temperature (60^oC) which could increase the T2-value and decrease the diffusion constant. Since

the temperature goes into the Stokes-equation the calculated particle size would not change. Nevertheless it has to be considered that the distribution of structural units in the silicate solutions changes with increasing temperature. Furthermore there is exchange between the silicate units which increases with increasing temperature and thus causes the T2-values to decrease (see section 4.2.2 of this chapter).

A further possibility is the dilution of the silicate solution, which should work in favour of an increase in T2-values. However the disadvantage of this is that the particle size would change (see section 5-1.3) and the true size of the colloidal material in concentrated silicate solutions would not be represented.

All this leads to the conclusion that the method of choice is the use of the stimulated echo sequence. This sequence uses three 90^{o}x-pulses to generate the echo. Before the second and after the third pulse a pulsed field gradient (PFG) is switched on for a defined length of time. The duration of the PFG is still limited by the T2-decay of the echo but the signal decay in the gap between the second and third pulses is only due to T1-decay. Thus this gap can be used to apply large values of Δ which, just like large δ-values, increase the signal attenuation.

Due to loss of magnetisation between the first two 90^{o} pulses it is not possible to achieve a situation, even if using the pulse sequence for the stimulated echo, where δ and Δ are of a length to produce sufficient signal attenuation and a reasonably visible silicon spectrum is obtained which has not decayed to an unobservable level due to other influences than the PFG.

The last possibility to obtain silicon self-diffusion constants from PFG-experiments was to use the extra scope in the field gradient unit for the power adjustment. This allows the cutting out of some resistors in the circuit and yields an output-current increased maximally by a factor of 10 (with a coil-resistance of 3Ω this is an improvement of a factor of maximally 30 in the output-voltage). This extra scope in the power adjustment was not used before out of safety reasons as the effect on the probe was not established.

It was found that an increase in the output-current of 6 was sufficient to produce a signal attenuation down to 12% of the original signal at reasonable quality. An increase in the output current by a factor of 10 produced even better signal attenuation.

In the following pages all experiments are listed which have successfully been carried out on a sodium silicate solution with 25wt% SiO_2 and Rm=4.0 enriched in ^{29}Si to the 96%-level. The attenuation of the resonances is taking the peak-intensities as well as the peak-areas into account. The latter can not be obtained by straightforward integration as there is an overlap of resonances. Therefore a line-fit has to be carried out, for which the Pascal program Linesim.3000 was used. In all experiments the scattering of the individual values is too big to treat the slopes as if there was a distribution of particle sizes. Thus the slopes were treated as if there were particles of one average size.

Tables 6-19 to 6-23
Self-diffusion constants of silicate species, obtained using an increase in the output-current of a factor of **6**

Table 6-19
Self-diffusion constant of protons in water (literature value) obtained under the following conditions:
NS = 16
relaxation delay = 1 s
Δ = 10 ms
TAU = 4 ms

δ/ms	**$\delta^2(\Delta-\delta/3)$**	**attenuation**
0.1	0.1	0.987
0.2	0.4	1.0
0.3	0.89	0.987
0.4	1.58	0.905
0.5	2.46	0.785
0.6	3.53	0.658
0.7	4.79	0.563
0.8	6.23	0.443
0.9	7.86	0.354
1.0	9.67	0.266

slope = 0.143
correlation = 99.7%

D/cm^2 s^{-1} = 2.3E-5

Figure 6-9
Self-diffusion measurement of protons in water:

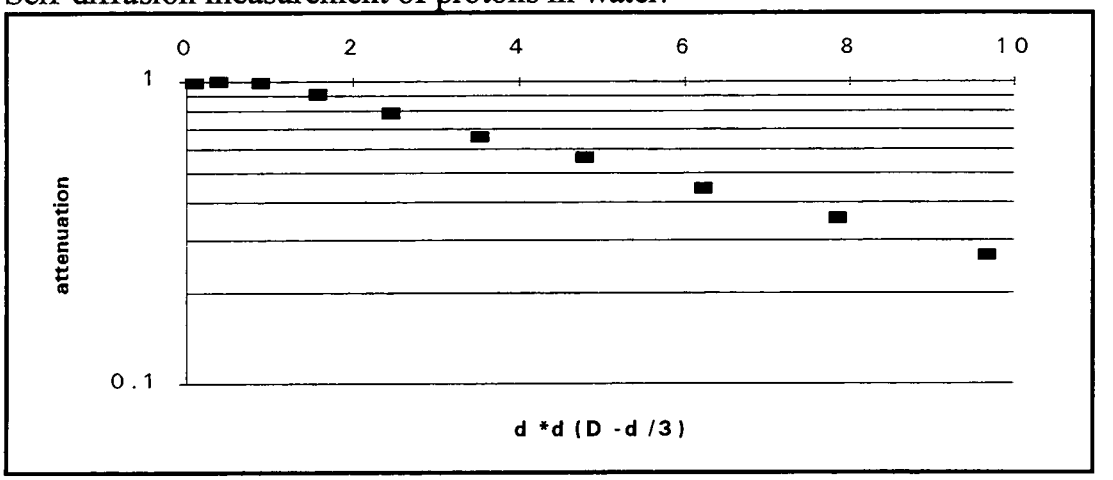

Tables 6-20 to 6-23
Self-diffusion constants of silicate species, obtained under the following conditions:
Δ = 50 ms
δ up to 4.5 ms
d6 = d7 = 6 ms
TAU = 44 ms
NS = 32
relaxation delay = 60 s
90°-pulse = 23 μs
acquisition time = 0.02 s
receiver gain = 10

The results using peak intensities are represented in tables 6-20, 6-21 and figure 6-9 and using peak areas in tables 6-22, 6-23 and figure 6-11.

Table 6-20
Attenuation of peak intensities under the influence of a pulsed field gradient in a sodium silicate solution with 25wt% SiO_2 and Rm=4.0

δ/ms	$\delta^2(\Delta-\delta/3)$	Q1	Q2	Q3	Q4
1	49.7	0.75	0.889	0.917	0.884
1.5	111.4	0.7	0.785	0.767	0.581
1.8	160.1	0.625	0.785	0.739	0.581
2	197.3	0.575	0.741	0.711	0.651
2.3	260.4	0.575	0.741	0.722	0.698
2.5	307.3	0.75	0.667	0.694	0.581
2.8	384.7	0.5	0.59	0.58	0.54
3	441.0	0.5	0.59	0.64	0.44
3.3	532.5	0.375	0.52	0.56	0.40
3.5	598.2	0.13	0.67	0.63	0.35
3.8	703.7	0.13	056	0.69	0.3
4	778.7	-	0.39	0.39	0.19
4.3	898.0	-	0.41	0.41	0.23
4.5	982.1	-	0.37	0.33	0.1

Table 6-21
Self-diffusion constants for structural units using the attenuation of peak intensities in a sodium silicate solution with 25wt% SiO_2 and Rm=4.0

	Q1	Q2	Q3	Q4
slope	- 1.167E-3	- 2.585E-4	- 3.819E-4	- 6.908E-4
correlation	87%	63%	90%	94%
$D/m^2\ s^{-1}$	7.4 E-13	1.6 E-13	2.4 E-13	4.4 E-13
r/m	3.2 E-9	14.6 E-9	9.8 E-9	5.4 E-9

Figure 6-10

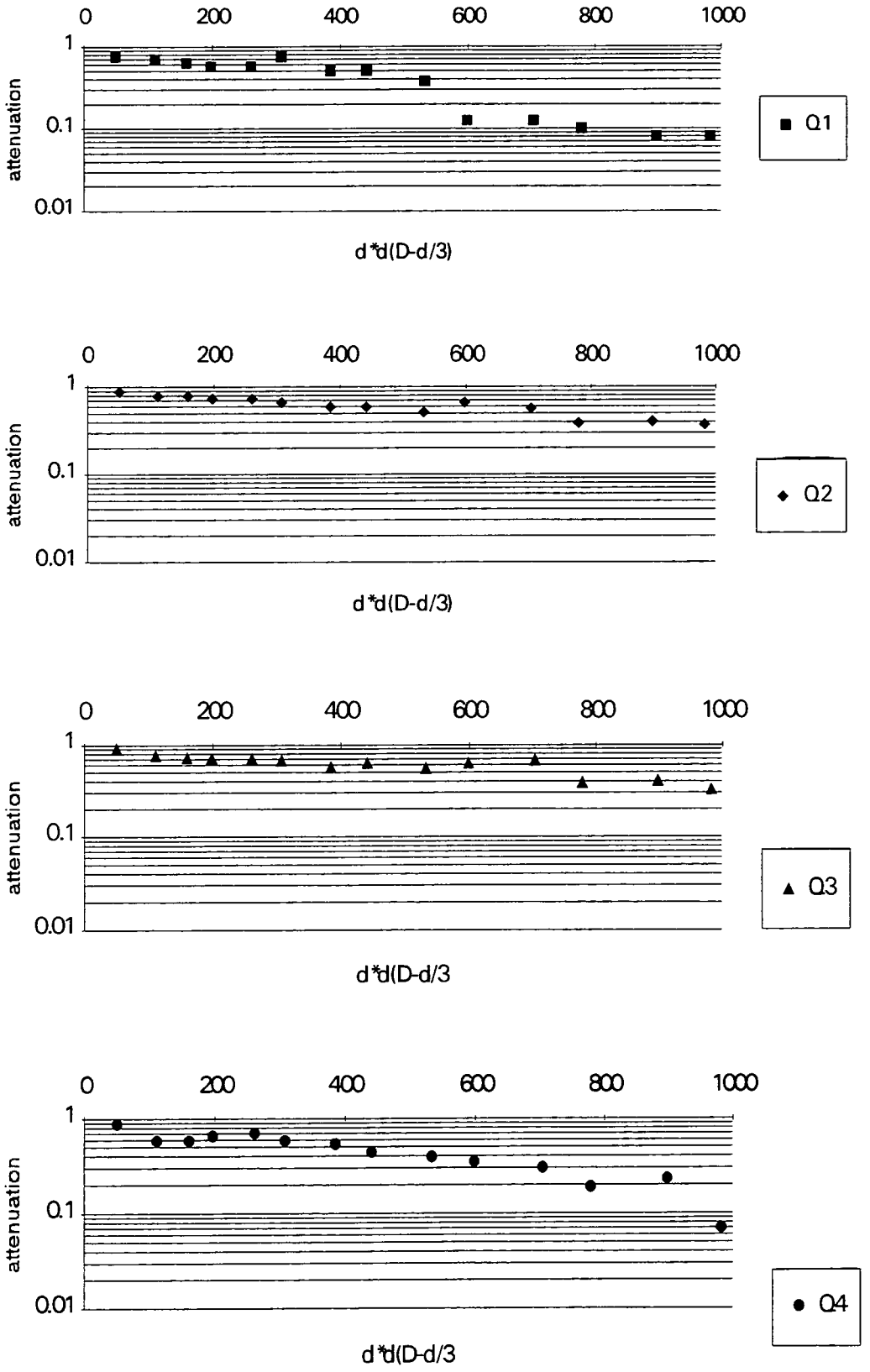

Table 6-22
Attenuation of peak areas under the influence of a pulsed field gradient in a sodium silicate solution with 25wt% SiO_2 and Rm=4.0

δ/ms	$\delta^2(\Delta-\delta/3)$	Q1	Q2	Q3	Q4
1	49.7	0.75	0.87	0.9	0.97
1.5	111.4	0.66	0.84	0.77	0.61
1.8	160.1	0.81	0.81	0.73	0.65
2	197.3	0.72	0.77	0.69	0.81
2.3	260.4	0.63	0.88	0.8	1.0
2.5	307.3	0.8	0.69	0.7	0.71
2.8	384.7	0.63	0.74	0.69	0.87
3	441.0	0.63	0.64	0.63	0.55
3.3	532.5	0.42	0.56	0.57	0.68
3.5	598.2	0.38	0.72	0.65	0.55
3.8	703.7	0.38	0.58	0.71	0.48
4	778.7	0.18	0.51	0.43	0.48
4.3	898.0	0.13	0.51	0.5	0.48
4.5	982.1	0.13	0.4	0.33	0.39

Table 6-23
Self-diffusion constants for structural units using the attenuation of peak areas in a sodium silicate solution with 25wt% SiO_2 and Rm=4.0

	Q1	Q2	Q3	Q4
slope	-7.72 E-4	-4.66 E-4	-3.85 E-4	-4.88 E-4
correlation	94.4%	92.8%	81.9%	76.3%
$D/m^2\ s^{-1}$	4.9 E-13	3.0 E-13	2.4 E-13	3.1 E-13
radius/m	4.9 E-9	8.1 E-9	9.8 E-9	7.7 E-9

Figure 6-11

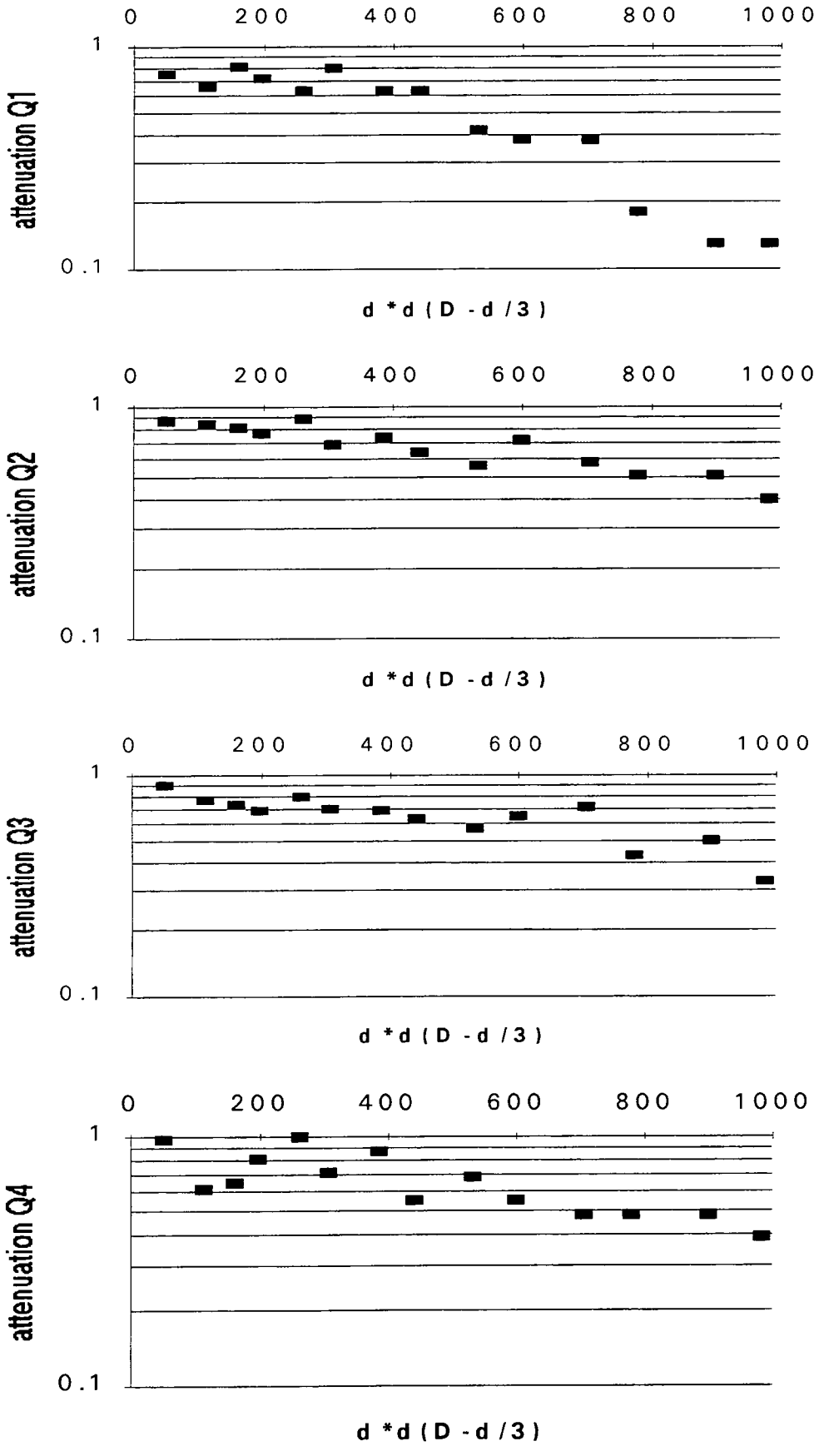
0
200
400
600
800
1000
1
0.1
attenuation Q1
d *d (D - d / 3)
attenuation Q2
attenuation Q3
attenuation Q4

Tables 6-24 to 6-32
Self-diffusion constants of silicate species using an increase in the output-current of a factor of **10**

Table 6-24
Self-diffusion constant of protons in water (literature value) obtained under the following conditions:
NS = 16
relaxation delay = 1 s
Δ = 50 ms
TAU = 44 ms

Table 6-24

δ/ms	**$\delta^2(\Delta-\delta/3)$**	**attenuation**
0.05	0.12	0.91
0.1	0.50	0.74
0.15	1.12	0.55
0.2	2.0	0.34
0.25	3.12	0.19
0.3	4.49	0.09
0.35	6.11	0.04

slope = -0.543

correlation = 99.98 %

D/cm^2 s^{-1} = 2.3E-5

Figure 6-12
Self-diffusion measurement of protons in water
1H NMR spectra of the attenuation of the half-echo

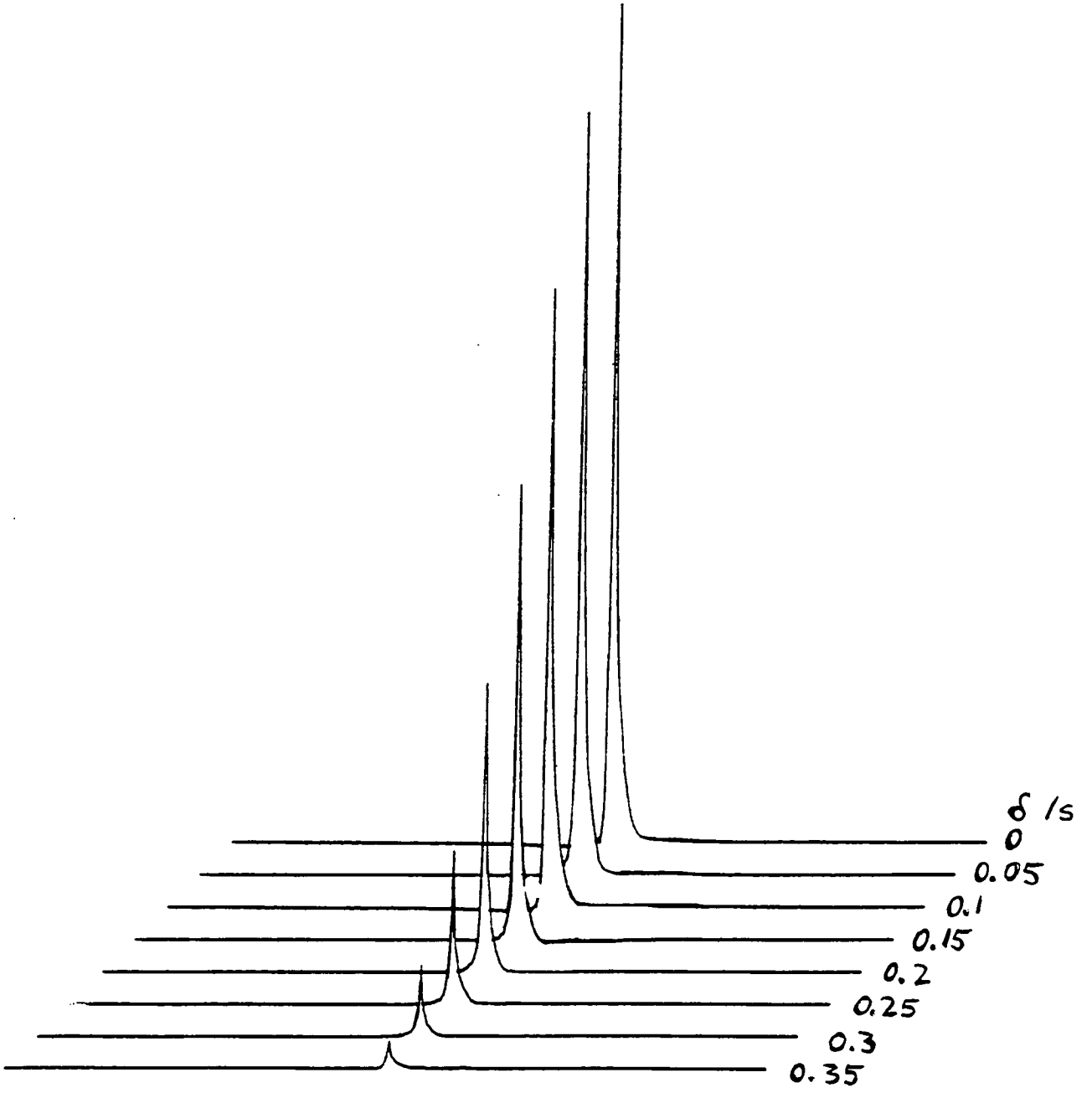

Figure 6-13
Self-diffusion measurement of protons in water :

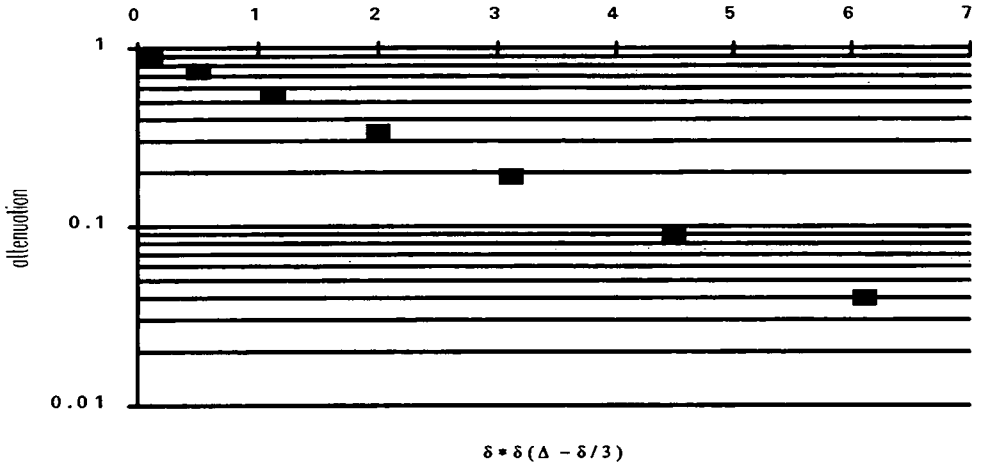

Tables 6-35 to 6-38
Self-diffusion constants of silicate species obtained under the following conditions:
Δ = 50 ms
δ up to 4.5 ms
d6 = d7 = 6 ms
TAU = 44 ms
NS = 32
relaxation delay = 60 s
90°-pulse = 18 μs
acquisition time = 0.02 s
receiver gain = 10

The results using peak areas are represented in tables 6-25, 6-26 and figure 6-13 and the results using peak intensities are represented in tables 6-27, 6-28 and figure 6-14.

Table 6-25
Attenuation of peak areas under the influence of a pulsed field gradient in a sodium silicate solution with 25wt% SiO_2 and Rm=4.0

δ/ms	$\delta^2(\Delta-\delta/3)$	Q1	Q2	Q3	Q4
0.5	12.5	0.70	0.58	0.70	0.84
1	49.7	0.80	0.66	0.74	0.95
1.5	111.4	0.85	0.82	0.92	0.92
2	197.3	0.94	0.81	0.88	1.0
2.5	307.3	-	-	-	-
3	441.0	0.83	0.71	0.83	0.92
3.5	598.2	0.24	0.63	0.82	0.81
4	778.7	0.12	0.25	0.33	0.23
4.5	982.1	0.08	0.2	0.33	0.39

Table 6-26
Self-diffusion constants for structural units using the attenuation of peak areas in a sodium silicate solution with 25wt% SiO_2 and Rm=4.0

	Q1	Q2	Q3	Q4
slope	-2.50 E-3	-1.23 E-3	-9.03 E-4	-1.14 E-3
correlation	0.913	0.821	0.770	0.774
$D/m^2\ s^{-1}$	4.2 E-13	2.0 E-13	1.5 E-13	1.9 E-13
r/m	5.7 E-9	11.7 E-9	15.9 E-9	12.6 E-9

Figure 6-14
Self-diffusion measurement for silicon in silicate species
in a sodium silicate solution containing 25wt% SiO_2 and Rm=4.0

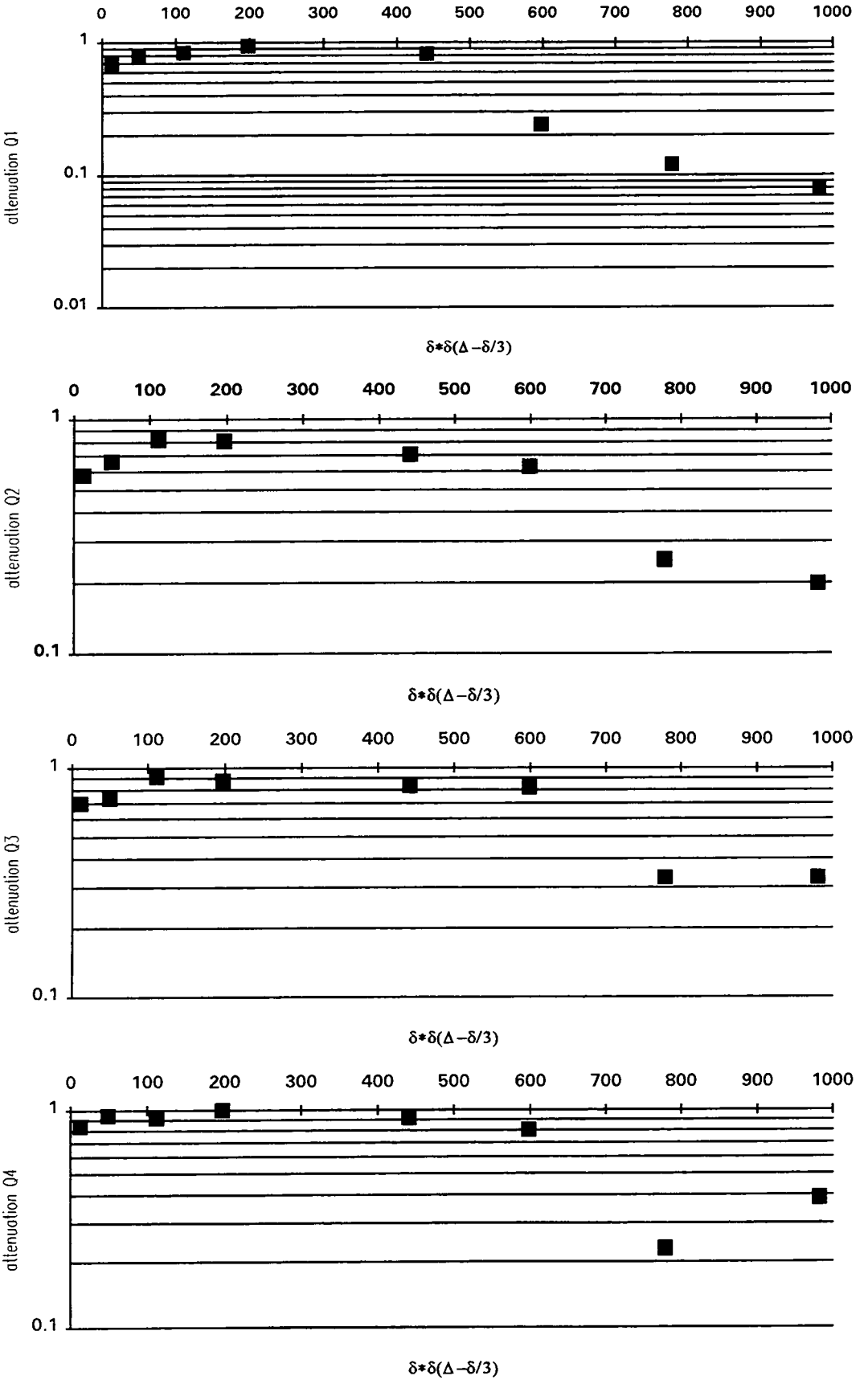

Table 6-27
Attenuation of peak intensities under the influence of a pulsed field gradient in a sodium silicate solution with 25wt% SiO_2 and Rm=4.0

δ/ms	$\delta^2(\Delta-\delta/3)$	Q1	Q2	Q3	Q4
0.5	12.5	0.74	0.84	0.84	1.0
1	49.7	0.60	0.85	0.85	1.0
1.5	111.4	0.71	1.0	0.99	0.98
2	197.3	0.69	1.0	0.98	0.97
2.5	307.3	-	-	-	-
3	441.0	0.65	0.96	0.91	0.91
3.5	598.2	0.17	0.91	0.86	0.85
4	778.7	0.12	0.52	0.61	0.58
4.5	982.1	0.10	0.41	0.48	0.51

Table 6-28
Self-diffusion constants for structural units using the attenuation of peak intensities in a sodium silicate solution with 25wt% SiO_2 and Rm=4.0

	Q1	Q2	Q3	Q4
slope	-2.25 E-3	-6.21 E-4	-5.69 E-4	-6.82 E-4
correlation	0.927	0.679	0.815	0.929
$D/m^2\ s^{-1}$	3.7 E-13	1.0 E-13	0.9 E-13	1.1 E-13
r/m	6.4 E-9	23.1 E-9	25.2 E-9	21.0 E-9

Figure 6-15

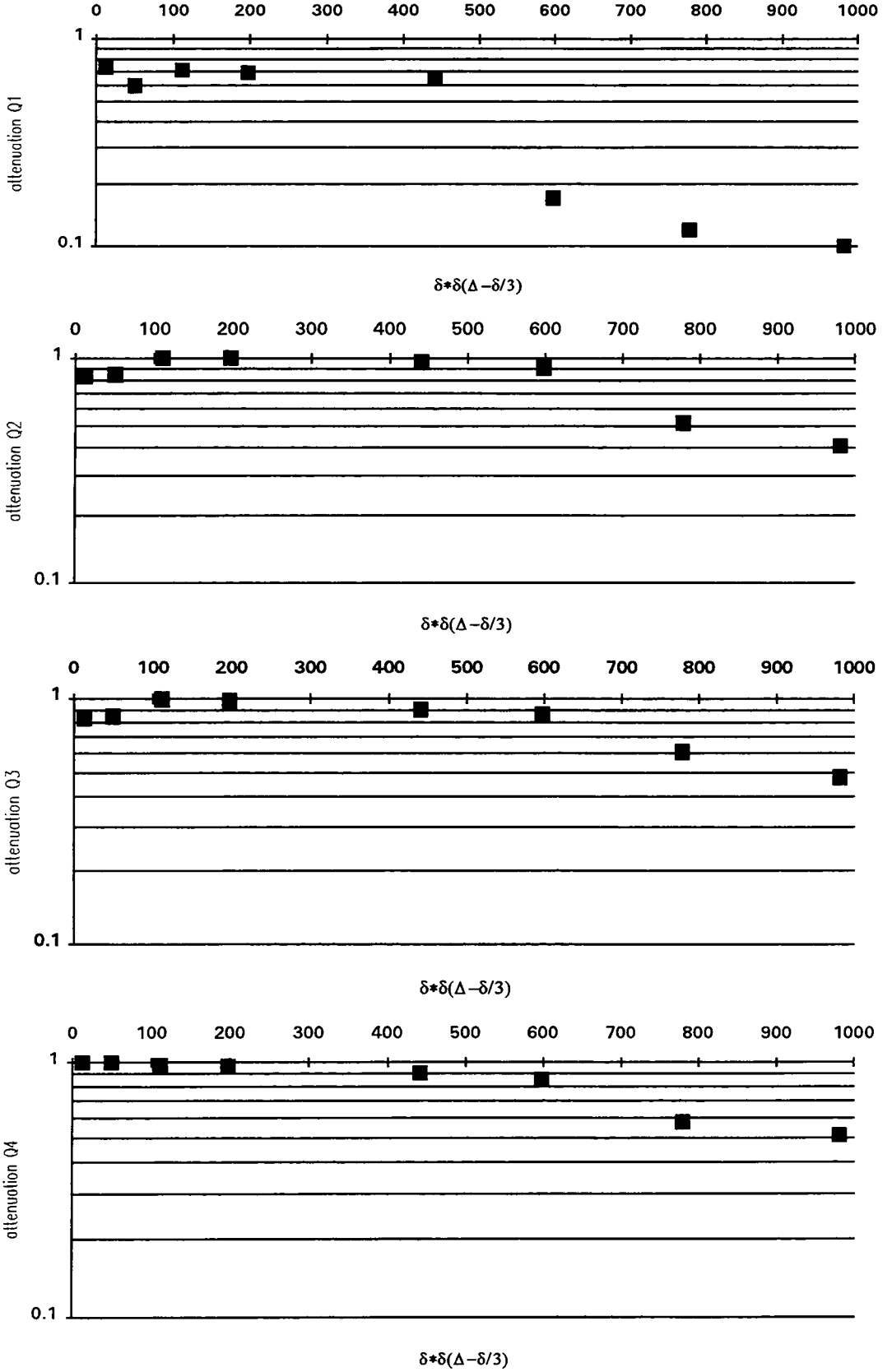
0 100 200 300 400 500 600 700 800 900 1000
1
0.1
attenuation Q1
δ*δ(Δ−δ/3)
attenuation Q2
attenuation Q3
attenuation Q4

Tables 6-29 to 6-32
Self-diffusion constants of silicate species, obtained under the following conditions:
Δ = 50 ms
δ up to 7.0 ms
d6 = d7 = 10 ms
TAU = 40 ms
NS = 32
relaxation delay = 60 s
90^{o}-pulse = 18 μs
acquisition time = 0.02 s
receiver gain = 10

The 29Si NMR spectra for the attenuation of the half-echos are given in figure 6-16. The results using peak areas are represented in tables 6-29, 6-30 and figure 6-17 and the results using peak intensities are represented in tables 6-31, 6-32 and figure 6-18.

Figure 6-16
^{29}Si NMR spectra for the attenuation of the half-echos
of the species in a sodium silicate solution containing 25wt% SiO_2 and Rm=4.0
enriched in ^{29}Si

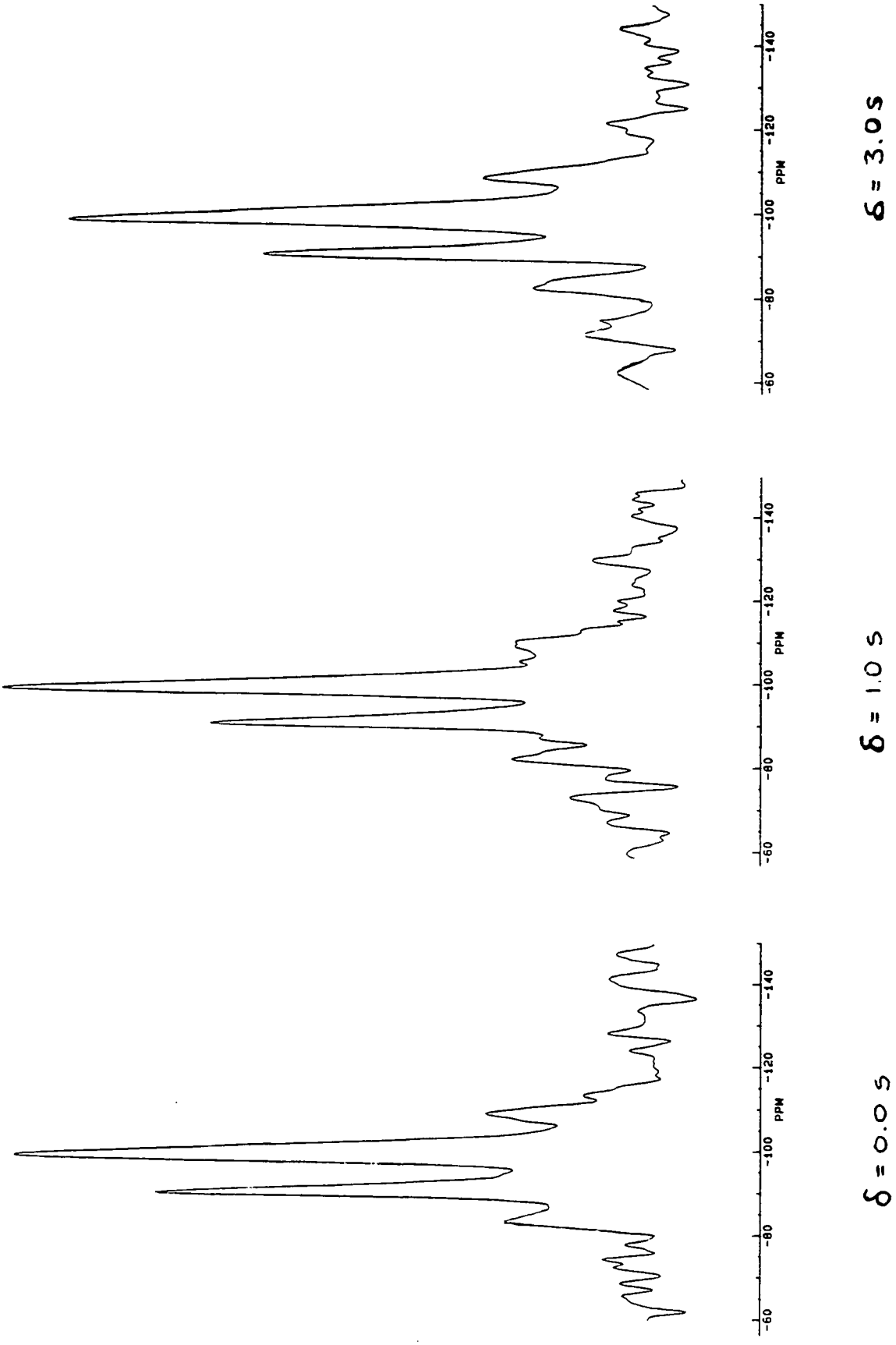

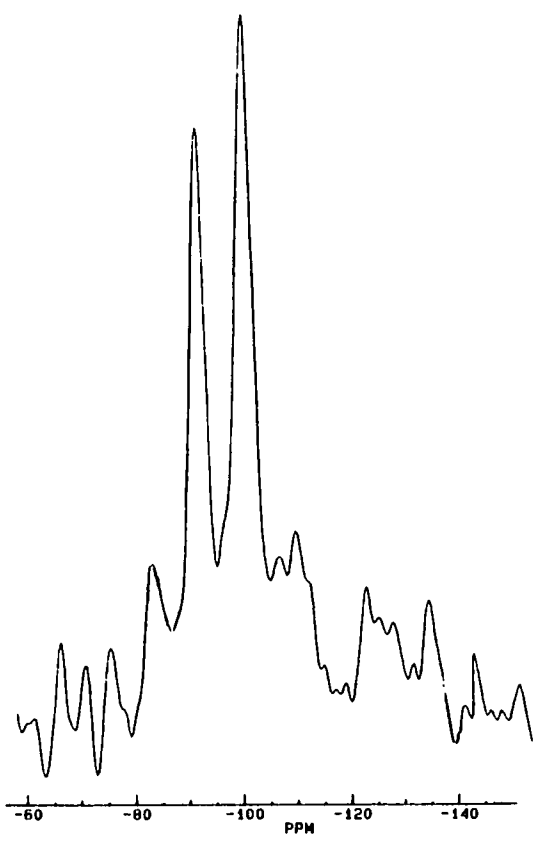

δ = 4.0s

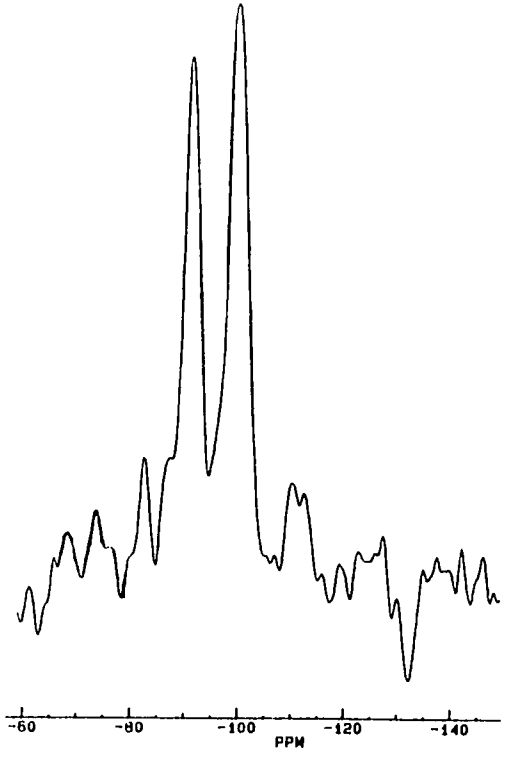

δ = 4.5s

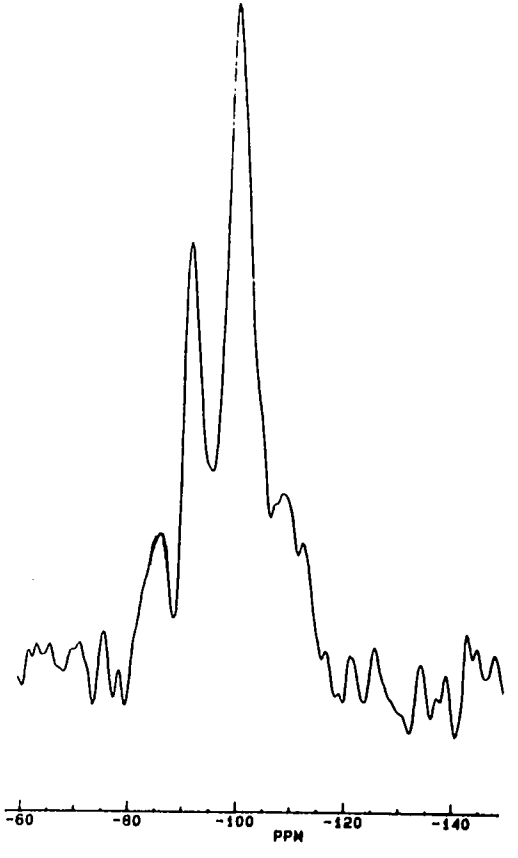

δ = 5.0s

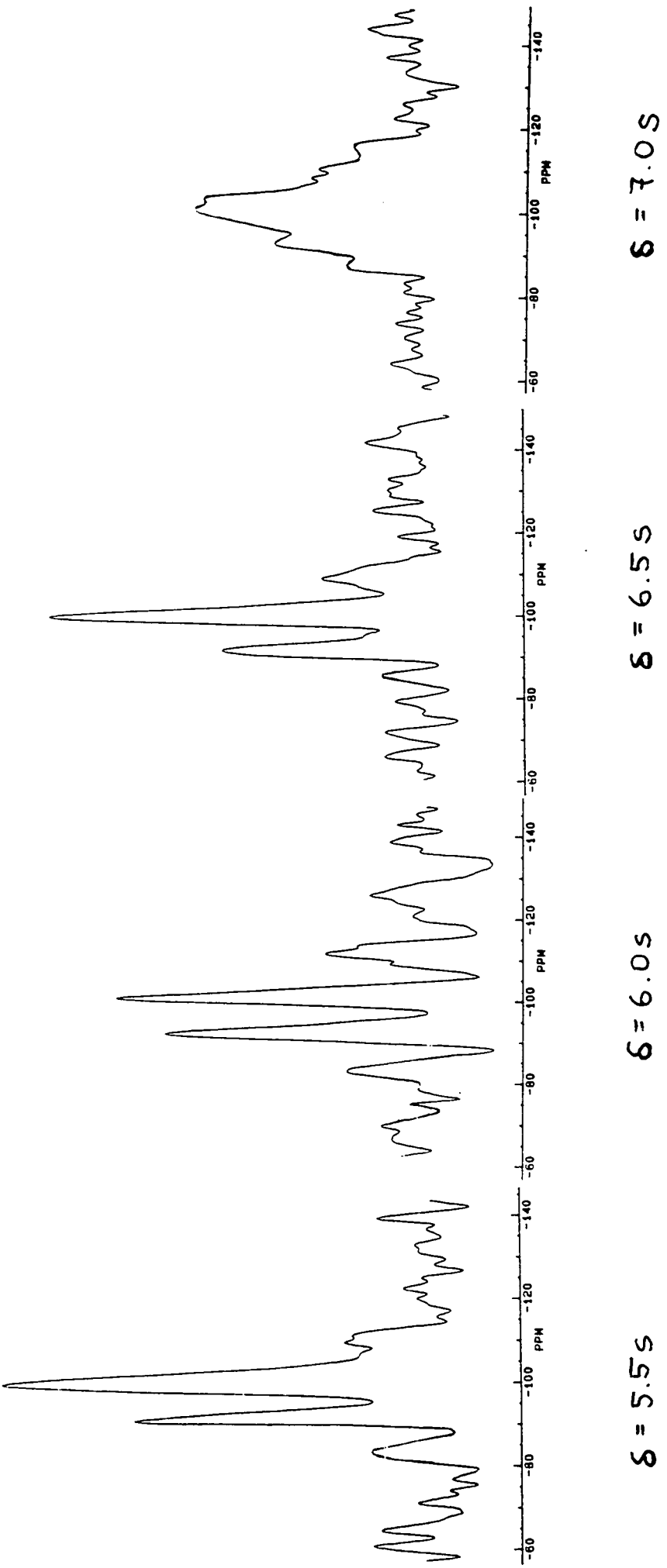
δ = 5.5s
δ = 6.0s
δ = 6.5s
δ = 7.0s
PPM
-60
-80
-100
-120
-140

Table 6-29

Attenuation of peak areas under the influence of a pulsed field gradient in a sodium silicate solution with 25wt% SiO_2 and Rm=4.0

δ/ms	$\delta^2(\Delta-\delta/3)$	Q1	Q2	Q3	Q4
1	49.7	0.88	0.83	1.0	0.93
3	441.0	0.60	0.68	0.83	0.89
4	778.7	0.20	0.47	0.48	0.44
4.5	982.1	0.30	0.49	0.69	0.22
5.0	1208.3	0.16	0.47	0.85	0.69
5.5	1457.0	0.06	0.23	0.47	0.34
6.0	1728.0	0.03	0.22	0.29	0.21
6.5	2020.9	0.04	0.18	0.27	0.28
7.0	2335.7	0.02	0.14	0.24	0.31

Table 6-30

Self-diffusion constants for structural units using the attenuation of peak areas in a sodium silicate solution with 25wt% SiO_2 and Rm=4.0

	Q1	Q2	Q3	Q4
slope	-1.76 E-3	-8.20 E-4	-6.57 E-4	-5.54 E-4
correlation	0.969	0.973	0.891	0.717
$D/m^2\ s^{-1}$	2.9 E-13	1.4 E-13	1.1 E-13	0.9 E-13
r/m	8.2 E-9	17.5 E-9	21.9 E-9	25.9 E-9

Figure 6-17

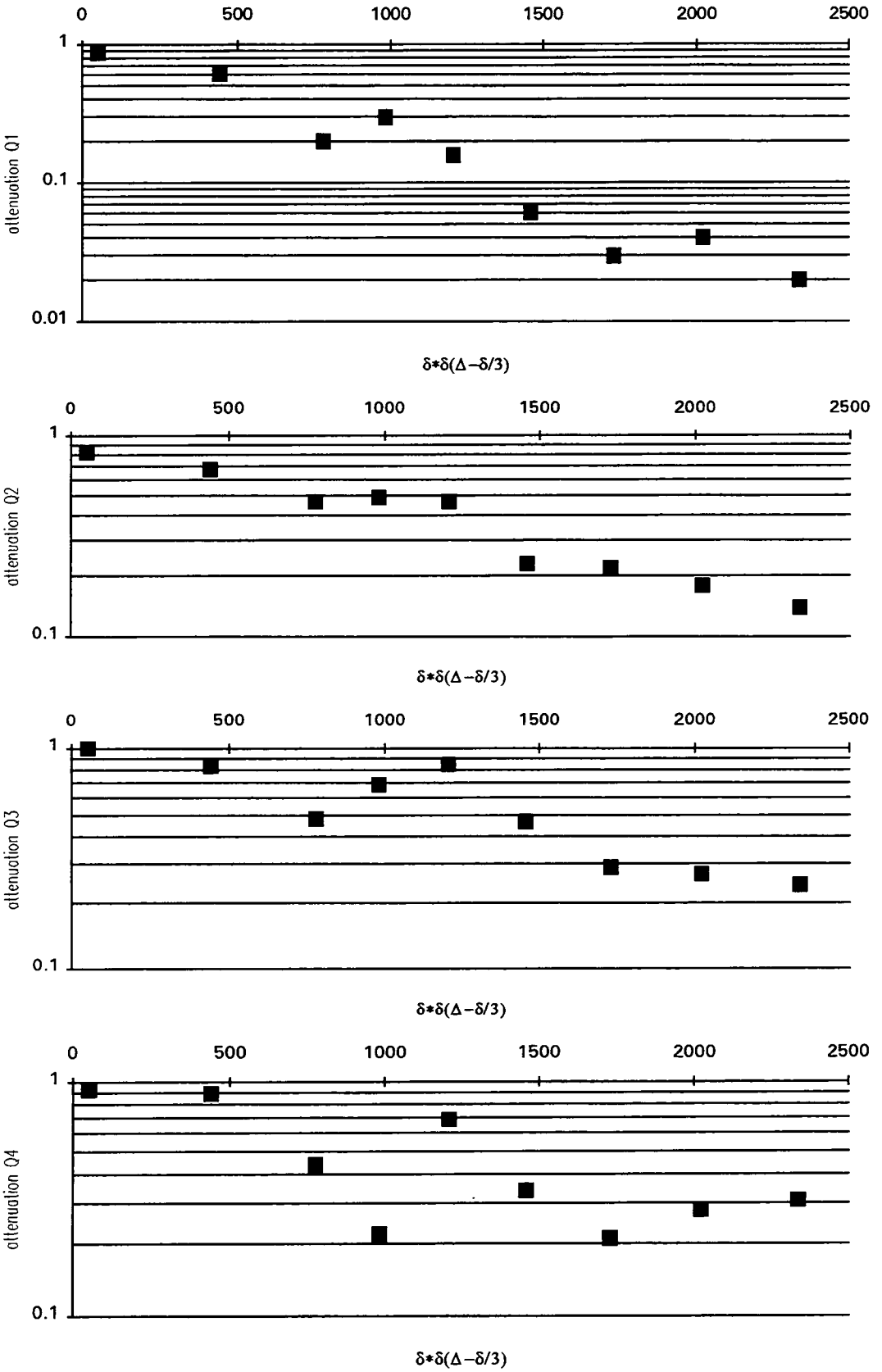
0
500
1000
1500
2000
2500
1
0.1
0.01
attenuation Q1
δ*δ(Δ−δ/3)
attenuation Q2
attenuation Q3
attenuation Q4

Table 6-31

Attenuation of peak intensities under the influence of a pulsed field gradient in a sodium silicate solution with 25wt% SiO_2 and Rm=4.0

δ/ms	$\delta^2(\Delta-\delta/3)$	Q1	Q2	Q3	Q4
1	49.7	0.72	0.67	1.0	1.0
3	441.0	0.59	0.60	1.0	1.0
4	778.7	0.33	0.65	0.88	0.91
4.5	982.1	0.47	0.63	0.78	0.67
5.0	1208.3	0.21	0.52	0.91	1.0
5.5	1457.0	0.12	0.45	0.75	0.74
6.0	1728.0	0.07	0.42	0.55	0.81
6.5	2020.9	0.09	0.29	0.55	0.80
7.0	2335.7	0.03	0.20	0.34	0.54

Table 6-32

Self-diffusion constants for structural units using the attenuation of peak intensities in a sodium silicate solution with 25wt% SiO_2 and Rm=4.0

	Q1	Q2	Q3	Q4
slope	-1.39 E-3	-5.03 E-4	-4.36 E-4	-2.04 E-4
correlation	0.948	0.907	0.905	0.720
$D/m^2\ s^{-1}$	2.3 E-13	0.84 E-13	0.73 E-13	0.40 E-13
r/m	10.3 E-9	28.6 E-9	32.9 E-9	60.2 E-9

Figure 6-18

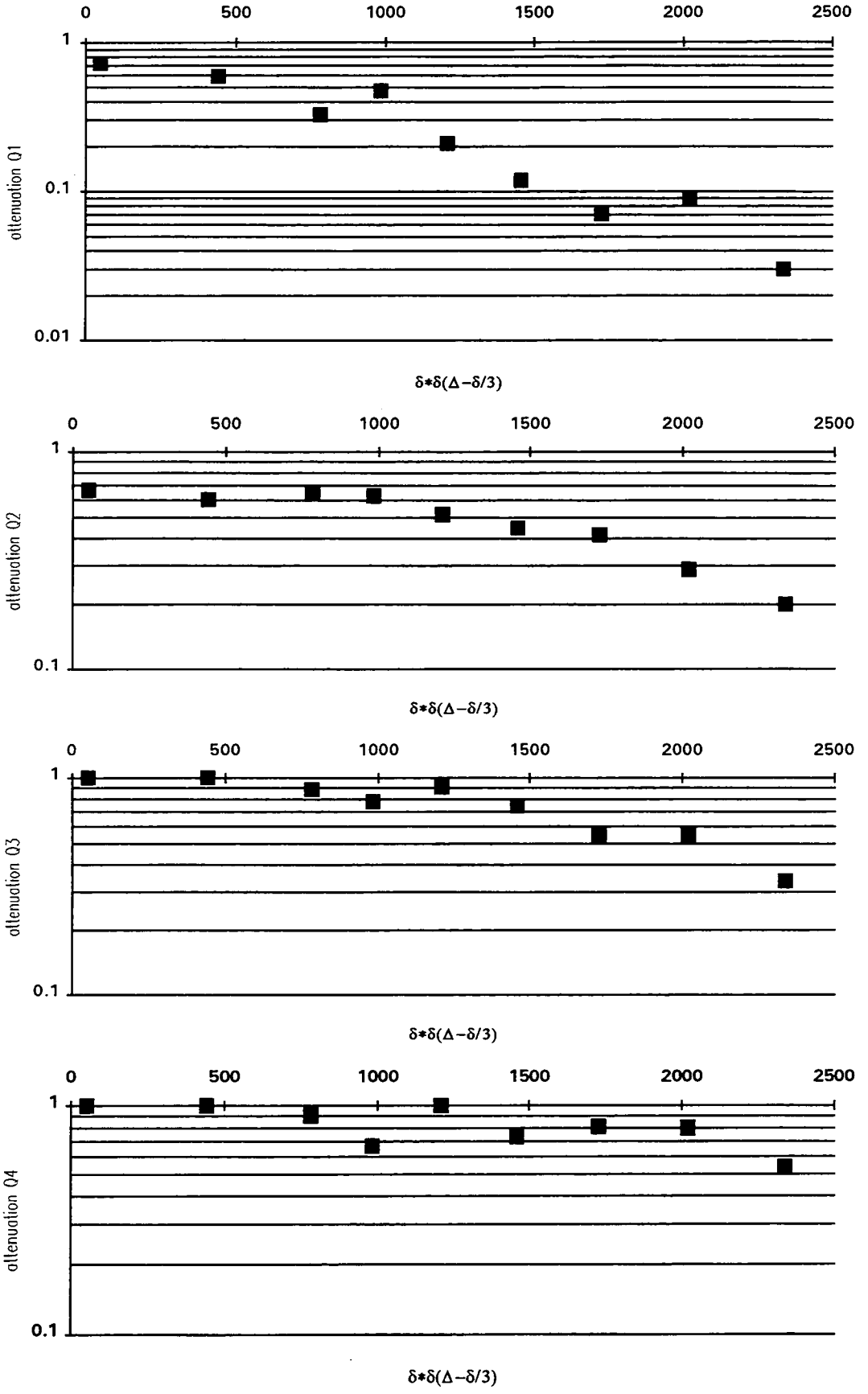
0
500
1000
1500
2000
2500
1
0.1
0.01
attenuation Q1
δ*δ(Δ−δ/3)
attenuation Q2
attenuation Q3
attenuation Q4

Generally there is more confidence in the attenuation obtained by using the areas (tables 6-26 and 6-30) than by just using the peak intensities (tables 6-21, 6-23, 6-28 and 6-32). The areas take changes in the width and the intensity of the resonances into account and are thus more sensitive to changes caused by the field gradient. It can be assumed that the results obtained at a higher gradient power (tables 6-24 to 32) present more confident results than those obtained at the lower gradient power (tables 6-19 to 6-23) since the higher gradient power produces a bigger attenuation of the resonances. Furthermore the experiments with a gradient pulse separation of 10 ms (tables 6-30 and 6-32) instead of 6 ms (tables 6-21, 6-23, 6-26, 6-28) present the more confident results, as higher gradient pulse durations can be used thus achieving a larger attenuation. Taking all this into account, it can be concluded that table 6-31 represents the results with the biggest confidence.

According to this the self-diffusion constant of the Q1 units is a factor two faster than the self-diffusion of Q2 units. The Q2 units generally diffuse slightly faster than the Q3 units, which in turn diffuse faster than the Q4 units. It has to be remembered, however, that all self-diffusion constants are for the average of the respective unit. This means that all values obtained are averages for all possible connectivities of the observed units to other units as well as for a distribution of particle sizes. The slower self-diffusion of Q4 units compared to Q3 units is due to the fact that there is a distribution of particle sizes in the silicate systems as opposed to an average particle size.

Particle radii :

Using the Stokes equation, values for particle radii are obtained. Although these are only averages, a general idea of the size of the colloidal material in highly-condensed silicate solutions is achieved for the first time. Macromolecules as large as 1 μm can often be uniformly dispersed through a fluid medium and thus form colloidal solutions. The lower limit of particle size for colloidal solutions is around 1 nm. Smaller particles would become

indistinguishable from true solutions. The upper limit is usually set at a radius of 1 μm[21]. According to the results presented in table 6-35, the size of colloidal particles in silicate solutions with a high degree of condensation ranges from about 8 nm to about 26 nm (8 nm to 18 nm for the smaller units, Q1 and Q2 and 22 nm to 26 nm for the larger units, Q3 and Q4).

4. Silicon-silicon Exchange

4.1 Room temperature

4.1.1 Exchange monitored *via* T2-values

T2-values have been measured with a pulse programme for the Hahn echo experiment (discussed in further detail in chapter 3-2.3). This pulse programme can only be used in the case of systems with no chemical exchange. In the case of chemical exchange the intensities of resonances in the spectra with long inter-pulse delays will be decreased not only by loss of magnetisation in the xy-plane due to spin-spin relaxation but also due to exchange. This means that the attenuation of the resonances does not follow equation [17].

$\ln M_t - \ln M_0 = -t/T2$ [17]

The longer the interpulse delay, t, the more will the intensities be affected by loss of xy-magnetisation caused by exchange. The result is that the graph of (ln Mt-ln Mo) versus t will have the form of an exponential decay instead of a linear decay.

In these investigations a representative sodium silicate solution with 25wt% SiO_2 and Rm=4.0 is used for the investigations. To allow a decision about the form of the decay, the experiment was carried out using the Hahn echo pulse sequence with a large number of interpulse delays being increased in small steps.

As shown in figure 6-19 below, the intensities of the Q3 and Q4 resonances decay in a non-logarithmic way (non-linear in a logarithmic plot).

Figure 6-19
(lnM_t - lnM_0) versus t in s for the Q3 and Q4 units in
a sodium silicate solution containing 25wt% SiO_2 with Rm=4.0

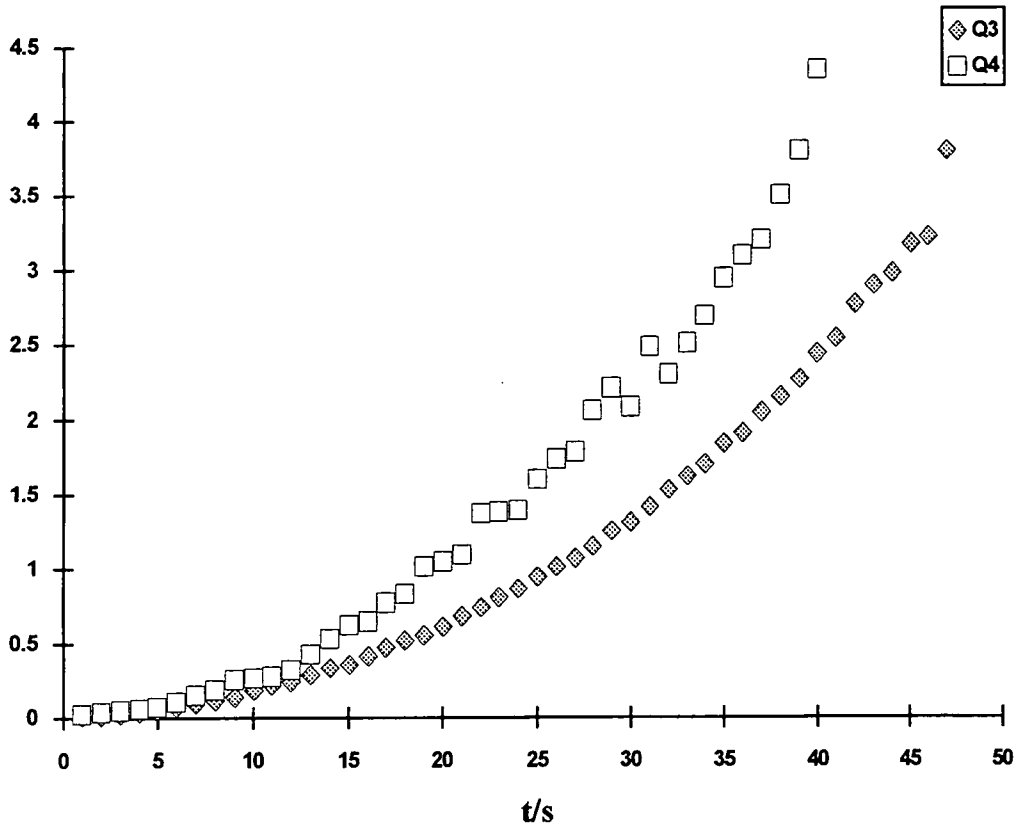

Therefore it is concluded, that Q3 and Q4 units in highly condensed silicate solutions participate in chemical exchange processes. If even Q3 and Q4 units undergo exchange, it can be assumed that the units with lower connectivities (Q0, Q1 and Q2) undergo exchange as well.

4.1.2 2D Exchange Spectroscopy (2D EXSY)

The conclusion derived from the previous section is of a merely qualitative nature. We know that all structural units in a highly condensed silicate solution undergo chemical exchange. However, the species they are in exchange with and the rate of exchange are not known. Both can be obtained using 2D exchange spectroscopy. This technique is described in detail in chapter 3-2.4. With 2D EXSY it is possible to study partially overlapping

spectra. Furthermore dynamic processes can be monitored as a function of the mixing time, whose variation turns the experiment into a 3D technique[25].

So far only exchange rates for the monomer resonance in silicates with far smaller degrees of condensation and without colloidal material have been monitored[15-18]. These exchange rates were not measured for a particular exchange process. The exchange rate constant determined on the basis of approximate kinetic evaluations *via* the linewidth of the Q0 resonance[15] is 17 s^{-1} at 4°C. This method, however, is not very accurate compared to exchange rates determined *via* T2-values, which yield exchange rate constants for the monomer of $k \leq 2.8\ s^{-1}$ for a silicate with Rm=1.0 and $k \leq 24\ s^{-1}$ for a silicate with Rm=0.3 at 4°C[16]. The exchange rate seems to increase with decreasing Rm-value. Harris et al. used selective inversion recovery experiments to monitor chemical exchange[17,18]. It was stated that the doubly deprotonated monomer ($H_2SiO_4^{2-}$) is of negligible importance in mediating Si-Si exchange compared to the mono deprotonated monomer ($H_3SiO_4^-$)[19]. Two-dimensional exchange spectroscopy was used to qualitatively model exchange pathways of silicon in potassium silicate solutions with low Rm-values (Rm=1.0 and Rm=0.5) using only one mixing time[20]. As the rate of exchange relative to the mixing time becomes higher (for long mixing times), the cross peaks broaden, move closer together and eventually coalesce into a broad peak (as in 1D NMR-spectra)[29]. The investigations reported here are the first ones to successfully monitor the entire exchange processes in a highly condensed silicate solution qualitatively as well as semi-quantitatively.

Since a silicate system containing ^{29}Si in natural abundance (4.7%) is far too insensitive for these investigations, a representative highly condensed sodium silicate solution with a SiO_2 concentration of 25wt% and Rm=4.0, enriched in ^{29}Si to the 95.65 %-level, was used. The mixing time was varied in order to find the approximate rate of exchange for the silicate units.

The results are presented in figure 6-20 and summarised in table 6-33.

Figure 6-20
2D EXSY at room temperature
for exchange between silicate species in a sodium silicate solution containing 25wt% SiO_2 and Rm=4.0 (enriched in ^{29}Si)
relaxation delay 60 s, transients 16, acquisition time 0.01 s,
128 data points in F1 and F2 direction

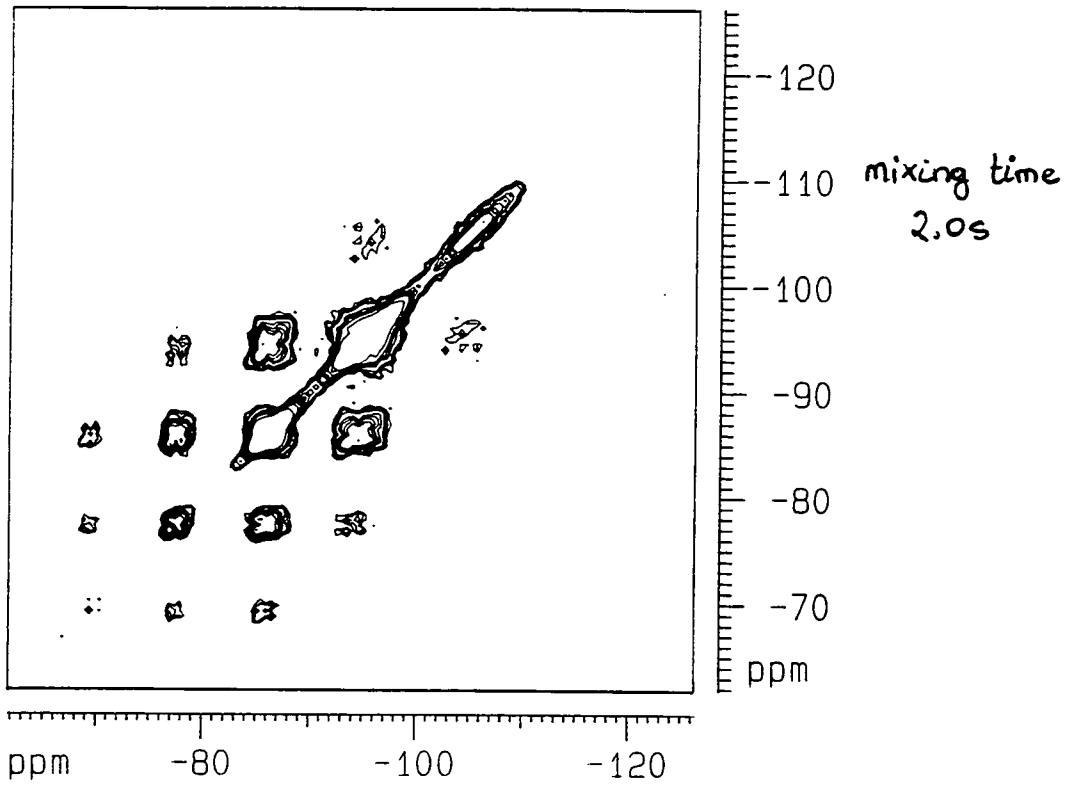

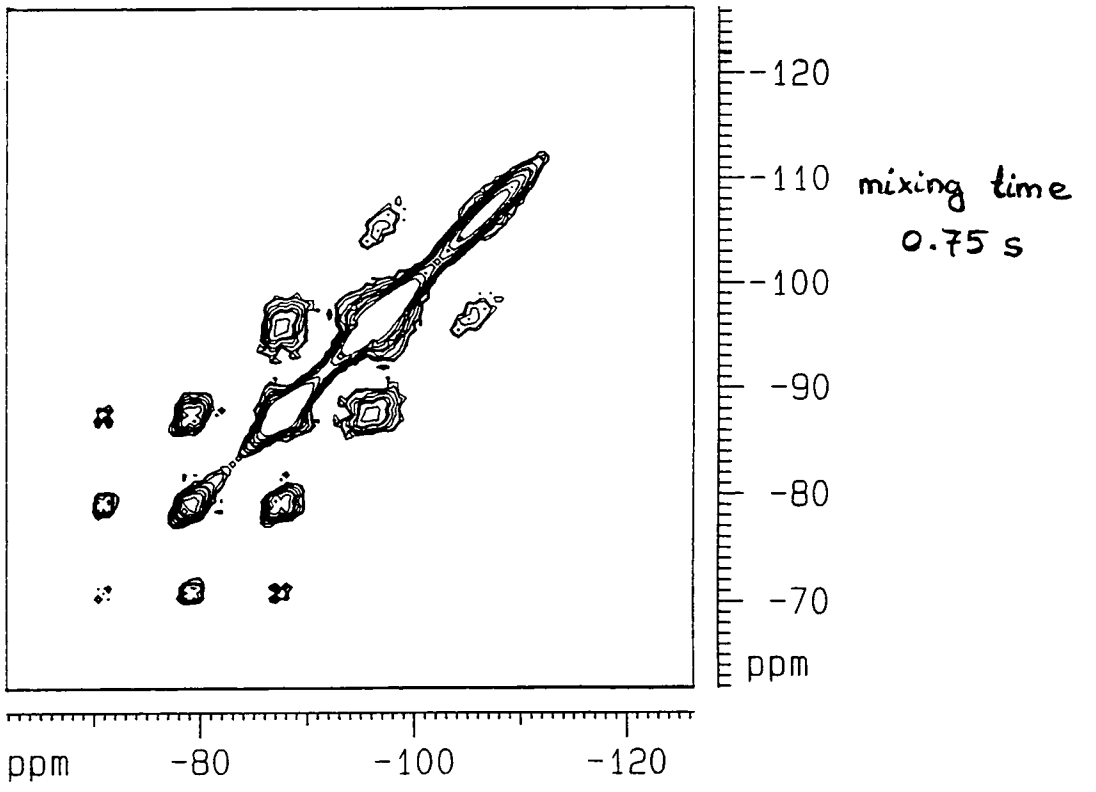

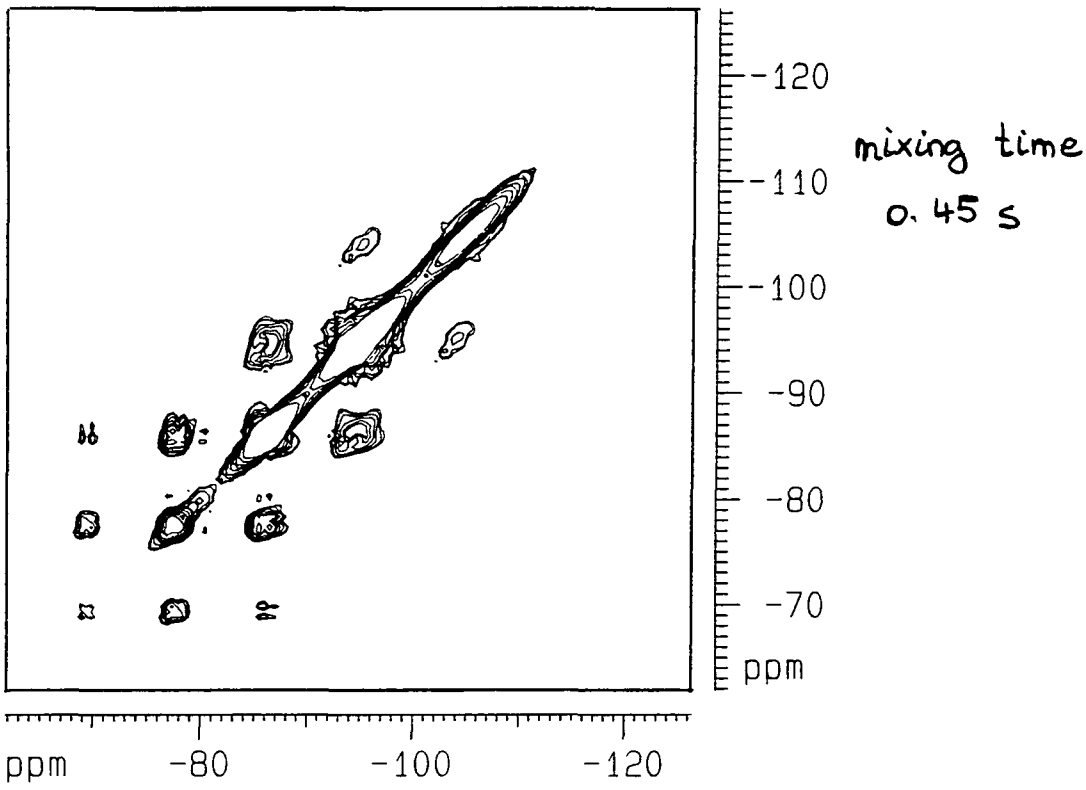

mixing time
0.45 s

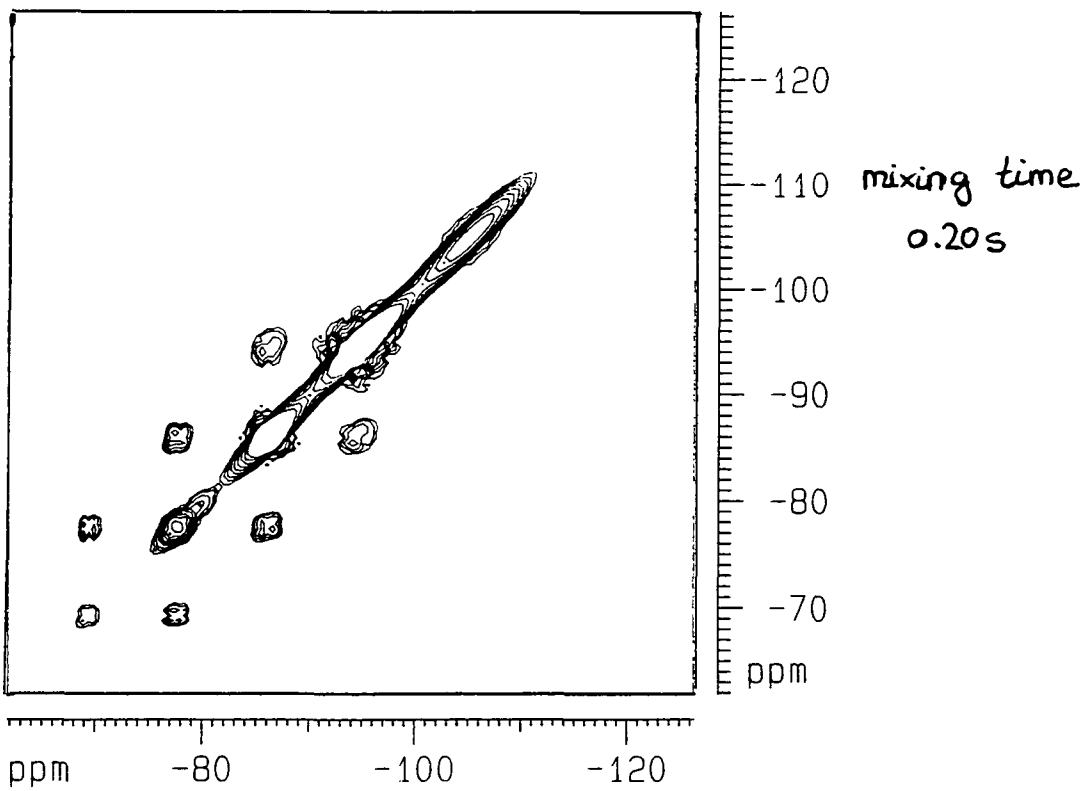

mixing time
0.20s

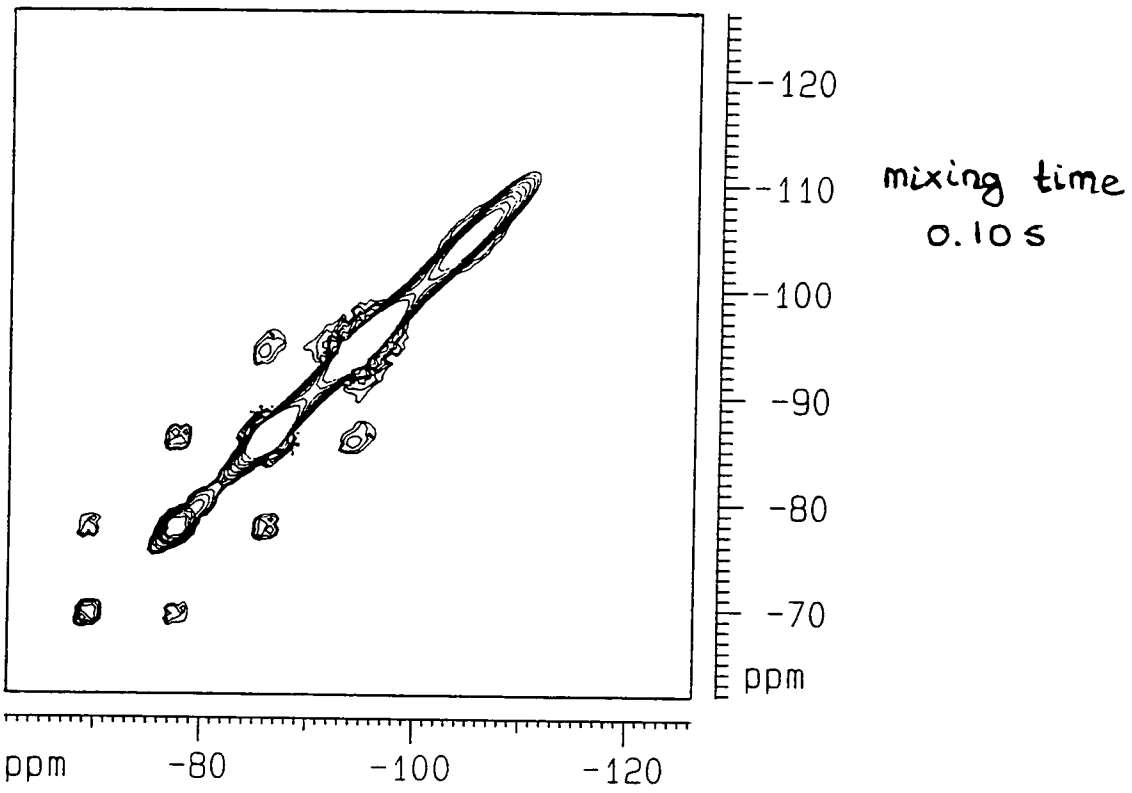

mixing time
0.10 s

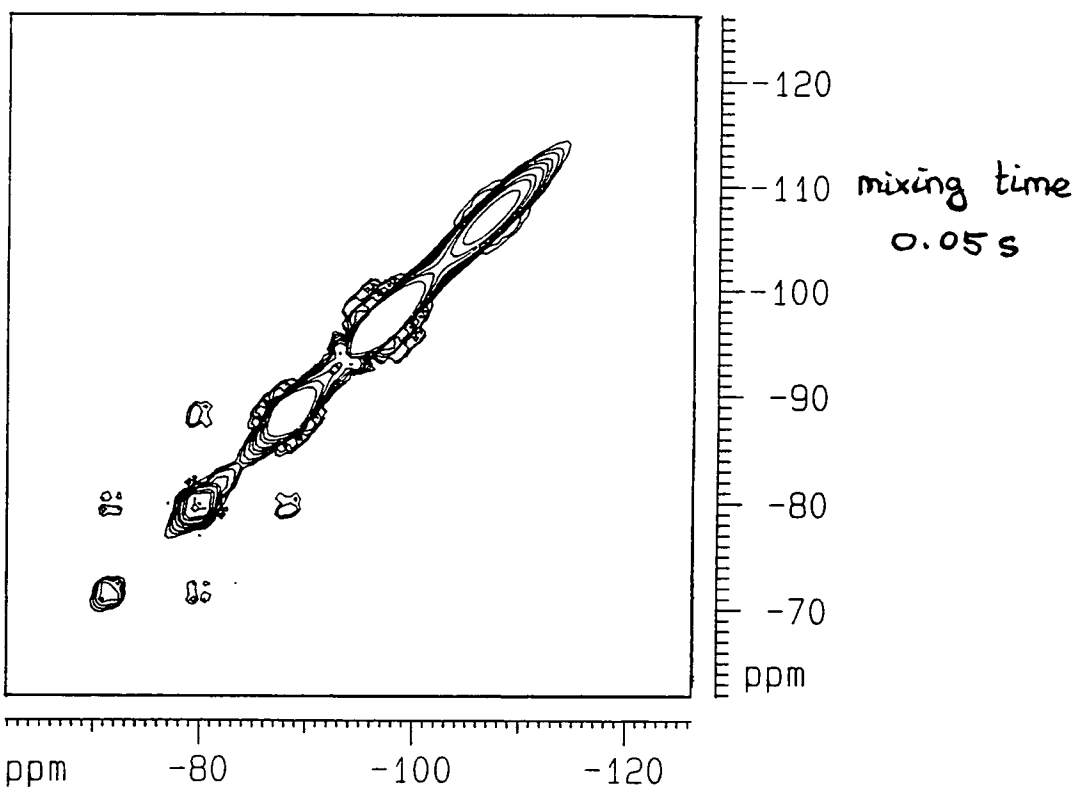

mixing time
0.05 s

Table 6-33
Exchange pathways in a
sodium silicate solution containing 25wt% SiO_2 with Rm=4.0
as monitored by 2D exchange spectroscopy

	Q0	Q1	Q2	Q3	Q4
Q0		×	×		
Q1	×		×	×	
Q2	×	×		×	
Q3		×	×		×
Q4				×	

All structural units present in a highly condensed silicate solution are involved in chemical exchange processes with the unit showing the next lower and the next higher connectivity. Even exchange involving two steps in the connectivity can be monitored for the Q3 and Q2 units (the Q1 and Q0 units respectively).

If several exchange processes combine to exchange networks, it is not possible to derive exchange rates from cross-peak intensities, and it becomes necessary to record a series of 2D exchange spectra with different mixing times, including some very short ones[29]. In this case a numerical evaluation of the dependence of cross-peak intensities (appearance of cross-peaks) on the mixing time yields a semi-quantitative measure of the exchange rate constants. It is desirable to determine the rates from the initial build-up of the cross-peak intensities, since the intensities for longer mixing times depend also on leakage mechanisms, which tend to reduce the transferred magnetisation[37]. If k is much less than 1/T1, the frequency labelled z-magnetisation will disappear before it has a chance to migrate and give rise to cross-peaks. The mixing time for detecting exchange at rate k varies as a function of kT1. Two equations are possible,

their applicability depending on the ratio between the spin-lattice relaxation times and k^{37} (for further details the reader is referred to chapter 3-2.4).

mixing time = $(0.5)k^{-1}$ if $k \sim T1^{-1}$ [18]

mixing time = $(1.5)k^{-1}$ if $k \sim (10)T1^{-1}$ [19]

From an evaluation of exchange rate constants and T1-values it is obvious that equation [19] has to be chosen for the calculation of rate constants for exchange. The mixing time, which was taken for the calculation of the rate constant for the exchange, is the lower limit, which is defined as the mixing time, where exchange cross peaks first become apparent. Using this lower limit of the mixing times for the calculation, results in the values reported for the rate constants being upper limits (maximum rate constants). These maximum pseudo first order rate constants characterise the minimum exchange lifetimes of the silicate species ($k_{max} = (t_{min})^{-1}$). In table 6-34 the lower limits for the mixing time of the structural units involved in exchange processes and the maximum exchange rate constants are presented.

Table 6-34
Lower limits for the mixing time and maximum rate constants at 25°C
for the structural units involved in chemical exchange
in a sodium silicate solution containing 25wt% SiO_2 with Rm=4.0

exchange process	**mixing time (lower limit)/s**	**maximum rate constants for exchange/s^{-1}**
Q3 - Q4	0.45	3
Q3 - Q2	0.1	15
Q3 - Q1	2.0	1
Q2 - Q1	0.05	30
Q2 - Q0	0.45	3
Q1 - Q0	0.05	30

Generally the rate of exchange for the structural units is the faster, the lower the degree of condensation of the structural units involved in the exchange. The exchange involving two connectivities, as for instance between Q0 and Q2 units, is about a factor of 10 slower than the exchange involving only one connectivity, as for instance between Q0 and Q1. Generally the mean lifetimes of the individual species are of the order of 10^{-2} s or longer and can thus be placed in the region of slow exchange, which is characterised by the line separation being much larger than the actual linewidth[29].

The fact that exchange between Q3 and Q4 units can be observed supports the conclusions made in chapter 5 about the porous structure of the colloidal particles in silicate sols. For Q3 - Q4 exchange to be operative, there must be a large amount of contacts between Q3 and Q4 units, which is only found in systems with high porosity. All species apart from the Q4 units can exchange with more than one other silicate species in the solution, so that lifetimes for structural units will necessarily be an average over all the exchange processes they are involved in. The fact that Q3 - Q1 exchange as well as Q2 - Q0 exchange is very much slower than exchange between Q3 and Q2 or exchange between Q2 and Q1 units shows that some of the Q2 units are connected to Q3 units and some are connected to Q1 units. This means that separate Q3 - Q2 links along with separate Q2 - Q1 links, rather than Q3 - Q2 - Q1 links, are found in the silicate solutions. This supports findings in section 3 of this chapter.

4.2 Increased temperature

4.2.1 T2-values

If the temperature is increased, there are two effects influencing the spin-spin relaxation times measured using the CPMG pulse sequence. One is the increase in particle mobility, the other is the increase in the exchange rate

between the structural units. The former will cause an increase in the T2-values while the latter will result in their decrease.

The results presented in table 6-35 show that an increase in the temperature of 35°C from 25°C to 60°C causes a decrease in the spin-spin relaxation times of all structural units.

Table 6-35
Spin-spin relaxation times measured with the CPMG sequence
using a pulse spacing of 1.5ms between 90°x and 180°y pulse
at 25°C and 60°C for a sodium silicate solution with 25wt% SiO_2 and Rm=4.0

structural unit	T2 in s at 25°C	T2 in s at 60°C
Q0	57	25
Q1	58	22
Q2	49	14
Q3	31	15
Q4	20	18

This decrease in the T2-values with increasing temperature can be explained by an increase in the rate of chemical exchange, which outweighs the increase in mobility.

4.2.2 2D EXSY

The findings described in the previous section are of a qualitative nature. For more quantitative information the technique of 2D (3D) exchange spectroscopy has to be used.

The variation of the mixing time shows that an increase in the temperature from 25°C to 45°C results in an increase in the rate of exchange for all exchange processes. The 2D exchange spectra are shown in figure 6-21. The rate constants for chemical exchange, calculated with equation [19], using the upper limit of the mixing times at which chemical exchange is still observed, are presented in table 6-36 below.

Table 6-36
Maximum rate constants for exchange at 25°C and 45°C for exchange processes in a sodium silicate solution containing 25wt% SiO_2 with Rm=4.0

exchange process	**maximum rate constants for exchange at 25°C /s^{-1}**	**maximum rate constants for exchange at 45°C /s^{-1}**	**Ea_{max} /$kJmol^{-1}$**
Q3 - Q4	3	33	100
Q3 - Q2	15	100	80
Q3 - Q1	1	33	140
Q2 - Q1	30	100	50
Q2 - Q0	3	33	100
Q1 - Q0	30	100	50

The rate of exchange generally is increased if the temperature is raised. This rate-increase generally is independent of the thermodynamics of the exchange (endothermic or exothermic)[23]. Since it can be assumed that the exchange processes are of the same order at the two temperatures investigated (25°C and 45°C), the dependency of the rate constant, k, on the temperature is described by the Arrhenius equation (equation [20])[23,24]. A plot of lnk versus 1/T will yield a graph with a slope of $-E_a/8.314$.

$$k = k_m * \exp\left(-\frac{E_a}{k_B N_A T}\right) \qquad [20]$$

The interval where E_a for chemical reactions generally can be found is from 5 to 400 kJ/mol[23]. For a successful exchange process, the participants have to absorb a certain potential energy, the activation energy. This characterises the energy barrier between the potential energy of the two participants in the exchange. The probability that the participants can acquire this energy is given by the Boltzman distribution and is proportional to $E_a(k_BN_AT)^{-1}$. Only those units are capable of undergoing exchange, which have a kinetic energy as large as the activation energy[24]. Considering the

total number of units, the part which is capable of undergoing exchange processes is characterised by k/k_m.

Naturally activation energies obtained with just two points are only approximations. Nevertheless they give us an idea of the region in which activation energies for chemical exchange between silicate species are found. The activation energies obtained with equation [20[are between 140 kJ/mol and 50kJ/mol. Exchange processes involving changes over two connectivities require higher activation energies than required for changes over one connectivity. The activation energy required for exchange processes generally is the higher the higher the connectivity of the structural units involved is. However, the activation energy needed for the exchange between Q4 and Q3 units is only a factor of two larger than for the exchange between species of low connectivity (Q0-Q1 and Q1-Q2 exchange). The relatively low activation energy for the exchange between Q3 and Q4 units supports the conclusions made about the highly porous nature of the colloidal material in highly condensed silicate solutions.

Figure 6-21
2D EXSY at 45°C
for exchange between silicate species in a sodium silicate solution containing 25wt% SiO_2 and Rm=4.0 (enriched in ^{29}Si)
relaxation delay 60 s, transients 16, acquisition time 0.01 s,
128 data points in F1 and F2 direction

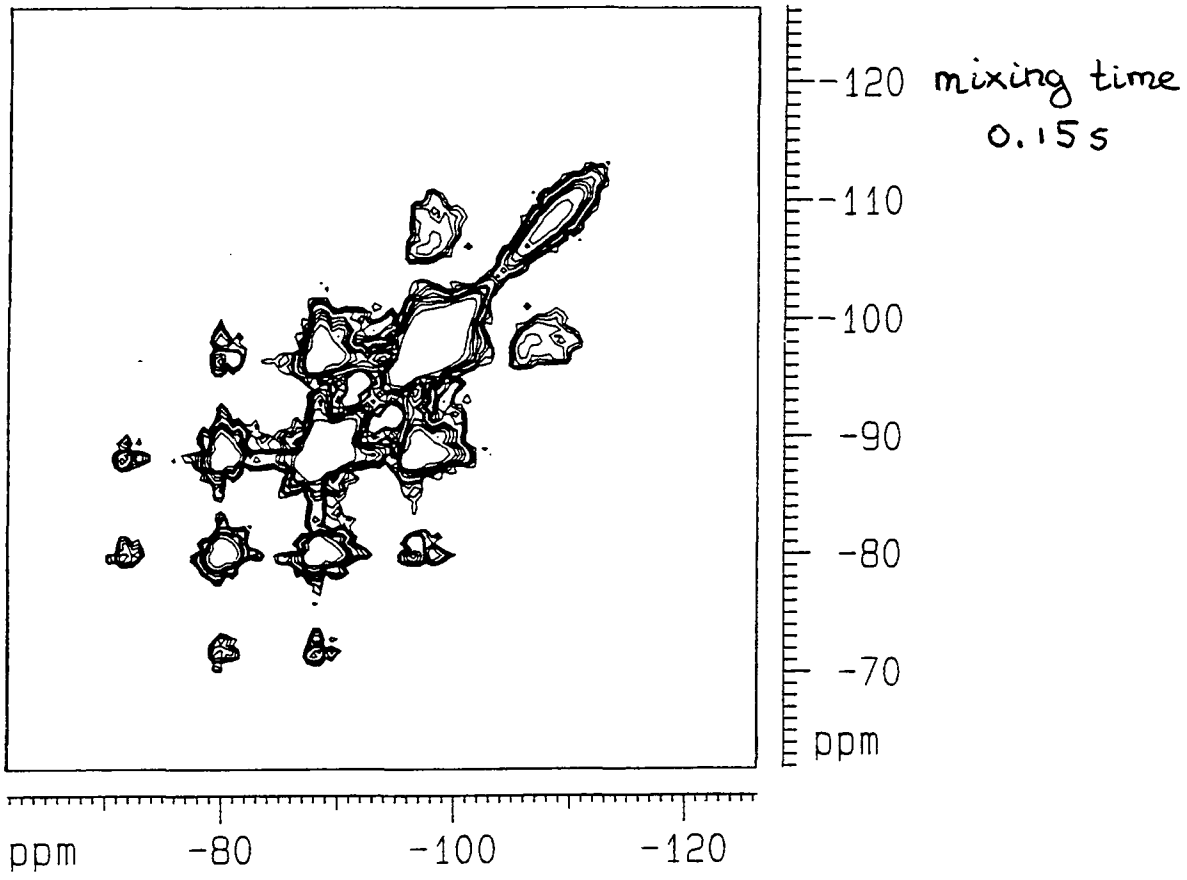

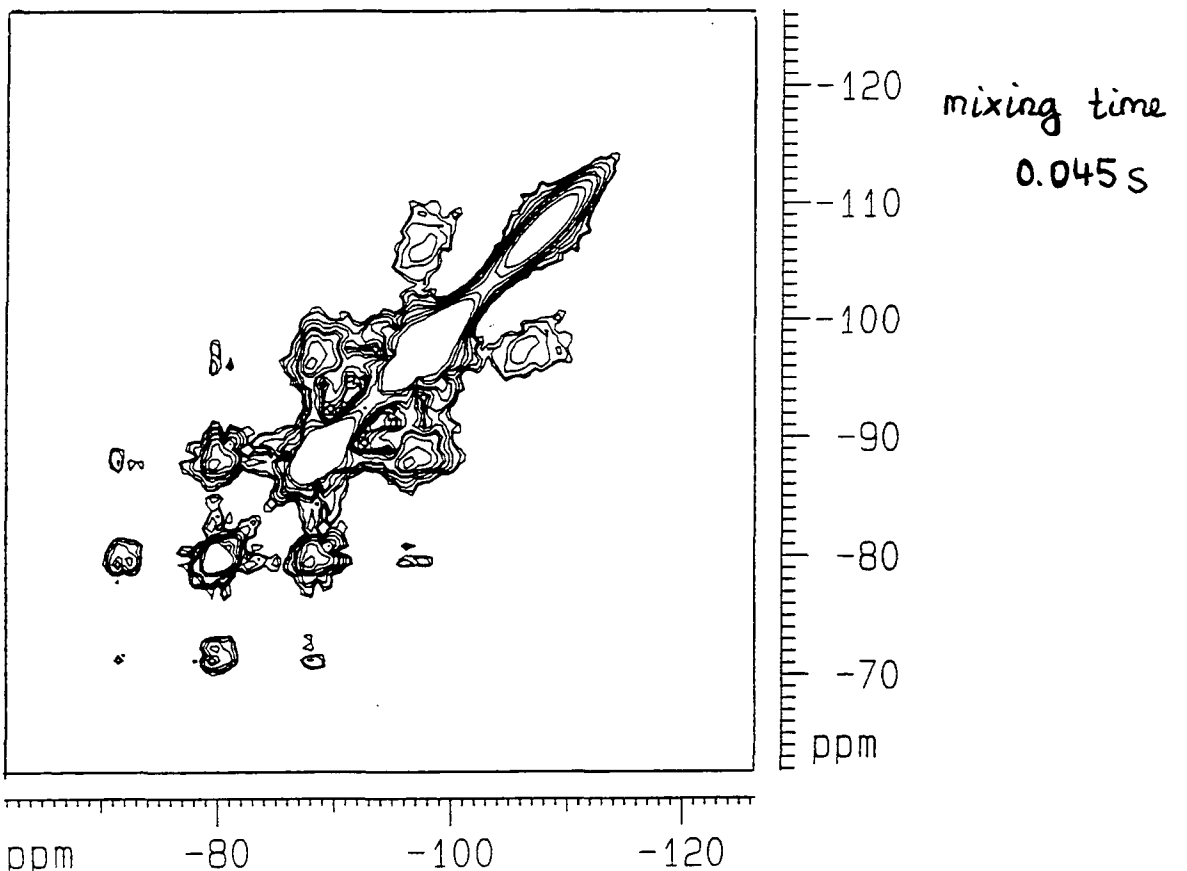

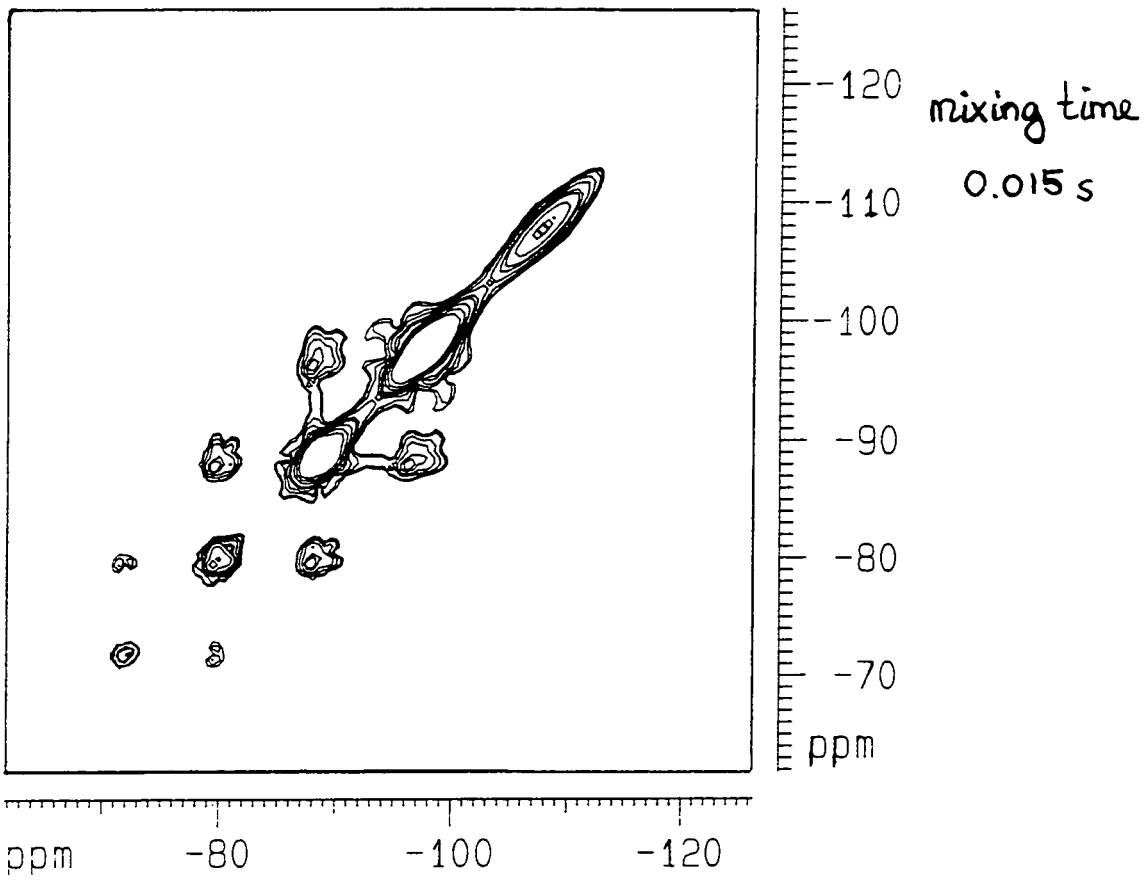
-120
-110
-100
-90
-80
-70
ppm
ppm
-80
-100
-120
mixing time
0.015 s

5. Si-H Distances

The distances between silicon and protons in Si-OH bonds can be calculated *via* known average Si-O and average O-H bond lengths in combination with average Si-O-Si and H-O-H angles. Naturally the distances thus obtained will only be approximate. Another way to calculate the rAX-distances (Si-H distances) is to use the correlation times, which have been worked out by comparing experimental T1-values at two different fields (see section 2.2 of this chapter), in combination with the experimentally measured T1-value. This method to achieve the Si-H distances will reveal if the correlation times, calculated in section 2.2 from experimental T1-values, are in the right range and prove if the theory for T1-relaxation worked out in section 2.1 is appropriate.

The following equations are needed:

$$\frac{1}{20}(2\pi R)^2 = 1.1258 * 10^{-51} * rAX^{-6} \qquad [21]$$

$$\frac{1}{T1} = 1.1258 * 10^{-51}[J(\omega x - \omega A) + 3J(\omega A) + 6J(\omega x + \omega A)] * rAX^{-6} \qquad [22]$$

$$1.1258 * 10^{-51}[J(\omega x - \omega A) + 3J(\omega A) + 6J(\omega x + \omega A)] = F_{calc} \qquad [23]$$

$$\frac{rAX^6}{T1} = F_{calc} \qquad [24]$$

$$rAX = \sqrt[6]{F_{calc} * T1} \qquad [25]$$

R is the dipolar coupling constant and is proportional to rAX^{-6}

rAX is the Si-H-distance

The values for F_{calc} at the appropriate field have been calculated for a range of τ_c-values using equations [22] to [25] with the help of a BASIC programme. Then the rAX distances were calculated using the appropriate F_{calc} values for the correlation times, obtained from experimental T1 values at different fields

for the structural units in a silicate system, in combination with the experimentally measured T1-values at the appropriate field (T1 = T1exp). The results for the silicon-proton distances in sodium silicate solutions (sols) and gels, obtained using equation [25], are reported in tables 6-37 and 6-38.

Table 6-37
Average Si-H distances in m for sodium silicate solutions

structural unit	30wt% SiO_2 and Rm=2.6	25wt% SiO_2 and Rm=4.0
Q0	1.5 ± 0.2 E-10	1.6 E-10
Q1	1.5 ± 0.2 E-10	1.7 E-10
Q2	1.8 ± 0.05 E-10	1.9 ± 0.1 E-10
Q3	1.7 E-10	2.0 ± 0.1 E-10

Table 6-38
Average Si-H distances in m for sodium silicate gels

structural unit	33wt% SiO_2 and Rm=3.4	30wt% SiO_2 and Rm=4.0
Q0	-	-
Q1	1.8 E-10	1.9 E-10
Q2	1.8 E-10	1.7 E-10
Q3	1.8 E-10	2.0 E-10

In this calculation of the rAX-distances, however, a number of effects occurring in real silicate systems have been neglected. These are :

1. the number of attached protons
2. the possibility of anisotropic motion
   (more than one correlation time)

These can be neglected for the calculation of τ as the correlation time is calculated from a ratio of T1-values, since all of the above mentioned effects are affecting the T1-values at two different fields in the same way and therefore are cancelled out by taking the ratio of T1-values at different fields.

Number of attached neighbouring protons:

So far the number of neighbouring protons has not been taken into account in the calculation of the Si-H distances. In contrast to the calculation of silicon correlation times, where the factors characterising the number of neighbouring protons go into all the equations no matter at what field and thus are cancelled by dividing one by the other, they have to be taken into account for the calculation of the rAX-value in the calculated T'calc. as well as in the experimentally measured T1-values.

The values, reported in tables 6-37 and 6-38, are the values for one Si-O-H distance, thus:

for one Si-O-H distance in Q3 units the result is: $(T1)^{-1} = F_{calc} * (rAX)^{-6}$

for two Si-O-H distances in Q2 units the result is: $(T1)^{-1} = F_{calc} * 2(rAX)^{-6}$

for three Si-O-H distances in Q1 units the result is: $(T1)^{-1} = F_{calc} * 3(rAX)^{-6}$

for four Si-O-H distances in Q0 units the result is: $(T1)^{-1} = F_{calc} * 4(rAX)^{-6}$

Here it is assumed that the values for the structural units Q0, Q1, Q2 and Q3 include only nearest neighbour interactions. The Q4-unit has not got any directly attached protons but can have protons in the neighbourhood as there are holes or caves in the colloidal particles which are big enough for water molecules (1). Furthermore Q3-units with direct Si-O-H bonding to protons are attached to the Q4-units on the surfaces (particle surface and caves or holes) which are attached to other Q4-units (2). Finally there are Q4-units near particle surfaces or near holes or caves that are directly attached to Q3-units (3). Thus the interactions which are included in the relaxation of Q4-silicon by protons are only long-range interactions with water (1) next next neighbour interactions(2) and next nearest neighbour proton-interactions (3). The possible interactions of silicon in Q4 units with protons are illustrated in figure 6-22.

Figure 6-22
Possible interactions of silicon in Q4 units with protons

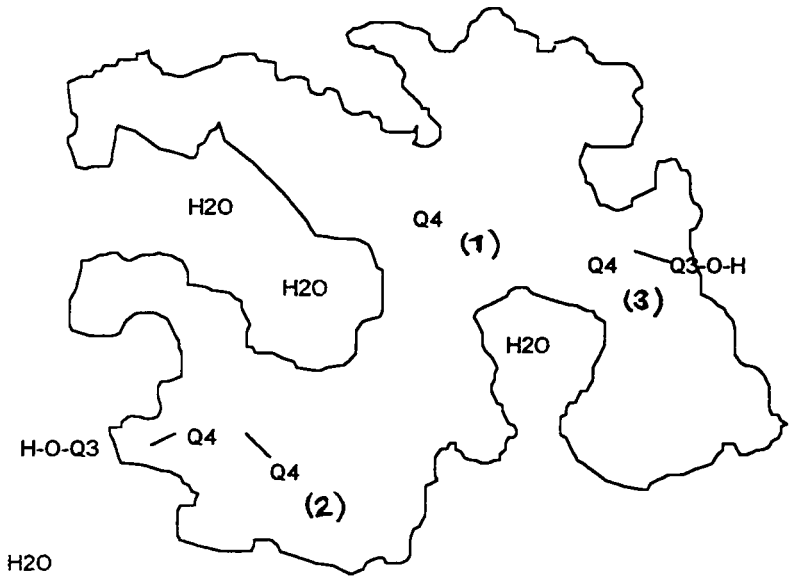

It can be concluded, that generally the experimental T1-values can be described by two major contributions if relaxation is dominated by dipolar interaction with protons:

1. direct Si-O-H interaction (next neighbour interactions)
2. indirect silicon-proton interactions which can be:
   a) next-nearest neighbour interactions (Si-O-Si-O-H)
   b) next next-nearest neighbour interactions (Si-O-Si-O-Si-O-H)
   c) long-range interactions with pore-water

The spin-lattice relaxation times of all structural units except the Q4 units can be influenced by the direct as well as the indirect dipolar silicon proton interactions. Thus subtracting the longitudinal relaxation rate due to 'indirect' interactions from the relaxation rate measured by inversion recovery for the overall interactions with protons yields the relaxation rate due to next neighbour (direct) interactions. All indirect interactions are characteristic for the interactions silicon can undergo with protons if it is located in Q4-units. This explains why average silicon proton distances for the Q4 units can not be calculated as there would be too much speculation involved. Out of the three

above-mentioned possibilities for indirect interactions, the next-nearest neighbour interactions are the ones which contribute most strongly to Si-Q4 relaxation *via* protons. This is because the Si-H distance is shorter than for the other two indirect interactions and because of the porous structure of colloidal particles results in a relatively large surface area and therefore a large number of Q4-Q3 bonds.

The contribution of Si-O-H bonds to the ^{29}Si relaxation rate due to direct dipolar interactions of silicon with next neighbour protons is :

1 Si-O-H for Q3 units (n=1)

2 Si-O-H for Q2 units (n=2)

3 Si-O-H for Q1 units (n=3)

4 Si-O-H for Q0 units (n=4)

The following equations are needed for the calculation of the relaxation rate due to direct interactions taking the number of attached protons and the indirect interactions into account:

$$R_{total} = nR_{direct} + R_{indirect} \qquad [26]$$

$$R_{direct} = \frac{1}{n} R_{total} - \frac{1}{n} R_{indirect} \qquad [27]$$

with $R_{indirect} = RQ4$

The new T1-values (T1*) and F_{calc}-values (F_{calc}*) taking the number of neighbouring protons and the nature of the interaction into account are reported in tables 6-39 to 6-44 and used in the calculation of the better approximation to Si-O-H distances.

Table 6-39

Best approximation for silicon proton distances in a sodium silicate solution with 25wt% SiO_2 and Rm=4.0 (field with ^1H resonance frequency 600MHz):

structural unit	T1exp.*/s (600MHz)	F_{calc}* 600MHz/m^6 s^{-1}	rAX*/m
Q0	54.7	5.5E-61	1.8E-10
Q1	43.3	9.7E-61	1.9E-10
Q2	34.5	2.1E-60	2.0E-10
Q3	25.7	4.6E-60	2.2E-10

Table 6-40

Best approximation for silicon proton distances in a sodium silicate solution with 25wt% SiO_2 and Rm=4.0 (field with ^1H resonance frequency 500MHz):

structural unit	T1exp.*/s (500MHz)	F_{calc}* 500MHz/m^6 s^{-1}	rAX*/m
Q0	61.5	5.7E-61	1.8E-10
Q1	50.4	1.12E-60	2..0E-10
Q2	31.5	2.46E-60	2.1E-10
Q3	22.7	5.2E-60	2.2E-10

Table 6-41

Best approximation for silicon proton distances in a sodium silicate solution with 25wt% SiO_2 and Rm=4.0 (field with ^1H resonance frequency 250MHz):

structural unit	T1exp.*/s (250MHz)	F_{calc}* 250MHz/m^6s^{-1}	rAX*/m
Q0	-	-	-
Q1	43.5	1.3E-60	2.0E-10
Q2	37.4	3.65E-60	2.3E-10
Q3	27.2	8.2E-60	2.5E-10

Table 6-42
Best approximation for silicon proton distances in a sodium silicate gel with 30wt% SiO_2 and Rm=4.0 (field with ^1H resonance frequency 600MHz):

structural unit	T1exp.*/s (600MHz)	F_{calc}* 600MHz/m^6 s^{-1}	rAX*/m
Q0	-	-	-
Q1	47.2	1.67E-60	2.1E-10
Q2	46.5	1.28E-60	2.0E-10
Q3	29.3	4.42E-60	2.2E-10

Table 6-43
Best approximation for silicon proton distances in a sodium silicate gel with 30wt% SiO_2 and Rm=4.0 (field with ^1H resonance frequency 500MHz):

structural unit	T1exp.*/s (500MHz)	F_{calc}* 500MHz/m^6s^{-1}	rAX*/m
Q0	-	-	-
Q1	44.8	1.9E-60	2.1E-10
Q2	33.8	1.34E-60	1.9E-10
Q3	23.9	5.7E-60	2.3E-10

Table 6-44
Average silicon proton distances in a sodium silicate sol and gel with 25wt% SiO_2/30wt% SiO_2 and Rm=4.0

structural unit	**25wt% SiO_2 Rm=4.0**	**30wt% SiO_2 Rm=4.0**
Q0	1.8 E-10 m	-
Q1	2.0 ± 0.05 E-10m	2.1 E-10m
Q2	2. 1 ± 0.12 E-10m	2.0 ± 0.05 E-10m
Q3	2.3 ± 0.14 E-10m	2.3 ± 0.05 E-10m

The average bond-distance for a Si-O bond in solid silicates is 1.6E-10m[30,32], the bond-distance for an O-H bond is 0.93E-10m[31]. The bond-

angle for a Si-O-Si angle is reported to be 130°-155°[30,32] and the value for the H-O-H angle is 105°[31]. Thus the Si-H distance is between 2.0E-10m and 2.35E-10m. The values for the average Si-H distance in SiOH bonds calculated using literature values are in good agreement with the ones calculated using the experimental T1-values and correlation times. The silicon proton distances for the less condensed species are shorter than for the highly condensed ones. The results discussed in detail in chapter 5-5 show that the majority of surface groups are in the hydrated state (SiOH). The calculated distances account for Si-OH distances but not for $Si\text{-}O^{-}$ $(H_2O)_6Na^{+}$ distances.

Anisotropic correlation time

The usual case of intramolecular anisotropic correlation times occurs in systems like

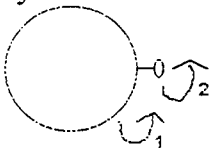

where there are two independent correlation times (**1** and **2**). The whole particle rotates with $\tau 1$ and the small connected part additionally rotates with $\tau 2$. This cannot be the case for structural Si-units like Q4, Q3, Q2 and Q0 as these are interlinked in a way which makes this sort of system impossible. It is only for Q1-units that this anisotropic rotation is possible.

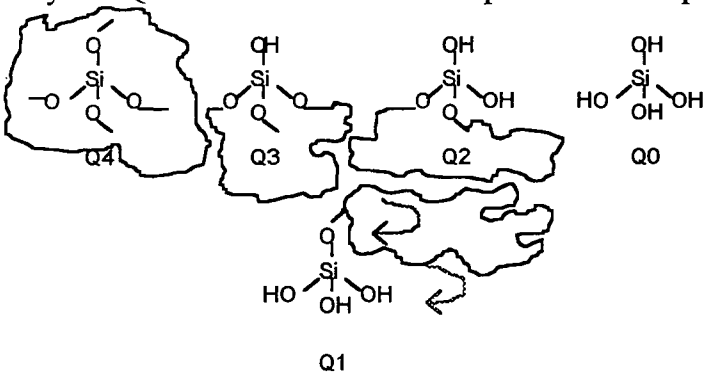

Intramolecular anisotropic rotation can occur in large colloidal particles where parts of the particle can rotate independently to other parts. Thus there would be Q3-units and Q4-units with different rotational correlation times.

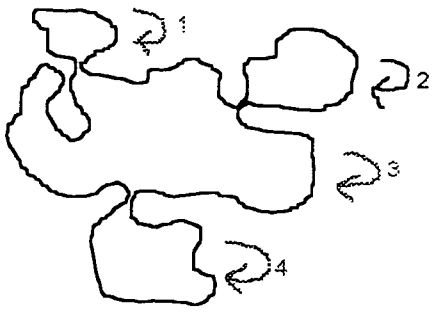

This, however, is unlikely to occur in many of the colloidal silicate particles as the prerequisite for this independent rotation of parts of the molecule is that the connection between the parts is sufficiently mobile. This is normally not the case as there is strong interlinking between most of the units which condense randomly. Thus the particle is quite stiff and rotates as a whole.

6. Proton Mobility

6.1 Relaxation time measurements

Relaxation time measurements for protons can give valuable information about the mobility of protons in silicate systems. The protons in highly condensed silicate systems can be found in a number of different surroundings. They can be attached on surface silanol groups, and they can be attached to water molecules, the latter being the bonds most protons are engaged in. Water molecules in turn can be found in a number of different surroundings, as free water, hydrogen bonded to the silanol surface groups, in the hydration shell of sodium ions and in the pores of colloidal material.

Proton spin-lattice relaxation times were measured using the inversion recovery sequence and for the measurement of spin-spin relaxation times the CPMG pulse sequence was used, since the protons participate in exchange processes.

In the investigated silicate solutions the only visible proton peak is the water-resonance (δ = 5.6 to 5.1ppm). Free water molecules and water molecules in the hydration shell of sodium ions as well as protons in Si-OH groups are expected to undergo exchange which is fast on the NMR-timescale,

and therefore their protons cannot be distinguished by NMR. The surface groups in silica gel can act as proton donors. The proton exchange mechanism with surface groups requires the presence of a structural network of adsorbed species capable of acting as proton acceptors[35]. However, very strong hydrogen bonds (as those for instance formed with OH groups of a decationized zeolite) seem to hinder the exchange of the SiOH protons with protons of free water[35].

As shown in tables 6-45 and 6-46 the spin-lattice relaxation times for protons in the viscous silicate solutions are in every case longer than the spin-spin relaxation times which indicates that either the proton-correlation times are longer than $1/\omega o$ and/or the presence of proton-proton exchange in these systems is a significant influence. To check this, proton relaxation times were measured at two different fields (at a proton resonance frequency of 200MHz and 600MHz). Since within error limits these are identical, it can be concluded that proton mobility is characterised by rotational correlation times, which are on the high motion side of the T1-minimum. Therefore an increase in the ^{1}H T1-value means an average increase in the proton mobility. The proton T1- and T2-values of a sodium silicate solution with Rm=2.0 are particularly small compared to those of a sodium silicate solution with Rm=4.0, which leads to the conclusion that the protons in the silicate solution with the higher sodium content (lower degree of condensation) are less mobile than in a silicate solution of lower sodium content. This is in good agreement with the smaller diffusion coefficient for protons measured for the silicate with Rm=2.0 (section 6.2) and indicates that the sodium ions play a crucial role in the structuring of water in the silicate solution by co-ordinating water in their hydration shell. This agrees with results reported for ^{23}Na mobility in section 7.

Table 6-45
Sin-lattice relaxation times in ms for protons in sodium silicate solutions at two different field strengths

	32wt% SiO_2 Rm=2.0	30wt% SiO_2 Rm=3.4	25wt% SiO_2 Rm=3.8	25wt% SiO_2 Rm=4.0
T1 / ms on the CXP200	156	837	973	1007
T1 / ms on the VXR600	158	833	988	1001

Table 6-46
Spin-spin relaxation times in sodium silicate systems

	25wt% SiO_2 **Rm=2.0**	32wt% SiO_2 **Rm=2.0**	25wt% SiO_2 **Rm=4.0**	28wt% SiO_2 **Rm=4.0**
T2 / ms	389	18	663	61

6.2 Self-diffusion of protons

Self-diffusion constants of protons provide additional information on the mobility of the water in silicate systems. In dealing with translational motion, there is a range of situations, which are illustrated in figure 6-23, from free self-diffusion in homogeneous liquids to hindered diffusion of water adsorbed on particle surfaces to more restricted or limited diffusion of the type experienced by liquids in porous substances, for instance.

Figure 6-23
Translational molecular mobility :

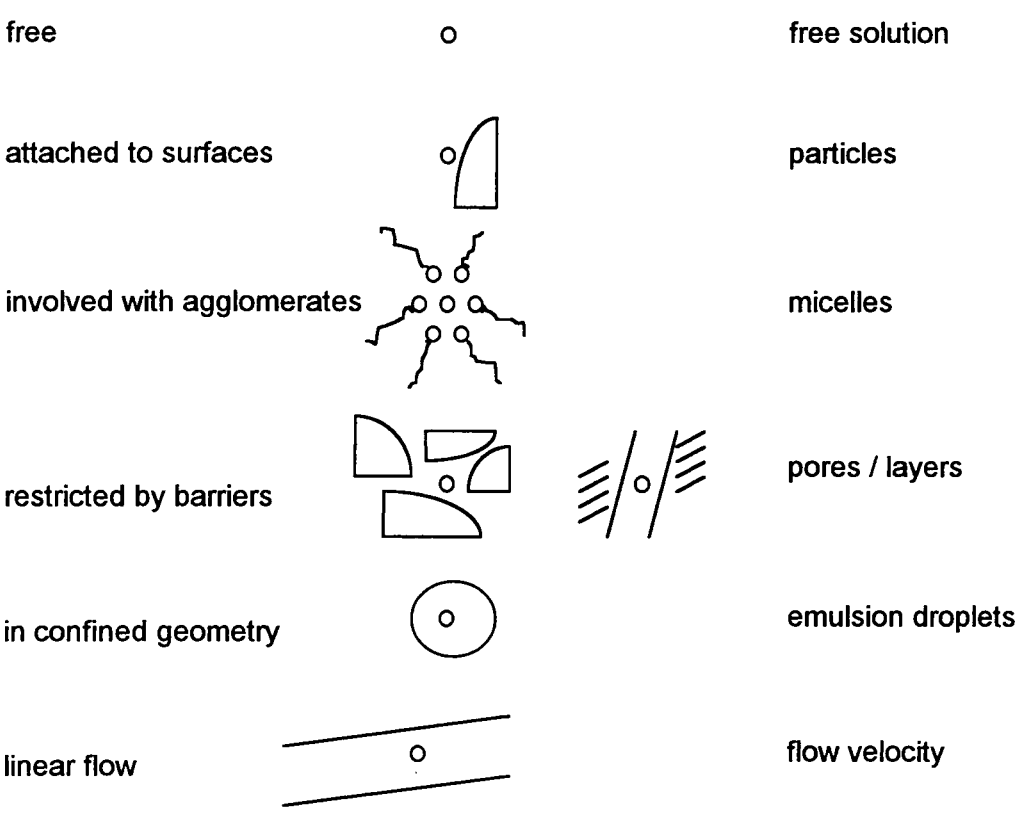

The self-diffusion constants of protons in silicate sols and gels with Rm-values of 2.0 and 4.0 are measured using the PFG sequence shown in figure 3-7 of chapter 3-2.6. Any static magnetic field gradient will impose a fixed distribution of precession frequencies on the spins that causes them to lose their phase coherence after the 90^{o}_{x} pulse. Following the 180^{o}_{y} pulse, the spins will completely refocus provided they do not diffuse. If, however, dephasing due to translational diffusive motion occurs across the field gradient during the time of the Spin Echo experiment, some 'phase memory' will be lost and the height of the echo correspondingly reduced.

The attenuation of the proton spectra is shown in figures 6-24 and 6-25. The plots of the half-echo attenuation versus $\delta^2(\Delta-\delta/3)$ are presented in figures 6-26 to 6-29. The resulting self-diffusion constants are given in table 6-47.

Table 6-47
Self-diffusion constants for protons in silicate systems

	25wt% SiO_2 **Rm=2.0**	32wt% SiO_2 **Rm=2.0**	25wt% SiO_2 **Rm=4.0**	28wt% SiO_2 **Rm=4.0**
D_{self} / m^2 s^{-1}	3.3E-6	0.9E-6	6.8E-6	5.1E-6

The self-diffusion of protons in two silicate solutions with identical SiO_2 contents is about half as slow for the silicate solution with the high sodium hydroxide content (Rm=2.0) as for the one with half the sodium hydroxide content (Rm=4.0). This leads to the conclusion that the rotational (section 6.1) as well as the translational mobility of water molecules co-ordinated in the hydration shell of sodium ions is severely limited compared to free water in the silicate system. Furthermore it can be assumed that free water and water in the ions' hydration shell dominate in the proton (water) resonance and that water in the pores of the colloidal material represents only a fraction of the total water in the silicate sols. In silicates with high sodium ion contents (high alkalinity) the mobility of water molecules generally is restricted according to the large fraction of water molecules in the hydration shell (6 molecules per sodium ion). In the silicate solutions with identical silica contents, the one with Rm=2.0 engages 78% of the total water content in the sodium hydration shells, whereas in the silicate with Rm=4.0 only 43% of the total water molecules are found in co-ordination links to sodium ions. An increase in the SiO_2 concentration at constant alkalinity (Rm-value) results in a decrease in the self-diffusion coefficient of the protons.

Figure 6-24

Self-diffusion measurement for protons in sodium silicate solutions and gels

25R2 = 25wt% SiO_2 and Rm=2.0

32R2 = 32wt% SiO_2 and Rm=2.0

25R4 = 25wt% SiO_2 and Rm=4.0

29R4 = 29wt% SiO_2 and Rm=4.0

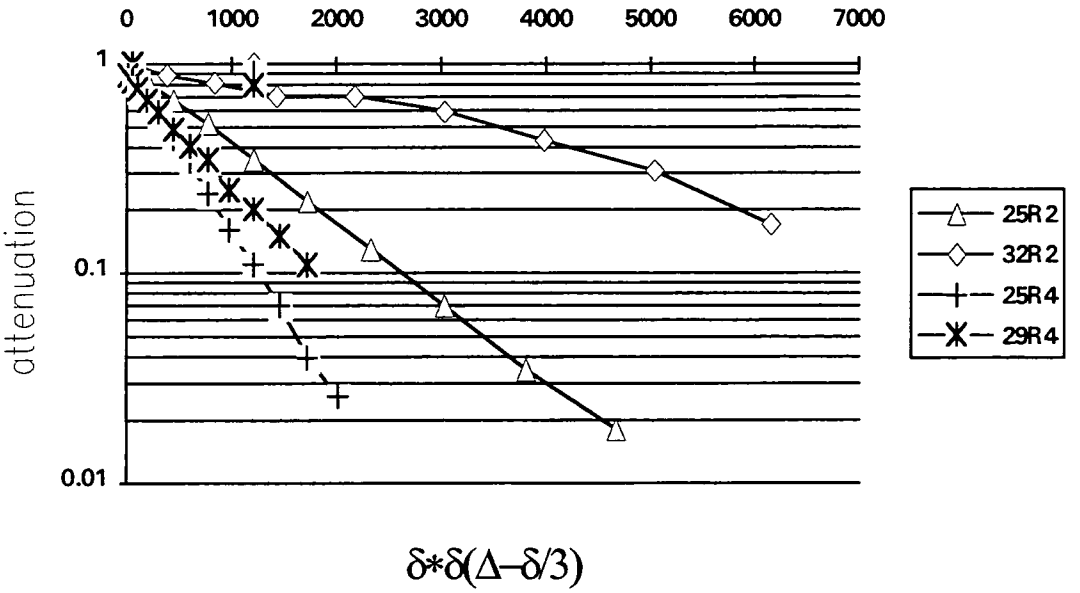

Figure 6-25

Self-diffusion measurement for protons in sodium silicate solutions and gels

1H NMR spectra of the attenuation of the half-echo

relaxation delay 6s, 32 transients, acquisition time 2s, interpulse delay (intergradient delay) 50ms for a), c), d) and 25ms for b)

a) 25wt% SiO_2 and Rm=2.0 (sol)

b) 32wt% SiO_2 and Rm=2.0 (sol)

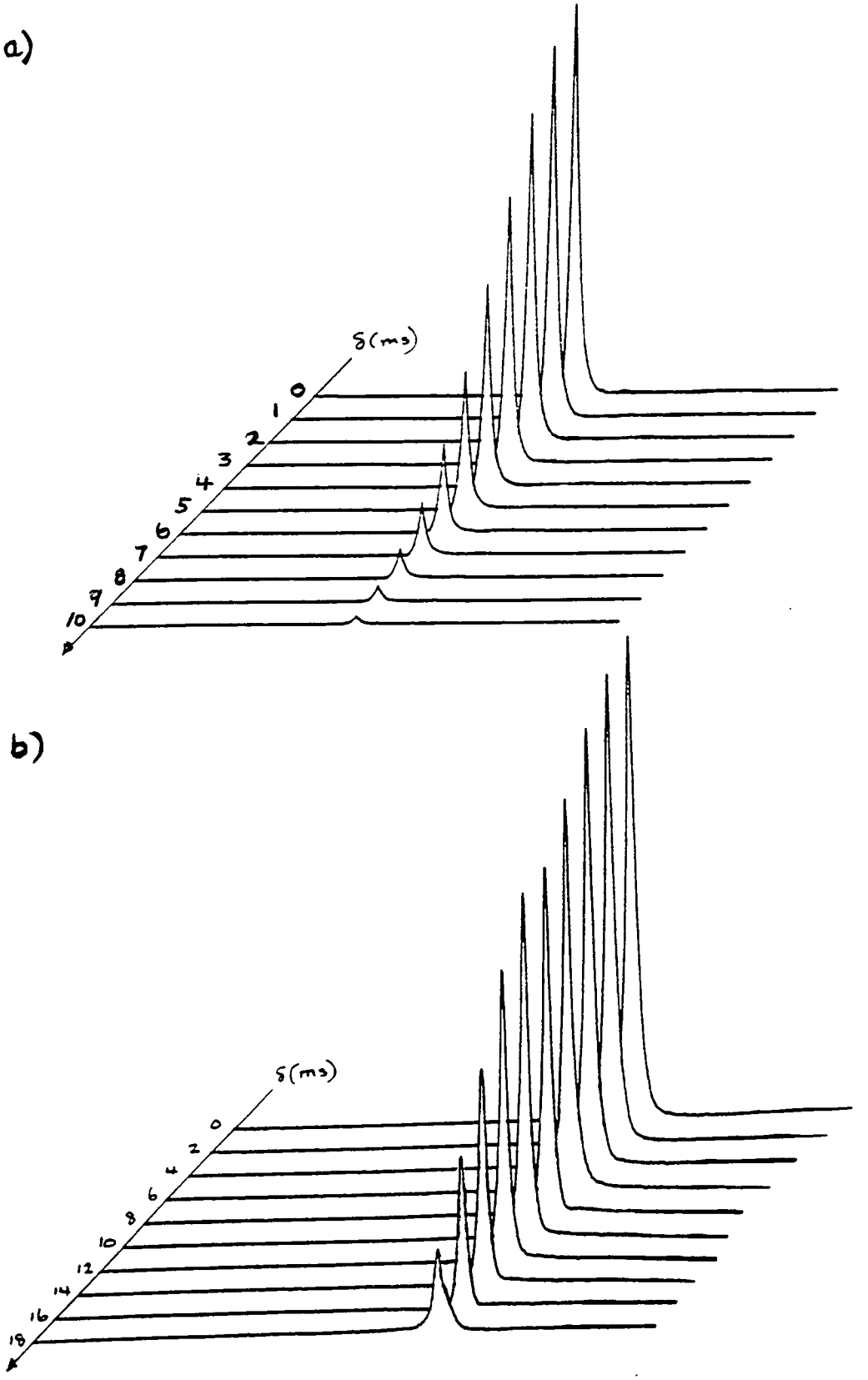

c) 25wt% SiO_2 and Rm=4.0 (sol)

d) 29wt% SiO_2 and Rm=4.0 (gel)

c)

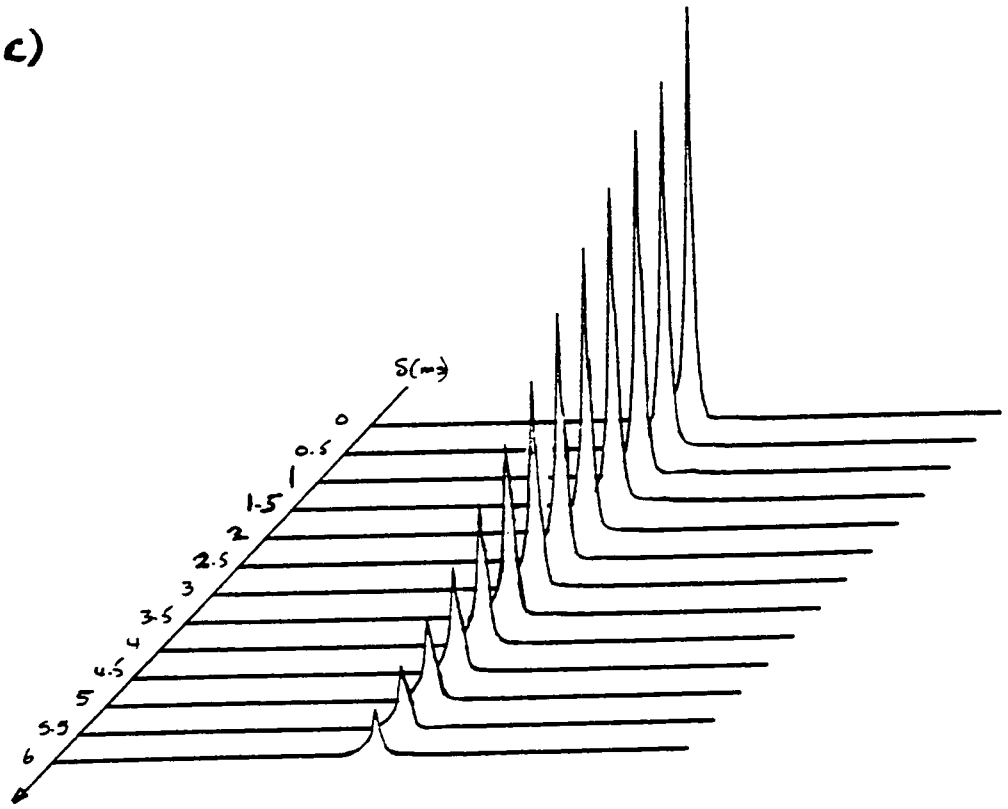

d)

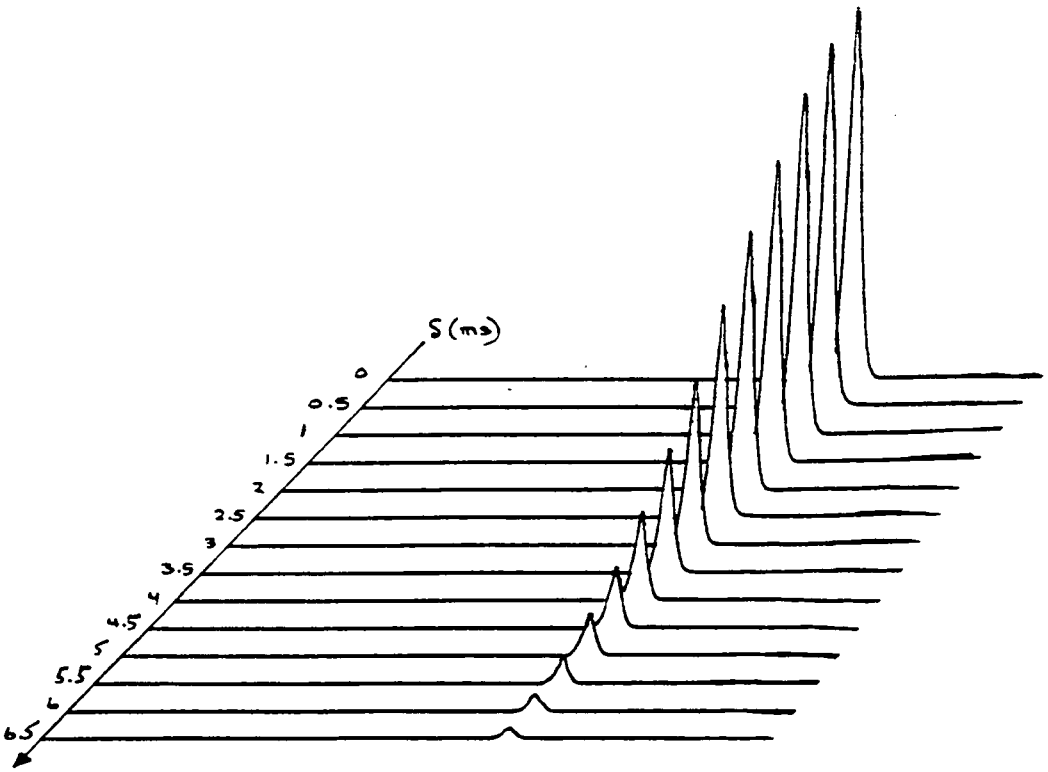

7. Sodium Mobility

Sodium ions can exert a great influence on the structuring in silicate solutions. This suggestion is reinforced by observations made in section 6.2. The influence of sodium ions on the general mobility of species in the silicate systems is mainly caused by structuring of the water by the cation and is particularly apparent in silicates with high sodium-ion contents (low Rm-values). It is important to check if observations made for protons, which are of an indirect nature, can be made for sodium and thus lead to direct conclusions.

A number of sodium silicate systems have been investigated using ^{23}Na NMR spectroscopy. ^{23}Na single-pulse MAS spectra were acquired and ^{23}Na spin-spin relaxation times were measured using the CPMG sequence. The results are presented in table 6-48 below.

Table 6-48
Chemical shifts, linewidth at half-height for two spin rates and T2-values for the ^{23}Na MAS resonance in sodium silicate sols and gels

	chemical shift δ	linewidth at half-height spin rate 90Hz	linewidth at half-height spin rate 2000Hz	T2-value
32wt% SiO_2 Rm=2.0 (**sol**)	36.9ppm	800Hz	781Hz	0.5ms
30wt% SiO_2 Rm=3.4 (**sol**)	36.7ppm	293Hz	276Hz	1.3ms
25wt% SiO_2 Rm=4.0 (**sol**)	38.3ppm	201Hz	208Hz	1.7ms
29wt% SiO_2 Rm=4.0 (**gel**)	38.5ppm	300Hz	268Hz	1.2ms

The ^{23}Na resonance in a silicate solution with 32wt% SiO_2 and Rm=2.0 is particularly broad, whereas in the silicate solutions with lower alkalinity the linewidth is smaller and decreasing the higher the Rm-value for

the silicate solution is. In all silicate solutions the ^{23}Na lines show little narrowing if the spinning speed is increased from 90Hz to 2000Hz. T2-values measured by CPMG match, within experimental error, the T2*-values obtained from the linewidth using equation [28].

$$\Delta_{1/2} = \frac{1}{\pi T2^*} \qquad [28]$$

They are lower for a sol than the corresponding gel. Proton-coupled and proton-decoupled spectra show no difference, therefore there is no scalar coupling between sodium ions and protons. This is due to exchange of water molecules as well as proton exchange on water molecules. Apart from the influence of the correlation time, linewidths for ^{23}Na resonances are affected by the spin quantum number, the quadrupole moment and the electric field gradient. Generally there can be two reasons for sodium resonances not to show quadrupolar broadening. One is rapid isotopic tumbling of the sodium ions, which tends to average the quadrupolar energy by randomly varying the angle between the vector of the Bo-field and the electric field gradient, q_{zz}. This gradient is fixed in the molecular framework so that as the molecule tumbles the quadrupolar energy is modulated. This averaging, however, is not sufficient to give a sharp line if $\tau c \sim 1/\omega o^7$. It has been shown that MAS does not make any difference for the ^{29}Si spectrum of a representative highly condensed silicate solution when the ^{29}Si correlation times for the species in the silicate solution are in the region of $1/\omega o^{22}$. Thus it has to be considered that though MAS makes only a very slight difference to the sodium resonances, the ^{23}Na correlation times can be near $1/\omega o$. The other reason for sodium resonances not to show quadrupolar broadening is the local symmetry at the nucleus. Quadrupolar broadening of the sodium resonances will be minimal if the nucleus in question is in a symmetrical surrounding (the important factor is electrical symmetry). This is the case for sodium ions surrounded by a symmetrical hydration shell of 6 water molecules (octahedral symmetry). Furthermore the linewidths of the +1/2 / +3/2 transitions of bound sodium ions

can be significantly reduced when the former are in rapid exchange with a large population of rapidly tumbling free ions[36]. The sodium T2-value in silicate systems is mainly influenced by the sodium mobility (the correlation time). Two factors account for the low mobility of sodium ions in a silicate solution with a low Rm-value (Rm=2.0) and a high sodium content. First the amount of surface groups in the ionised state is larger than in silicates with higher Rm-values (chapter 5-5) and thus there is a percentage of hydrated sodium ions bound near the surface *via* electrostatic interactions.

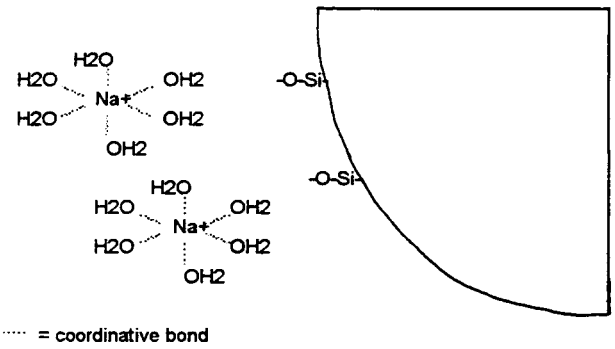

Moreover these sodium ions will be fairly immobile if they participate in interparticle interactions (Si-O$^-$ $Na^+(H_2O)_6$ $^-$O-Si). However, in a sodium silicate solution with Rm=2.0 quadrupolar broadening is assumed to contribute to the broad ^{23}Na lines, since the electrostatic interaction with SiO^- bonds can slightly distort the octahedral symmetry around the ^{23}Na ions and thus give rise to a quadrupolar contribution to the linewidth. Second the sodium ions take water out of the systems, which is bound in the hydration shell. The more sodium ions in the system, the larger is the percentage of the total water engaged in the hydration shells and thus the slower the overall mobility. It is interesting that even in a gel the sodium ions are more mobile than in a silicate sol with high sodium content. This indicates a strong influence of sodium ions on the structuring of the solution especially in systems with a high sodium content caused by the water in the solution being engaged in the hydration shells of sodium ions. It can be concluded that characteristic parameters of the silicate species in silicate systems such as the sol/gel-

transition or the overall mobility are not only determined by the condensation characteristics of the silicate structures but also by the sodium ion content.

7.1 Dilution-study

The dilution of a sodium silicate solution with 30wt% SiO_2 and Rm=3.4 shows a shifting of the sodium-resonance to higher frequency and a narrowing of the resonance-line with increasing dilution. Increasing the MAS rate makes no difference to the ^{23}Na-linewidth in the highly diluted solutions (13wt% and 5%wt% SiO_2), whereas in the more concentrated solutions (25wt% and 30wt% SiO_2) the linewidth is slightly decreased (5% and 6%) (see table 6-49).

Table 6-49
Sodium chemical shifts and linewidths at two spinning speeds for a range of SiO_2 concentrations in a sodium silicate solution with Rm=3.4

	chemical shift δ	linewidth at half-height spin rate 90Hz	linewidth at half-height spin rate 2000Hz
30wt%	36.7ppm	293Hz	276Hz
25wt%	37.0ppm	208Hz	198Hz
13wt%	37.9ppm	90Hz	90Hz
5wt%	38.2ppm	20Hz	20Hz

8. Conclusions

The silicate systems under investigation are of a highly complex nature, which makes a detailed analysis very difficult and in some cases the range, where a physical parameter is found, rather than a distinct value has to be reported. Nevertheless reliable trends have been established with good repeatability and high confidence in many cases, where no information was available before. This states the value and importance of these experiments.

On the basis of a working model for the spin-lattice relaxation times the range of rotational correlation times for the silicate species in a number of highly condensed silicate systems was obtained. This is the first time that ^{29}Si T1-values in highly viscous silicate systems in sol and gel form with a high degree of condensation have reliably been determined for all structural units (even the ones in colloidal particles). It is an achievement that these have been analysed in a quantitative way.

For the first time self-diffusion of silicate species in a highly condensed silicate solution was investigated and self-diffusion coefficients in the range of 0.9E-13 cm^2 s^{-1} for the Q4 units to 2.9E-13 cm^2 s^{-1} for the Q1 units were obtained.

These results open the possibility to get an idea of the approximate size of the colloidal material present in these highly-condensed silicate solutions. The average particle sizes range from 8 nm for the smaller particles to 26 nm for the larger particles. This is the first time that sizes of colloidal particles in highly-condensed silicate solutions have been obtained experimentally, since obstacles like the sensitivity of silicate systems to the atmosphere and their relatively small size range made the determination of the particle size impossible so far.

Chemical exchange in a highly-condensed silicate solution was monitored and maximum exchange rate constants for all exchange processes including exchange between the units with the highest connectivities, Q3 and Q4 units, were obtained. This has never been attempted before. Exchange

rates at room temperature range from 30 s^{-1} for the species with the low connectivities, Q0 and Q1, to 3 s^{-1} for the units with high connectivities, Q3 and Q4. A temperature increase of 20°C increases the exchange rate constants by a factor of 3 for the former and a factor of 10 for the latter. Approximate activation energies for the exchange processes were obtained using the Arrhenius equation, which are in the range of 50 kJ/mol to 140kJ/mol.

Though most investigations in this thesis are concerned with the behaviour of silicon, the mobility of protons (water mobility) and the sodium ion mobility are other important factors in understanding these very complex systems. It was found that the mobility of water molecules in the hydration shells of sodium ions is severely limited compared to free water. Therefore sodium ions, in their ability as co-ordinators of water molecules in an octahedral hydration shell, play an important role in the overall mobility for silicate systems and an important physical parameter for silicate systems like the sol/gel-transition is not only influenced by condensation characteristics of the silicate species but also by the sodium ion content.

Literature :

1 S. D. Kinrade, T. W. Swaddle, J. Am. Chem. Soc. **108** (1986) 7159

2 G. Engelhardt, Z. Chem. **15**, No.12 (1975) 495

3 C. G. Levy, J. D. Cargioli, P. C. Juliano, T. D. Mitchell, J. Am. Chem. Soc. **95** (1973) 3445

4 J. Mason Ed.), Multinuclear NMR, Plenum Press, New York, London (1987)

5 R. K. Harris, B. E. Mann, NMR and the Periodic Table, Academic Press, New York, London (1978)

6 J. Schraml, J. M. Bellama, Determination of Organic Structures by Physical Methods, Vol.6, Ch.4, Academic Press, New York, London, San Francisco (1976)

7 R. K. Harris, Nuclear Magnetic Resonance Spectroscopy, Longman Scientific & Technical, New York (1987)

8 A. Abragam, The Principles of Nuclear Magnetism, Oxford at the Clarendon Press (1961)

9 R. K. Harris, R. H. Newman, J. Chem. Soc. Faraday Trans. II, **73** (1977) 1204

10 E. G. Smith, J. W. Rockliffe, P. I. Riley, J. of Colloid Interface Sci. **131** (1989) 29

11 J. E. Tanner, J. Chem. Phys. **52** (1970) 2523

12 P. W. Atkins, Physical Chemistry, 2nd Ed., Oxford University Press (1982)

13 E. Fukushima, S. B. W. Roeder, Experimental Pulse NMR, Addison-Wesley Publishing Company, London (1981)

14 K. J. Packer, C. Rees, D. J. Tomlinson, Molecular Physics **18** (1970) 421

15 G. Engelhardt, D. Hoebbel, J. Chem. Soc. Chem. Commun. **8** (1984) 514

16 L. Griffiths, C. S. Cundy, R. J. Plaisted, J. Chem. Soc. Dalton (1986) 2265

17 C. J. Creswell, R. K. Harris, P. T. Jageland, J. Chem. Soc. Chem. Commun. (1984) 1261

18 R. K. Harris, J. Jones, C. T. G. Knight, R. H. Newman, J. Mol. Liquids **29** (1984) 63

19 S. D. Kinrade, T. W. Swaddle, J. Chem. Soc. Chem. Commun. (1986) 120

20 C. T. G. Knight, R. J. Kirkpatrick, E. Oldfield, J. Magn. Reson. **78** (1988) 31

21 R. J. Hunter, Foundations of Colloid Science, Vol.1, Clarendon Press, Oxford (1992)

22 E. K. F. Bahlmann, R. K. Harris, K. Metcalfe, E. G. Smith, Magn. Reson. Chem. **31** (1993) 743

23 A. Blaschette, Allgemeine Chemie, Vol.2, Akademische Verlagsgeselschaft, Frankfurt am Main (1974)

24 H. R. Christen, Grundlagen der Allgemeinen und Anorganischen Chemie, Otto Salle Verlag, Verlag Sauerlaender, Frankfurt am Main (1988)

25 R. R. Ernst, G. Bodenhausen, A. Wokaun, Principles of Nuclear Magnetic Resonance in One and Two Dimensions, Oxford Science Publications, Clarendon Press, Oxford (1991)

26 C. P. Slichter, Principles of Magnetic Resonance, 3rd Ed., Springer Verlag, Berlin, london (1989)

27 A. V. McCormick, A. T. Bell, C. J. Radke, J. Phys. Chem. **93** (1989) 1737

28 C. T. G. Knight, R. K. Harris, Magn. Reson. Chem. **24** (1986) 872

29 J. Schraml, J. M. Bellama in: Determination of Organic Structures by Physical methods, F. C. Nachod, J. J. Zuckerman, E. W. Randall (Eds.), Vol.6, Ch.4, Academic Press, New York, London, San Francisco (1976)

30 J. V. Smith, C. S. Blackwell, Nature **303** (1983) 223

31 Handbook of Chemistry and Physics, 64th edition, CRC Press

32 L. E. Sutton (Ed.), Interatomic Distances Supplement 1956-1959, Special Publication, No.18, The Chemical Society, London (1965)

33 M. I. Cruz, W. E. Stone, J. J. Fripat, J. Phys. Chem. **36** (1972) 3078

34 S. J. Seymour, M. I. Cruz, J. J. Fripat, J. Phys. Chem. **77** (1973) 2847

35 H. A. Resing, C. G. Wade, Magnetic Resonance in Colloid and Interface Science, ACS Symposium Series 34, Am. Chem. Soc. Washington (1976)

36 L. Lerner, D. A. Torchia, J. Am. Chem. Soc. **108**, No.15 (1986) 4264

37 A. E. Derome, Modern NMR Techniques for Chemistry Research, Vol.6, Pergamon Press, Oxford, New York (1987)

38 E. K. F. Bahlmann, Diplomarbeit, Technical University of Braunschweig (1992)

7. Additive influence

The aim of this chapter is to investigate the influence of various additives on the structuring and mobility in silicate systems on either side of the sol/gel-transition, the biggest and most important group of additives studied being surfactants. All additives interact in some way with the colloidal particles in the silicate systems. Adsorption on the particle surfaces can alter the particle characteristics, whereas dissolution in the aqueous phase can change the ionic strength of the solution causing precipitation and affecting the colloidal particles this way.

The distribution of structural units will give information about changes in the average particle sizes while the rotational correlation times show how the additive affects the particle mobility. All in all, the addition of additives to a silicate system can give valuable information about its behaviour and stability, and the technological, environmental and biological importance of additive-interaction with colloidal particles can hardly be overestimated.

A. Surfactant influence

The stability of colloidal dispersions in a liquid bulk phase often requires the presence of adsorbed surfactants at the interface. Industrially important effects produced by the surfactant can be (i) enhanced wetting of the solid by a liquid phase, (ii) the reduction of interfacial energies to promote formation of small particle sizes, or (iii) the formation of a stabilising layer to prevent particle coagulation[1].

Surfactants are amphiphilic molecules constituted of a hydrophobic and a hydrophilic part. In the presence of water they tend to form condensed phases

called micelles where polar/apolar contacts are avoided. The concentration of surfactant characteristic for this point is the critical micelle concentration (cmc)[1,12]. It has been found that in many cases the concentration of surfactant characteristic for the maximum amount adsorbed on silica surfaces coincides with the critical micelle concentration[18].

Three types of surfactant of the categories anionic , cationic and non-ionic have been used, with the main emphasis on surfactants containing C_{12}-chains (lauryl groups) as the alkyl chain. The anionic surfactant sodium dodecylsulfate (SDS) is very commonly used, the C_{12}-chain being of a medium length, providing a hydrophobic surfactant tail of reasonable length without the hydrophobic part dominating the amphiphilic nature of the surfactant as the alkyl chain does in soaps.

The surfactants used in this work are the following:

Anionic surfactants:

- Sodium dodecylsulfate " sodium laurylsulfate " (SDS)

  cmc (in water at 25°C) = $8 * 10^{-3}$ M

- Sodium hexylsulfate (SHS)

Cationic surfactant :

- Dodecyltrimethylammonium bromide " laurylbromide "

  cmc (in water at 25°C) = $14 * 10^{-3}$ M

Non-ionic surfactant :

- Hexaethyleneglycolmono n-dodecylether " laurylether "

  cmc (in water at 25°C) = $0.07 * 10^{-3}$ M

The investigations were started at the point where the concentration of anionic and cationic surfactant do not exceed their cmc in water at 25°C. At this

point the SDS and the laurylbromide were not completely soluble. Although the concentration of the non-ionic surfactant laurylether was exceeding the cmc in water at 25°C by more than 20 times it dissolved completely (Chapter 7-1.3). In further investigations the surfactant concentrations were taken to a point where the maximum amount of surfactant is dissolved. In the case of SDS the surfactant was added beyond the limit of dissolution where it forms a mixed crystalline and hexagonal phase in the silicate solution (Chapter 7-1.6.1).

1. Silicate systems with complete SiO_2-dissolution

1.1 General information

The influence of the surfactant on the structural units in the silicate solution is manifested mainly by the effect on the colloidal particles in the system. Since in these particles Q4 units are forming the cores and Q3 units are the surface-units the effect of the surfactant on the structures in the silicate system can be described in terms of the Q3/Q4-ratio, which characterises changes in the colloidal material.

Quantitative experiments have been carried out to investigate if there is any precipitation of silica under the influence of the surfactant due to a salting-out effect caused by the surfactant which results in silica that is not observed in the ^{29}Si solution-state spectrum. It was confirmed that in all cases the silicon in the system is observed quantitatively. Thus the observed changes in the distribution of structural units are entirely due to changes within the silicate solutions.

1.2 Preparation and Equilibration

All surfactants have been added to silicate solutions which had reached equilibrium. After the addition of the surfactant the solutions were given at least

24 hours to equilibrate before any spectra were recorded. This time period was found to be sufficient to allow full equilibration of the structural units under the influence of the surfactant. This is shown by the example of a highly condensed silicate solution which had reached its equilibrium. To this solution 1wt% sodium hexylsulfate was added and spectra were recorded at fixed time intervals up to a total time of 46 hrs. The results are as in Table 7-1.

Table 7-1
Distribution of structural units versus the time (in minutes) after the addition of SHS to a silicate solution with 25.5wt% SiO_2 and Rm=3.8

	0	**53**	**106**	**159**	**212**	**318**	**848**	**1908**	**2756**
Q0	0.6	0.7	0.1	0.2	0.3	0.8	0.7	0.5	0.6
Q1	4.4	3.2	2.7	3.0	2.6	2.7	2.4	2.3	2.5
Q2	22.7	22.5	23.7	23.9	23.8	23.4	23.2	23.5	23.3
Q3	52.2	55.5	55.6	55.3	56.0	56.1	56.6	56.4	56.6
Q4	20.1	18.1	17.9	17.6	17.3	17.0	17.1	17.2	17.0
Q3/Q4	**2.6**	**3.1**	**3.1**	**3.1**	**3.2**	**3.3**	**3.3**	**3.3**	**3.3**

A stable equilibrium has been established in the silicate solution approximately 14 hours after the addition of the surfactant SHS to the silicate solution. It has to be considered that the applicability of this value to other silicate-surfactant systems is dependent on the surfactant used. The amount of SHS dissolved in the silicate solutions is bigger than the amount of dissolved SDS and it is possible that SHS produces the observed effect on the structural distribution in the silicate solution more quickly than SDS does. Therefore the value for the establishment of the equilibrium can only be taken as a guide if applied to other silicate -surfactant systems.

1.3 Surfactant dissolution

The level of dissolution of the surfactant in the silicate solutions was investigated by making use of the method of quantification described in chapter 4. Proton spectra were used for the quantification. Since the proton spectra were recorded in rotor inserts made of Teflon FEP it was not possible to use an internal reference. Thus it had to be ensured that dielectric changes between the standard and the investigated sample were negligible. This was achieved by using a solution of surfactant as a standard which contains the surfactant at the same concentration as in the silicate solution and with the same alkalinity. Furthermore, the intensity of the water signal had to be reduced. This was achieved by using D_2O instead of H_2O as a solvent (for the sodium silicate solution deuterated water instead of protonated water was used in the preparation). To investigate if the alkalinity of the silicate solution causes a change in the surfactant which is not due to interactions with the silicate system each solution of the surfactant in D_2O has been prepared without the addition of NaOH and with the addition of NaOH. These spectra were compared with the spectrum of the surfactant in the silicate solution. The investigated sodium silicate solution contains 30wt% SiO_2 with Rm=2.6.

The investigations have been carried out on a Bruker CXP200 spectrometer. One of the results (with laurylbromide) has been checked on a Varian VXR400 where we get better resolution of the resonances, and the result matched the one obtained on the Bruker CXP200.

The results of the quantification are reported in Table 7-2.

Table 7-2

Dissolution of surfactants in a sodium silicate solution with 30wt% SiO_2 and Rm=2.6 using the method of quantification

SDS	c*=8mM:	3 % dissolved	($c_{dissolved}$=0.3mM)
SHS	c*=8mM:	20 % dissolved	($c_{dissolved}$=1.6mM)
Laurylbromide	c*=14mM:	26 % dissolved	($c_{dissolved}$=3.6mM)
Laurylether	c*=2mM:	98 % dissolved	($c_{dissolved}$=2.0mM)

c* denotes the concentration of surfactant in the standard which is the same as placed into the silicate solution

% dissolved relates to the amount of dissolved surfactant detected by the method of quantification relative to the concentration of surfactant in the standard

$c_{dissolved}$ is the concentration of surfactant dissolved in the aqueous phase of the silicate solution or adsorbed on the particle surfaces (surfactant that can not be centrifuged to the bottom of the silicate solution)

The surfactant which is most easily dissolved in a silicate solution is the non-ionic surfactant laurylether. It fully dissolves in the silicate solution to a concentration which exceeds its critical micelle concentration in water by a factor of almost 30. Laurylether is not charged, so the salinity of the silicate system has the smallest effect on its dissolution. Thus it is not salted out by the silicate solution. It is known that an increase in the salinity of the system causes a

decrease in the critical micelle concentration of non-ionic surfactants and surface coverage at lower surfactant concentrations than in systems with low salinity[18]. The anionic surfactant SDS is the least dissolved in the silicate solution. The concentration of SDS dissolved in the silicate solution is only 3% of its critical micelle concentration in water. This indicates that the salinity of the silicate solution prevents the dissolution of SDS in the aqueous phase (the salinity of the silicate solution is directly proportional to the electrolyte concentration). The anionic surfactant SHS dissolves to 20% of it's critical micelle concentration. This shows that the anionic surfactant with a shorter hydrophobic chain is less easily salted out by the silicate solution. The cationic surfactant laurylbromide dissolves to 26% of its cmc in water. Adsorption of the surfactant's positively charged head groups on the charged $Si\text{-}O^-$ is possible, but the salinity of the silicate solution has an effect on the dissolution of the charged surfactant so that it does not dissolve completely. The case where the salinity exerts the smallest effect is the non-ionic surfactant.

The resonances in the proton spectra of surfactants can give information about their behaviour in alkaline media and in the silicate system. All surfactants under investigation have a very similar structuring.

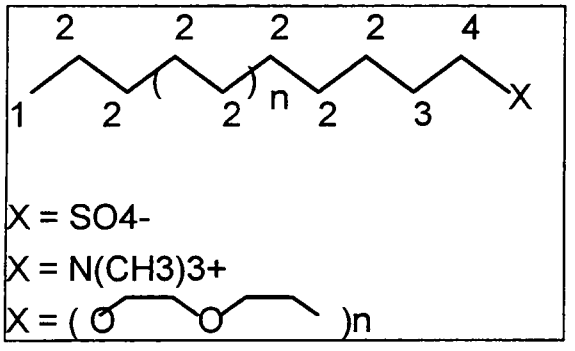

The proton resonances all surfactants under investigation have in common are at :

$\delta_1 \cong 0.1$ ppm $\Rightarrow$ methyl group at the end of the CH_2-chain

$\delta_2 \cong 1.3$ ppm $\Rightarrow$ methylene groups in $-(CH_2)_n$-chain

$\delta_3 \cong 1.8$ ppm $\Rightarrow$ methylene group next nearest to functional polar group

$\delta_4 \cong 3$ to 4 ppm $\Rightarrow$ methylene group adjacent to functional polar group

The proton spectra of the surfactant SDS in D_2O with and without the addition of NaOH show identical chemical shifts. The proton resonances of SDS in the silicate solution are much broader than the resonances of SDS in solution without any silicate units (Figure 7-1). This shows that the surfactant is not changed by the alkalinity of the silicate system. The broadened lines for the proton resonances of the dodecane chain in the silicate solution suggest that there is some restriction in the movement of the surfactant which is caused by the adsorption of its hydrophobic tail on the surface of colloidal particles *via* dispersion forces.

In the case of SHS, proton spectra of the surfactant in D_2O with and without the addition of NaOH and in the sodium silicate solution are identical (Figure 7-2). This suggests that although showing an effect on the distribution of structural units in the silicate solution, SHS seems to retain its mobility in the silicate system.

The proton spectra of the cationic surfactant laurylbromide in D_2O with and without the addition of NaOH are identical (Figure 7-3). This shows that the alkalinity of the silicate system exerts no effect on laurylbromide. The proton spectrum of laurylbromide in the silicate solution only shows a weak and broad proton resonance for the methyl groups attached to the nitrogen at δ=3.15ppm (as shown in Figure 7-3). This can be explained by immobilisation of the polar heads of the surfactant by adsorption on charged surface sites which causes a broadening of the lines.

In the case of the non-ionic surfactant laurylether the proton spectra in D_2O with and without the addition of NaOH are identical. This shows that laurylether is not hydrolysed in a system with the alkalinity of the silicate solution. In the proton spectrum of the laurylether in the silicate solution the resonance for the oxyethylenic chain at 3.7ppm is shifted to 1.1ppm and the main resonance of the dodecane chain is shifted from 1.3ppm to -0.3ppm along with broadening of the resonances, the resonance of the ethyleneoxide protons being more affected than the resonance of the hydrophobic chain. This indicates that the non-ionic surfactant laurylether is strongly adsorbed on the uncharged surface sites of the colloidal particles *via* hydrogen bonding with the polar chain. This causes increased shielding of the protons and immobilises the surfactant, the polar oxyethylenic chain being more affected than the hydrophobic chain.

Figure 7-1
Proton NMR spectra of SDS in :
a) D_2O
b) D_2O with NaOH (same alkalinity as silicate)
c) sodium silicate solution with 30wt% SiO_2 and Rm=2.6 in D_2O
They were acquired on the Bruker CXP200 with 128 transients, relaxation delay of 10s, acquisition time of 0.08s, spectral width of 50ppm

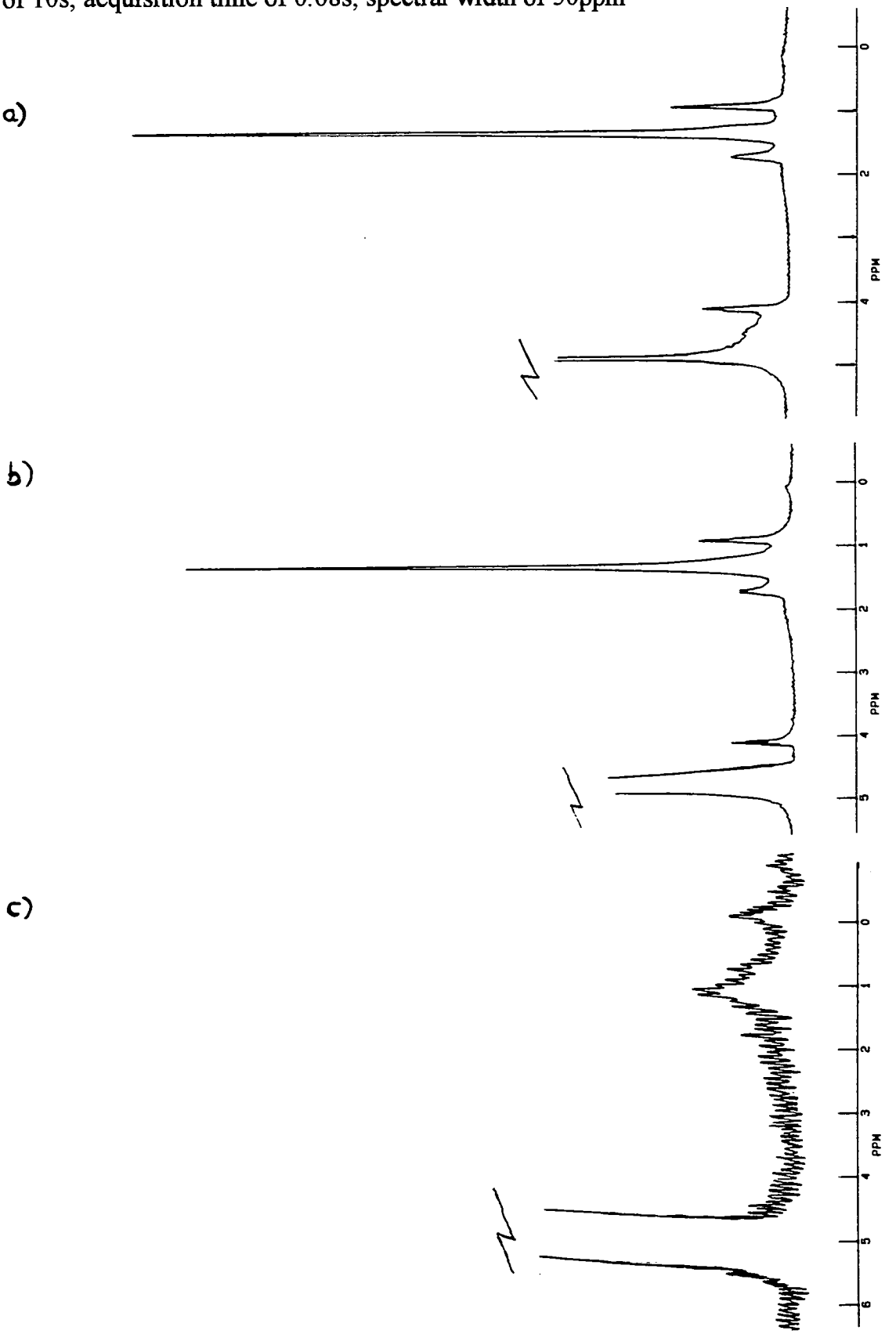

Figure 7-2
Proton NMR spectra of SHS in :
a) D_2O
b) D_2O with NaOH (same alkalinity as silicate)
c) sodium silicate solution with 30wt% SiO_2 and Rm=2.6 in D_2O
were acquired on the Bruker CXP200 with 128 transients, relaxation delay of 10s, acquisition time of 0.08s, spectral width of 50ppm

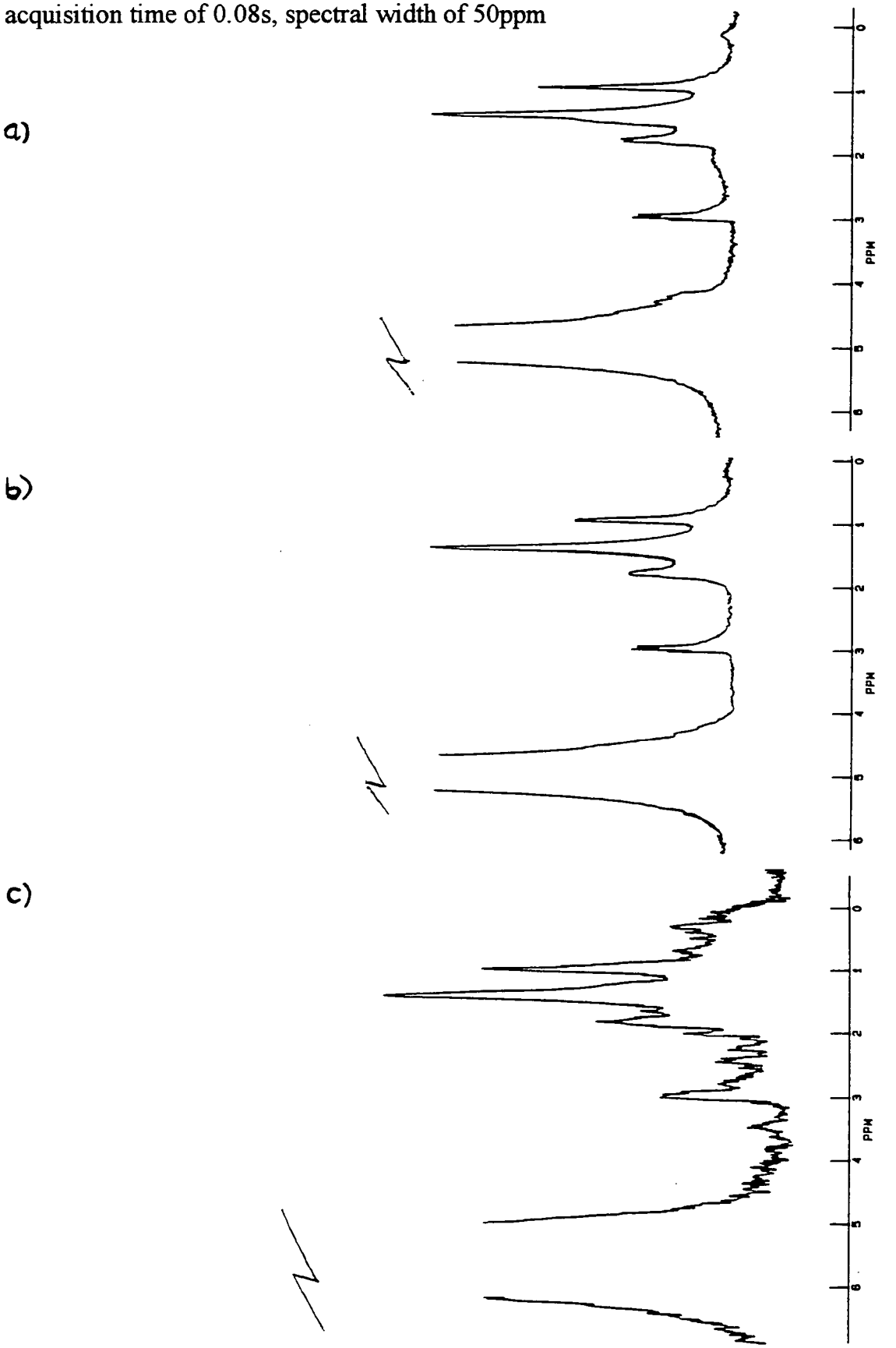

Figure 7-3
Proton NMR spectra of laurylbromide in :
a) D_2O
b) D_2O with NaOH (same alkalinity as silicate)
c) sodium silicate solution with 30wt% SiO_2 and Rm=2.6 in D_2O
were acquired on the Bruker CXP200 with 128 transients, relaxation delay of 10s, acquisition time of 0.08s, spectral width of 50ppm

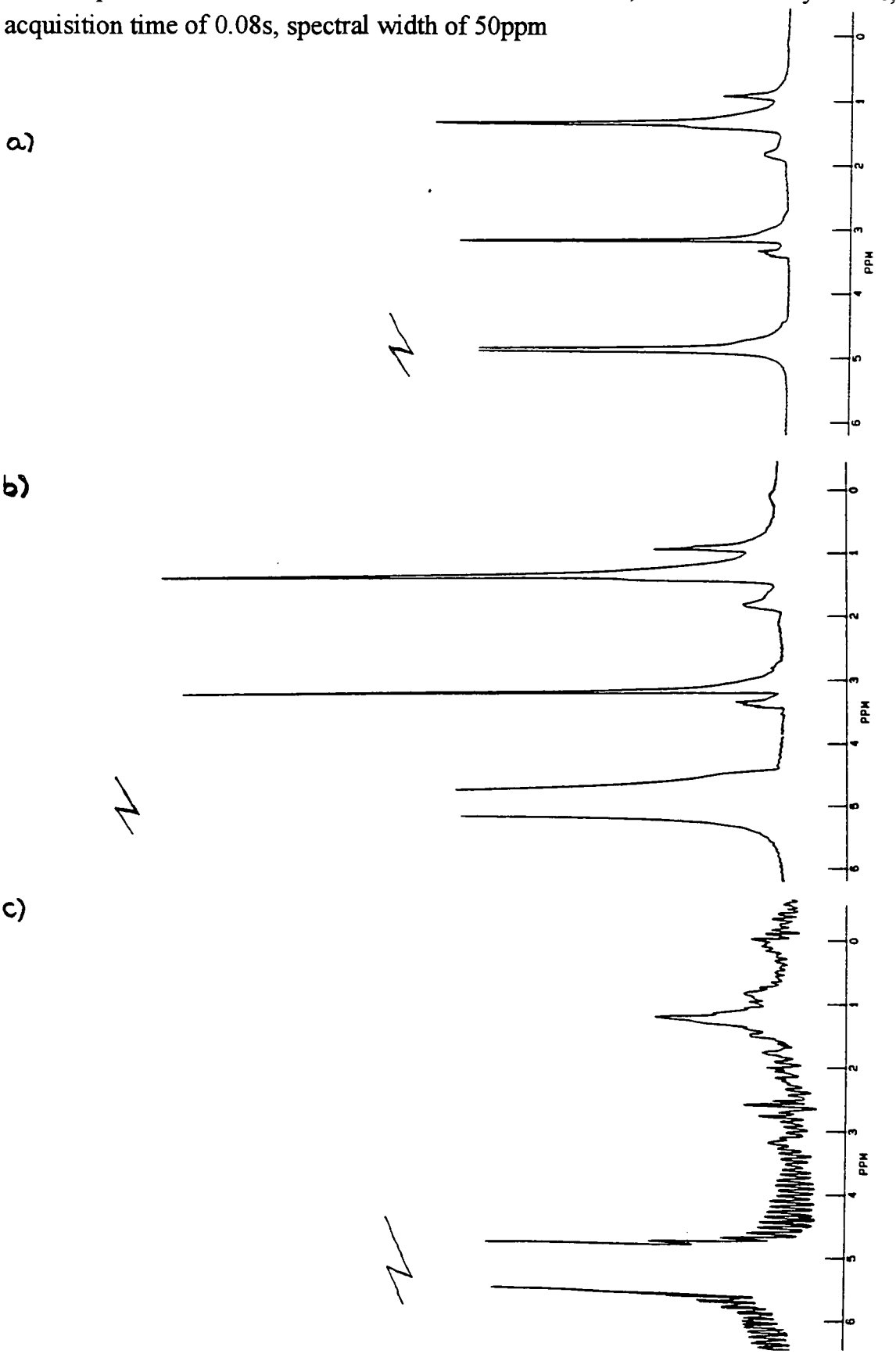

Figure 7-4
Proton NMR spectra of laurylether in :
a) D_2O
b) D_2O with NaOH (same alkalinity as silicate)
c) sodium silicate solution with 30wt% SiO_2 and Rm=2.6 in D_2O
were acquired on the Bruker CXP200 with 128 transients, relaxation delay of 10s, acquisition time of 0.08s, spectral width of 50ppm

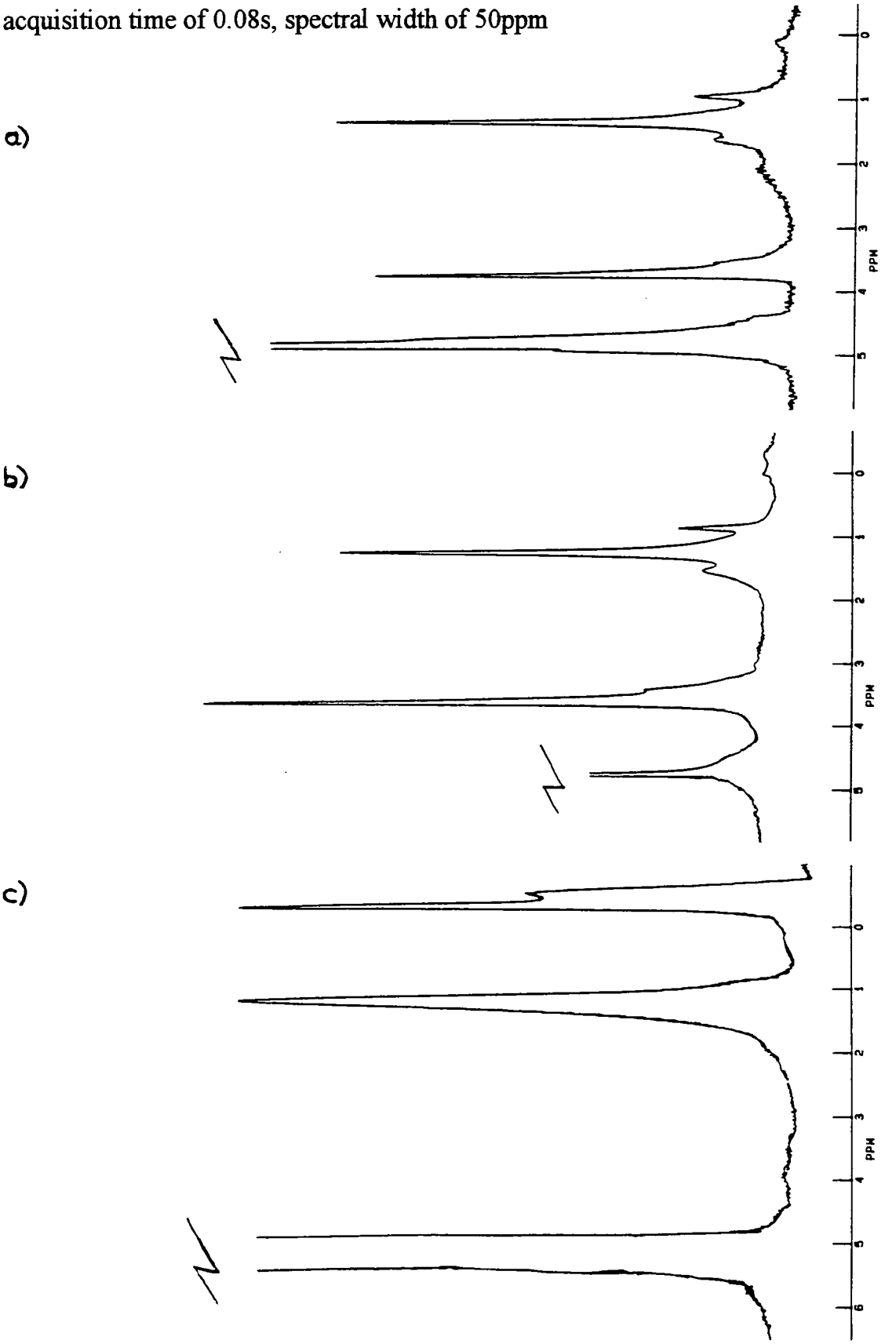

1.4 Surfactant effect on structural behaviour

Generally, all the investigated surfactants shift the distribution of structural units in the silicate system towards an increased number of Q3-units parallel to a decreased number of Q4-units (Table 7-1 and 7-3 to 7-14). Considering the nature of the colloidal particles in the systems, this experimental observation goes along with an increase in the surface area of the particles parallel to a decrease in the core area. Therefore the general effect of the surfactants appears to be a decrease in the size of the colloidal particles. This effect, which is observed in the case of all surfactants and all silicate systems which have been investigated, is only small. Nevertheless it was found to be very consistent by the repetition of experiments and when a new preparation of the whole system was done. The results for a representative sodium silicate solution containing a large amount of colloidal particles, 25.5wt% SiO_2 Rm=3.8, have been checked by preparing a new stock-solution and adding surfactants accordingly. The results show the same tendency as established in previous results. The addition of the surfactants does not cause any change in the pH-value of the silicate systems.

It is concluded that there is a small but consistent and thus relevant decrease in the size of colloidal particles due to the surfactant. This conclusion is supported by DSC (differential scanning calorimetry) measurements, which show a decrease in the amount of pore water (water trapped in the pores of the colloidal particles) of 20% to 30% of the amount of pore water in a silicate without surfactants upon the addition of surfactants. Figures 7-5 and 7-6 show typical 29Si NMR spectra of silicate/surfactant systems in comparison with the silicate solution without surfactant. The changes in the structuring of the silicate systems are not visible in these ^{29}Si NMR spectra and only detailed integration and repetition of experiments convinces of the observed effect. It was found that spherical silica particles of 500-700A can be synthesised as stable dispersions by

controlled hydrolysis of TEOS in non-ionic surfactant/cyclohexane/water reverse micellar systems, the presence of surfactant limiting the particle size produced[17]. This is an example of a surfactant producing a decrease in the average particle size documented in the literature, though the mechanism can not be adapted to the systems investigated here.

The decrease in the average particle size caused by the surfactant does not revert to the old state with time but stays constant, which can be seen in the constant amount of Q4-units (Table 7-5). Nevertheless in the case of the non-ionic surfactant there is a tendency for a decrease in the less condensed units Q0, Q1, Q2cyc and Q2, indicating condensation. This, however, does not go any further than to increasing the amount of Q3 surface units (Table 7-5). These observations indicate that there is a fairly complete surface coverage by the non-ionic surfactant If there was no surface coverage by the surfactant the condensation of Q3-units to Q4 units could occur as it does in a surfactant-free system (Chapter 5.1). If the surface is covered by adsorbed surfactant at least a part of the Q1 and Q2 units have to be connected to the particle surfaces to be able to condense to Q3-units. If these Q1 and Q2 units were not connected to the Q3-surface units it would be very difficult for them to access a surface with adsorbed surfactant for the condensation.

The addition of SDS in concentrations where it is only partially dissolved produces very different reactions. If it exceeds the cmc in water by a factor of 10 it does not change the structuring in the silicate solution, as shown in Table 7-10. However, a further drastic increase in the concentration of SDS to 9wt% affects the structuring in the silicate and results in the silicate solution not being fluid at room temperature any more but it does not cause precipitation (For further discussion see Chapter 7-1.6.1). In the former concentration the surplus SDS (undissolved SDS) is on the bottom of the silicate solution as a precipitate whereas

in the higher concentration the SDS forms a liquid crystalline phase containing the silicate.

In diluted silicate solutions the effect of the anionic surfactant SDS on the silicate structuring is much more pronounced than in the concentrated systems, as can be seen in Table 7-11 and 7-12. This can be explained by the fact that the solubility of the surfactant is higher in the dilute system, which has got a lower alkalinity and a smaller ion content. Of course there are less contact points for the surfactant in a dilute solution than in a concentrated solution but this seems to be more than compensated by the increased amount of surfactant dissolved in the system.

If the non-ionic surfactant is added to its maximum concentration, which was determined to be 1.4wt% (39mM), the average particle size decreases compared to the effect created by laurylether at a concentration of 2mM (0.0025wt%) but the change is only slight (Table 7-7). The addition of more non-ionic surfactant than 1.4 wt% does not cause precipitation of the silicate but results in a surfactant phase separating from the silicate and resting on top of the silicate solution. The structuring in the silicate system stays the same as for the silicate solution containing 1.4 wt% non-ionic surfactant.

Sodium hexylsulfate is a short-chain anionic surfactant. The dissolution of short-chain surfactants is less affected by the ionic influence of the silicate solution than is the dissolution of long-chain surfactants (Table 7-2). Thus SHS is more soluble than SDS in the sodium silicate solutions. Table 7-8 shows that the effect caused by the addition of SHS is stronger than for the same amount of SDS, which is due to the fact that more SHS can dissolve in the silicate solution than SDS. However it should be mentioned that the addition of 1.0wt% SHS to the silicate solution causes precipitation of the silicate and the separation of two phases, the bottom phase consisting of the precipitated silicate, and the top phase

being an aqueous phase containing the surfactant. Therefore there is a tendency for a higher Q4 content parallel to a lower Q3 content than found in the initial silicate solution, which both characterise an increase in the average particle size (which usually goes along with the precipitation of a silicate). In the silicate solution containing SHS, however, the amounts of Q3 and Q4 units only revert back to the state of the initial silicate solution. The average particle size compared to the silicate containing 8mM SHS increases due to the precipitation but this does not proceed any further than the average article size in the silicate solution without SHS (Table 7-8). ^{29}Si NMR spectra illustrating the effect of SHS are presented in Figure 7-7.

A mixture of two surfactants, the non-ionic laurylether and the anionic SHS in the weight ratio 1:1 at concentrations of 0.7 wt% , does not cause a great change in the structures apart from a very slight decrease in particle size (Table 7-9). This effect of the surfactant mixture on the silicate solution, however, is smaller than the effect caused by the addition of any one of the two surfactants on its own to the silicate solution. This indicates that the two surfactants interact with each other and thus cannot be taken into account for the silicate surfactant interaction.

The values for the structural distributions that are reported in the following tables are average values over at least two experiments.

Table 7-3
Distribution of structural units in % in a
sodium silicate solution with 32wt% SiO_2 and Rm = 2.0

structural unit	without surfactant	with laurylsulfate c=8mM
Q0	1.0	1.2
Q1	11.4	12.4
Q2cyc	2.7	4.0
Q2	46.3	49.8
Q3	37.6	32.2
Q4	1.0	0.4
Q3/Q4	**37.6**	**80.5**

Table 7-4
Distribution of structural units in % in a
sodium silicate solution with 30.0 wt% SiO_2 and Rm=2.6

structural unit	without surfactant	with SDS c=8mM	with laurylbromide c=14mM	with laurylether c=0.2mM
Q0	0.7	0.8	0.6	0.8
Q1	6.7	6.6	6.6	6.8
Q2cyc	1.5	1.2	1.0	1.2
Q2	36.5	36.6	37.2	35.3
Q3	47.2	47.9	48.8	48.8
Q4	7.4	6.9	5.8	7.1
Q3/Q4	**6.4**	**6.9**	**8.4**	**6.9**

Table 7-5
Distribution of structural units in % in a
sodium silicate solution with 30.0 wt% SiO_2 and Rm=2.6

structural unit	with SDS c=8mM after 1 year	with laurylether c=0.2mM after 1 year
Q0	0.5	0.4
Q1	5.6	3.9
Q2cyc	0.8	0.7
Q2	37.9	33.2
Q3	48.2	54.8
Q4	7.0	7.0
Q3/Q4	**6.9**	**7.4**

Table 7-6
Distribution of structural units in % in a
sodium silicate solution with 25.5 wt% SiO_2 and Rm=3.8

structural unit	without surfactant	with SDS c=8mM	with laurylbromide c=14mM
Q0	0.6	0.4	0.1
Q1	4.4	2.5	1.7
Q2cyc	0.0	0.1	0.06
Q2	22.7	23.3	23.0
Q3	52.2	58.6	57.84
Q4	20.1	15.1	17.3
Q3/Q4	**2.6**	**3.9**	**3.3**

Table 7-7
Distribution of structural units in % in a
sodium silicate solution containing 25.5 wt% SiO_2 with Rm=3.8

structural unit	without surfactant	with laurylether c=0.2mM	with laurylether c= 39mM*
Q0	0.6	0.2	0.5
Q1	4.4	2.7	1.8
Q2cyc	0.0	0.1	0.0
Q2	22.7	24.1	23.4
Q3	52.2	55.3	57.2
Q4	20.1	17.6	17.1
Q3/Q4	**2.6**	**3.1**	**3.3**

* the laurylether concentration of 39mM corresponds to c=1.4wt%

Table 7-8
Distribution of structural units in % in a
sodium silicate solution with 25.5 wt% SiO_2 and Rm=3.8

structural unit	without surfactant	with SHS c=0.1wt%*	with SHS c=1wt%**	with SHS c=3wt%
Q0	0.6	0.5	0.5	0.3
Q1	4.4	2.8	2.5	2.4
Q2cyc	0.0	0.4	0.0	0.0
Q2	22.7	22.5	21.7	22.7
Q3	52.2	59.2	57.5	51.8
Q4	20.1	14.6	17.8	19.8
Q3/Q4	**2.6**	**4.1**	**3.2**	**2.6**

* the SHS concentration of 0.1wt% corresponds to c=8mM

** at the concentration of c=1wt% the SHS causes precipitation in the silicate system

Table 7-9
Distribution of structural units in % in a
sodium silicate solution containing 25.5 wt% SiO_2 with Rm=3.8

structural unit	without surfactant	with SHS:laurylether in ratio 1:1 (c=0.7 wt%)
Q0	0.6	0.7
Q1	4.4	2.8
Q2cyc	0.0	0.0
Q2	22.7	22.8
Q3	52.2	55.8
Q4	20.1	17.9
Q3/Q4	**2.6**	**3.1**

Table 7-10
Distribution of structural units in % in a
sodium silicate solution with 25 wt% SiO_2 and Rm=4.0

structural unit	without surfactant	with SDS c=8mM	with SDS c=80mM
Q0	0.7	0.8	1.1
Q1	3.3	3.0	2.8
Q2cyc	0.0	0.0	0.0
Q2	21.4	22.2	23.5
Q3	52.3	53.2	52.6
Q4	22.3	20.8	20.0
Q3/Q4	**2.3**	**2.6**	**2.6**

Table 7-11
Distribution of structural units in % in a sodium silicate solution with 15 wt% SiO_2 and Rm=2.6 diluted from 30wt% SiO_2 and Rm=2.6

structural unit	without surfactant	with SDS c=4 mM
Q0	2.4	1.3
Q1	9.1	9.2
Q2cyc	2.1	1.1
Q2	38.1	37.0
Q3	35.8	43.9
Q4	12.5	7.5
Q3/Q4	**2.9**	**5.9**

Table 7-12
Distribution of structural units in % in a sodium silicate solution with 8.0wt% SiO_2 with Rm = 4.0 diluted from 25wt% SiO_2 with Rm=4.0

structural unit	without surfactant	with "laurylbromide" c=5 mM
Q0	3.3	2.8
Q1	5.3	6.3
Q2cyc	0.0	0.0
Q2	23.5	25.2
Q3	53.4	55.7
Q4	14.5	10.0
Q3/Q4	**3.7**	**5.6**

Figure 7-5

^{29}Si NMR spectra of a sodium silicate solution with 30wt% SiO_2 and Rm=2.6

a) without surfactant

b) with SDS

c) with laurylbromide

d) with laurylether

a) to c) acquired on the Varian VXR300 with 1020 transients, relaxation delay 80s, spinning speed 600Hz (at the magic angle)

d) acquired on the Bruker AMX500 with120 transients, relaxation delay 80s acquisition time 0.06s, spectral width 200ppm

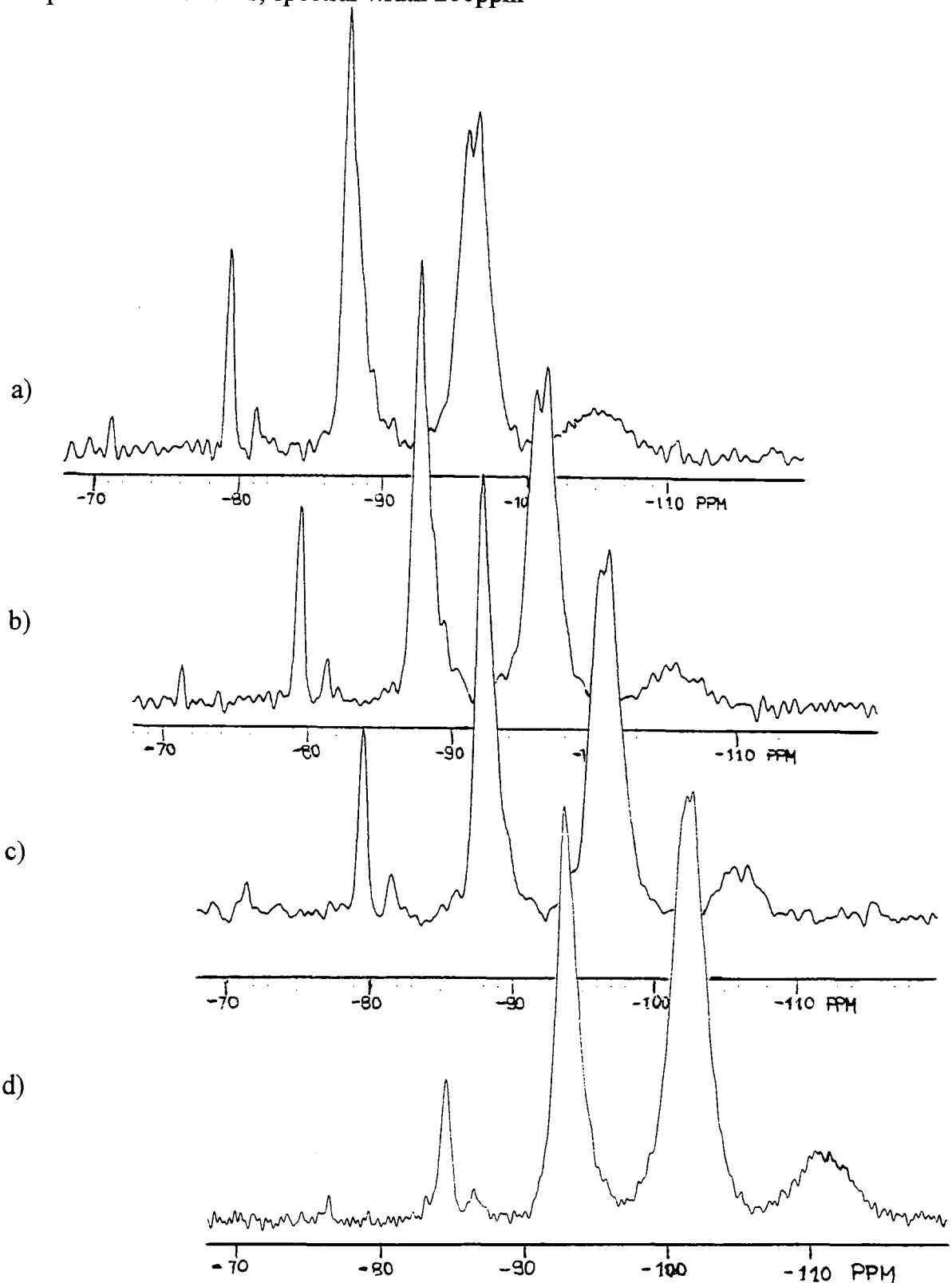

Figure 7-6

^{29}Si NMR spectra of a sodium silicate solution with 25.5wt% SiO_2 and Rm=3.8

a) without surfactant

b) with 8mM SDS

c) with 14mM laurylbromide

d) with 2mM laurylether

a) to d) acquired on the Bruker AMX500

120 transients, relaxation delay 100s, acquisition time 0.04s, spectral width 200ppm

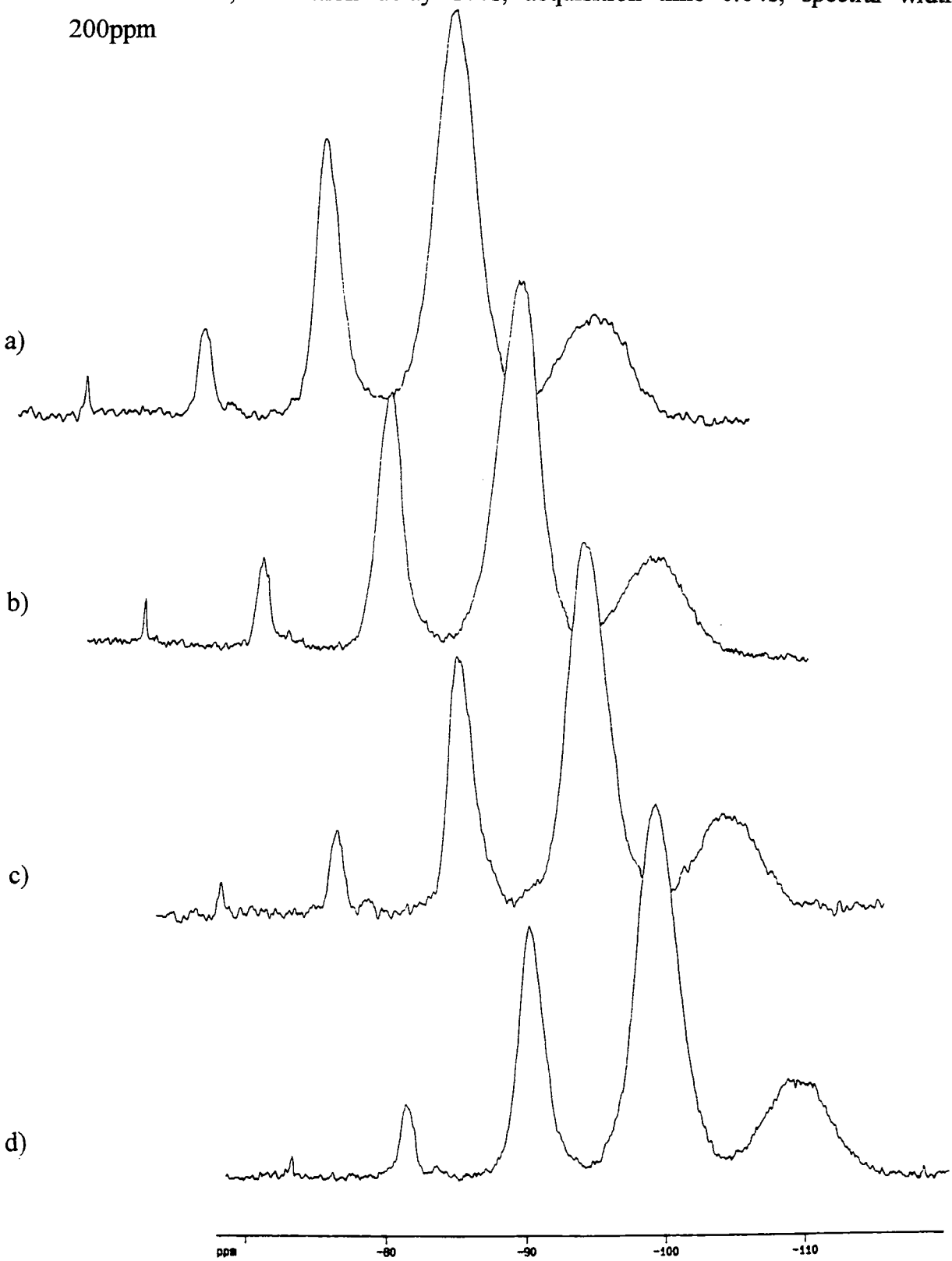

Figure 7-7

^{29}Si NMR spectra of a sodium silicate solution with 25.5wt% SiO_2 and Rm=3.8

a) without surfactant

b) with 8mM SHS

c) with 1wt% SHS

d) with 3wt% SHS

a) to d) acquired on the Bruker AMX500 with 160 transients, acquisition time 0.06s, spectral width 200ppm, a) and b) relaxation delay 100s, c) and d) relaxation delay 140s

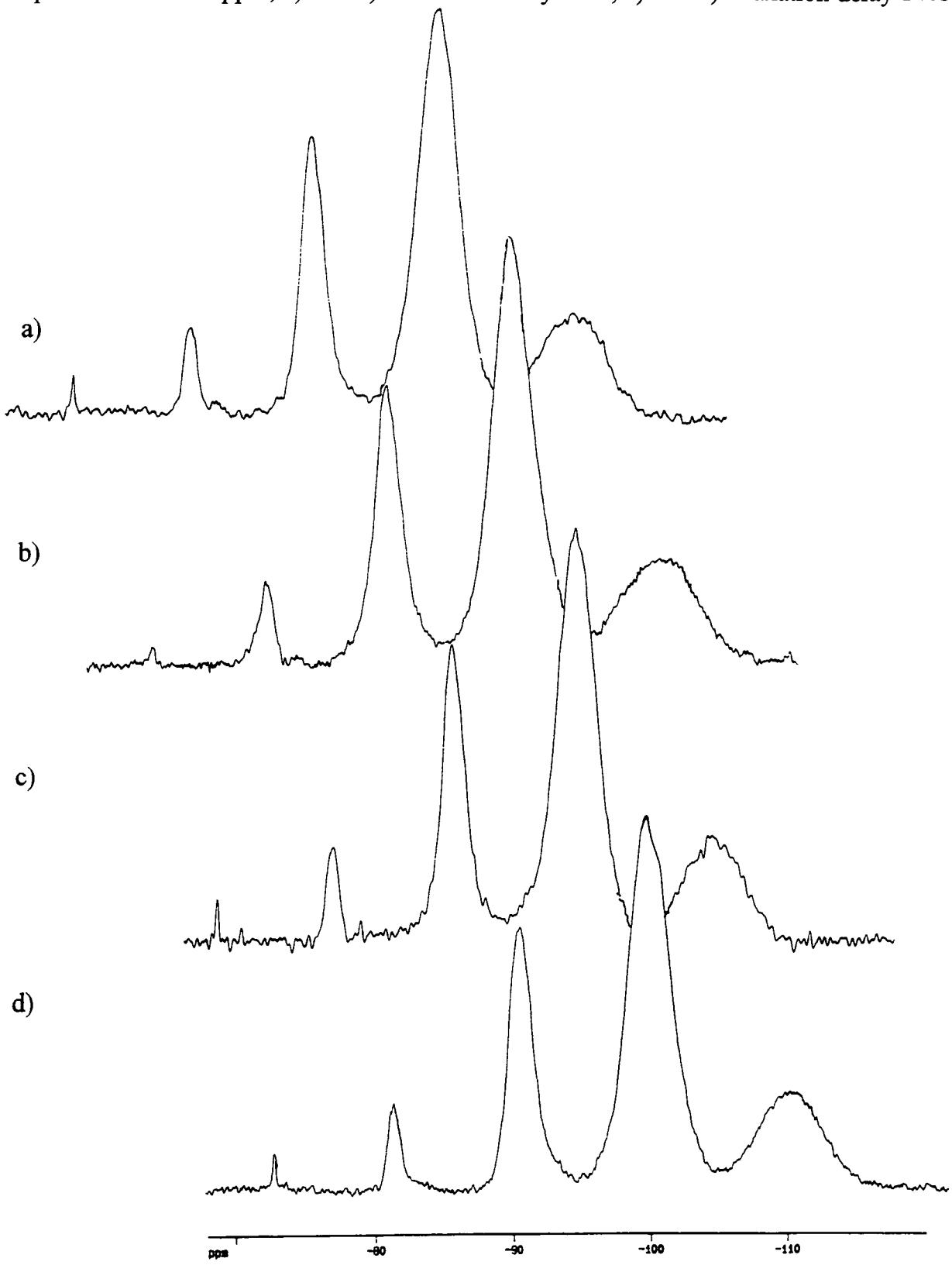

1.5 The shifting of the sol/gel-transition

The transition from a sol to a gel is a property which is characteristic for the composition of a silicate system. Any change of this property caused by additives is very important for industrial applications, particularly in the adhesives industry.

The effect of the anionic surfactants SHS and SDS on the sol/gel-transition has been investigated. SHS (8mM) was added to a sodium silicate solution with 25.5wt% SiO_2 and Rm=3.8. After leaving the solution for 1 day to equilibrate it was concentrated by heating and evaporating water to the point when the sol/gel-transition was passed according to the procedure described in Chapter 3-4.1.1. This point was not passed until a SiO_2 concentration of 33wt% was reached (Table 7-13). At a SiO_2 concentration of 27.5wt%, which is the point where the silicate without any surfactant passes the sol/gel-transition, the silicate containing 8mM of SHS was still in the sol-region. Thus the addition of sodium hexylsulfate shifts the SiO_2 concentration for the sol/gel-transition from 27.5wt% to 33wt%. The sol/gel-transition of the same silicate solution containing SDS instead of SHS was less affected by the surfactant and the transition to the gel is passed at an SiO_2 concentration of 30 wt% instead of 27.5wt% without SDS. The results are in Table 7-13.

Both silicate gels show a slight increase in the amount of Q3 units and a slight decrease in the amount of Q4 units (Table 7-14). The structuring in a silicate system generally does not show substantial changes when the transition to the gel is passed (Chapter 5-2). The addition of surfactants, which in these experiments are already in equilibrium with the silicate before the system is concentrated, only causes a small change. SHS is dissolved to a greater extent than SDS and thus generally affects the systems more than SDS.

Table 7-13
Sodium silicate solution with Rm=3.8

	without surfactant	with SDS	with SHS
sol/gel-transition	at 27.5wt% SiO_2	at 30wt% SiO_2	at 33wt% SiO_2

Table 7-14
Distribution of structural units:
sodium silicate gels with Rm=3.8

structural unit	30wt% SiO_2 without surfactant	30wt% SiO_2 with SDS c=8mM	33wt% SiO_2 with SHS c=8mM
Q0	0.0	0.0	0.3
Q1	3.0	3.5	2.7
Q2cyc	0.0	0.0	0.0
Q2	24.3	21.7	23.4
Q3	51.5	54.2	54.3
Q4	21.2	18.6	19.3
Q3/Q4	**2.4**	**2.9**	**2.8**

1.6 Silicate systems with the anionic surfactant in the liquid crystal phase

1.6.1 The addition of SDS

Sodium silicate systems on both sides of the sol/gel-transition have been investigated. The anionic surfactant SDS is added at a concentration of 9wt% to silicate systems with Rm-values smaller than or equal to 4.0 and mixed into the

silicate at room temperature as much as possible. Then the mixture is heated and at already ~ 60°C a clear homogeneous phase is formed which is left for another 20 minutes at this temperature. After cooling to room temperature the result is a white homogeneous phase which is not fluid. This situation is not caused by the silicate solution passing the sol/gel-transition but by the SDS forming a phase which restricts movement in the system. In the case of a silicate solution with 25wt% SiO_2 and Rm=4.0 the addition of 9wt% SDS causes a restriction of movement for the silicate units and the silicate does not flow at room temperature any more. In spite of this, the Q3- and Q4-units do not show any tendency for further condensation but in contrast show the same effect on the amount of Q3- and Q4-units as is observed for all surfactants, characterising a decreasing particle size (Table 7-15). This is illustrated in Figure 7-8. Even in a silicate gel the addition of 9wt% SDS is followed by a decrease in particle size as shown in Figure 7-9 (Table 7-19). Though it is much more difficult for a surfactant to interact with a locked-up gel structure than with a sol, the heating of both systems to homogenise the SDS gives it the chance to shift the equilibrium of the exchange between silicate units, since all motion is increased at a raised temperature. It was found that in the presence of surfactants forming liquid crystalline phases nucleation for the growth of particles is restricted by the microdomains and a large number of small particles can result[13].

Figure 7-8

^{29}Si NMR spectra of a sodium silicate solution with 25wt% SiO_2 and Rm=4.0

a) without surfactant

b) with 9wt% SDS

a) and b) were acquired on the Bruker AMX500 with 140 transients, acquisition time 0.04s, spectral width 200ppm, a) relaxation delay 100s, b) relaxation delay 140s

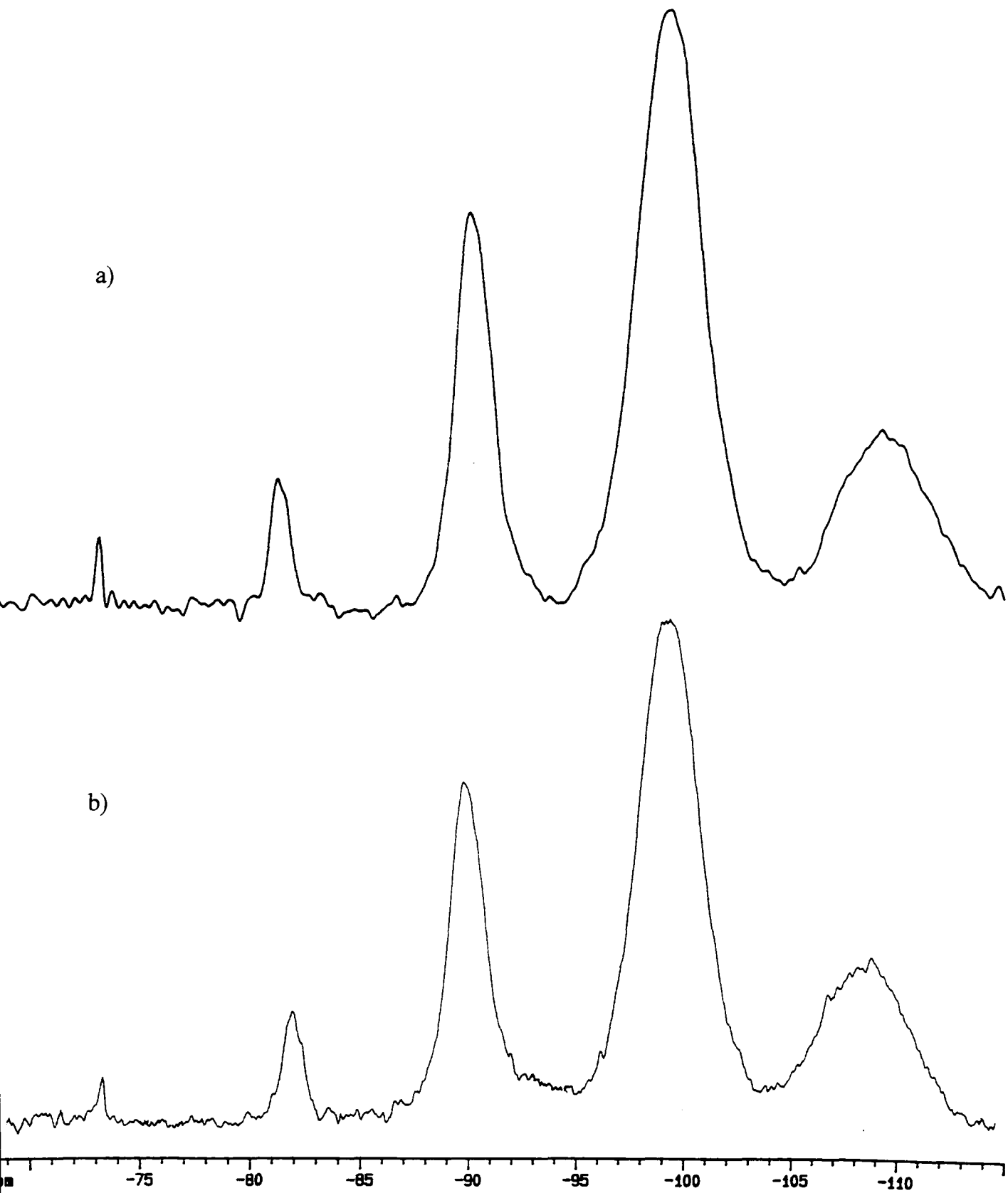

Figure 7-9
^{29}Si NMR spectra of a sodium silicate gel with 33wt% SiO_2 and Rm=3.4
a) without surfactant
b) with 9wt% SDS
a) and b) acquired on the Varian VXR300 with 1040 transients, acquisition time 0.04s, spectral width 300ppm, a) relaxation delay 120s, b) relaxation delay 150s

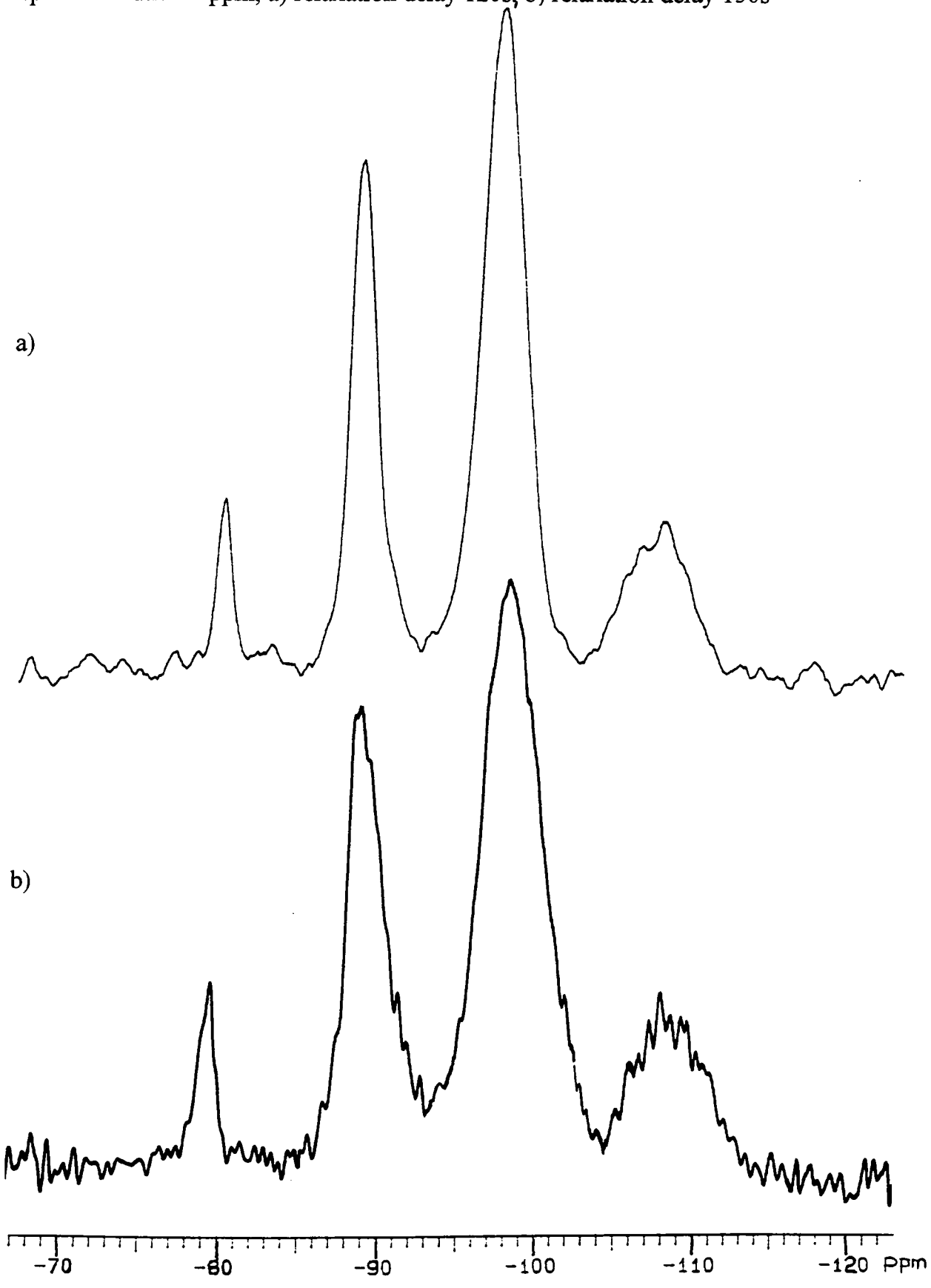

The silicon-proton distances in the silicate systems containing SDS in a liquid crystalline phase (tables 7-18 and 7-21) remain unchanged within the error limits compared to the pure silicate systems.

A comparison of the T2-values of the silicate/SDS solution with the T2-values of the silicate solution without SDS as presented in Table 7-16 shows that the mobility of Si-units decreases compared to the surfactant-free solution when the surfactant SDS is added to 9wt%-level. The rotational correlation times for the structural units in the silicate systems with and without SDS are calculated *via* spin-lattice relaxation times at different Bo-fields (Tables 7-17 and 7-20). As illustrated in Figure 7-10 the correlation times for the structural units in a silicate system on the sol-side of the sol/gel-transition increase when 9wt% SDS is added, the correlation time of the Q2-unit by a factor of 2, the correlation times of Q3- and Q4-units by a factor of about 6.

Figure 7-10
Comparison of correlation times without and with 9 wt% SDS for a sodium silicate solution with 25wt% SiO_2 and Rm=4.0

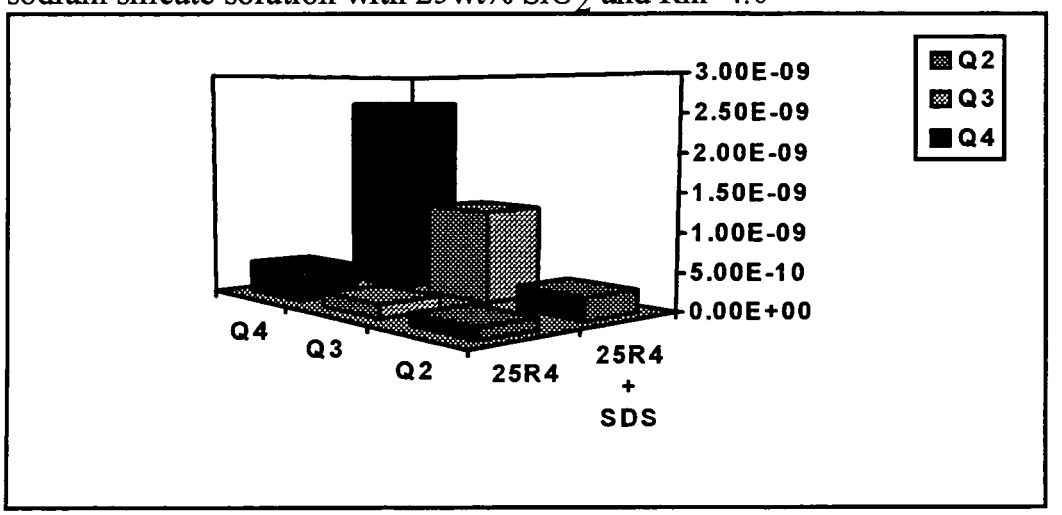

This indicates that the mobility of the Q2-units is less restricted by the interaction with a liquid crystal phase than the mobility of Q3- and Q4-units. It can be concluded that in the sol there is still scope for the movement of small particles in the liquid crystal phase of the SDS whereas the mobility of larger particles is severely restrained.

In contrast, figure 7-11 shows the increase in correlation times for a silicate gel in interaction with SDS in a liquid crystalline phase. In this case the mobility of the Q2-units decreases by a factor of about 5 whereas for the Q3- and Q4-units the decrease is only by a factor of 2.

Figure 7-11
Comparison of correlation times for a silicate gel
containing 33wt% SiO_2 with Rm=3.4 without and with 9wt% SDS:

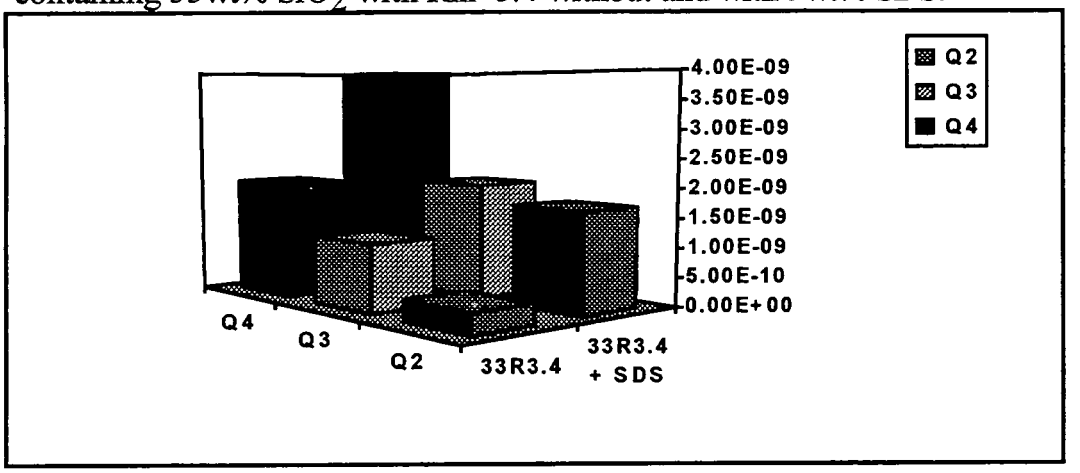

The silicate gel is in a state of low mobility before the SDS is added and it is particularly the silicate units with a higher degree of condensation (Q3- and Q4-units) whose mobility is most affected by the forming of a locked up gel-structure (Chapter 5-2). Thus the decrease in mobility for these structural units is relatively small compared to the decrease in mobility for the Q2-units which remain fairly mobile even in a gel (Chapter 6-2.2). The fact that the interaction with the liquid

crystalline phase restricts the overall mobility of the silicate solution as well as the silicate gel indicates that the silicate particles are locked up in the SDS phase.

Phase diagrams explore the numerous phases a SDS/water system passes with varying surfactant concentration at varying temperatures[8,9]. The three most common liquid crystal phases are the lamellar phase, where bilayers of amphiphilic molecules arranged in sheets are separated by water[13], the hexagonal phase where cylinders of surfactant are arranged in a two-dimensional hexagonal lattice and the cubic phase where the primary units are short rod-like aggregates which are connected at each end and form two interwoven but independent three-dimensional networks[8].

To characterise the structure the SDS forms when added in high concentration to a silicate system, investigations by optical microscopy were carried out (Figure 7-12). SDS was observed in the solid phase where it is crystalline. Then water was added and the SDS in water was heated. The phase-transition to a hexagonal phase occurs at 26°C and the phase transition to a lamellar phase takes place at 58°C. The silicate systems under investigation contain 33.0 wt% SiO_2 with Rm=3.4 and 25wt% SiO_2 with Rm=4.0. The former is past the sol/gel-transition and the latter is on the sol side of the sol/gel-transition. Both contain 9wt% SDS. From the previous investigations of the SDS/water system it can be concluded that at room-temperature the SDS in both silicates is found in a mixed phase. The SDS is in crystalline form, in the form of precipitated fine needles as well as forming a hexagonal phase underlying the crystalline phase in the background. Both phases reflect the light in a characteristic way and can thus most clearly be seen using the polariser. The structure of the SDS phases is very similar in both silicate systems. Further investigations by optical microscopy to understand the behaviour of the SDS in

these systems were carried out by heating the silicate-SDS systems to temperatures up to 75°C (Figure 7-13). At a temperature of 34°C the crystalline phase dissolves into the hexagonal phase. No transition from the hexagonal phase into a lamellar phase can be seen even when the temperature is raised to 75°C.

Figure 7-12
Optical microscopy on SDS
a) in crystalline form
b) in aqueous solution non-heated
c) in aqueous solution heated
d) in a sodium silicate system with 33wt% SiO_2 and Rm=3.4 at room temperature
e) in a sodium silicate system with 25wt% SiO_2 and Rm=4.0 at room temperature

a)

SDS dry t = 25°C

b)

SDS with H_2O t = 22°C

c)

crystalline phase

hexagonal phase

t = 26°C

hexagonal phase

with polariser

t = 26 °C

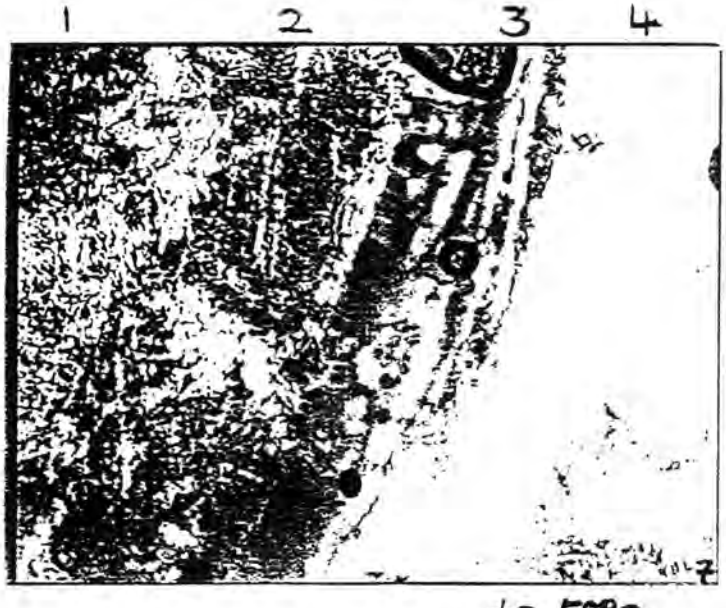

t = 58°C

4 phases

1 crystalline phase

2 lamellar phase
L_α (mobile)

3 intermediate phase

4 hexagonal phase
H_1

2 3

with polariser

t = 58 °C

d)

e)

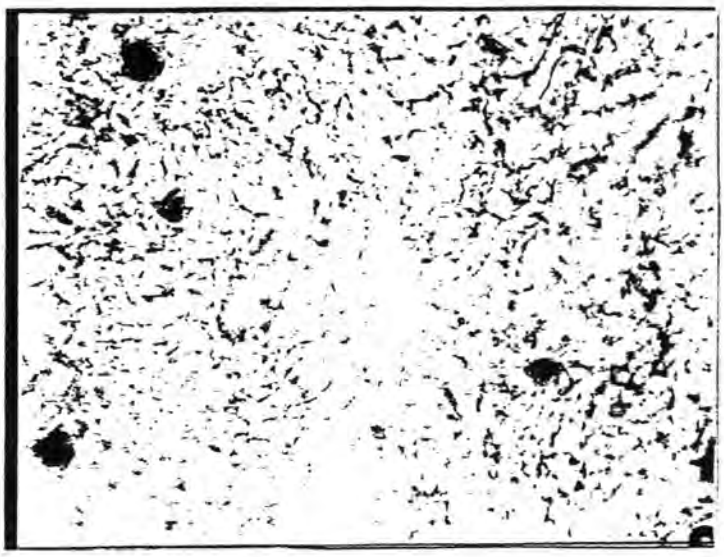

Figure 7-13
Optical microscopy on SDS with increasing temperature in
a) sodium silicate system with 33wt% SiO_2 and Rm=3.4
b) sodium silicate system with 25wt% SiO_2 and Rm=4.0

a)

crystals on hexagonal background

$t = 22\,^{\circ}C$

hexagonal phase crystals dissolved

$t = 26 - 36\,^{\circ}C$

no changeover to lamellar phase

$t = 66\,^{\circ}C$

b)

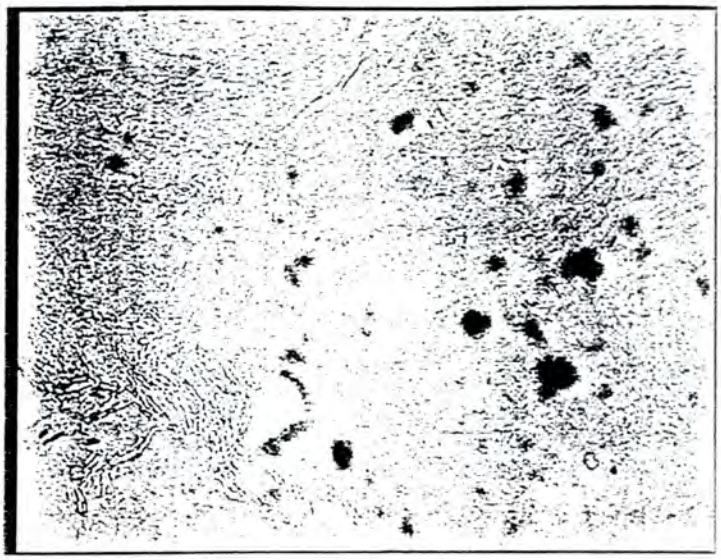

crystals on hexagonal background

without polariser
$t = 22°C$

crystals dissolving into hexagonal phase

with polariser
$t = 28°C$

hexagonal phase

with polariser
$t = 70°C$

It can be concluded that SDS forms a hexagonal liquid crystal phase in silicate systems with Rm-values ≤ 4.0 when added in high concentration (9wt%). The silicate structures seem to be arranged in the two-dimensional network in a way that does not influence the structuring formed at increased temperature and that does not disturb the formation and stability of a two-dimensional SDS network. It can be assumed that the changes in the structural distribution in both silicates take place during the period where the temperature is increased. The fact that the hexagonal phase, which is fairly rigid compared with the highly mobile lamellar phase, does not change into a lamellar phase at high temperature indicates that the silicate particles and the SDS are locked up in the hexagonal phase. Presumably the silicate prevents the arrangement of the SDS in sheets with water in between them as silicate particles would be too big to fit in-between normal intersheet distances.

Silicate system in sol form :

Table 7-15
Distribution of structural units in a
sodium silicate solution 25 wt% SiO_2 Rm=4.0 :

structural unit	without surfactant	with SDS c=9 wt%
Q0	0.7	0.2
Q1	3.3	2.4
Q2cyc	0.0	0.0
Q2	21.4	20.9
Q3	52.3	58.3
Q4	22.3	18.2
Q3/Q4	**2.3**	**3.2**

Table 7-16
T2-values in s measured with the CPMG sequence (Bruker AMX500):

structural unit	without surfactant	with SDS c=9 wt%
Q0	360 ms	-
Q1	107 ms	51 ms
Q2cyc	-	-
Q2	71 ms	46 ms
Q3	54 ms	34 ms
Q4	35 ms	23 ms

Table 7-17

T1-values in s at different fields measured by inversion recovery and calculation of the rotational correlation time τc using the ratio T1(600)/T1(500):

structural unit	without surfactant at 500 MHz	with SDS c=9 wt% at 500 MHz	with SDS c=9 wt% at 600 MHz	τc
Q0	8.4	-	-	-
Q1	8.8	9.6	10.8	3.5E-10 s
Q2cyc	-	-	-	-
Q2	8.5	9.8	10.9	3.0E-10 s
Q3	10.2	11.7	13.8	1.2E-9 s
Q4	18.5	26.5	34.8	2.6E-9 s

Table 7-18

Calculation of Si-H distances considering the amount of neighbouring protons:

structural unit	rSiH
Q0	-
Q1	2.0E-10 m
Q2	2.0E-10 m
Q3	2.2E-10 m

Silicate system in gel form :

Table 7-19
Structural distribution in a
sodium silicate gel containing 33wt% SiO_2 with Rm=3.4 :

structural unit	without surfactant	with SDS c=9wt%
Q0	0.0	0.0
Q1	5.6	2.8
Q2cyc	0.0	0.0
Q2	25.6	27.1
Q3	50.2	56.3
Q4	18.6	13.8
Q3/Q4	**2.7**	**4.1**

Table 7-20
T1-values in s at different fields measured by inversion-recovery and calculation of the rotational correlation time τc using the ratio T1(600)/T1(500):

structural unit	without surfactant at 500MHz	with SDS c=9wt% at 500MHz	with SDS c=9wt% at 600MHz	τc
Q0	7.9	-	-	-
Q1	8.1	9.7	10.2	1.3E-10 s
Q2cyc	-	-	-	-
Q2	8.6	9.1	11.4	1.7E-9 s
Q3	10.1	11.3	14.5	2.0E-9 s
Q4	22.0	24.7	33.6	4.0E-9 s

Table 7-21
Calculation of Si-H distances considering the amount of neighbouring protons:

structural unit	rSiH
Q0	-
Q1	(1.9 ± 0.05) E-10 m
Q2	(2.1 ± 0.05) E-10 m
Q3	2.2E-10 m

1.6.2 The addition of SHS

It has been investigated whether using SHS, which is more soluble in silicate solutions than SDS, as an anionic surfactant instead of SDS forms an ordered phase with the silicate and possibly exerts a greater effect on the silicate structures than SDS. However, the addition of 9wt% SHS to a sodium silicate solution containing 25wt% SiO_2 with Rm=4.0 results in a non-homogeneous mixture (two phases) where a part of the silicate has precipitated or strongly coagulated and an aqueous phase has separated. Nevertheless 95 % of the 29-Si in the precipitated part of the silicate can still be detected by solution-state NMR (AMX 500) with a broad peak underlying the Q1-, Q2-, Q3- and Q4-resonance which vanishes in MAS solid-state NMR (Figure 7-14).

Figure 7-14

^{29}Si NMR spectra of a sodium silicate solution with 25wt% SiO_2 and Rm=4.0

a) without surfactant acquired on the Varian VXR300

b) with 9wt% SHS acquired on the Varian VXR300 with MAS

a) and b) 1080 transients, acquisition time 0.04s, spectral width 300ppm, a) relaxation delay 100s, b) spin rate 1200Hz, relaxation delay 150s

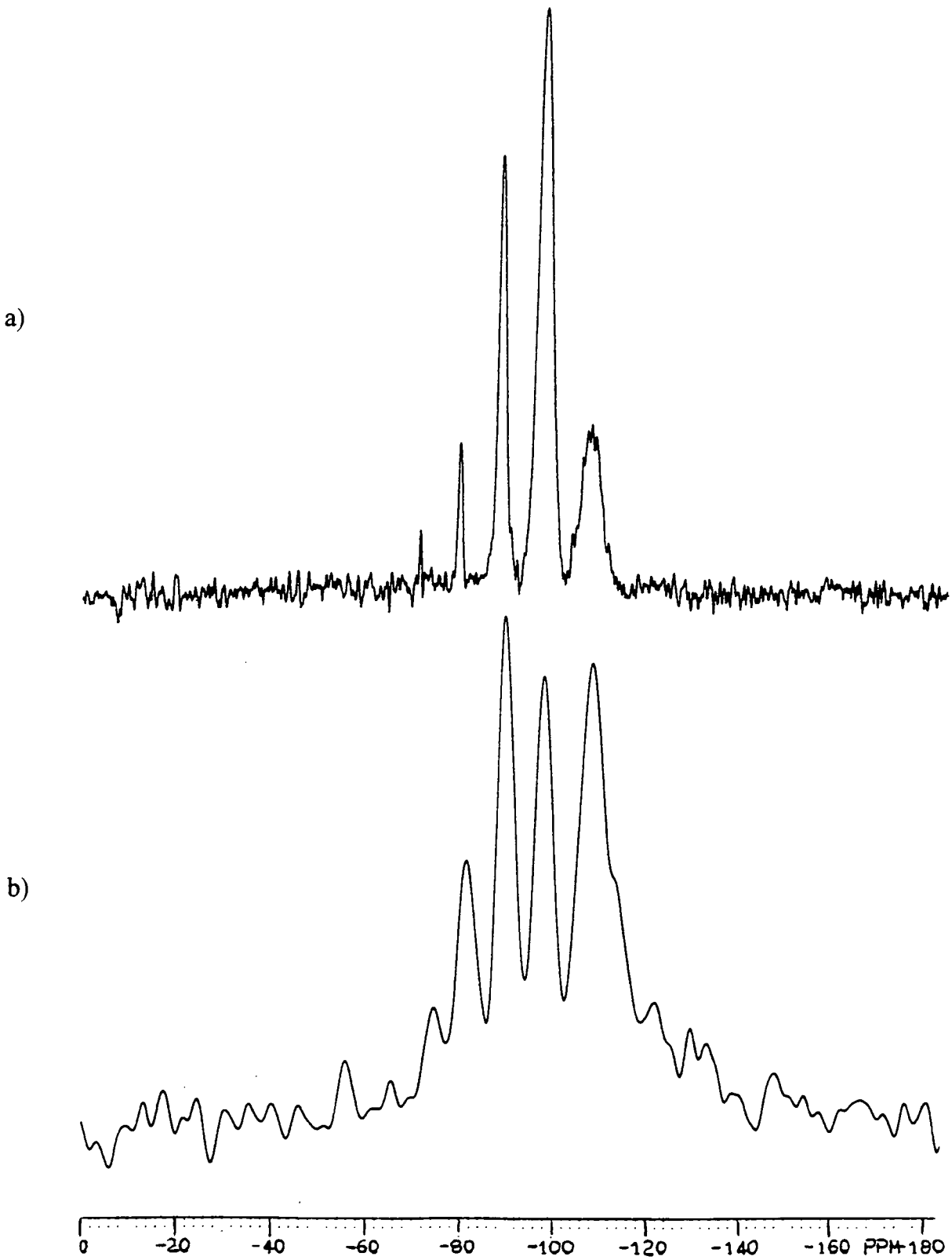

The change in the structuring of the silicate system upon addition of 9wt% SHS is interesting not only for the drastically decreasing amount of Q3-units along with an increase in the amount of Q4-units, but also for an increasing number of Q0- and Q1-units (Table 7-22). The former is characteristic for the increasing degree of condensation of the silicate system whereas the latter indicates a tendency towards less condensed units at the same time. This suggests that the process taking place is a gradual coagulation to highly-condensed partially-insoluble networks rather than a sudden precipitation of big 'lumps' of silica. It is assumed that only a part of the surface units (Q3-units) undergoes further condensation whereas the other part decondenses. In Chapter 6-4 it was established that Q3-units exchange with Q4-units as well as with Q2- and even Q1-units and that the structuring in silicate systems is determined by the exchange equilibria. It can be assumed that the change in the structuring caused by SHS is mainly due to a change in the exchange equilibria of the Q3 surface units.

Table 7-22
Structural distribution in a
sodium silicate system with 25wt% SiO2 and Rm=4.0

structural unit	without surfactant (sol)	with 9wt% SHS (precipitate)
Q0	0.7	5.3
Q1	3.3	15.1
Q2cyc	0.0	0.0
Q2	21.4	21.7
Q3	52.3	21.1
Q4	22.3	36.8

1.7 Heat-influence

Silicate-surfactant systems have been investigated under the influence of increased temperature, providing information on the structures in the solutions. The systems studied contain a high level of surfactant whilst still being solutions. The general idea behind these experiments is that at increased temperature the exchange between all species is more rapid (Chapter 6-4.2) and the exchange equilibrium shifts towards structures with a lower degree of condensation (Chapter 5-1.5). This means that at raised temperature the increase in the exchange rate from more-condensed to less-condensed species is bigger than that for the exchange from less-condensed to more-condensed species. Therefore it should be easier for the surfactant to shift the equilibrium of the exchange towards smaller particles, as the tendency for this process is existing anyway at higher temperature. It has to be considered, however, that agglomeration of micelles upon heating has been documented in the literature[14]. This can result in surfactant being taken out of the silicate/surfactant interaction.

In these experiments sodium silicate solutions with 25.5wt% SiO_2 and R_m=3.8 containing laurylether in the maximum amount dissolved (c=1.4wt%) and SHS in high concentration (c=1wt%) were heated to 65°C and 85°C for 4 hours. During the last three hours of heating the ^{29}Si NMR spectra were recorded at the respective temperatures. After the heat-treatment the silicate/surfactant solutions were left at room temperature for 6 weeks to re-establish equilibrium (Chapter 5-1.5) after which their structural distribution was compared to the starting position before heat-treatment. The results are presented in Tables 7-23 and 7-24.

At increased temperature the structuring in the silicate solutions containing surfactants shows the same tendency for a decrease in the amount of Q3- and Q4-units as in silicate solutions which do not contain surfactants. The general tendency going from the more-condensed towards the less-condensed units is not

affected by the surfactants. After the re-equilibration to room temperature the structuring in the silicate solutions shows an average particle size which is slightly smaller than the one in the starting system.

Taking into account that the starting temperature 25°C was increased to 85°C and that an increase of the temperature to only 45°C results in an increase in the Si-Si exchange rate of a factor of more than 10 compared to that at room-temperature, it is concluded that heat-treatment has only a minor influence on the effect of surfactants on the structuring in silicate solutions.

Table 7-23
Distribution of structural units for a
sodium silicate solution 25.5wt% SiO_2 ; Rm=3.8 with laurylether
concentration of dissolved laurylether = 1.4wt%

structural unit	at 25°C	at 65°C	at 85°C	at 25°C*
Q0	0.5	0.0	0.0	0.3
Q1	1.8	4.2	7.0	2.2
Q2	22.4	27.3	32.5	23.0
Q3	57.2	53.4	47.6	58.0
Q4	18.1	15.1	12.9	16.5
Q3/Q4	**3.2**	**3.5**	**3.7**	**3.5**

* 6 weeks after heat-treatment to 85°C for 2 hrs

Table 7-24
Distribution of structural units for a
sodium silicate solution 25.5wt% SiO_2 ; Rm=3.8 with SHS (c= 1.0wt%)

structural unit	at 25°C	at 85°C	at 25°C*
Q0	0.5	0.0	0.0
Q1	2.5	1.1	2.3
Q2	21.7	28.8	22.4
Q3	56.5	53.5	57.3
Q4	18.8	16.6	18.0
Q3/Q4	**3.0**	**3.2**	**3.2**

* 6 weeks after heat-treatment to 85°C for 2 hrs

1.8 Surfactant interaction with colloidal particles

In water/surfactant systems micelle formation is promoted by the thermodynamically unfavourable dissolution of the hydrophobic tails of the surfactant in water and the mutual attraction of the tails due to dispersion forces[1,3]. The micelle has a liquid-like character and can be regarded as a microscopic droplet[3]. It is possible to distinguish between rapid internal motions (in the range of 10^{-11}s) and slow overall motions (10^{-9}s and upwards) in surfactant aggregates. Fast motion occurs in the hydrocarbon chains whereas slow motion is dominated by micelle rotation and surfactant molecule lateral diffusion along the micelle surface[5].

It was established (chapter 5-5) that the surfaces of the colloidal particles in highly viscous silicate solutions with Rm-values bigger than 2.0 is mainly

uncharged. Nevertheless there are sites carrying charges resulting from the alkaline cleavage of Si-O-Si bonds.

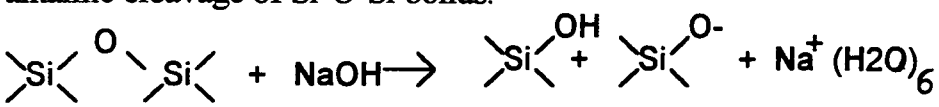

The starting point for the preparation of highly viscous silicate solutions is a dispersion of undissolved silica in a sodium hydroxide solution. This undissolved silica consists of silica particles whose surface area is covered with Si-OH groups which are mainly Q3-units. To dissolve these particles Si-O-Si bonds are hydrolysed to the extent that the amount of OH-ions in the system allows. These can either deprotonate Si-OH groups or hydrolyse Si-O-Si bonds. In any case a charged surface unit is produced. Since not all surface units are attacked by hydroxyl ions there is a considerable amount of Si-OH groups remaining in the system and the higher the molar ratio is, the higher is the ratio of uncharged to charged sites. Thus in the adsorption of additives there is a certain contribution of electrical effects along with the mechanisms present on polar, uncharged surfaces.

Adsorption of a surfactant on a solid/liquid interface is mainly controlled by three factors: the nature of the surfactant (including the nature of the head-group which determines the functionality and the nature of the hydrophobe), the nature of the solid surface and the nature of the liquid environment[1]. The forces which can be involved in the adsorption of surfactants at the solid/liquid interface are electrostatic interactions (illustrated in C, overleaf) , hydrogen bonding and dipolar interactions (illustrated in B, overleaf), dispersion forces and Van der Waals attractions (illustrated in A, overleaf)[1]. Adsorption usually occurs on a molecular level[1]. If a bilayer is adsorbed it will be via chain-chain interactions[2].

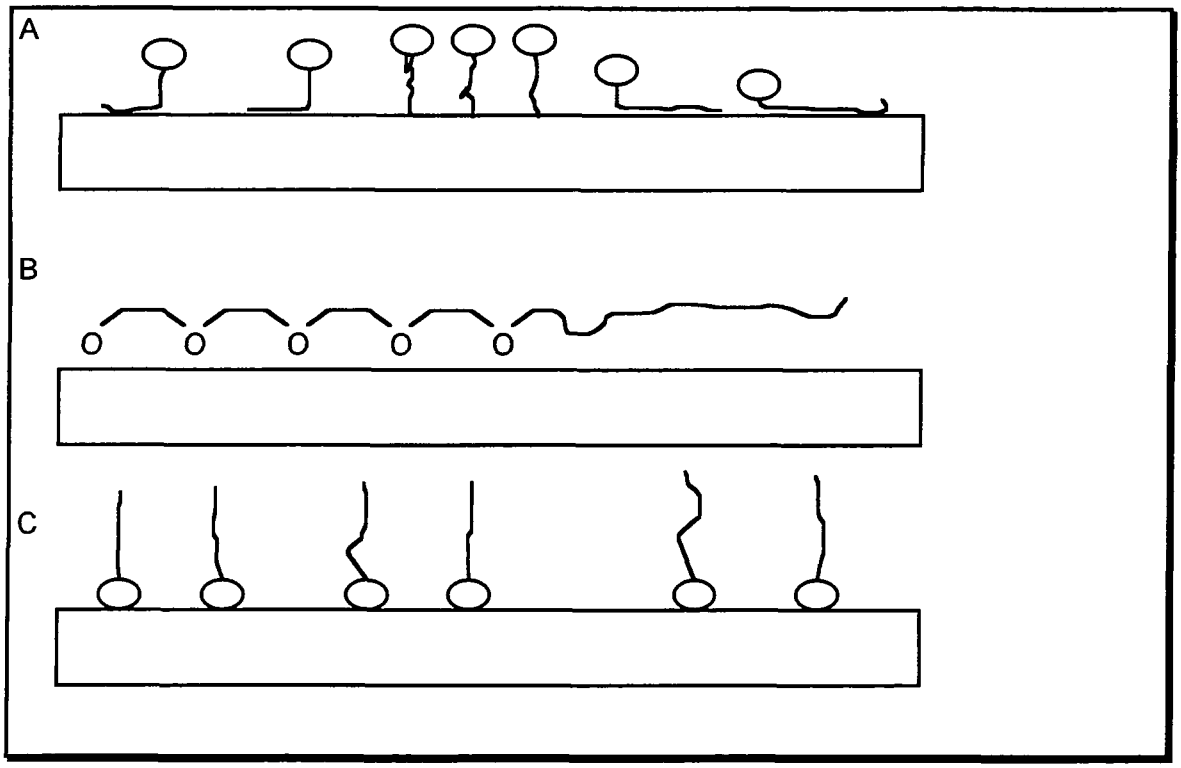

A small change in the characteristics of the system can cause a major change in the adsorption[1]. Hydration effects at the particle/solution interface are disrupted by the adsorbed surfactant[2].

The hydrogen bonding of large organic molecules and surfactants is considerably reduced by a surface charge as the large hydrated sodium ion which is adsorbed on the charged sites prevents the attachment not only on the charged site but also on the neighbouring sites[22]. This however is only of importance in silicate systems with low Rm-values, as in systems with higher Rm-values and lower alkalinity uncharged SiOH groups dominate on the surface of the colloidal particles.

The only case when the electrical effect on the adsorption mechanism has to be taken into account is the addition of surfactants with a cationic headgroup. Here the cationic headgroup competes with hydrated sodium ions in the adsorption on the charged sites. In the presence of charged sites the hydrophobic interaction

between alkyl chains on the silica surface is reported to be small[16]. There are two possibilities for the adsorption of charged surfactants on surfaces carrying charges. First, adsorption can be promoted by the charge difference then there is a changeover of mechanism to adsorption *via* Van der Waals forces onto sites with equal charge, for example on the crystal edges of kaolinit. This mechanism, however, is unlikely for the adsorption of cationic surfactants on silica surfaces. Second, adsorption can be promoted by the charge difference, and further adsorption occurs through bilayer formation on the monolayer[2]. Lee et al. found that the adsorption of the cationic surfactant $C_{16}TAB$ on silica occurs as a thick layer with head groups at both the silica surface and oriented into the bulk solution even at surfactant concentrations below the cmc[11]. The adsorption of surfactants on ionic surfaces is enhanced by salt-addition[2].

Surfactants with anionic headgroups do not adsorb *via* electrical effects. The charge balance on the charged surface sites is provided by hydrated sodium ions. The adsorption of cationic and anionic surfactants is considerably reduced by a surface charge as the large hydrated sodium, which is adsorbed on the charged sites, prevents the attachment not only on the charged site but also on the neighbouring sites[22]. This however is only of importance in silicate systems with low Rm-values, since in systems with higher Rm-values and lower alkalinity uncharged Si-OH groups dominate on the surface of the colloidal particles.

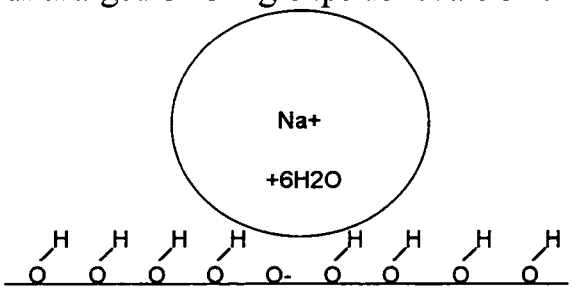

On polar uncharged surfaces the electrolyte content is expected to have a less pronounced effect upon adsorption of surfactants than on charged surfaces[1]. Potential forces at a polar uncharged surface include dispersion forces, dipolar interactions and hydrogen bonding[7]. The balance between the dispersion forces and the polar interactions determines the orientation of the surfactant molecules on the surface. If the former predominates, the hydrophobic tails align on the surface. If, however, the latter predominates, the hydrophilic head group will be at the surface and the tail oriented towards the aqueous phase. Dispersion forces are relatively weak but long-range. They are always present but not always dominant. The adsorption increases with increasing chain length. The drive for the dispersion forces or hydrophobic bonding is the tendency of the hydrophobic chains to be pushed out of the aqueous environment[1,4]. If the head groups are derivatives of strong acids such as sulphuric acid salts (SDS, SHS) or derivatives of strong bases such as quaternary ammonium ions the adsorption on polar uncharged surfaces *via* dispersion force interactions prevails. From this it can be concluded that the anionic surfactants SDS and SHS adsorb on the silica surface via dispersion forces. These are stronger for SDS than for SHS but it has to be considered that more SHS is dissolved than SDS, so for these surfactants there are two reciprocal effects. Materials like polyoxyethylenes can interact strongly with OH-groups on the surface *via* hydrogen bonding with the ethyleneoxide chains. Non-ionic surfactants are found to adsorb onto polar uncharged surfaces in a loose-packed monolayer with molecules parallel to the surface[1]. It was found that an increase in the length of the polyoxyethylene chain enhances adsorption at low concentrations and decreases the adsorption density[10]. The hydrophobicity of the surface is dependent on the ethyleneoxide chain length as well as the hydrophobic chain length[1,10]. In a surfactant mixture the surfactant with the longer chain displaces the one with the shorter chain[6]. In a mixture of an anionic with a non-

ionic surfactant the stronger hydrogen bonds with the non-ionic prevail over dispersion forces and it is assumed that the non-ionic will displace the anionic surfactant on the surface.

It can be said that all surfactants used in the present investigations adsorb on the surface of the colloidal particles in silicate systems *via* different mechanisms which depend on the nature of the surfactant. In chapter 6-4 it was established that the exchange equilibrium between silicate units in silicate systems gives rise to the distribution of structures observed in the silicate spectra. To understand the effect surfactants exert on the structuring in the silicate systems the fact that Q3-surface units exchange with Q4-units is of particular importance. The adsorption of surfactants onto the surface units of colloidal particles inhibits the recondensation of Q3-units and thus causes the equilibrium of the exchange to be shifted to the less condensed units.

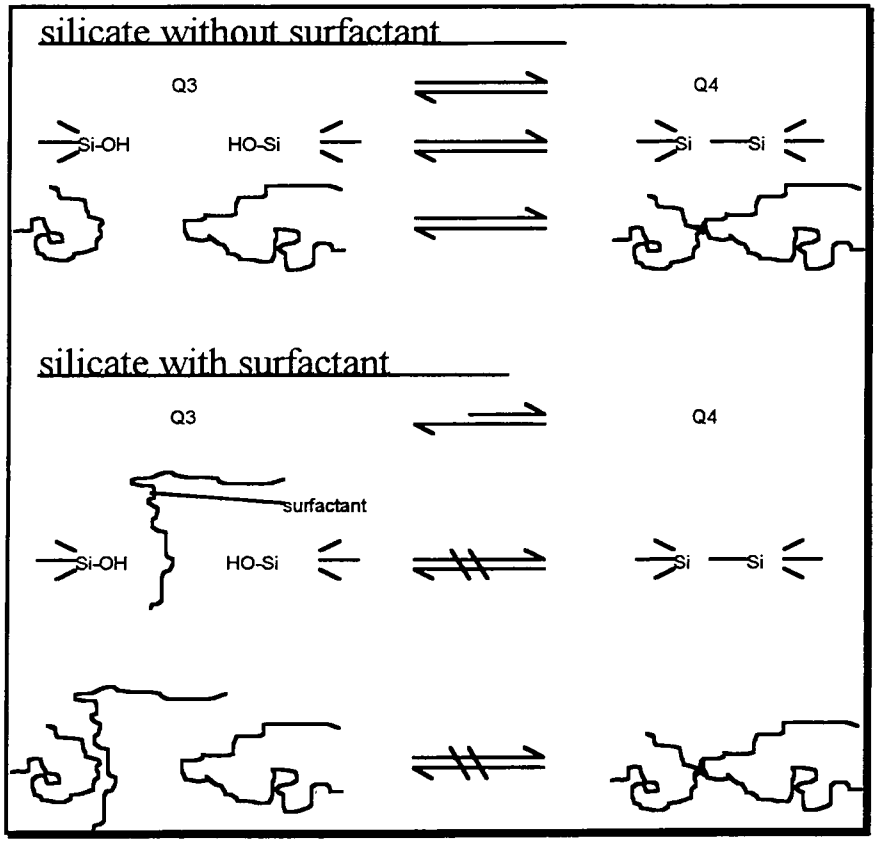

2. Silicate systems with incomplete SiO_2-dissolution

2.1 Introduction

The aim in this paragraph is to produce silicate systems with Rm-values bigger than 4.0, the emphasis being placed on systems with Rm-values of 4.5 and 5.0. The molar ratio of Rm=4.0 is reported to be the precipitation boundary of SiO_2 in silicate solutions[26,27]. It was investigated if this boundary can be shifted with the use of surfactants. Since surfactants seem to cause a decrease in the size of colloidal particles there is the possibility that by decreasing the average particle size in a silicate solution with undissolved silica more silica can be brought into solution.

The amount of dissolved silica was determined using the method of quantification described in chapter 4. In contrast to colloidal silica particles which are dissolved and stabilised, undissolved silica sinks to the bottom of the silicate solutions and can thus easily be separated by decanting. To make sure that this method only picks up silicon in silicate units which are dissolved in the silicate solution, the amount of silica dissolved in the silicate solutions is investigated after decanting and thus separating from the undissolved silica on the bottom. Therefore any silicon in undissolved silica is disregarded in the quantification.
Although the task was to produce sodium silicate systems containing 20wt% SiO_2 with Rm-values of 4.5 and 5.0, in the majority of experiments reported in this paragraph these compositions could not be achieved. The initial composition of the systems before separation from the undissolved silica, which is the starting point for all systems in this paragraph, is reported in terms of notional SiO_2 concentration (SiO_{2n})and notional Rm-value (Rm_n). The amount of silica dissolved in the silicate systems determines their real composition and thus their actual SiO_2 concentration and Rm-value, which are reported in terms of real SiO_2 concentration and real Rm-value.

In this paragraph the real composition of the silicate systems is determined *via* the amount of silica dissolved. It could be argued that this could also be obtained by separating, drying and weighing of the undissolved silica. This, however , is not feasible due to the high viscosity combined with the high sensitivity of the silicate systems.

2.2 Preparation

The silicate systems with notional Rm-values > 4.0 were prepared by dissolving fumed silica in sodium hydroxide solution. The systems were left at room temperature for six weeks and the amount of dissolved silica was determined. After this the surfactant was added to the system, which was then left to equilibrate at room temperature for at least two weeks before the NMR analysis. The silicates without surfactant were heated in order to check if the increased temperature promotes further dissolution of silica than can be achieved at room temperature. The only silicate system containing surfactant to be heated was the case of the addition of 9wt% SDS. This silicate SDS system was heated to 70°C to homogenise the surfactant in the silicate solution and yielded a homogeneous phase at 70°C. After cooling to room temperature the result was a white but not completely homogeneous phase which is non-fluid at room temperature and a slight phase separation due to precipitation occurs.

2.3 SiO_2-solubility

The silica in silicate systems with notional Rm-values bigger than 4.0 did not dissolve completely without heating the system as shown in tables 7-25.1 and 7-26.1. In a sodium silicate solution with $cSiO_{2n}$=20wt% and Rm_n=4.5 80% of the silica is dissolved whereas in the same solution but with Rm_n=5.0 it is only

71%. Without heat-treatment the actual molar ratio of SiO_2 to Na_2O can not be increased above Rm=3.6. The initial composition of the systems makes no change to the end-result.

The amount of dissolved silica increases when the systems are kept at increased temperature for a certain time. After heating to 70°C to 80°C for 10 hours it dissolved completely in a silicate with Rm=4.5 (Table 7-30.2) and stayed in solution when the silicate was brought back to room temperature. This is remarkable as the Rm of 4.0 was claimed to be the precipitation boundary of silica. In a silicate with Rm_n=5.0 heating increases the level of dissolved silica to 91% (Table 7-26.2). It can be concluded that heat-treatment can produce silicate systems with Rm-values as high as 4.6 with SiO_2 concentrations of about 20wt%.

However, the silica also dissolved completely in a silicate solution with Rm=4.5 when SDS (sodium dodecyl sulfate) was added (c=8mM) without having to heat the solution (Table 7-25.4). In a silicate solution with Rm=5.0 89% of the silica dissolved under the influence of 8mM SDS (Table 7-26.4). This demonstrates that the addition of SDS causes the same effect as heat-treatment in producing silicate solutions with Rm-values of 4.5 at SiO_2 concentrations of about 20wt% and can thus replace the heat-treatment.

At a concentration of only 3mM the effect of the SDS is reduced (Table 7-25.3) and a Rm-value of only 3.9 is obtained. Thus the influence of the surfactant SDS is subject to its concentration. The dissolution of silica in non heat-treated silicates under the influence of a surfactant, however, never exceeds the level of dissolution achieved with heat treatment. Leaving the silicate solutions containing 8mM SDS for up to 7 months exerts no effect on the dissolution of the silica. Thus there is no reverse effect caused by salting-out and the systems are stable (Table 7-25.5 and 7-26.5).

The addition of SDS in a high concentration (c=9wt%) gives rise to the formation of a liquid crystalline SDS phase in the silicate and increases the level of dissolution compared to the level of silica dissolution in the same silicate without SDS (Table 7-26.6) although the mobility of the system is decreased. This means that a small increase in the Rm-value above Rm=4.0 is achieved and the composition of the system changes to 15wt% SiO_2 with Rm=4.2. However, compared to the silicate with 8mM SDS, where SDS does not form a liquid crystalline phase, the level of SiO_2 dissolution is smaller. This is due to a slight precipitation of the silicate caused by the large amount of SDS in the system, which goes along with the results presented in Table 7-28.2 indicating an increase in the average particle size in this system.

As shown in Table 7-25.6 the cationic surfactant dodecyl-trimethylammonium bromide only causes a slight increase in the level of silica dissolution in increasing the Rm-value of the silicate solution from 3.6 to 3.7 and is thus less effective than SDS.

A sodium silicate solution of Rm=5.0 where only 70% of the usual concentration is taken as initial concentration (14wt% SiO_2) was investigated and it was found that without heat-treatment the silica is not completely dissolved to this level without the addition of a surfactant (Table 7-26.3).Nevertheless a composition of 12wt% SiO_2 and Rm=4.4 can be obtained.

Furthermore it was found that the anionic surfactant sodium hexylsulfate (SHS) is more effective for the dissolution of silica than SDS (Table 7-26.7). This can be explained as SHS is less salt-sensitive than SDS. Under the influence of SHS a silicate solution with the highest Rm-value (Rm=4.8) found in these investigations was achieved.

The tendencies reported before have been reconfirmed in a new preparation of the same samples at Rm=4.5 and Rm=5.0. The effect observed is repeatable and therefore seems to be genuine.

Tables 7-25.1 to 7-25.6
Sodium silicate solutions with $cSiO_{2n}$=20wt% and Rm_n=4.5

(% dissolved SiO2 describes the ratio of the amount of silica initially given into the system (20wt% SiO2) to the amount of dissolved silica determined after separation from the undissolved silica and quantification)

Table 7-25.1
20wt% SiO_2 Rm=4.5 no heating, 6 weeks after preparation

detected :	average :	dissolved SiO_2 :
16.4wt% SiO_2		
16.0wt% SiO_2	15.9 ± 0.4wt% SiO_2	80 %
15.4wt% SiO_2		

actual composition :
16wt% SiO2 and Rm=3.6

Table 7-25.2
20wt% SiO_2 Rm=4.5 heating to 70-80°C for 10 hrs
6 weeks after preparation

detected :	average :	dissolved SiO_2 :
19.8wt% SiO_2		
20.4wt% SiO_2	20.0 ± 0.3wt% SiO_2	100 %
19.7wt% SiO_2		

actual composition :
20wt% SiO2 and Rm=4.5

Table 7-25.3
after 6 weeks with 3mM SDS without heating :

detected :	average :	dissolved SiO_2 :
17.2wt% SiO_2		
16.7wt% SiO_2	17.2 ± 0.4 wt% SiO_2	86 %
17.8wt% SiO_2		

actual composition :
17wt% SiO2 and Rm=3.9

Table 7-25.4
20wt% SiO_2 Rm=4.5 with 8mM SDS, no heating
6 weeks after preparation

detected :	average :	dissolved SiO_2 :
19.9wt% SiO_2	-	99.5%

actual composition :
20wt% SiO2 and Rm=4.5

Table 7-25.5
after 7 months with 8mM SDS without heating :

detected :	average :	dissolved SiO_2 :
20.2wt% SiO_2		
20.0wt% SiO_2	20.1± 0.1wt% SiO_2	100 %
20.0wt% SiO_2		

actual composition :
20wt% SiO2 and Rm=4.5

Table 7-25.6

20wt% SiO_2 Rm=4.5 with 14mM laurylbromide, no heating

6 weeks after preparation

detected :	average :	dissolved SiO_2 :
16.3wt% SiO_2	16.6 ± 0.3wt% SiO_2	83 %
16.9wt%SiO_2		

actual composition :

17wt% SiO2 and Rm=3.7

Tables 7-26.1 to 7-26.7

Sodium silicate solutions with $cSiO_{2n}$=20wt% and Rm_n=5.0

(% dissolved SiO2 describes the ratio of the amount of silica initially given into the system (20wt% SiO2) to the amount of dissolved silica determined after separation from the undissolved silica and quantification)

Table 7-26.1

20wt% SiO_2 Rm=5.0, not heated, after leaving for 10 weeks

detected :	average :	dissolved SiO_2 :
14.7wt% SiO_2		
14.2wt% SiO_2	14.2 ± 0.4wt% SiO_2	71%
13.8wt% SiO_2		

actual composition :

14wt% SiO2 and Rm=3.6

Table 7-26.2

20wt% SiO_2 Rm=5.0, heated to 70°C for 10 hrs, after leaving for 10 weeks

detected :	average :	dissolved SiO_2 :
17.3wt% SiO_2		
18.5wt% SiO_2	18.2 ± 0.7wt% SiO_2	91%
18.9wt% SiO_2		

actual composition :

18wt% SiO2 and Rm=4.6

Table 7-26.3

14wt% SiO_2 Rm=5.0, not heated, after leaving for 10 weeks

detected :	average :	dissolved SiO_2 :
12.4wt% SiO_2	-	89%

actual composition :

12wt% SiO2 and Rm=4.4

Table 7-26.4

20wt% SiO_2 Rm=5.0 with 8mM SDS, not heated, after leaving for 10 weeks

detected :	average :	dissolved SiO_2 :
17.1wt% SiO_2		
17.5wt% SiO_2	17.7 ± 0.5 wt% SiO_2	89%
18.4wt% SiO_2		

actual composition :

18wt% SiO2 and Rm=4.5

Table 7-26.5

20wt% SiO_2 Rm=5.0 with 8mM SDS, not heated, after leaving for 5 months

detected :	average :	dissolved SiO_2 :
17.7wt% SiO_2		
17.2wt% SiO_2	17.5 ± 0.2 wt% SiO_2	87%
17.5wt% SiO_2		

actual composition :

18wt% SiO2 and Rm=4.5

Table 7-26.6

20wt% SiO_2 Rm=5.0 with 9wt% SDS, heated to 70°C for
10 minutes to homogenise, not completely homogeneous, after 18 weeks

detected :	average :	dissolved SiO_2 :
16.6wt% SiO_2	-	83%

actual composition :

15wt% SiO2 and Rm=4.2

Table 7-26.7

20wt% SiO_2 Rm=5.0 with 8mM SHS, not heated, after leaving for 10 weeks

detected :	average :	dissolved SiO_2 :
17.8wt% SiO_2		
18.9wt% SiO_2	19 ± 1.0wt% SiO_2	95%
19.3wt% SiO_2		
20.5wt% SiO_2		

actual composition :

19wt% SiO2 and Rm=4.8

2.4 Structural distribution under surfactant influence

Tables 7-27.1, 7-27.2, 7-28.1 and 7-28.2 summarise the structural distribution characterising the behaviour of the silicate systems under heat and surfactant influence. In all the investigated cases an increase in the amount of Q3 units was observed. Heat-treatment generally increases the SiO_2 concentration and the Rm-value of the silicate solutions and therefore an increased amount of Q3- and Q4-units is found. It has to be born in mind throughout these investigations that the effect on the structuring is not only caused by heat-treatment or surfactant addition but also by the increased level of SiO_2-dissolution which changes the composition of the system. The comparison of a silicate solution with Rm=5.0 containing 14 wt% SiO_2 with the same system containing 20wt% SiO_2 indicates that the average particle size in the former is smaller than in the latter.

The addition of the surfactant SDS results in a constant amount of Q3-units along with a slight decrease in the amount of Q4-units compared to a silicate solution without SDS with the same notional composition but a real composition of 14wt% SiO_2 and Rm=3.6. This indicates that a slight decrease in the degree of condensation takes place which can be related to a slight decrease in particle size.

in the real SiO_2 concentration and the Rm-value is. The addition of 8mM SHS produces the largest Rm-value achieved in these investigations. In this case both the amounts of Q3- and Q4-units stay constant compared to heat-treated silicate solutions where the level of SiO_2 concentrations and Rm-values are only slightly smaller than obtained with the addition of SHS. The structuring in the silicate/surfactant systems is stable within a period of 7 months. The addition of 9wt% SDS to the silicate solutions causes a decrease in the amount of Q3-units and an increase in the amount of Q4-units. This indicates an increase in particle size produced by the precipitation of the silicate under the influence of 9wt% SDS.

Table 7-27.1 and 7-27.2
Distribution of structural units in sodium silicate solutions with $cSiO_{2n}$=20wt% and Rm_n=4.5

Table 7-27.1

	without surfactant not heated	without surfactant heated to 70°C for 10 hrs
actual composition	16wt% SiO_2 Rm=3.6	20wt% SiO_2 Rm=4.5
Q0	0.0	0.0
Q1	1.8	1.0
Q2cyc	0.0	0.0
Q2/Q3cyc	24.6	20.0
Q3	50.8	53.4
Q4	22.8	25.6

Table 27.2

	with 3mM SDS	with 8mM SDS	with 8mM SDS after 7 months	with 14mM laurylbromide
actual composition	17wt% SiO_2 Rm=3.9	20wt% SiO_2 Rm=4.5	20wt% SiO_2 Rm=4.5	17wt% SiO_2 Rm=3.7
Q0	0.0	0.2	0.2	0.4
Q1	1.2	2.3	2.5	2.2
Q2cyc	0.0	0.0	0.0	0.0
Q2/Q3cyc	21.4	18.6	18.5	22.7
Q3	53.9	56.7	56.0	50.8
Q4	23.5	22.2	22.8	23.9

Table 7-28.1 and 7-28.2
Distribution of structural units in sodium silicate solutions with $cSiO_{2n}$=20wt% and Rm_n=5.0

Table 7-28.1

	without surfactant not heated	without surfactant heated to 70°C for 10 hrs
actual composition	14wt% SiO_2 Rm=3.6	18wt% SiO_2 Rm=4.6
Q0	0.3	0.0
Q1	1.2	1.7
Q2cyc	0.0	0.0
Q2	24.1	16.2
Q3	51.4	54.5
Q4	23.0	27.6

Table 7-28.2

	with 8mM SDS	with 8mM SDS after 5 months	with 9wt% SDS	with 8mM SHS
actual comp.	18wt% SiO_2 Rm=4.5	17wt% SiO_2 Rm=4.4	15wt% SiO_2 Rm=4.2	19wt% SiO_2 Rm=4.8
Q0	0.0	0.0	0.4	0.4
Q1	1.0	0.9	1.8	1.2
Q2cyc	0.0	0.0	0.0	0.0
Q2	20.9	21.2	15.2	16.1
Q3	54.7	55.0	50.2	54.3
Q4	23.4	22.9	32.4	28.0

2.5 The shifting of the sol/gel-transition

A sodium silicate solution containing 8mM SDS was concentrated from 20wt% SiO_2 Rm=4.5 to a notional SiO_2 concentration of 30wt% by heating to 80°C for 40 minutes with evaporation of water (The procedure is more accurately described in chapter 3-4.1.2). The silicate had an increased viscosity but had not passed the sol/gel-transition. It has to be considered that the whole composition of the system changes during the procedure (see table 7-29.1). The SiO_2 concentration increases and the Rm-value decreases during the concentration of the silicate but the notional SiO_2 concentration of 30wt% was not obtained. A sodium silicate system with an Rm-value of 4.0, which does not contain SDS, has passed the transition from a sol to a gel at a SiO_2 concentration of 27wt% (see chapter 5-2). Thus it can be concluded that the presence of the anionic surfactant SDS in silicate systems with Rm-values > 4.0 shifts the sol/gel-transition of a silicate solution to higher SiO_2 concentrations and the silicate with

SDS locks up to the gel-structure at higher silica concentrations than a silicate without SDS.

Table 7-29.1
sodium silicate solution with 30wt% SiO_2, Rm=4.5 and 8mM SDS

detected :	average :	dissolved SiO_2 :
26.6wt% SiO_2		
25.1wt% SiO_2	27 ± 1.2wt% SiO_2	90%
28.0wt% SiO_2		

Table 7-30
Distribution of structural units :
sodium silicate solutions

structural unit	27wt% SiO_2 Rm=4.1 with 8mM SDS
Q0	0.1
Q1	1.0
Q2cyc	0.0
Q2	18.3
Q3	55.1
Q4	25.5

2.6 Conclusions

From the experimental results the general conclusion can be drawn that surfactants added to silicate solutions with Rm-values bigger than 4.0, where the silica is not completely dissolved, assist in the dissolution. The addition of a surfactant has the same effect on the dissolution of silica as heat-treatment at 70°C

for 10 hours. It is known from results discussed in chapter 5 that at increased temperature the amount of Q3- and Q4-units decreases and that systems with maximal Rm-values of 4.0 resume the structuring they had at room temperature after a certain time. From information given in Chapter 6 we know that at increased temperature (at 45°C) the rate constant for exchange between structural units increases by a factor of more than 10. Silicate systems with Rm-values up to 4.0 are heated to promote the dissolution of silica. Thus it is assumed that in silicates with Rm-values bigger than 4.0 the heating only assists in decreasing the time-scale of the SiO_2-dissolution. Surfactants cause a decrease in the amount of Q4-units in silicates. In silicate systems with undissolved silica this opens the possibility to dissolve more silica till the amount of Q4 reaches a limiting factor which has been further discussed in chapter 5-1.2.

B. Other additives than surfactants

1. The effect of NaCl addition

The addition of NaCl is interesting for two reasons. First the salt influence generally is of considerable interest in silicate solutions. Second the addition of the surfactant SDS involves the addition of sodium ions which could affect the structures in the silicate solution. It had to be investigated if the effect of the anionic surfactants SDS and SHS on the structuring in the silicates is possibly caused by sodium ions.

It was found that the addition of more than 6wt% NaCl to a representative sodium silicate solution with 25wt% SiO_2 and Rm=4.0 causes precipitation so that

the system is no longer homogenous. If NaCl is added to an extent which does not cause precipitation the silicate solutions proceed very slightly to the more condensed region (Table 7-31 to 7-33). It is assumed that this is due to sodium ions taking water out of the system for their hydration.

The effect of the anionic surfactants SDS and SHS is the reverse effect to that caused by sodium ions. It can be concluded that the additional sodium ions added with the anionic surfactants do not affect the structuring. Generally it can be said that in concentrations where it does not cause precipitation NaCl has no significant effect on the structuring in silicate solutions. Sodium ions in high concentrations seem to take so much water for their hydration shell out of the silicate system that precipitation is caused.

The addition of a sodium salt to a silicate solution does not change the Rm-value, since this is defined as the ratio of silica to sodium oxide (sodium hydroxide) dissolved in the system and thus characterises the silicate system in terms of alkalinity rather than sodium ion content.

Table 7-31
Structural distribution for sodium silicate solution 25.5wt%SiO_2 ; Rm=3.8

structural unit	without NaCl	with NaCl c=8mM
Q0	0.9	0.6
Q1	4.7	4.0
Q2cyc	0.0	0.0
Q2/Q3cyc	23.2	22.1
Q3	51.5	53.9
Q4	19.7	20.4

Table 7-32

Structural distribution for sodium silicate solution 30wt%SiO_2 ; Rm=2.4

structural unit	without NaCl	with 4wt%NaCl
Q0	0.85	0.6
Q1	8.6	7.2
Q2cyc	2.3	2.2
Q2/Q3cyc	38.75	37.8
Q3	44.8	46.6
Q4	4.7	5.6

Table 7-33

Structural distribution for sodium silicate solution 25wt%SiO_2 ; Rm=4.0

structural unit	without NaCl	with 5.5wt% NaCl
Q0	0.7	0.4
Q1	3.3	3.1
Q2cyc	0.0	0.0
Q2/Q3cyc	21.4	20.1
Q3	52.3	53.6
Q4	22.3	22.8

2. Addition of $CaCl_2*6H_2O$

In certain cases a structure-directing effect of calcium ions in silicates has been reported[23]. These investigations however do not deal with silicate solutions on the border of the sol/gel-transition as the present studies do. The adsorption of $CaCl_2$ on SiOH-bonds takes place above a pH of 5[21]. It has been confirmed that each Ca^{2+} ion is only linked to one SiOH-group[21].

$SiOH + Ca^{2+}$ ------- $SiOCa^{+} + H^{+}$

The chelation of calcium ions by sodium silicates was observed by determining the total free calcium content in a silicate solution using a calcium electrode[19].

In the investigated highly-condensed silicate solutions the addition of $CaCl_2*6H_2O$ leads to precipitation of the silicate. The result is a white solid suspended in aqueous solution. All investigations have been on the resulting suspensions in the original state 1 day after addition of the $CaCl_2$. The intensities reported in table 7-34 are measured with the deconvolution program (DECON) with the data sent from the VXR300 to an Archimedes computer.

The addition of 2.1mmol $CaCl_2*6H_2O$ per g silicate corresponds to the addition of as many Ca^{2+}-ions as there are Na^{+}-ions in the solution. As demonstrated in Figure 7-15 this caused severe precipitation and only Q3- and Q4-units are remaining in the system as shown in figure 7-15.

Generally the adsorption of charged species changes the surface properties, and uncharged colloids are not stable any more. It can be assumed that the bonding of calcium ions to the surface, which disturbs the electrostatic equilibrium in the system by producing a charged surface along with releasing protons (the latter acidifying the system)[21], is responsible for the precipitation of the silicate. Since the calcium ions are added in the fully hydrated form as $CaCl_2*6H_2O$ they do not take water out of the system for their hydration. Much less calcium ions are needed to precipitate the silicate than sodium ions, which

indicates that silicate solutions are more sensitive to the adsorption of ions than to hydration effects.

Table 7-34
Distribution of structural units (VXR300):
sodium silicate solution with 25wt% SiO2 and Rm=4.0

structural unit	without $CaCl_2*6H_2O$	with 2.1mmol $CaCl_2*6H_2O$ per g silicate
Q0	0.7	0.0
Q1	3.3	0.0
Q2cyc	0.0	0.0
Q2	21.4	0.0
Q3	52.3	49.0
Q4	22.3	51.0

Figure 7-15

^{29}Si NMR spectra of a sodium silicate solution with 25wt% SiO_2 and Rm=4.0

a) without additive

b) with 2.1mmol $CaCl_2*6H_2O$

a) and b) acquired on the Varian VXR300 with 1040 transients, acquisition time 0.04s, spectral width 300ppm, a)relaxation delay 100s, b) and c) relaxation delay 160s

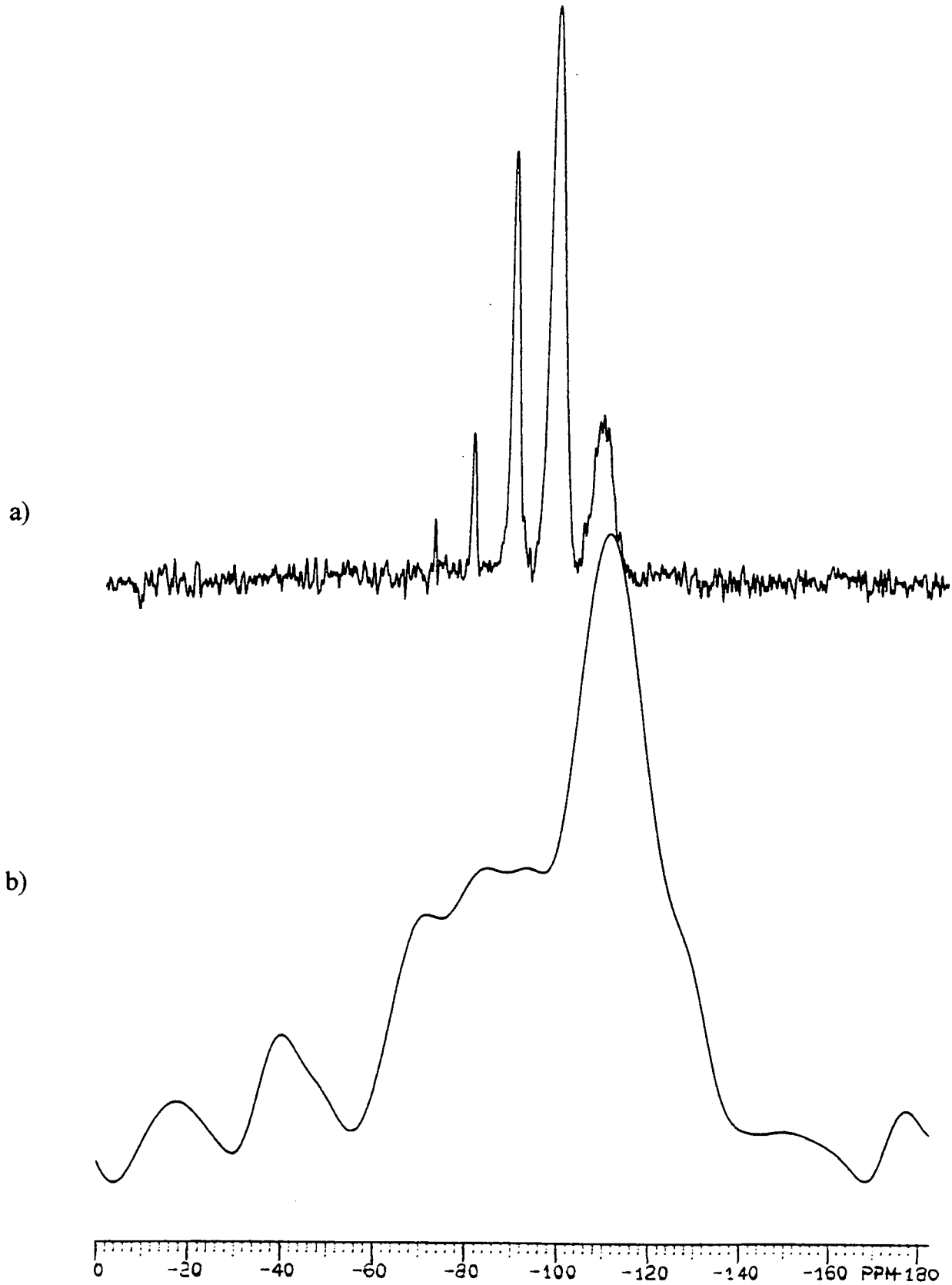

3. $FeCl_3$ in silicate solutions

In previous investigations it was found that Fe^{3+} ions adsorb strongly onto silica surfaces[22]. In chapter 3-5 the addition of a small amount of $FeCl_3$ was studied and it was found that in low concentration the T1-values are shortened while the structuring does not change. The addition of $FeCl_3$ in concentrations of 3wt% and 9wt% drastically changes the nature of the silicate. A silicate precipitate is formed, but unlike the precipitation of silicates under the influence of additives like NaCl or $CaCl_2 * 6H_2O$, the volume of the aqueous phase which separates is extremely small. Table 7-35 shows that the addition of 3wt% $FeCl_3$ only results in a slight increase in the degree of condensation of the silicate, whereas $FeCl_3$ in a concentration of 9wt% causes a drastic increase in the amount of Q4-units at the cost of Q3-units. This indicates an increase in the particle size characteristic of a precipitate rather than a gel.

If there is more than a certain amount of $FeCl_3$ in the system the constitution of the silicate changes from a gel to a precipitate. $FeCl_3$ reacts as a weak acid in aqueous solution[24] and it can be concluded that the coordination of water in the hydration shell of Fe^{3+}, along with the release of protons, is responsible for the gelation of the silicate.

$FeCl_3 + H_2O = FeCl_3[OH^-] + H^+$

Table 7-35
Distribution of structural units sodium silicate solution 25wt% Rm=4.0

structural unit	without $FeCl_3$	with 3wt% $FeCl_3$	with 9wt% $FeCl_3$
Q0	0.7	0.0	0.0
Q1	3.3	0.0	0.0
Q2	21.4	20.0	18.4
Q3	52.3	54.8	30.3
Q4	22.3	24.2	51.3

4. The effect of lauric acid

Lauric acid was chosen as a representative C_{12}-organic acid for the investigation of the effect of fatty acids on silicate solutions. The addition of lauric acid in a concentration of 1.3wt% does not affect the silicate. If the concentration of lauric acid is increased to 10wt% precipitation is caused. Most affected by this are Q3- and Q4-units, whereas Q1- and Q2-units stay relatively unaffected, as shown in Figure 7-16 and Table 7-36.

Lauric acid can adsorb on the silica surface with the hydrophobic chain via dispersion forces or via the hydrophilic carboxyl group with hydrogen bonding. In both cases the resulting effect should not be the precipitation of the silicate. Therefore the acidity of lauric acid is assumed to be the reason for the precipitation. Since lauric acid is a weak organic acid[25] the release of protons at low acid concentration has no effect, and high acid concentrations are required to cause precipitation of the silicate.

Table 7-36

Distribution of structural units in a sodium silicate solution 25wt% Rm=4.0

structural unit	without Lauric acid	with 1.3wt% Lauric acid	with 10wt% Lauric acid
Q0	0.7	0.0	0.0
Q1	3.3	2.7	1.4
Q2	21.4	20.0	16.0
Q3	52.3	52.3	29.5
Q4	22.3	25.0	53.0

Figure 7-16

^{29}Si NMR spectra of a sodium silicate solution with 25wt% SiO_2 and Rm=4.0

a) without surfactant

b) with 1.3wt% lauric acid

c) with 10wt% lauric acid

a) to c) acquired on the Varian VXR300 with 1040 transients, acquisition time 0.04s, spectral width 300ppm, a)relaxation delay 100s, b) and c) relaxation delay 140s

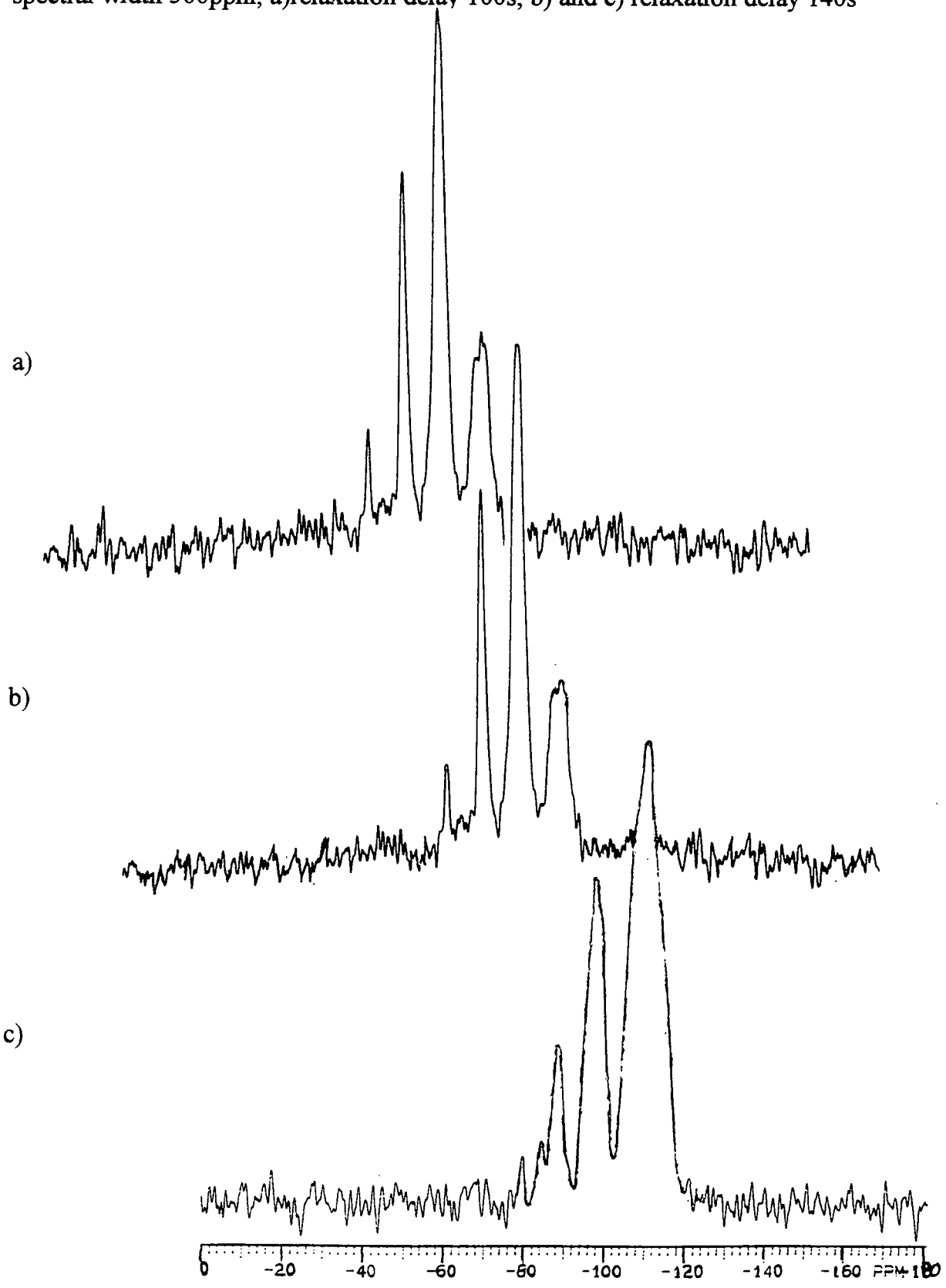

5. Polyethylene glycols as additives

Polyethylene glycols are industrially important additives and their effect on silicate systems is of great commercial interest. Polyethylene glycols (PEG400 and PEG1500) were added to an equilibrated commercial sodium silicate solution containing 28 wt% SiO_2 with an Rm-value of 3.4. It has been found that the adsorption of polar polymers onto the silica surface causes an immobilisation of solvent molecules[19].

Both glycols added in amounts of 1 wt% and 3 wt% caused the separation of an aqueous phase. This takes up 15 vol% of the total volume in the case of the addition of 3 wt% PEG400. Quantitative investigations by ^{13}C-NMR and ^{29}Si-NMR show that the aqueous phase contains the PEG but no silicate. The phase containing the silicate has the consistency of a gel that is produced by evaporation of water from a silicate solution. Further confirmation that the effect caused by polyethyleneglycols is a gelation rather than a precipitation is presented in Figure 7-17 and Table 7-37, which show that although a water-phase separates the Si-structures are not affected to a great extent.

It is remarkable that the addition of a polyethylene glycol in a concentration of only 1wt% causes the separation of a water phase whereas the addition of 3wt% the non-ionic surfactant laurylether, which adsorbs via the same mechanism through the oxyethylenic chain like PEG, produces a slightly decreased particle size. It is assumed that PEG, which has many more polar sites than laurylether, competes strongly with the silicate system for hydration water, and at concentrations of 1wt% it takes so much water out of the system that the system passes the sol/gel-transition.

Table 7-37
Distribution of structural units
sodium silicate solution commercial 28wt% SiO_2, Rm=3.4

1 without any PEG

2 with 1 wt% PEG400 (20hrs after addition)

3 with 3 wt% PEG400 (24 hrs after addition)

4 with 3 wt% PEG400 (4 weeks after addition)

5 water-phase which has separated from the silicate/PEG mixture (4 weeks after the PEG400-addition)

This water-phase has been measured quantitatively using the method of quantification and it was found to contain 1 wt% SiO_2.

The corresponding gel-phase was analysed with 13C-quantification and it was established that it contains only negligible amounts of PEG400.

6 with 1wt% PEG1500 (24 hrs after addition)

7 with 1wt% PEG1500 (4 weeks after addition)

	1	2	3	4	5	6	7
Q0	0.1	0.4	0.3	0.3	0.0	0.3	0.4
Q1	2.8	3.0	3.7	3.8	19.5	3.8	3.5
Q2	27.8	27.4	28.2	28.7	36.0	28.7	25.5
Q3	55.8	55.6	53.1	53.6	39.0	53.6	56.8
Q4	13.5	13.8	14.7	13.6	0.0	13.6	13.8

Figure 7-17

^{29}Si NMR spectra of

a) commercial sodium silicate solution with 28wt% SiO_2 and Rm=3.4

b) with 3wt% PEG400

c) with 3wt% PEG1500

a) to c) acquired on the Bruker AMX500 with acquisition time 0.06s, spectral width 200ppm, relaxation delay 150s, 180 transients

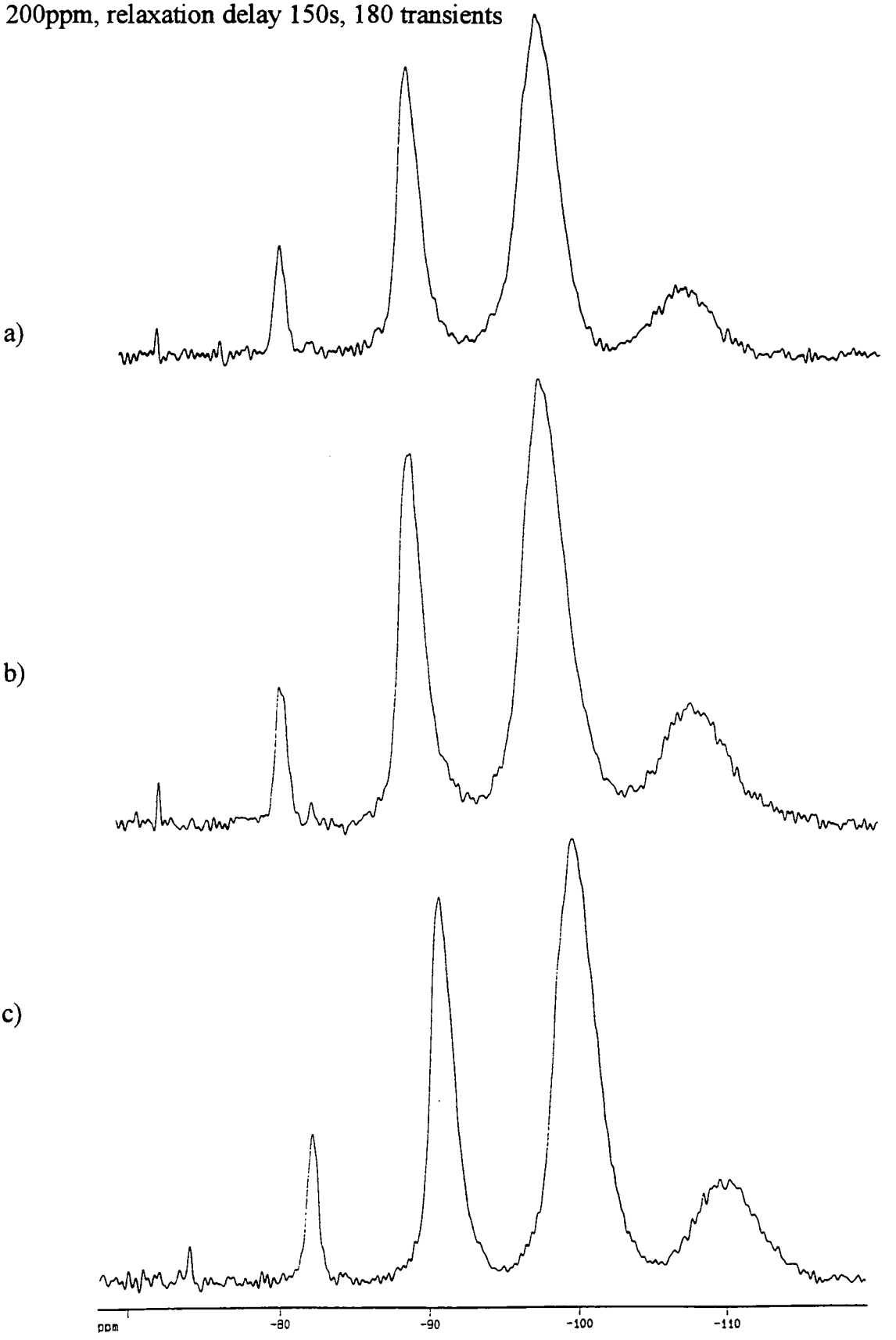

Literature:

1 D. Myers, C. Drew, Surfactant Science and Technology, 1.Surface Active Agents, VCH Weinheim, New York (1988)

2 G. D. Parfitt, C. H. Rochester, Adsorption from Solution at the Solid/Liquid Interface, Academic Press London, New York (1983)

3 B. Ranby, Physical Chemistry of Colloids and Macromolecules, Blackwell Scientific Publications Oxford, London, Edinburgh (1984), B. Lindman, H. Wennerstrom, 67

4 C. Tanford, The Hydrophobic Effect, John Wiley New Yok (1980)

5 H. Walderhaug, O. Soederman, P. Stilbs, J. Phys. Chem. **88** (1984) 1655

6 J .F. Scamehorn (Ed.), Phenomena in Mixed Surfactant Systems, ACS Symposium Series 311 (1968)

7 K. Shinoda (Ed.), Solvent Properties of Surfactant Solutions, Edward Arnold London (1968)

8 P. Kekicheff, C. Grabielle-Madelmont, M. Ollivon, J. of Colloid and Interface Science **131**, No.1 (1989) 112

9 P. Kekicheff, J. of Colloid and Interface Science **131**, No.1 (1989) 133

10 P. Somasundaran, E. D. Snell, E. Fu, Q. Xu, Abstracts of Papers of the American Chemical Society **200** (1990) 134

11 E. M. Lee, E. A. Simister, R. K. Thomas, Langmuir **6** (1990) 1031

12 B. Lindman, H. Wennerstrom, Topics in Chemstry, No.87: Micelles, Springer Verlag Berlin (1980), 1

13 E. C. O'Sullivan, R. C. Patel, A. J. I. Ward, J. of Colloid and Interface Science **146**, No.2 (1991) 582

14 S. E. Friberg, P. Botherol (Ed.), Microemulsions: Structure and Dynamics, CRC Press Boca Raton (1987)

15 P. K. Dutta, D. Robins, Langmuir **7** (1991) 1048

16 P. Waengerund, G. Olofsson, J. of Colloid and Interface Science **152**, No.2 (1992) 393

17 K. Osseo-Asare, F. J. Arriagada, Colloids and Surfaces **50** (1990) 321

18 R. Denoyel, J. Rouquerol, J. of Colloid and Interface Science **143**, No.2 (1991) 555

19 C.-Z. Yang, S.-Y. Tang, J. Surface Sci. Technol. **5**, No.3 (1989) 377

20 G. P. van der Beek, M. A. Cohen Stuart, T. Cosgrove, Langmuir 7, No.2 (1991) 333

21 E. Tadros, J. Lyklema, J. Electroanal. Chem. Interfacial Electrochem. **22** (1969) 1

22 R. K. Iler, The Chemistry of Silica, John Wiley & Sons New York (1979)

23 G. Engelhardt, D. Michel, High Resolution Solid State NMR of Silicates and Zeolites, John Wiley & Sons (197)

24 H. R. Christen, Grundlagen der Allgemeinen und Anorganischen Chemie, Salle & Sauerlaender Verlag Frankfurt a. M. (1988)

25 H. Kaufmann, Grundlagen der Organischen Chemie, 7. Aufl., Birkhauser Verlag Basel, Boston (1986)

26 I. L. Svensson, S. Sjoeberg, L-O. Oehman,
J. Chem. Soc. Faraday Trans. I, **82** (1986) 3635

27 R. K. Iler, Soluble Silicates, J. S. Falcone (Ed.), ACS Symposium Series **194** (1982) 95

Appendix

List of Lectures and Seminars

Colloquia, Lectures and Seminars given by invited Speakers
from Aug 1991 to April 1994

1991

Oct 17	Dr. J. A. Salthouse, University of Manchester Son et Lumiere - a demonstration lecture
Oct 31	Dr. R. Keeley, Metropolitan Police Forensic Science Modern Forensic Science
Nov 6	Prof. B. F. G. Johnson, Edinburgh University Cluster - surface analogies
Nov 7	Dr. A. R. Butler, St. Andrews University Traditional Chinese herbal drugs : a different way of treating disease
Nov 13	Prof. D. Gani, St. Andrews University The chemistry of PLP-dependent enzymes
Nov 20	Dr. R. More O'Ferrall, University College, Dublin Some acid-catalysed rearrangements in organic chemistry
Nov 28	Prof. I. M. Ward, IRC in Polymer Science, University of Leeds The SCI lecture : the science and technology of oriented polymers
Dec 4	Prof. R. Grigg, Leeds University Palladium-catalysed cyclisation and ion-capture processes
Dec 5	Prof. A. L. Smith, ex Unilever Soap, detergents and black puddings
Dec 11	Dr. W. D. Cooper, Shell Research Colloid Science : theory and practice

1992

Jan 22	Dr. K. D. M. Harris, St. Andrews University Understanding the properties of solid inclusion compounds
Jan 29	Dr. A. Holmes, Cambridge University Cycloaddition reactions in the science of the synthesis of piperidine and indolizidine natural products
Jan 30	Dr. M. Anderson, Sittingbourne Research Centre, Shell Research Recent advances in the safe and selective chemical control of insect pests
Feb 12	Prof. D. E. Fenton, Sheffield University Polynuclear complexes of molecular clefts as models for copper biosites
Feb 13	Dr. J. Saunders, Glaxo Group Research Limited Molecular modelling in drug discovery

Feb 19	Prof. E. J. Thomas, Manchester University Applications of organostannanes to organic synthesis
Feb 20	Prof. E. Vogel, University of Cologne Porphyrins : molecules of interdisciplinary interest
Feb 25	Prof. J. F. Nixon, University of Sussex Phoosphalkynes : new building blocks in inorganic and organometallic chemistry
Feb 26	Prof. M. L. Hitchman, Strathclyde University Chemical vapour deposition
Mar 5	Dr. N. C. Billingham, University of Sussex Degradable Plastics - Myth or magic?
Mar 11	Dr. S. E. Thomas, Imperial College Recent advances in organoiron chemistry
Mar 12	Dr. R. A. Hahn, ICI Imagedata Electronic Photography - an image of the future
Mar 18	Dr. H. Maskill, Newcastle University Concerted or stepwise fragmentation in a deamination-type reaction
Apr 7	Prof. D. M. Knight, Philosophy Department, University of Durham Interpreting experiments : the beginning of electrochemistry
May 13	Dr. J.-C. Gehret, Ciba Geigy, Basel Some aspects of industrial agrochemical research
Oct 15	Dr. M. Glazer, Dr. S. Tarling, Oxford University & Birbeck College, London It pays to be British - the chemists role as an expert witness in patent litigation
Oct 20	Dr. H. E. Bryndza, Du Pont Centra Research Synthesis, reactions and thermochemistry of metal (alkyl) cyanide complexes and their impact on olefin hydrocyanation catalysis
Oct 22	Prof. A. Davies, University College, London The behaviour of hydrogen as a pseudometal
Oct 28	Dr. J. K. Cockcroft, University of Durham Recent developments in powder diffraction
Oct 29	Dr. J. Emsley, Imperial College, London The shocking history of phosphorus
Nov 4	Dr. T. P. Kee, University of Leeds Synthesis and co-ordination chemistry of silylated phosphites
Nov 5	Dr. C. J. Ludman, University of Durham Explosions, a demonstration lecture
Nov 11	Prof. D. Robins, Glasgow University Pyrrolizine alkaloids : biological activity, biosynthesis and benefits
Nov 12	Prof. M. R. Truter, University College, London Luck and logic in host-guest chemistry

Mar 17	Dr. R. J. K. Taylor, University of East Anglia Adventures in natural product synthesis
Mar 24	Prof. I. O. Sutherland, University of Liverpool Chromogenic reagents for cations
May 13	Prof. J. A. Pople, Carnegie-Mellon University, Pittsburgh, USA Applications of molecular orbital theory
May 21	Prof. L. Weber, University of Bielefeld Metallo-phospha alkenes as synthons in organometallic chemistry
Jun 1	Prof. J. P. Konopelski, University of California, Santa Cruz Synthetic adventures in enantiomerically pure acetals
Jun 2	Chiral discrimination in the stereospecific polymerisation of alpha olefins
Jun 7	Prof. R. S. Stein, University of Massachusetts Scattering studies of crystalline and liquid crystalline polymers
Jun 16	Prof. A. K. Covington, University of Newcastle Use of ion selective electrodes as detectors in ion chromatography
Jun 17	Prof. O. F. Nielsen, H. C. Oersted Institute, University of Kopenhagen Low-frequency IR- and Raman studies of hydrogen bonded liquids
Oct 4	Prof. F. J. Fehder, University of California and Irvine Bridging the gap between surfaces and solution with sessilquioxanes
Oct 20	Dr. P. Quayle, University of Manchester Aspects of aqueous ROMP chemistry
Oct 23	Prof. R. Adams, University of South Carolina The chemistry of metal carbonyl cluster complexes containing platinum and iron, ruthenium or osmium and the development of a cluster based alkyne hydrogenation catalyst
Oct 27	Dr. R. A. Jones, Cavendish Laboratory Perambulating polymers
Nov 10	Prof. M. N. R. Ashford, University of Bristol High-resolution photofragment translational spectroscopy : a new way to watch photodissociation
Nov 17	Dr. A. Parker, Laser support Facility Applications of time resolved raman spectroscopy to chemical and biochemical problems
Nov 24	Dr. P. G. Bruce, University of St. Andrews Synthesis and application of inorganic materials
Dec 1	Prof. M. A. McKervy, Queens University, Belfast Functionalised Calixerenes

1994

Jan 19	Prof. O. Meth-Cohen, Sunderland University Friedel's folly revised

Jan 26	Prof. J. Evans, University of Southampton Shining light on catalysis
Feb 2	Dr. A. Masters, University of Manchester Modelling water without using pair potentials
Feb 9	Prof. D. Young, University of Sussex Chemical and biological studies on the coenzyme tetrahydrofolic acid
Feb 16	Dr. R. E. Mulvey, University of Strathclyde Structural patterns in alkali metal chemistry
Feb 23	Prof. P. M. Maitlis FRS, University of Sheffield Why rhodium in homogeneous catalysis
Mar 2	Dr. C. Hunter, University of Sheffield Non-covalent interactions between aromatic molecules
Apr 20	Prof. P. Parsons, University of Reading New methods and strategies in natural product synthesis